

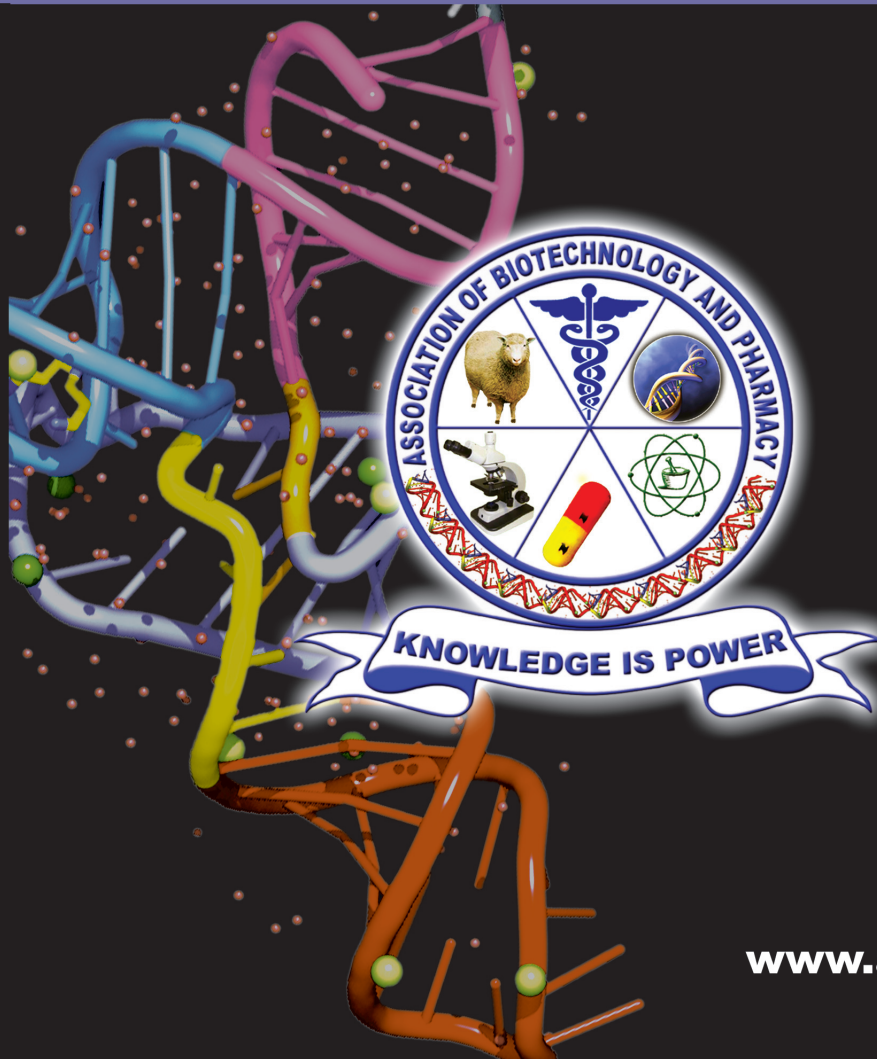
ISSN 0973-8916

# Current Trends in Biotechnology and Pharmacy

Volume 14

Issue 1

January 2020



[www.abap.co.in](http://www.abap.co.in)

## Current Trends in Biotechnology and Pharmacy

ISSN 0973-8916 (Print), 2230-7303 (Online)

### Editors

Prof.K.R.S. Sambasiva Rao, India  
krssrao@abap.co.in

Prof. Karnam S. Murthy, USA  
skarnam@vcu.edu

### Editorial Board

Prof. Anil Kumar, India  
Prof. P.Appa Rao, India  
Prof. Bhaskara R.Jasti, USA  
Prof. Chellu S. Chetty, USA  
Dr. S.J.S. Flora, India  
Prof. H.M. Heise, Germany  
Prof. Jian-Jiang Zhong, China  
Prof. Kanyaratt Supaibulwatana, Thailand  
Prof. Jamila K. Adam, South Africa  
Prof. P.Kondaiah, India  
Prof. Madhavan P.N. Nair, USA  
Prof. Mohammed Alzoghaibi, Saudi Arabia  
Prof. Milan Franek, Czech Republic  
Prof. Nelson Duran, Brazil  
Prof. Mulchand S. Patel, USA  
Dr. R.K. Patel, India  
Prof. G.Raja Rami Reddy, India  
Dr. Ramanjulu Sunkar, USA  
Prof. B.J. Rao, India  
Prof. Roman R. Ganta, USA  
Prof. Sham S. Kakar, USA  
Dr. N.Sreenivasulu, Germany  
Prof. Sung Soo Kim, Korea  
Prof. N. Udupa, India

Dr.P. Ananda Kumar, India  
Prof. Aswani Kumar, India  
Prof. Carola Severi, Italy  
Prof. K.P.R. Chowdary, India  
Dr. Govinder S. Flora, USA  
Prof. Huangxian Ju, China  
Dr. K.S.Jagannatha Rao, Panama  
Prof. Juergen Backhaus, Germany  
Prof. P.B.Kavi Kishor, India  
Prof. M.Krishnan, India  
Prof. M.Lakshmi Narasu, India  
Prof. Mahendra Rai, India  
Prof. T.V.Narayana, India  
Dr. Prasada Rao S.Kodavanti, USA  
Dr. C.N.Ramchand, India  
Prof. P.Reddanna, India  
Dr. Samuel J.K. Abraham, Japan  
Dr. Shaji T. George, USA  
Prof. Sehamuddin Galadari, UAE  
Prof. B.Srinivasulu, India  
Prof. B. Suresh, India  
Prof. Swami Mruthinti, USA  
Prof. Urmila Kodavanti, USA

### Assistant Editors

Dr.Giridhar Mudduluru, Germany

Dr. Sridhar Kilaru, UK

Prof. Mohamed Ahmed El-Nabarawi, Egypt

Prof. Chitta Suresh Kumar, India

[www.abap.co.in](http://www.abap.co.in)

ISSN 0973-8916

# Current Trends in Biotechnology and Pharmacy

(An International Scientific Journal)

Volume 14

Issue 1

January 2020



[www.abap.co.in](http://www.abap.co.in)

Indexed in Chemical Abstracts, EMBASE, ProQuest, Academic SearchTM, DOAJ, CAB Abstracts, Index Copernicus, Ulrich's Periodicals Directory, Open J-Gate Pharmoinfonet.in Indianjournals.com and Indian Science Abstracts.

## **Association of Biotechnology and Pharmacy** (Regn. No. 28 OF 2007)

The *Association of Biotechnology and Pharmacy (ABAP)* was established for promoting the science of Biotechnology and Pharmacy. The objective of the Association is to advance and disseminate the knowledge and information in the areas of Biotechnology and Pharmacy by organising annual scientific meetings, seminars and symposia.

### **Members**

The persons involved in research, teaching and work can become members of Association by paying membership fees to Association.

The members of the Association are allowed to write the title **MABAP** (Member of the Association of Biotechnology and Pharmacy) with their names.

### **Fellows**

Every year, the Association will award Fellowships to the limited number of members of the Association with a distinguished academic and scientific career to be as Fellows of the Association during annual convention. The fellows can write the title **FABAP** (Fellow of the Association of Biotechnology and Pharmacy) with their names.

### **Membership details**

(Membership and Journal)		India	SAARC	Others
Individuals	– 1 year	Rs. 600	Rs. 1000	\$100
	LifeMember	Rs. 4000	Rs. 6000	\$500
Institutions (Journal only)	– 1 year	Rs. 1500	Rs. 2000	\$200
	Life member	Rs.10000	Rs.12000	\$1200

Individuals can pay in two instalments, however the membership certificate will be issued on payment of full amount. All the members and Fellows will receive a copy of the journal free.

**Association of Biotechnology and Pharmacy**  
(Regn. No. 28 OF 2007)  
#5-69-64; 6/19, Brodipet  
Guntur – 522 002, Andhra Pradesh, India



## Current Trends in Biotechnology and Pharmacy

ISSN 0973-8916

Volume 14 (1)	CONTENTS	January 2020
<b>Research Papers</b>		
Optimization Of Operating Parameters Using Response Surface Method For Biosorption of Zinc <i>P. Bangaraiah</i> DOI: 10.5530/ctbp.2020.1.1		7-15
Molecular evolution of Thermophilic <i>Geobacillus</i> species isolated from Tattapani Hotspring (India) and the Worldwide Distribution. <i>Parul Sharma, Sonika Gupta, Anuradha Sourirajan, David J. Baumler, Kamal Dev</i> DOI: 10.5530/ctbp.2020.1.2		16-32
Differential Loss of ROS homeostasis and activation of anti oxidative defense response in tea cultivar due to aluminum toxicity in acidic soil <i>Sanjenbam Sanjibia Devi, Bedabrata Saha, Sanjib Kumar Panda</i> DOI: 10.5530/ctbp.2020.1.3		33-43
Deciphering the Biological Activity of Recombinant Guinea Pig Proteins <i>Madhavan Omanakuttan, Vijaya R. Dirisala, Hanumohan R. Konatham, M. Madhuri, Malathi Jojula, Shradha Mawatwal, Rohan Dhiman</i> DOI: 10.5530/ctbp.2020.1.4		44-47
Pemphigus vegetans: a rare case report <i>InamdarSZ, Pradeep R, Akhila M, Jangond A, Pradeepthi K, Kulkarni RV</i> DOI: 10.5530/ctbp.2020.1.5		48-50
Comparative analysis of biofabricated silver nanoparticles as antibiofilm agents on <i>Pseudomonas aeruginosa</i> <i>Anju .S and J. Sarada</i> DOI: 10.5530/ctbp.2020.1.6		51-61
Statistical optimization of PolyHydroxyButyrate (PHB) production by novel <i>Acinetobacter nosocomialis</i> RR20 strain using Response Surface Methodology <i>Ranganadha Reddy A, Vidya Prabhakar K, Venkateswarulu T C, Krupanidhi S, Md. Nazneen Bobby, Abraham Peele K, P.Sudhakar, P. Vijetha</i> DOI: 10.5530/ctbp.2020.1.7		62-69
Extraction, Total phenol Content, Flavonoid content, Free Radical Scavenging Capacity and phytochemical screening of the Parts of Sri Lankan Pomegranate ( <i>Punica granatum</i> L.) Fruit <i>Udeshika Y Bandara, Chamindri Witharana and Preethi Soysa</i> DOI: 10.5530/ctbp.2020.1.8		70-80
Design and Development of Multifunctional Hybrids of Ferulic Acid and 1,3,4-Oxadiazoles for the Treatment of Alzheimer's Disease <i>Avanish Tripathi, Priyanka Kumari Choubey, Ankit Seth, Piyoosh Sharma, Manish Kumar Tripathi and Sushant Kumar Shrivastava</i> DOI: 10.5530/ctbp.2020.1.9		81-96
<b>Review Papers</b>		
Role of Nanoparticles as Antibiofilm Agents: A Comprehensive Review <i>Suruchi Chaudhary, Anurag Jyoti, Vikas Shrivastava and Rajesh Singh Tomar</i> DOI: 10.5530/ctbp.2020.1.10		97-110
Engineered nanoparticles: Hazards and Risk Assessment upon Exposure-A Review <i>Krishna Suresh Babu Naidu</i> DOI: 10.5530/ctbp.2020.1.11		111-122

## Information to Authors

The *Current Trends in Biotechnology and Pharmacy* is an official international journal of *Association of Biotechnology and Pharmacy*. It is a peer reviewed quarterly journal dedicated to publish high quality original research articles in biotechnology and pharmacy. The journal will accept contributions from all areas of biotechnology and pharmacy including plant, animal, industrial, microbial, medical, pharmaceutical and analytical biotechnologies, immunology, proteomics, genomics, metabolomics, bioinformatics and different areas in pharmacy such as, pharmaceutics, pharmacology, pharmaceutical chemistry, pharma analysis and pharmacognosy. In addition to the original research papers, review articles in the above mentioned fields will also be considered.

### Call for papers

The Association is inviting original research or review papers and short communications in any of the above mentioned research areas for publication in *Current Trends in Biotechnology and Pharmacy*. The manuscripts should be concise, typed in double space in a general format containing a title page with a short running title and the names and addresses of the authors for correspondence followed by Abstract (350 words), 3 – 5 key words, Introduction, Materials and Methods, Results and Discussion, Conclusion, References, followed by the tables, figures and graphs on separate sheets. For quoting references in the text one has to follow the numbering of references in parentheses and full references with appropriate numbers at the end of the text in the same order. References have to be cited in the format below.

Mahavadi, S., Rao, R.S.S.K. and Murthy, K.S. (2007). Cross-regulation of VAPC2 receptor internalization by m2 receptors via c-Src-mediated phosphorylation of GRK2. *Regulatory Peptides*, 139: 109-114.

Lehninger, A.L., Nelson, D.L. and Cox, M.M. (2004). *Lehninger Principles of Biochemistry*, (4<sup>th</sup> edition), W.H. Freeman & Co., New York, USA, pp. 73-111.

Authors have to submit the figures, graphs and tables of the related research paper/article in Adobe Photoshop of the latest version for good illumination and alignment.

Authors can submit their papers and articles either to the editor or any of the editorial board members for onward transmission to the editorial office. Members of the editorial board are authorized to accept papers and can recommend for publication after the peer reviewing process. The email address of editorial board members are available in website [www.abap.in](http://www.abap.in). For submission of the articles directly, the authors are advised to submit by email to [krssrao@abap.co.in](mailto:krssrao@abap.co.in) or [krssrao@yahoo.com](mailto:krssrao@yahoo.com).

Authors are solely responsible for the data, presentation and conclusions made in their articles/research papers. It is the responsibility of the advertisers for the statements made in the advertisements. No part of the journal can be reproduced without the permission of the editorial office.

## Optimization Of Operating Parameters Using Response Surface Method For Biosorption of Zinc

P. Bangaraiah<sup>1</sup>

<sup>1</sup>Department of Chemical Engineering, VFSTRUniversity, Vadlamudi, Guntur. A .P.  
Email:pbangaraiah79@gmail.com

### Abstract

The Biosorption of metals is an effective and environmental friendly process for the removal of heavy metals from aqueous solution. Biosorption of zinc by Tamarind fruit shell powder (*Tamarindus Indica L.*) was investigated in this study. The various operating parameters like agitation time, biomass dosage, initial metal ion concentration and pH were studied using Face centered composite design method under RSM and batch process. The optimum parameters using RSM are agitation time is 22.84 minutes, dosage is 0.78gm, initial ion concentration is 20.87 mg/l and pH is 6.98. The experimental data was analyzed using Freundlich and Langmuir isotherms. Langmuir isotherm is the best fit to the given data. The kinetic data is well suited to pseudo second order kinetics. Thermodynamic and equilibrium studies were investigated. The maximum percentage removal of zinc using tamarind fruit shell is 65.2. The tamarind fruit shell biomass is favorable for biosorption of zinc.

**Keywords:** Tamarind fruit shell powder; zinc; RSM; biosorption; isotherm

### 1 Introduction

Heavy metal pollution can arise from many sources but most commonly arise from the purification of metals. Rubber dye, wood preservatives and electroplating industries are the major sources for zinc pollution.

The search for alternate and innovate treatment techniques has focused attention on the use of biological materials for heavy metals

removal and recovery technologies and has gained important credibility during recent years because of the good performance and low cost of this complexed materials. Biosorbent materials are available in abundance, low in cost and found to be more efficient for the removal of heavy metals [1].

In this I am using Tamarind fruit shell as biomaterial and then results are obtained. The results are analyzed and conclusions are made. Heavy metals contamination of industrial effluents is one of the significant environmental problems due to their toxic nature and accumulation throughout the food chain as non-biodegradable pollutants. Iron is considered as an aesthetic contaminant. Ferrous iron gives water a disagreeable taste and produces an inky, black appearance when it combines with tea and coffee. It causes staining on laundries, fixtures and table ware. Iron is usually discharged to the environment through the effluent of many industries such as basic steel, inorganic chemicals, alkalis, chlorine, fertilizers and petroleum refining. Iron overload may lead to debilitating and life-threatening problems such as diabetes, heart failure, and poor growth. According to environmental pollution act the acceptable value of iron in drinking water is 0.3 mg/l. Therefore biosorption is potentially cost effective way of removing heavy metals from industrial wastewaters [2].

The present study, biosorbent was prepared from Tamarind tree. The tamarind fruit shells are collected from Jammalamadugu village in

Kadapa district. The biosorbent tamarind fruit shell powder (*Tamarindus Indica.L*) was used to carry out zinc removal. Batch experiments are carried out for kinetic, thermodynamic and equilibrium studies on the removal zinc from aqueous solution. The effect of various parameters such as agitation time, biosorbent dosage, initial metal ion concentration and pH has been studied [3-4].

### Materials and methods

**Preparation of biosorbent :** The Tamarind fruit shells are collected from Jammalamadugu in Kadapa district. The shells are washed with distilled water. Then these shells are dried for 24 hrs at 60°C using oven. The dried shells are crushed and the resulting powder is sieved to different sizes. The size fractions of biosorbent are stored for future use.

**Preparation of stock solution (aqueous solution) :** Known amount of ZnSO<sub>4</sub>.7H<sub>2</sub>O is dissolved in one liter of distilled water to prepare a stock solution. Samples of different concentrations of zinc are prepared by appropriate dilutions. The P<sup>H</sup> is adjusted with NaOH [5-6].  
**2.3 Batch Biosorption studies**

The aqueous solution of 30 ml is taken in a conical flask and one gm of biosorbent (Tamarind fruit shell powder) is added. The sample is agitated by using shaker at 120 rpm and 30°C for one minute. Similarly few more samples are prepared with varying agitation times. Then these samples are filtered and the filtrates are analyzed with Spectrophotometer. The % removal of zinc is calculated using  $(C_i - C_t) \times 100 / C_i$ . Graph is plotted between the agitation time and % removal of zinc to identify the optimum agitation time. Similarly the above procedure is followed to find the optimum initial metal ion concentration, dosage and pH [7].

**Response surface Methodology:** The applied optimization method is based on Face centered composite Designs under RSM to fit the second

order model. This is one of the best experimental designs used in the process optimization studies [8].

### Results And Discussion

**Effect of agitation time :** The effect of agitation time is determined by plotting the % removal of zinc against agitation time in Figure.1 with the process conditions of initial concentration of zinc ( $C_i$ ) = 20 mg l<sup>-1</sup>, biosorbent size (dp) = 82.5 μm, biosorbent dosage (w) = 1 gm, volume of aqueous solution, V = 30 ml. From Figure.1, it was observed that at initial period, the rate of biosorption is faster, because adequate surface area is available for the biosorption of zinc. As the agitation time increases, more amounts of zinc get biosorbed onto the surface of the biosorbent available. The maximum % removal is attained at 35 minutes. The % removal of zinc is 65.5. So the optimum agitation time is 35 minutes [9].

**Effect of Biosorbent dosage :** The effect of biosorbent dosage is determined by plotting biosorbent dosage with percentage removal of zinc in Figure.2. It was evident from the plot that the percentage removal of zinc from the aqueous solution increases with increases in biosorbent dosage from 0.1 gm to 1.0 gm. After this there was no change in percentage removal. The maximum % removal of zinc at 1.0 gm is 66.1. This is because of number of active sites available for metal removal would be more as amount of the biosorbent increases. So the optimum dosage is 1 gm.

**Effect of initial ion concentration :** The effect of initial concentration of zinc is observed by plotting the percentage removal of zinc against initial metal ion concentration in Figure.3. The percentage removal of zinc was decreased from 65.2 to 40.3 by increasing the initial metal ion concentration from 5 mg l<sup>-1</sup> to 60 mg l<sup>-1</sup>. This was attained due to constant amount of biosorbent exposed to more amount of adsorbate. It was observed that the high percentage removal of zinc attained in the start of biosorption. So the optimum initial metal concentration is 20 mg l<sup>-1</sup> [10].

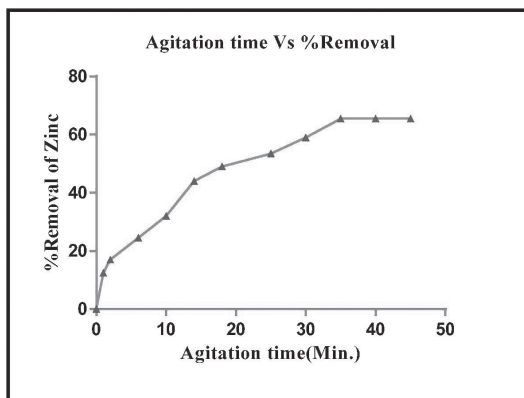
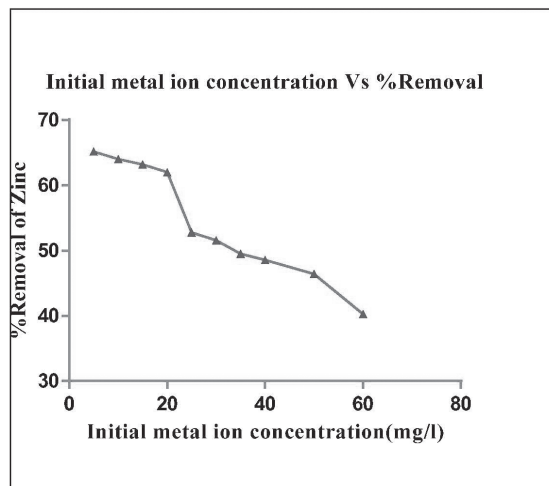


Figure.1 Effect of agitation time on % removal of zinc



e.3 Effect of initial metal ion concentration on % remo

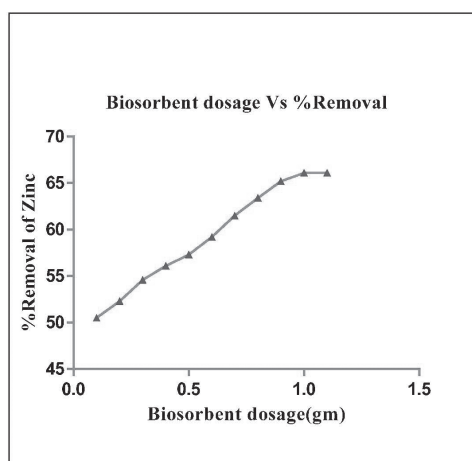
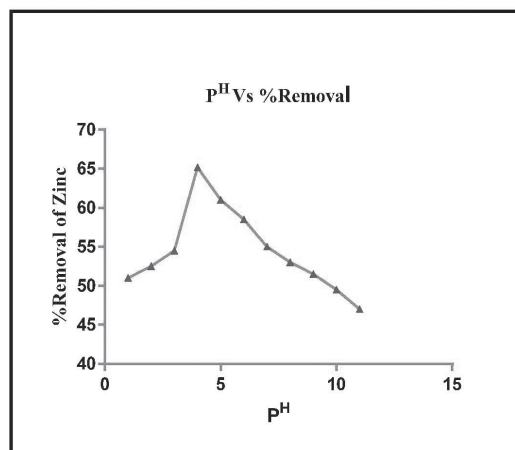


Figure.2 Effect of biosorbent dosage on % removal of zinc



**Effect of pH:** The effect of  $P^H$  is observed by plotting pH against percentage removal of zinc as shown in Figure.4. The % removal of zinc was increased from 51% to 65.2% as  $P^H$  is increased from 1 to 4. At higher  $P^H$  value, the capacity of the biosorbent recessed. The reduction in biosorption was occurred due to more numbers of OH-ions. Further increase in  $P^H$  value from 4 to 11, resulted to decrease in biosorption. So the optimum  $P^H$  was 4.

**Adsorption isotherms:** From Figure.5 and Figure.6, it was observed that the experimental

data is well correlated with Freundlich and Langmuir isotherms indicating favorable biosorption of zinc by the biosorbent of Tamarind fruit shell. Langmuir isotherms are more suitable than Freundlich isotherms for the removal of zinc.

**First order kinetics:** The kinetic data was analyzed by using Pseudo first order kinetic equation given in equation-1  $\log(q_e - q_t) = \log q_e - (K_{ad}/2.303) t$ . The data is obtained using optimum conditions of volume of solution is 30ml, biosorbent size,  $(d_p) = 97.5 \mu m$ , initial ion concentration of  $20 \text{ mg l}^{-1}$  and agitation time

35 minutes. Lagergren plot of  $\log(q_e - q_t)$  versus agitation time  $t$  is drawn in Figure. 7. From the plot it was observed that  $R^2$  is 0.960 and it not followed the perfect linearity. So Pseudo first order model is not best fit [11].

**Second order kinetics :** The Pseudo second order equation is given by equation-2.  $(t/q_t) = 1/K q^2 + 1 / q_e t$  The plot of  $(t/q_t)$  vs.  $t$  was drawn in Figure.8. From the plot it was observed that, the

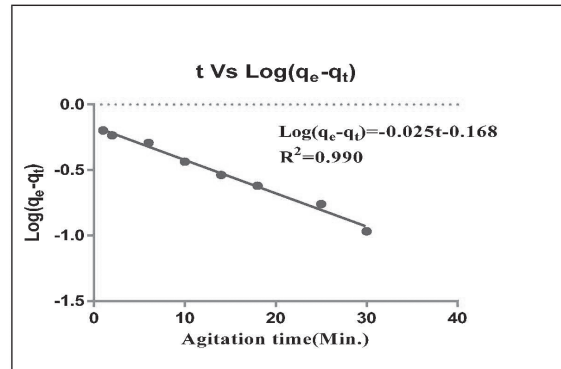


Figure.7 First order kinetics

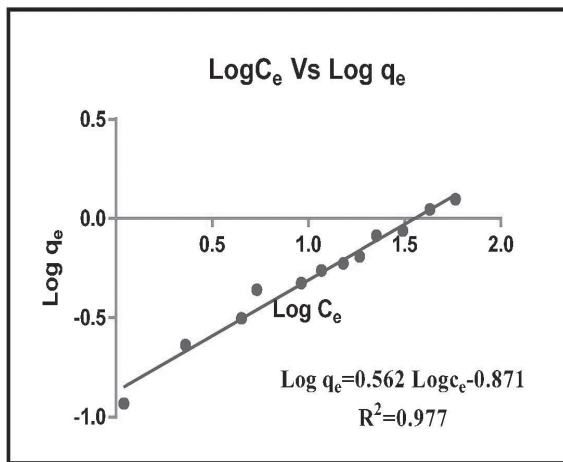


Figure.6 Langmuir isotherm

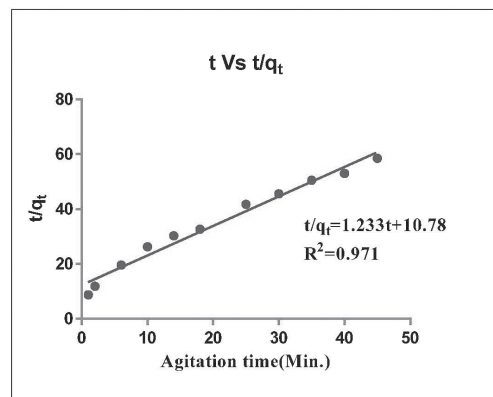
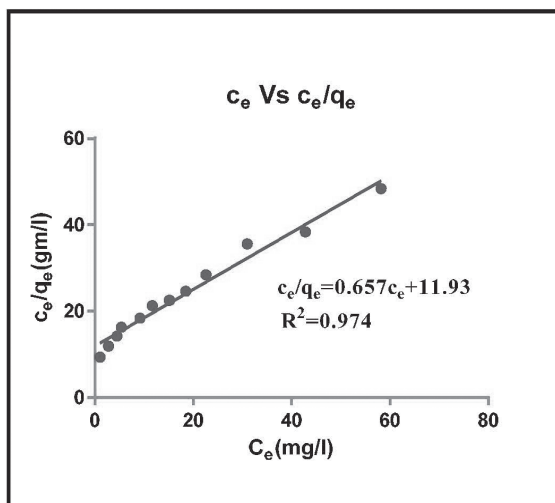


Figure.8 Second order kinetics

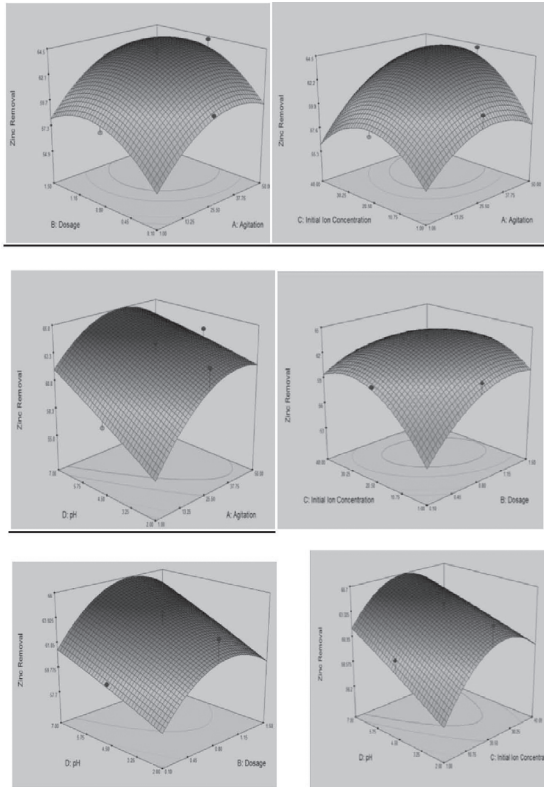


linearity of the plot ( $R^2 = 0.991$ ) confirms the suitability of pseudo second order rate equation [12].

**Thermodynamic study :** From Table.1, it was observed that the value of enthalpy is positive, it meant that the biosorption process is endothermic and the physical sorption play a role in biosorption of zinc and can easily be reversed by applying heat [equal to calculated ( $H$ ) value] to the adsorption system. The entropy values above zero confirm the irreversibility of the biosorption process. The -ve value of Gibbs free energy indicates the reaction is spontaneous [13].

**Statistical analysis :** The optimum parameters for biosorption of zinc on the surface of Tamarind





fruit shell powder were determined by means of FCCD under Response Surface Method (RSM). The results are shown in Table.2. The percentage removal of zinc was expressed by using following equation. The Final expression in terms of coded form is given in equation-3.  $(Y) = +63.72 + 2.24 * A + 1.55 * B + 1.26 * C + 2.03 * D + 0.013 * A * B + 0.93 * A * C - 0.97 * A * D - 1.89 * B * C + 0.24 * B * D - 0.77 * C * D - 2.46 * A^2 - 2.51 * B^2 - 3.31 * C^2 - 0.11 * D^2$

Where A,B,C,D are Agitation time, biosorbent dosage, initial ion concentration and pH respectively. The above equation represents how individual variables or double interaction affected zinc removal by using Tamarind fruit shell powder as a biosorbent. The  $R^2$  value indicate the quality of model. The equation demonstrated that the model is well fitted with  $R^2$  value of 0.9090. The calculated parameters and coefficients are indicated in Table.2. F-Values less than 0.0500 indicate model is significant. From Table.3, it was observed that the relationship between RSM predicted and experimental values of the response is good [14].

**Table 1 Thermodynamics on biosorption of zinc using tamarind fruit shell Initial**

S.No.	Conc., mg l <sup>-1</sup>	$\Delta H,$ J/mol	$\Delta S,$ K <sup>-1</sup> Jmol <sup>-1</sup>	$\Delta G$ at different temperatures Jmol <sup>-1</sup>			
				293° K	303° K	313°K	323°K
1	20	23.83	58.13	-17008.3	-17589.6	-18170.9	-18752.2
2	40	17.74	32.35	-9460.81	-9784.31	-10107.8	-10431.3
3	60	16.41	29.14	-8521.61	-8813.01	-9104.41	-9395.81
4	80	12.69	11.06	-3227.89	-3338.49	-3449.09	-3559.69
5	100	8.78	2.85	-826.27	-854.77	-883.27	-911.77



**Table 2 Response surface method for optimization**

Source	Sum of squares	df	Mean square	F-value	P-value Prob > F
<b>Model</b>	<b>747.54</b>	<b>14</b>	<b>53.40</b>	<b>21.69</b>	<b>&lt; 0.0001</b>
<i>A-Agitation</i>	<i>90.68</i>	<i>1</i>	<i>90.68</i>	<i>36.84</i>	<i>&lt; 0.0001 significant</i>
<i>B-Dosage</i>	<i>43.24</i>	<i>1</i>	<i>43.24</i>	<i>17.57</i>	<i>0.0008</i>
<i>C-Initial Ion Concentration</i>	<i>28.63</i>	<i>1</i>	<i>28.63</i>	<i>11.63</i>	<i>0.0039</i>
<i>D-pH</i>	<i>74.01</i>	<i>1</i>	<i>74.01</i>	<i>30.07</i>	<i>&lt; 0.0001</i>
<i>AB</i>	<i>2.500E-003</i>	<i>1</i>	<i>2.500E-003</i>	<i>1.016E-003</i>	<i>0.9750</i>
<i>AC</i>	<i>13.69</i>	<i>1</i>	<i>13.69</i>	<i>5.56</i>	<i>0.0324</i>
<i>AD</i>	<i>15.21</i>	<i>1</i>	<i>15.21</i>	<i>6.18</i>	<i>0.0252</i>
<i>BC</i>	<i>57.00</i>	<i>1</i>	<i>57.00</i>	<i>23.16</i>	<i>0.0002</i>
<i>BD</i>	<i>0.90</i>	<i>1</i>	<i>0.90</i>	<i>0.37</i>	<i>0.5539</i>
<i>CD</i>	<i>9.61</i>	<i>1</i>	<i>9.61</i>	<i>3.90</i>	<i>0.0669</i>
<i>A2</i>	<i>15.74</i>	<i>1</i>	<i>15.74</i>	<i>6.40</i>	<i>0.0231</i>
<i>B2</i>	<i>16.39</i>	<i>1</i>	<i>16.39</i>	<i>6.66</i>	<i>0.0209</i>
<i>C2</i>	<i>28.47</i>	<i>1</i>	<i>28.47</i>	<i>11.57</i>	<i>0.0040</i>
<i>D2</i>	<i>0.034</i>	<i>1</i>	<i>0.034</i>	<i>0.014</i>	<i>0.9077</i>
Residual	36.92	15	2.46		
<i>Lack of Fit</i>	<i>24.89</i>	<i>10</i>	<i>2.49</i>	<i>1.03</i>	<i>0.5182 not significant</i>
<i>Pure Error</i>	<i>12.03</i>	<i>5</i>	<i>2.41</i>		
Cor Total	784.46	29			

**Table 3 FCCD experimental design matrix and experimental responses**

Run	Agitation	Dosage	Conc.	pH	% Zinc	RSM	Residual
					Removal	Predicted	
1	1	0.1	1	2	46.2	45.76	0.44
2	50	0.1	1	2	48.5	50.32	-1.82
3	1	1.5	1	2	52.4	52.14	0.26
4	50	1.5	1	2	56.3	56.75	-0.45
5	1	0.1	40	2	50.8	51.76	-0.96
6	50	0.1	40	2	61.3	60.02	1.28
7	1	1.5	40	2	50.2	50.58	-0.38
8	50	1.5	40	2	58.6	58.90	-0.30
9	1	0.1	1	7	52.1	52.84	-0.74
10	50	0.1	1	7	54.9	53.50	1.40
11	1	1.5	1	7	59.9	60.17	-0.27
12	50	1.5	1	7	60.8	60.88	-0.08
13	1	0.1	40	7	57.2	55.74	1.46
14	50	0.1	40	7	58.8	60.10	-1.30
15	1	1.5	40	7	56.3	55.51	0.79
16	50	1.5	40	7	60.5	59.93	0.57
17	1	0.8	20.5	4.5	58.4	59.01	-0.61
18	50	0.8	20.5	4.5	64.2	63.50	0.70
19	25.5	0.1	20.5	4.5	59.9	59.65	0.25
20	25.5	1.5	20.5	4.5	62.6	62.75	-0.15
21	25.5	0.8	1	4.5	60.4	59.14	1.26
22	25.5	0.8	40	4.5	60.5	61.66	-1.16
23	25.5	0.8	20.5	2	63.5	61.57	1.93
24	25.5	0.8	20.5	7	63.8	65.63	-1.83
25	25.5	0.8	20.5	4.5	64.3	63.72	0.58
26	25.5	0.8	20.5	4.5	64.3	63.72	0.58
27	25.5	0.8	20.5	4.5	64.3	63.72	0.58
28	25.5	0.8	20.5	4.5	64.3	63.72	0.58
29	25.5	0.8	20.5	4.5	64.3	63.72	0.58
30	25.5	0.8	20.5	4.5	60.5	63.72	-3.22

**RSM Plots** : Figure.9, the RSM plots represent interaction effects of the factors. These graphs can be done by software. These plots are represented the effect of agitation time, dosage, initial ion concentration and pH on percentage removal of zinc [15].

#### **Conclusion :**

The Analysis of variance of the FCCD model demonstrates that the model is significant. Solution pH was the most significant factor affecting zinc removal. Therefore, the RSM not only gives the interactions between the factors but also helps to the recognition of possible optimum values of the studied factors. As per RSM the optimum agitation time is 22.84 minutes, dosage is 0.78 gm, initial ion concentration is 20.87 mg l<sup>-1</sup> and pH is 6.98. Batch biosorption experiments indicate that the adsorption equilibrium can be achieved in 35min. The kinetics data followed the pseudo-first order at different initial concentrations. The results of equilibrium data showed that the biosorption of zinc followed the Langmuir isotherm. Thermodynamic studies indicated that the zinc biosorption onto Tamarind fruit shell powder was spontaneous and endothermic [16].

#### **5 REFERENCES**

1. Umesh, K. G. and Harish, K. G. (2016) Optimization of Process Parameters for Metal Ion Remediation using Agricultural Waste materials, *International Journal of Theory and Applied Science*, 8:17-24.
2. Seyed ali, zamani, Robiah, A.W. Yunus, Samsuri, M. A. Mohd salleh and Bahareh, A. (2017) Removal of zinc from aqueous solution by optimized oil palm empty fruit bunches biochar as low cost adsorbent, *Bioinorganic chemistry and applications*, 1:1-9.
3. Anilkumar, B. Chitti Babu and N. Kavitha, G. (2016) Biosorption of Zinc on to *Gracilaria Corticata* (Red Algae) Powder and Optimization using Central Composite Design, *Journal of Applied Science and Engineering Methodologies*, 2:412-425.
4. Vishal, M. (2014) Biosorption of zinc ion: a deep comprehension, *Applied Water Science*, 4:311-332.5. Yang, C. Wang, J. Lei M, Xie. Zeng, G and Leo, G. (2010) Biosorption of zinc (II) from aqueous solution by dried activated sludge, *Journal of Environmental Sciences (China)*, 22:675-680.
6. Sangkyu Kam, Donghwan, Lee. and Mingyu, Lee. (2003) Biosorption of Copper and Zinc by Biomass of Marine Brown Algae in Cheju Island, *Environmental Engineering Research*, 2:181-190.
7. Zuleyha, B. Hasan, G. Ali, and A. Sezai, E. (2016) 'Biosorption of Zinc (II) from aqueous solutions by non living lichen biomass of *Xanthoria parietina* (L.)', *Environmental Engineering and Management Journal*, 15:2733-2740.
8. Adesola, N.A. Babarinde, J. Oyebamiji, B. and Olasumbo, B. A. (2008) Kinetic, isotherm and thermodynamic studies of the biosorption of zinc (II) from solution by maize wrapper *International Journal of Physical Sciences*, 3: 050-055.
9. Adesola, N.A. Babarinde, J. Oyebamiji, B. and Olasumbo, B.A. (2008) Isotherm and Thermodynamic Studies of the Biosorption of Zinc (II) from Solution by Maize Leaf, *The Pacific Journal of Science and Technology*, 9:196-202.
10. Ajitha, R. Meena Devi, V. N. and Murugan, M. (2015) Biosorption of Zn (II) from aqueous solution onto the Alexandrian laurel oil cake, *Journal of Chemical and Pharmaceutical Research*, 7:643-648.
11. Rezguia, A. Hannachia, Y. Guibal, E. and Boubakera, T. (2015) Biosorption of zinc

- from aqueous solution by dried activated sludge biomass, *Desalination and Water Treatment*, 56:2699-2705.
12. Bahia, M. Mohamed, A. Zenasnil, Merlin, A. and Béatrice, G. (2015) Biosorptive Removal of Zinc from Aqueous Solution by Algerian *Calotropis procera* Roots, *Journal of Environmental Protection*, 6 :735-743.
  13. S<sup>3</sup>awomir, W. (2015) Biosorption of lead (II) zinc (II) and nickel (II) from industrial wastewater by *Stenotrophomonas maltophilia* and *Bacillus subtilis*, *Polish Journal of Chemical Technology*, 17: 79-87.
  14. Guezzen, B. Didi, M.A. and Medjahed, B. (2017) 'Optimization of Process Parameters using Response Surface Methodology for the Removal of Zinc (II) by Solvent Extraction, *International Journal of Chemical, Molecular, Nuclear, Materials and Metallurgical Engineering*, 11:126-129.
  15. Rakesh, N. and King, P. (2013) Response Surface Methodology for optimization of Zinc biosorption by *Grewia Orbiculata* .L, *International Journal of Statistika and Matematika*, 5:06-15.
  16. Marandi, R. Doulati, F. Ardejani, H. and Amir, A. (2010) Biosorption of Lead (II) and Zinc (II) ions by pre-treated biomass of *phanerochaete chrysosporium*, *International Journal of Mining & Environmental Issues*, 1:1-9.

## Molecular evolution of Thermophilic *Geobacillus* species isolated from Tattapani Hotspring (India) and the Worldwide Distribution.

Parul Sharma<sup>1</sup>, Sonika Gupta<sup>1</sup>, Anuradha Sourirajan<sup>1</sup>, David J. Baumler<sup>2,3,4</sup>, Kamal Dev<sup>1,2,\*</sup>

<sup>1</sup>Faculty of Biotechnology, Shoolini University of Biotechnology and Management Sciences, Solan, Himachal Pradesh, India, PIN Code: 173212, <sup>2</sup>Department of Food Science and Nutrition, <sup>3</sup>Microbial and Plant Genomic Institute, and <sup>4</sup>Biotechnology Institute, University of Minnesota-Twin Cities St. Paul, Minnesota, USA

\*Corresponding Author: Email: kamaldevbhardwaj1969@gmail.com

### Abstract

Four thermophilic bacterial isolates PW11, PW12, PW13 and PS4 were isolated from Tattapani Hot Spring. The microbial isolates showed optimum growth at 70°C and at pH 6-7. Both Na<sup>+</sup> and K<sup>+</sup> ions were detected at 0.11 M and 1.7 mM respectively in the hot spring water. Interestingly, two bacterial isolates PW12 and PW13 showed growth in the presence of 0.5M KCl, whereas PW12 could grow in the presence of 0.75 M KCl and 0.75 M NaCl. All the four thermophilic isolates were rod shaped Gram-positive bacteria, and were analyzed by randomly amplified polymorphic DNA (RAPD) using five random primers and produced PCR fragments ranging from 250 – 6000 bp in size. Further, PW11, PW12, PW13 and PS4 were analyzed by PCR amplification of gene encoding 16S rDNA. 16S rDNA sequence analysis by BLAST search identifies PW13 as *Geobacillus thermoleovorans*, PW11 as *Geobacillus kaustrophilus*, PS4 and PW12 as *Geobacillus toebii* with GenBank accession nos. KF751757, KF751758, KF751759, and KJ509869 respectively.

**Keywords:** Thermophiles, RAPD, 16S rDNA sequencing, Phylogenetic relationship, *Geobacillus*, BLAST

### Introduction

There is a tremendous demand of thermophilic bacteria because of their

biotechnological importance as sources of thermostable enzymes and other products of industrial interest. Thermophilic microorganisms belong to Archaea and Bacteria live in Hot springs, thermal pools, and solfatares that are found throughout the world [1]. Since the discovery of thermophilic microorganisms and novel enzymes such as *Taq* Polymerase from *Thermus aquaticus*, large numbers of thermophilic enzymes have found industrial application including their importance as sources of thermostable enzymes (proteases, amylase, lipase, xylanase, cellulase, DNA restriction enzymes) and other products of industrial interest [2, 3, 4]. Thermophilic enzymes are advantageous in terms of high solubility of many reaction components and less risk of contamination. Considering that these microorganisms persist today in habitats that may have been present, and at times predominant, throughout Earth's geologic history, some assume that they represent lineage closely descendent from the first living microorganisms on the planet [5, 6]. Hot spring microbial communities have been extensively studied in many areas such as Yellowstone National Park in the United States [7, 8, 9, 10], Kamchatka hot springs in Russia, Icelandic hot springs [11, 12], Mt. Unzen hot springs in Japan [13], Ohwakudani hot springs in Japan [14], BorKhlueng hot springs in Thailand [15], Wai-o-tapu geothermal area in New Zealand [16], Tengchong hot Springs in China [17], and

Manikaran Hotspring of Himachal Pradesh [18]. The exploration and characterization of such microbial communities continues and is expected to simulate hypotheses about the structure, dynamics and distributions and phylogenetic relationship of thermophilic microbial populations from different geographical regions. Hot springs vary in terms of temperature, chemical composition and geographical location, which determine the nature of microorganisms. Therefore, exploration of the hot spring microbial communities all around the world would provide deeper insights into the evolution of species and microflora residing deep inside the earth's atmosphere. Unlike earlier microbiological work, recent development of techniques, such as the 16S rRNA approach [19] and genetic fingerprinting by RAPD [20] analysis revealed considerably more details and accurate analysis of microbial diversity and their evolution. Recently, *Geobacillus* species with hydrolytic activities have been characterized from Jordanian hot springs [21]. Nine different thermophilic bacterial isolates representing *Bacillus licheniformis* and *Aeribacillus pallidus* were characterized by molecular tests including fatty acid and BOX profiles, and 16S rDNA sequence from Pasinler Hot spring located in eastern Turkey [22].

Tattapani is one of the volcanic regions of Himachal Pradesh, India, situated in the snowy mountains of Himalayas. In this paper, we report the co-existence of thermophilic *Geobacillus spp.* from Tattapani hot spring of Himachal Pradesh that are distantly related to each other and represent diversified lineage based on phylogenetic evolution.

#### **Materials and methods**

**Collection of water and sludge samples from Tattapani hot spring** : Water and sludge samples were aseptically collected in a sterile falcon tubes from hot spring of Tattapani, district Mandi, Himachal Pradesh, India in the month of March 2011. Geothermal hot spring is located at 650 mt of altitude, Latitude: 31.383342 and Longitude: 77.199991 on the bank of Satluj river.

#### **Analysis of physical parameters of water sample**

Digital pH meter and glass mercury thermometer was used for the determination of pH and temperature of the water respectively at the source site. Further, water samples were analyzed by Argentometric method [23], conductivity meter and flame photometer methods for the determination of Na<sup>+</sup> and K<sup>+</sup> ions. Tap water was used as negative control. The Na<sup>+</sup> and K<sup>+</sup> ions were calculated from the standard curve of NaCl and KCl.

#### **Screening of water and sludge samples for thermophilic bacterial isolates**

25 ml water and soil sample (1g soil was mixed with 25 ml of sterile water) were centrifuged separately at 1000 rpm for 5 min to remove insoluble particles. The resultant supernatant was centrifuged at 10,000 rpm for 20 min. The bacterial pellet thus obtained was suspended in 1 ml LB broth medium and given codes as PW for water sample and PS for soil sample. Different volumes of 200, 300 and 400 µl were spread on LB agar medium. Plates were incubated at 60°C for 24h. Individual and isolated colonies were selected based on the colour, texture, morphology and size. The isolated colonies were successively streaked for three times on LB agar medium and pure cultures were preserved at -80°C in 50% glycerol.

#### **Biochemical characteristic features of thermophilic isolates**

Purified bacterial isolates were characterized on the basis of Gram's staining, cell morphology, motility and pigmentation. Further, enzymatic assays like oxidase, catalase, nitrate reduction, urease tests were performed to study the biochemical characteristics as described earlier [24].

#### **Effect of physical parameters on growth of thermophilic isolates**

To study the effect of temperature on growth, thermophilic isolates were streaked on LB agar medium and incubated at different temperature (40, 50, 60, 70 and 75°C) for 24h. Similarly, pH of the LB medium was adjusted to acidic pH of 5 and 6 by using 1N HCl and alkaline pH of 8, 9 and 10 using 5N NaOH to study



the effect of pH on growth of microbial isolate. Effect of NaCl and KCl on the growth of microbial isolates was studied by supplementing the LB agar medium with different concentration of NaCl and KCl (0.5, 0.75 and 1.0 M). Petri plates were incubated at 60°C for 24h in case of effect of pH, NaCl and KCl on growth of microbial isolates. To test the effect of various metal ions on growth of microbial isolates, chemicals used as nickel sulphate hexahydrate ( $\text{NiSO}_4 \cdot 6\text{H}_2\text{O}$ ), Zinc sulphate monohydrate ( $\text{ZnSO}_4 \cdot \text{H}_2\text{O}$ ), cobaltous nitrate hexahydrate  $\text{Co}(\text{NO}_3)_2 \cdot 6\text{H}_2\text{O}$ , mercuric chloride ( $\text{HgCl}_2$ ), manganese sulphate monohydrate ( $\text{MnCl}_2 \cdot \text{H}_2\text{O}$ ), Ferrous sulphate heptahydrate ( $\text{FeSO}_4 \cdot 7\text{H}_2\text{O}$ ), calcium chloride ( $\text{CaCl}_2$ ), Magnesium chloride ( $\text{MgCl}_2$ ), Copper sulphate ( $\text{CuSO}_4 \cdot 5\text{H}_2\text{O}$ ) and Cadmium sulphate ( $\text{CdSO}_4$ ) metal salts at concentrations of 10, 20, 50, 100, 150 and 200 ppm were supplemented in minimal M9 medium containing 1% Glucose. Cultures were incubated at 60°C for 24h and cell density was measured by measuring absorbance at 600 nm as compared to un-supplemented metal ions containing media as control.

**Effect of carbon and nitrogen sources on the growth of thermophilic isolates :** Various carbohydrates (glucose, starch, sucrose, fructose, trehalose, glycerol, lactose, raffinose, galactose, and sorbitol) and nitrogen sources (yeast extract, peptone, beef extract, casein hydrolysate, urea and ammonium chloride) were evaluated for the growth of thermophilic microorganisms in Minimal M9 media. All thermophilic bacterial isolates were streaked on M9 agar medium supplemented with 1% carbohydrates [w/v] and 0.5% nitrogen source [w/v]. The Petri plates were incubated at 60°C for 24 h and analyzed for growth.

**Molecular characterization of thermophilic isolates by RAPD and 16S rDNA analysis :** Total genomic DNA was extracted from the bacterial isolates using standard phenol: chloroform method [25]. Genomic DNA was separated on 1% agarose gel by using TAE buffer (40 mM Tris base, 1 mM EDTA and 20 mM glacial acetic acid) system and visualized by using gel documentation unit (Alpha Innotech). RAPD analysis was used as a method

to study the genetic variation among bacterial isolates. Amplification was carried out using decamer random primers 1K, 2K, 14K, 15K and 25K (Table 5) at annealing temperature of 40°C. The amplified products were resolved on 1.2% agarose gel and fragments generated by RAPD-PCR were analyzed by using alpha image viewer (Alpha Innotech) and numbered 0 (zero) and 1 (one) on the basis of absence and presence of bands respectively. Polymorphic band were analyzed by constructing phylogenetic tree using MVSP 3.2 version software (<https://www.mvsp.software.informer.com/3.2/>)

16S rDNA sequence was amplified using universal bacterial specific forward primer 27F and reverse primer 1492R [16]. Amplification was carried out at annealing temperature of 55°C. The gel purified PCR products were sequenced on both strands of DNA by using 27F and 1492R primers at Eurofins, Bangalore, India (<https://www.eurofins.com>). Complete nucleotide sequence was generated by removing the overlapping sequence and was subjected to BLASTN (<http://blast.ncbi.nlm.nih.gov>) search at NCBI database. The 16S rDNA sequences of related bacterial strains available in Genbank were used for the construction of dendrogram by using MEGA 4 software (<http://www.megasoftware.net>). The nucleotide sequences were submitted in the GenBank database (<https://www.ncbi.nlm.nih.gov/genbank/>).

## Results

Considering the wealth of amazing biodiversity of thermophiles, the present study was undertaken to determine the phylogenetic relationship among thermophilic bacteria isolated from water and sludge samples of Tattapani Hot Spring of Himachal Pradesh, India. Four bacterial isolates, three from water (PW11, PW12 and PW13) and one from sludge (PS4) were selected. The molecular approach by RAPD-PCR amplification was performed to understand the phylogenetic relationship of culturable bacterial diversity in the Tattapani Hot Spring. Moreover, the isolates were identified by PCR amplification



of 16S rDNA sequence and identified as *Geobacillus toebii* (PW12), *Geobacillus toebii* (PS4), *Geobacillus kaustophilus* (PW11) and *Geobacillus thermoleovorance* (PW13).

**Morphological and biochemical characteristic features of bacterial isolates :** Water and sludge samples were collected in the month of March, year 2011. Sludge sample was taken underneath water. At the time of sample collection, temperature of the hot spring water was recorded as 70°C and pH6. Tattapani hot spring showed the presence of white precipitates on the surface of water. Accordingly, Tattapani water contains 0.11M salt NaCl, which is ten times more than the tested tap water (0.012 M) of the Shoolini University. By using flame photometer, it was observed that Tattapani water sample contains 1.75 mM potassium ions as compare to 0.5 mM in salty water body and 0.04 mM in tap water (Table 1). All the four bacterial isolates were whitish to creamish in color, positive for Gram's reaction, long rods, non-motile, positive for oxidase, catalase and nitrate reduction test, urease activity was observed only for PW11 and PW12 (Table 2).

**Strict thermophiles and thermo-halotolerant present in the Tattapani Hot Spring :** All the 4 isolates showed growth between 50 - 75°C in LB agar medium with an optimum temperature 70°C (Fig. 1A). Also, detectable growth was observed for all the thermophilic isolates at 75°C within 10 h of incubation, whereas none of the bacterial strains could grow below or at 40°C even when incubated for 72 h. This indicates strict thermophilic nature of the bacterial isolates present in the Tattapani hot spring. However, growth at 37°C was detected for *Bacillus stearothermophilus* and *Bacillus thermoglucosidasius* [27]. Though, the optimum pH for growth was observed at pH 7, but all the isolates showed trace growth even at pH 5 and 8 (Table 3). No detectable growth was observed below pH 5 and above pH 8. Since we detected Na<sup>+</sup> and K<sup>+</sup> ions in the Tattapani hot spring water, we tested the growth of bacterial isolates in LB agar medium supplemented with different

concentrations of either NaCl or KCl (Fig. 1B). It is interesting to note that tap water contain equimolar of Na<sup>+</sup> and K<sup>+</sup> ions, but 7 and 120 fold more Na<sup>+</sup> and K<sup>+</sup> ions respectively, when compared to tap water. On the other hand, saltern water body has 2 fold more Na<sup>+</sup> ions and 3.4 fold less K<sup>+</sup> ions as compared to Hot spring water (Table 1). This is in agreement with the fact that the water isolates PW12 and PW13 could grow in the presence of 0.5 M KCl and only PW12 could grow in the presence of 0.75 M KCl (Table 3 and Fig. 1B). Though the Na<sup>+</sup> ions were detected 50% less in Tattapani water sample as compared to saltern water, none of the bacterial isolates except PW12 could grow in the presence of 0.75 M NaCl. This is surprising that, how only PW12 could grow in the presence of NaCl and KCl and why other bacterial isolates could not grow in the presence

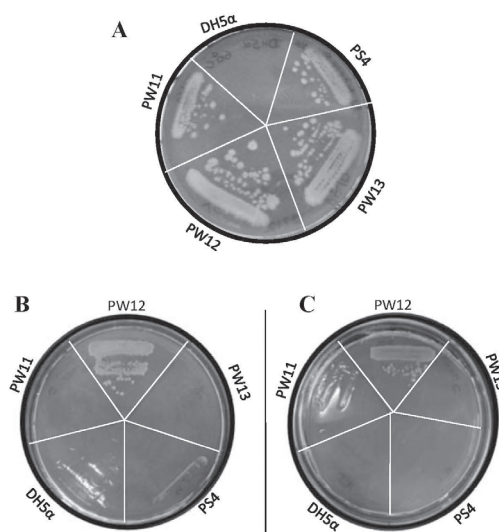


**Fig. 1.** Growth of thermophilic microorganisms. Individual and isolated colonies of different thermophilic microorganisms as indicated were streaked on LB agar medium. Petriplates were incubated at 60°C for 24 h and observed for growth (A). Thermophilic isolates were streaked on LB agar medium containing 0.75M KCl (B) and 0.75 M NaCl(C). Petriplates were incubated at 75°C after 24 h of incubation.

of NaCl and two of them even in the presence of KCl (Table 3). This raises a question whether thermophilic bacteria are present in the dormant stage or the doubling time in the natural habitat is in years. The bacterial isolate PW12 showed growth up to 0.75 M NaCl as well as in the presence of 0.75 M KCl and no growth in the presence of 1M NaCl or KCl. (Fig. 1B and Table 3) and classified as thermo-halotolerant.

**Heavy metal resistance by thermophilic microorganisms:** Thermophilic microorganisms were tested for their growth in minimal M9 medium supplemented with salts for the metal ions, such as Ni<sup>2+</sup>, Ca<sup>2+</sup>, Mn<sup>2+</sup>, Mg<sup>2+</sup>, Zn<sup>2+</sup>, Co<sup>2+</sup>, Cu<sup>2+</sup>, Hg<sup>2+</sup>, Fe<sup>2+</sup>, Cd<sup>2+</sup>. In general, Hg<sup>2+</sup> was most toxic metal ion followed by Cd<sup>2+</sup> (or Ni<sup>2+</sup> in case of PW13). Moreover, certain metal ions such as Ca<sup>2+</sup>, Zn<sup>2+</sup>, and Fe<sup>2+</sup> in case strain PS4; Ni<sup>2+</sup>, Mg<sup>2+</sup>, Zn<sup>2+</sup>, and Fe<sup>2+</sup>, in case strain PW12; and Ca<sup>2+</sup>, Zn<sup>2+</sup>, and Fe<sup>2+</sup> in case of PW13 stimulated the growth in the presence of metal ions as compared to non-metal supplementation growth. Interestingly, growth of strain PS4 was increased in the presence of even 200 ppm Ca<sup>2+</sup>, Mg<sup>2+</sup>, Zn<sup>2+</sup>, and Fe<sup>2+</sup>, whereas the growth of PW12 was inhibited by ~50% in the presence of 200 ppm Ca<sup>2+</sup>, Mg<sup>2+</sup>, Zn<sup>2+</sup>, and Fe<sup>2+</sup>. (Fig. 2A-D)

**Utilization of carbon and nitrogen sources by thermophilic bacterial isolates:** Thermophilic bacterial isolates showed growth in presence of starch, raffinose, trehalose and sucrose, but no detectable growth was observed in the presence lactose, fructose and sorbitol. The best nitrogen source for the growth of all thermophilic bacterial isolate was peptone followed by yeast extract and casein acid hydrolysate. No detectable growth was observed when urea was used as nitrogen source (Table 4).

**Thermophilic isolates of Tattapani are phylogenetically different:** The total genomic DNA of bacterial strains was isolated (Fig. 3A) and subjected to RAPD amplification using random decamer primers (Table. 5). Amplified products were resolved through 1.0% agarose gel electrophoresis as shown in Fig. 3B-F. The size

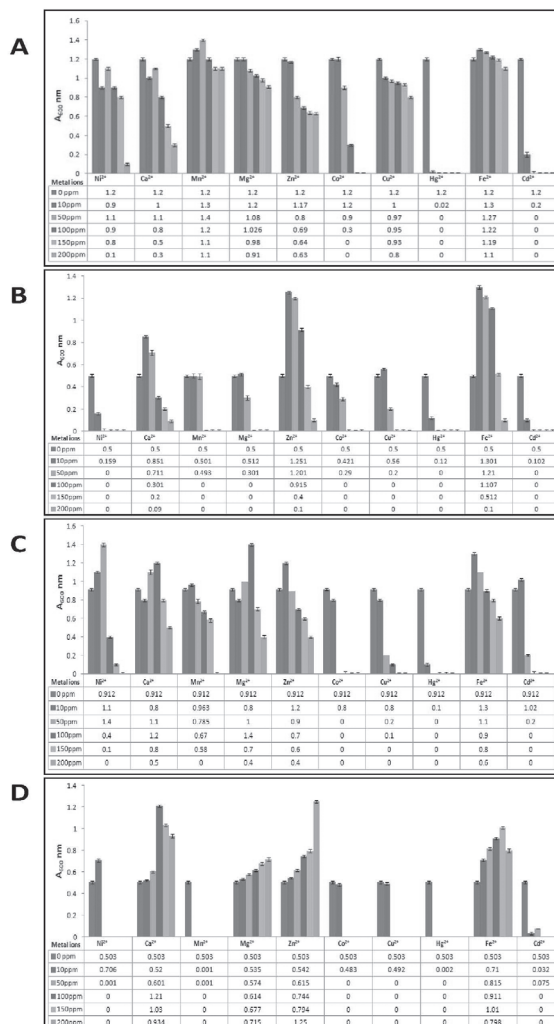


**Fig. 2.** Effect of metal ions on the growth of thermophilic microbial isolates. Minimal M9 liquid medium was supplemented with metal ions (Ni<sup>2+</sup>, Ca<sup>2+</sup>, Mn<sup>2+</sup>, Mg<sup>2+</sup>, Zn<sup>2+</sup>, Co<sup>2+</sup>, Cu<sup>2+</sup>, Hg<sup>2+</sup>, Fe<sup>2+</sup>, Cd<sup>2+</sup>) at 10-200 ppm. Cultures were incubated at 60°C for 24 h and growth was monitored by measuring absorbance at 600 nm and plotted against the various metal ions and their concentration as indicated for *Geobacillus kaustrophilus* strain PW11 (A), *Geobacillus thermoleovorans* strain PW13 (B), *Geobacillus toebii* strain PW12 (C) and *Geobacillus toebii* strain PS4 (D). Minimal M9 medium without metal ion supplementation served as control.

of each band was determined using Alpha imager software and the presence (1) or absence (0) of a particular band was recorded to generate a binary table. The data table was analyzed through the MVSP software. The levels of similarity in the RAPD fingerprints were calculated using Jaccard's correlation coefficient. Cluster analysis was performed using the unweighted pair group method with arithmetic mean (UPGMA). The relationships between the pattern profiles are displayed as dendrograms and expressed as percentage

similarity as shown in Fig. 3G. Primer 1K generated PCR products ranging 250-3000 bp (Fig. 3B), primer 2K as 250-1500 bp (Fig. 3C), primer 14K as 250 – 2000 bp (Fig. 3D), primer 15K as 750 – 2300 bp (Fig. 3E), and primer 25K between 200-1500 bp (Fig. 3F). The large number of polymorphic bands were observed with primer 1K, followed by 15K, 2K, 14K and 25K. The four thermophilic bacterial isolates divides into two groups, bacterial isolate PS4 and PW13 were closely related and isolate PW11 and PW12 are

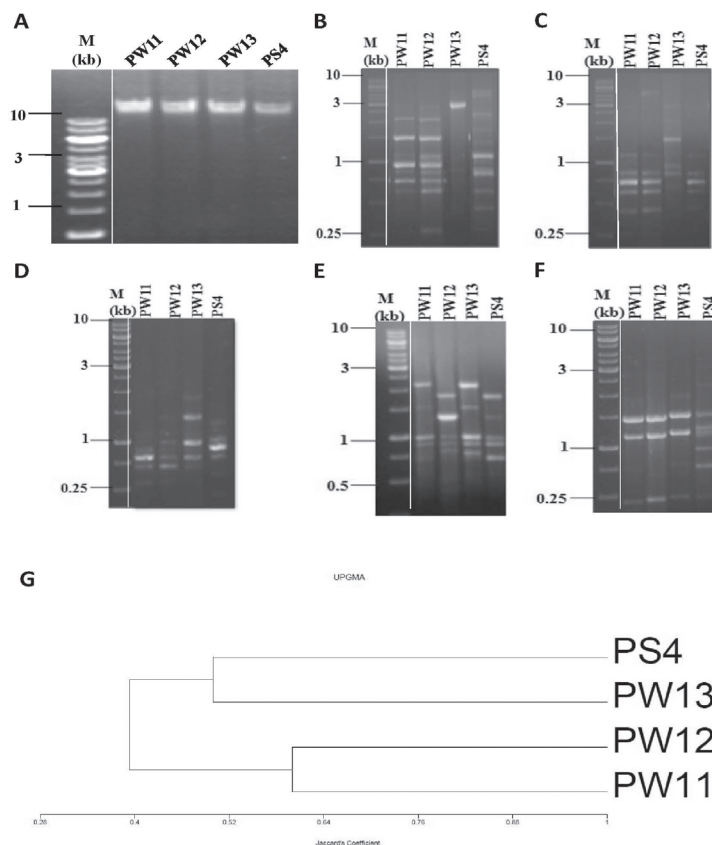


**Fig. 3.** Genomic DNA isolation and RAPD analysis of thermophilic isolates. Total genomic DNA of the thermophilic bacterial isolates as indicated was electrophoresed on 1% agarose gel, followed by staining with ethidium bromide (10 mg/ml) and visualized under gel documentation (A). The genomic DNA of seventeen individual isolates as indicated was subjected to RAPD-PCR amplification by using primer 1K (B), 2K (C), 14K (D), 15 K (E) and 25K (F). Reaction products were electrophoresed on 1.2 % agarose gel and visualized under gel documentation. M indicates the DNA molecular size marker (kb). Dendrogram showing estimated average genetic distance among different thermophilic isolates based on polymorphism generated by RAPD (G). The dendrogram was built using total number of polymorphic bands produced by random primers 1K, 2K, 14K, 15K and 25K.

evolved together (Fig. 3G). PS4, a sludge isolate has evolved with PW13, a water isolate. This is the first study that demonstrated different thermophilic bacterial isolates live in close association in water and sludge of Tattapani hot spring. It is surprising that bacterial isolate PW12 that could grow in the presence of KCl or NaCl evolved together with the bacterial isolates PW11 that could not grow in the presence of KCl or NaCl.

**Geobacillus spp. were predominantly found in the Tattapani Hot Spring :** To identify the bacterial isolates, total genomic DNA of four isolates (PW11, PW12, PW13 and PS4) was subjected to PCR amplification of 16S rDNA using standard set of two primers (Table 5). 16S rDNA amplified a ~1.5. kbs fragment in all the four isolates. Gel purified DNA fragments were sequenced on both the strands, and we obtained 1409, 1410, 1432 and 1421 bp sequence from PS4, PW11, PW12 and PW13 respectively. Similar nucleotide sequences were identified by BLASTN search. The 16S rDNA sequence of identified strains exhibited >95% similarity with the sequences of the bacteria currently assigned to the genus *Geobacillus*. The highest level of sequence similarity of isolates PS4 and PW12 was 99% and 98% respectively with *Geobacillus toebii* SK-1. *Geobacillus toebii* PW12 and *Geobacillus toebii* PS4 form separate and coherent cluster with *Geobacillus toebii* SK-1 [44]. Further, it is interesting that *Geobacillus toebii* PW12 could grow in the presence of up to 0.75 M KCl or 0.75 M NaCl and classified as thermohalotolerant in contrast to *Geobacillus toebii* PS4, which could not even grow in the presence of 0.5 M NaCl or 0.5 M KCl. It was also observed that *Geobacillus toebii* PW12 produces urease, whereas *Geobacillus toebii* PS4 does not produce urease. PW11 and PW13 showed 99% similarity with *Geobacillus kaustophilus* and *Geobacillus thermoleovorance* respectively. *Geobacillus thermoleovorans* PW13 showed 99% similarity with *Geobacillus thermoleovorans* LEH-1[47].

Further, to establish the phylogenetic position of the newly isolated strains, 16S rDNA of PS4, PW11, PW12 and PW13 and the *Geobacillus spp* (isolated from hot springs, compost, geothermal soil, crude oil, gold mine and deep ocean sediments) reported worldwide and reviewed by Daniel [8] were used to construct Phylogenetic tree as shown in Fig 4. The GenBank accession numbers for the reference 16S rDNA gene sequence and the newly isolated strains are shown in Table 6. Phylogenetic analysis of the 47 *Geobacillus spp.* including four newly isolates formed five phylogenetically coherent and discrete groups. *Geobacillus thermoleovorans* PW13 and *Geobacillus toebii* PW12 are closely related to each other and formed independent phylogenetic clad with *Geobacillus Kaue* NB (AF411066.1), as a part of one of the five groups. *Geobacillus toebii* PS4, a sludge isolate formed an independent clad in a separate group. On the other hand, *Geobacillus kaustophilus* PW11 formed a distinct outgroup not related to known *Geobacillus kaustophilus*.

The 16S rDNA sequences of all the bacteria have been submitted to the NCBI GenBank databases under the accession no.KF751757 (*Geobacillus thermoleovorans* strain PW13), accession no.KF751758 (*Geobacillus kaustophilus* strain PW11), accession no.KF751759 (*Geobacillus toebii* strain PS4) and accession no.KJ509869 (*Geobacillus toebii* strain PW12)

*Geobacillus* strain PW11, PW12, PW13 and PS4 are novel subspecies of *Geobacillus*, for which the new names *Geobacillus kaustophilus* PW11, *Geobacillus toebii* PW12, *Geobacillus thermoleovorans* PW13, and *Geobacillus toebii* PS4 respectively are proposed.

#### Discussion

Temperature is one of the hall mark environmental factors that set the limit for the growth of organisms. Exceptionally, certain group of microorganism lives at temperature as high as more than 100°C and are classified as hyperthermophiles. They are present in thermal



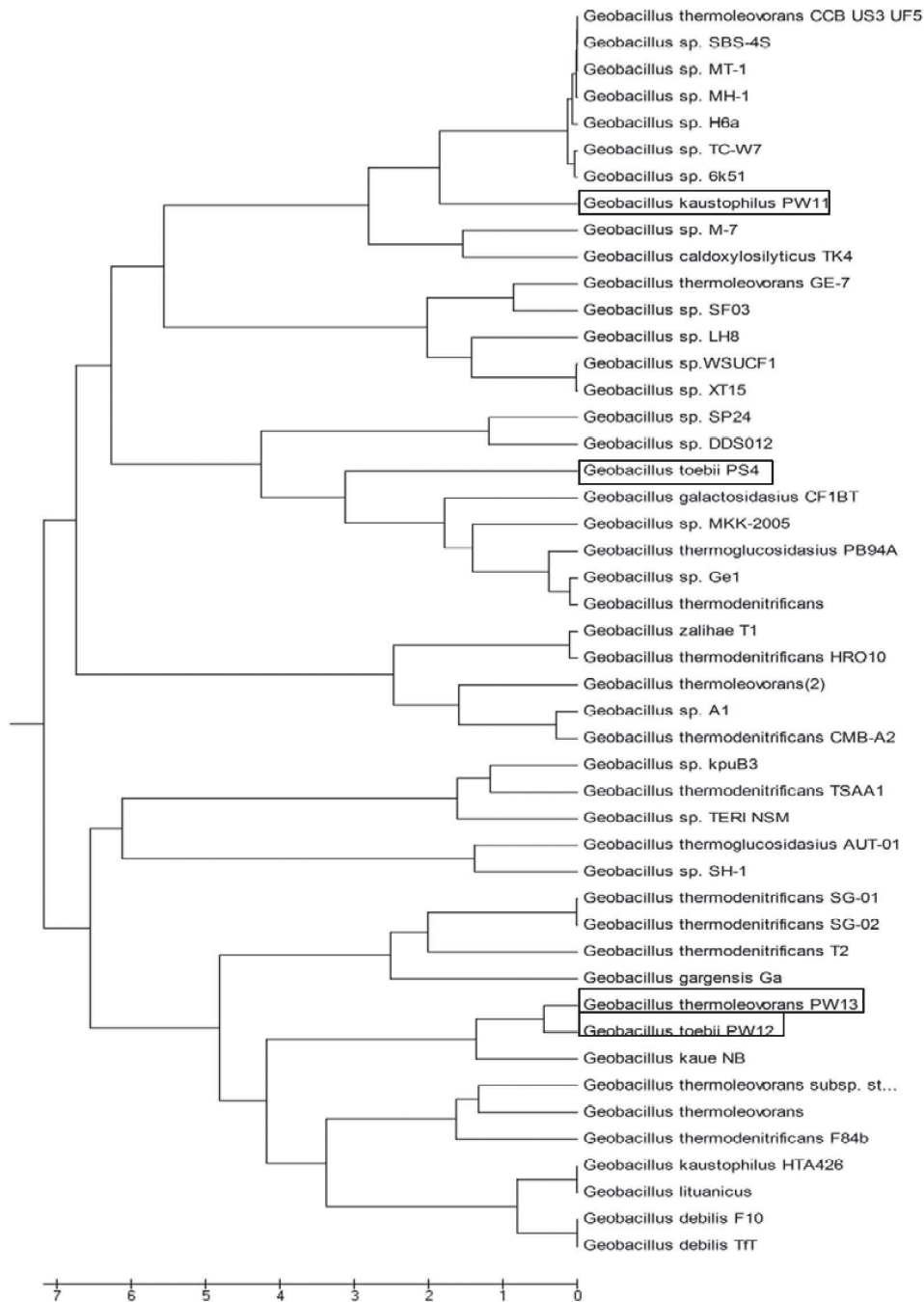


**Fig. 4.** 16S rDNA based dendrogram of *Geobacillus* sp. Dendrogram showing phylogenetic relationship of newly isolated *Geobacillus* sp. from all over the world.

**Table 1.** Estimation of Na<sup>+</sup> and K<sup>+</sup> ions in water sample of Tattapani hot spring

Method	Tattapani Hot spring water	Tap water
Conductivity meter	0.11 M NaCl	0.014 M NaCl
Volumetric analysis	0.12 M NaCl	0.013 M NaCl
Flame photometer	0.11 M Na <sup>+</sup> ions 1.7 mM K <sup>+</sup> ions	0.013 M Na <sup>+</sup> ions 0.014 mM K <sup>+</sup> ions

**Table 2.** Biochemical characteristics of thermophilic isolates

Strain	Colour	Shape	Gram's staining	Catalase	Oxidase	Nitrate	Urease	Motility
PW11	Creamish	Long rods	+	+	+	+	+	-
PW12	Creamish	Long rods	+	+	+	+	+	-
PW13	Creamish	Long rods	+	+	+	+	-	-
PS4	Whitish	Long rods	+	+	+	+	-	-

**Table 3.** Effect of physical parameters on growth of thermophilic isolates.

Isolate	Growth Temperature (°C)					Growth pH					Growth in presence of salts					
											NaCl (M)			KCl (M)		
	40	50	60	70	75	5	6	7	8	9	0.5	0.75	1	0.5	0.75	1
PW11	-	+	++	+++	+++	+	++	+++	+++	-	-	-	-	-	-	-
PW12	-	+	++	+++	+++	+	+++	+++	++	-	+++	++	-	++	+++	-
PW13	-	+	++	+++	+++	+	+++	+++	++	-	-	-	-	++	-	-
PS4	-	+	++	+++	+++	+	++	+++	+	-	-	-	-	-	-	-
DH5α	+	-	-	-	-	-	-	-	-	-	-	-	-	-	-	-

Plus (+) sign indicate the visible difference in the size of individual and isolated colony, when streaked on LB agar medium, minus (-) sign indicate no detectable growth. Three plus (+++) signs are indicative of more visible growth as compare to two plus (++) signs

**Table 4.** Utilization of carbon and nitrogen sources by thermophilic isolates.

Isolate	Basal M9	M9 medium + 1% carbon source						M9 medium + 0.5% nitrogen source		
	Glucose + NH <sub>4</sub> Cl	Lactose/ Fructose/ Sorbitol	Galactose	Raffinose	Starch	Trehalose	Sucrose	Beaf extract/ Urea	Yeast extract/ Casein acid hydrolysate	Peptone
PW11	-	-	+	++++	++++	+++	++	-	++	+++
PW12	-	-	+	+++	+++	++++	+++	-	+	+++
PW13	-	-	+	+++	+++	++++	++++	-	++	+++
PS4	-	-	+	+++	+++	++++	++	-	++	+++
Isolate	Basal M9	M9 medium + 1% carbon source						M9 medium + 0.5% nitrogen source		
	Glucose + NH <sub>4</sub> Cl	Lactose/ Fructose/ Sorbitol	Galactose	Raffinose	Starch	Trehalose	Sucrose	Beaf extract/ Urea	Yeast extract/ Casein acid hydrolysate	Peptone
PW11	-	-	+	++++	++++	+++	++	-	++	+++
PW12	-	-	+	+++	+++	++++	+++	-	+	+++
PW13	-	-	+	+++	+++	++++	++++	-	++	+++
PS4	-	-	+	+++	+++	++++	++	-	++	+++

Plus (+) sign indicate the visible difference in growth of thermophilic isolates, when streaked on M9 agar medium supplemented with carbon and nitrogen sources, minus (-) sign indicate no detectable growth. Four plus (++++) signs are indicative of more visible growth as compared to three plus (+++), which is more than two plus (++) signs.

**Table 5.** Primers used in the current study

S. No.	Name	Sequence (5'-3')	Length (nt)	Tm (°C)	Reference
1	1K	CAGGCCCTTC	10	40	This study
2	2K	TGCCGAGCTG			
3	14K	TTCGAGCCAG			
4	15K	GATGACCGCC			
5	25K	GTCGCCGTCA			
6	27F	AGAGTTTGATCTGGCTCAG	19	45	Lane et al, 1991
7	1492R	ACCTTGTTACGACTT	15		

"nt" nucleotides



**Table 6.** Worldwide distribution of *Geobacillus sp* [30]

Geographic location	Isolation source	Isolate name	Gene bank acc. no
Germany	Agricultural produce (bast fiber)	<i>Geobacillus thermoglucosidasius</i> strain PB94A	FJ491390.1
Japan	Compost	<i>Geobacillus sp. kpuB3</i>	AB292801.1
Japan	Compost	<i>Geobacillus thermodenitrificans</i> strain TSAA1	JX262152.1
U.S.A.	Compost	<i>Geobacillus sp. WSUCF1</i>	GU289510.1
Italy	Compost	<i>Geobacillus galactosidasius</i> strain CF1BT	AM408559.1
India	Crude oil (paraffinic)	<i>Geobacillus sp. TERI NSM</i>	EF199739.2
Mariana Trench	deep ocean sediment (10,897 m)	<i>Geobacillus kaustophilus</i> HTA426	NR_074989.1
USA (Yellowstone NP)	Geothermal soil	<i>Geobacillus sp. M-7</i>	FJ896054.1
Italy	Geothermal soil	<i>Geobacillus sp. A1</i>	HM776457.1
Greece	Geothermal soil, sediment, seawater	<i>Geobacillus sp. SP24</i>	JN692241.2
South Africa	Gold mine (50°C water)	<i>Geobacillus thermoleovorans</i> strain GE-7	AY450926.1
China	Hot spring	<i>Geobacillus sp. TC-W7</i>	GQ866911.1
Iran	Hot spring	<i>Geobacillus sp. MKK-2005</i>	DQ309334.1
Iran	Hot spring	<i>Geobacillus sp. LH8</i>	DQ192572.1
Malaysia	Hot spring	<i>Geobacillus thermoleovorans</i> CCB_US3_UF5	NR_074931.1
USA (Montana)	Hot spring	<i>Geobacillus thermoglucosidasius</i> strain AUT-01	JGU356031.1
Pakistan	Hot spring	<i>Geobacillus sp. SBS-4S</i>	AB306519.1
Turkey	Hot spring	<i>Geobacillus caldoxylosilyticus</i> strain TK4	AY248718.1
Turkey	Hot spring	<i>Geobacillus kaue</i> strain NB	AF411066.1
Turkey	Hot spring	<i>Geobacillus sp. Ge1</i>	HE613733.2
Russia	Hot spring (microbial mat)	<i>Geobacillus gargensis</i> strain Ga	NR_115167.1
China	Hot spring	<i>Geobacillus sp. 6k51</i>	DQ141699.1
Thailand	Hot spring	<i>Geobacillus sp. H6a</i>	EU248957.1
Pacific Ocean	Hydrothermal field	<i>Geobacillus sp. MT-1</i>	DQ288898.1
Canada	Compost (manure)	<i>Geobacillus thermodenitrificans</i> strain CMB-A2	GQ293454.1
Turkey	Oil well (pipeline sediment)	<i>Geobacillus thermodenitrificans</i> subsp. <i>calidus</i> strain F84b	EU477773.2
China	Oil well (production water)	<i>Geobacillus sp. SH-1</i>	DQ839487.1
China	Oil well (production water)	<i>Geobacillus sp. XT15</i>	HQ891030.1
Japan	Deep subterranean	<i>Geobacillus thermoleovorans</i>	AB034902.1

	petroleum reservoir		
Lithuania	Oilfield	<i>Geobacillus lituanicus</i>	AY044055.1
China	Oilfield reservoir (deep subterranean)	<i>Geobacillus sp. MH-1</i>	FJ874632.1
Singapore	Sewage sludge	<i>Geobacillus sp. SF03</i>	AY327448.1
U.K.	Silage (Italian rye grass)	<i>Geobacillus sp. DDS012</i>	EF426762.1
Germany	Soil	<i>Geobacillus thermodenitrificans HRO10</i>	AJ785764.1
Northern Ireland	Soil	<i>Geobacillus debilis strain F10</i>	AJ564608.1
Northern Ireland	Soil	<i>Geobacillus debilis strain Tft</i>	AJ564616.1
Iran	Soil	<i>Geobacillus zalihae strain T1</i>	AY166603.1
Taiwan	Sugar refinery wastewater	<i>Geobacillus thermoleovorans</i>	AY074879.1
South Korea	Wood chips composted with swine manure	<i>Geobacillus thermodenitrificans strain SG-01</i>	FJ481105.1
South Korea	Wood chips composted with swine manure	<i>Geobacillus thermodenitrificans strain SG-02</i>	FJ481104.1
Japan	Hot spring	<i>Geobacillus thermodenitrificans</i>	AB546234.1
China	Hot spring	<i>Geobacillus thermodenitrificans strain T2</i>	EF570295.1
India	Hot spring (current study)	<i>Geobacillus kaustophilus strain PW11</i>	KF751758.1
India	Hot spring (current study)	<i>Geobacillus thermoleovorans strain PW13</i>	KF751757.1
India	Hot spring (current study)	<i>Geobacillus toebii strain PW12</i>	KJ509869.1
India	Hot spring (current study)	<i>Geobacillus toebii strain PS4</i>	KF751759.1

hot springs, volcanic areas, geothermal vents and mud holes, and solfataric fields [31]. Extremophiles are a valuable source of industrially important novel biocatalysts [32, 33] and has been reviewed [34, 35, 36, 37]. There is a great need to explore the different geographical regions that may be occupied with microbes with varied biotechnological potential. We isolated four thermophilic bacterial strains from water and sludge sample of un-explored Tattapani Hot spring, situated in Himachal Pradesh. Thermophiles can be generally classified as moderate thermophiles (growth optimum 50-60°C), extreme thermophiles (growth optimum 60-80°C) and hyperthermophiles

(growth optimum 80-110°C) [38]. Bacterial strains isolated in the current study could grow optimally between 60-75°C and are classified as extreme thermophiles (Table 3). Hyperthermophilic bacterial isolates PW11, PW13, and PS4 have been previously shown to produce metal inducible and extracellular amylase activity (39). Moreover, PW12 showed growth in medium supplemented with 0.75 M NaCl and 0.75 M KCl, suggesting a halotolerant nature of the strain.

There have been few studies involving RAPD-PCR of thermophilic bacteria isolated from Hot Springs. In the current study, four thermophilic bacterial strains were studied for their biochemical

characteristics and phylogenetic relationship. 16S rRNA gene sequences analysis has been widely used when designating the phylogenetic position of prokaryotic organisms and constitute the basis of the modern bacterial taxonomy [40]. Gram positive, rod-shaped, endospore-forming thermophilic bacilli grouped into the genus *Geobacillus* [27].

Thermophilic bacteria related to the genus *Geobacillus* have been widely isolated from geothermal and man-made environments throughout the world [41, 42, 43]. Eight *Geobacillus* spp. have been isolated from Jordanian hot springs. Optimal temperature for growth of the isolates was 60 to 65°C and the optimal pH was 6 to 8. Maximal homology of all eight isolates to genus *Geobacillus* was observed. Five of these isolates showed greater than 98% homology with *Geobacillus stearothermophilus* and one isolate showed 100% homology with *Geobacillus thermoglucosidasii* [44].

*Geobacillus* spp. was predominantly found in the Tattapani Hot Spring, which remained unexplored. Till date, there is no report on the isolation and characterization of microorganisms from Tattapani Hot Spring as reviewed by Daniel et al [30]. 16SrDNA gene sequencing results revealed that all the four bacterial isolates showed >95% similarity with *Geobacillus* sp. Thermohalophiles have adapted the combination of environmental stresses. *Halothermothirx orenii* is a strictly anaerobic thermohalophilic bacterium isolated from sediment of a Tunisian salt lake. It grows optimally at 60°C (maximum of 70°C) with 10% NaCl [45]. In present study *Geobacillus toebii* PW12 isolate shows growth upto 75°C and in presence of 4.2% NaCl as well as 5.4% KCl. *Geobacillus toebii* PW12 is very unique in terms of growth in presence of NaCl and KCl.

Thermophilic water isolates *G. toebii* strain PW12 is a thermo-halotolerant, whereas *G. toebii* strain PS4 isolated from sludge do not grow in the presence of NaCl or KCl. The effects of heavy metals (Ni<sup>2+</sup>, Zn<sup>2+</sup>, Co<sup>2+</sup>, Hg<sup>2+</sup>, Mn<sup>2+</sup>, Cr<sup>6+</sup>, Cu<sup>2+</sup>, Fe<sup>3+</sup> and Cd<sup>2+</sup>) on microorganism growth were studied at concentrations ranging from 10-200

ppm. The isolation of heavy metal resistant microorganisms and the understanding of the mechanisms they use in order to remove this kind of pollutants may contribute to the development of improved detoxification processes. A novel subspecies of *Geobacillus toebii* (*Geobacillus toebii* subsp. *decanicus*) was isolated by Poli et al [46]. It grows at temperatures between 55–75°C, utilize hydrocarbon and showed resistance to heavy metals. Most of the microorganism isolated in the current study showed resistance to all heavy metals tested during the growth and only Cd<sup>2+</sup> and Zn<sup>2+</sup> caused a decrease in growth when added even at 10 ppm concentrations. Two strains of thermophilic bacteria, *Geobacillus thermantarcticus* and *Anoxybacillus amylolyticus*, were employed to investigate the biosorption of heavy metals including Cd<sup>2+</sup>, Cu<sup>2+</sup>, Co<sup>2+</sup>, and Mn<sup>2+</sup> ions [47]. Ozdemir et al [30] studied the biosorption of Cd<sup>2+</sup>, Cu<sup>2+</sup>, Ni<sup>2+</sup>, Mn<sup>2+</sup> and Zn<sup>2+</sup> by *Geobacillus toebii* sub-species *decanicus* and *Geobacillus thermoleovorans* sub-species *Stromboliensis* [48]. Thermophilic isolates from Tattapani hot spring showed resistance to various heavy metal ions such as Co<sup>2+</sup>, Zn<sup>2+</sup>, Cd<sup>2+</sup>, Cu<sup>2+</sup>, and Mn<sup>2+</sup>, whereas the growth of all the four isolates was inhibited in the presence of Hg<sup>2+</sup>. More recently, Sharma et al [49] identified thermophilic *Flavobacterium* and *Anoxybacillus* from Unexplored Tattapani Hot spring situated of North Western Himalayas. In a different study, thermophile diversity and ecology of microbial mat samples collected from the iron rich hot springs of Brandvlei and Calitzdorp was studied for the first time [50]. In conclusion, the newly isolated *Geobacillus* spp. from the unexplored Tattapani hot spring helps in understanding the *Geobacillus* spp. biodiversity in different geographical regions and their evolutionary relationship with other *Geobacillus* isolated from the rest of the World. Recently, polygenomic studies showed that the genus *Geobacillus* consists of two distinct genera, viz., major *Geobacillus* and minor *Parageobacillus* [51]. The *G. toebii* PW12 reported in the current study is more closely related to *Parageobacillus* and hence named as *Parageobacillus toebii* PW12. Most recently, Sharma et al [52] has

sequenced the genome of hyper thermophilic, halotolerant *Parageobacillus toebii* PW12 with genome size of 3,210,377 bp. The genome of *Parageobacillus toebii* PW12 showed G+C content of 42.05%, and 3,382 coding sequences (CDS), 80 tRNAs, 5 noncoding RNAs (ncRNAs), and 4 CRISPR arrays were predicted.

#### Acknowledgement

The authors are thankful to Shoolini University, Solan for providing financial and infrastructural support for this study.

#### Conflict of interest

The authors declare no financial or commercial conflict of interest.

#### References

- [1] Waring, G.A. (1965). Thermal springs of the United States and other countries of the World. A summary. Geological Survey Professional paper 492 revised by R. R. Blankenship and R. Bentall, US Government Printing Office, Washington, D.C.
- [2] Bergquist, P.C., Morgan, H. W. (1992). The molecular genetics and biotechnological application of enzyme from extremely thermophilic eubacteria. In: Herbert, R.A., Sharp, R. J., (Eds) Molecular biology and biotechnology of extremophiles, Chapman and Hall, New York, pp. 44–45.
- [3] Lama, L., Calandrelli, V., Gambacorta, A., Nicolaus, B. (2004). Purification and characterization of thermostable xylanase and beta-xylosidase by the thermophilic bacterium *Bacillus thermantarcticus*. *Research in Microbiology*, 155: 283–289.
- [4] Schallmeyer, M., Singh, A., Ward, O. P. (2004). Developments in the use of *Bacillus* species for industrial production. *Canadian Journal of Microbiology*, 50: 1–17.
- [5] Baross, J. A. (1998). Do the geological and geochemical records of the early Earth support the prediction from global phylogenetic models of a thermophilic cenancestor? In Wiegel, J., Adams, M. W. W., (ed.) *Thermophiles: The Keys to Molecular Evolution and the Origin of Life*, Taylor & Francis, Inc., Philadelphia, PA, pp. 3–18.
- [6] Schwartzman, D. W. (1998). Life was thermophilic for the first two-thirds of Earth history, In Wiegel, J., Adams, M. W. W., (ed.) *Thermophiles: The Keys to Molecular Evolution and the Origin of Life*, Taylor & Francis, Inc., Philadelphia, PA, pp. 33–43.
- [7] Hugenholtz, P., Pitulle, C., Hershberger, K. L., Pace, N. R. (1998). Novel division level bacterial diversity in a Yellowstone hot spring. *Journal of Bacteriology*, 180: 366–376.
- [8] Reysenbach, A. L., Ehringer, M., Hershberger, K. (2000). Microbial diversity at 83°C in Calcite Springs, Yellowstone National Park: another environment where the Aquificales and Korarchaeota coexist. *Extremophiles*, 4: 61–67.
- [9] Blank, C. E., Cady, S. L., Pace, N. R. (2002). Microbial composition of near-boiling silica-depositing thermal springs throughout Yellowstone National Park. *Applied and Environmental Microbiology*, 68: 5123–5135.
- [10] Meyer-Dombard, D. R., Shock, E. L., Amend, J. P. (2005). Archaeal and bacterial communities in geochemically diverse hot springs of Yellowstone National Park, USA. *Geobiology*, 3: 211–227.
- [11] Perevalova, A. A., Kolganova, T. V., Birkeland, N. K., Schleper, C., Bonch-Osmolovskaya, E. A., Lebedinsky, A. V. (2008). Distribution of Crenarchaeota representatives in terrestrial hot springs of Russia and Iceland. *Applied and Environmental Microbiology*, 74: 7620–7628.
- [12] Kvist, T., Ahring B. K., Westermann, P. (2007). Archaeal diversity in Icelandic hot springs. *FEMS Microbiology Ecology*, 59: 71–80.



- [13] Takai K., Sako, Y. A. (1999). Molecular view of archaeal diversity in marine and terrestrial hot water environments. *FEMS Microbiology Ecology*, 28: 177–188.
- [14] Kato, S., Itoh T., Yamagishi, A. (2011). Archaeal diversity in a terrestrial acidic spring field revealed by a novel PCR primer targeting archaeal 16S rRNA genes. *FEMS Microbiology Letters*, 319: 34–43.
- [15] Kanokratana, P., Chanapan, S., Pootanakit K., Eurwilaichitr, L. (2004). Diversity and abundance of Bacteria and Archaea in the BorKhlueng Hot Spring in Thailand. *Journal of Basic Microbiology*, 44: 430–444.
- [16] Childs, A. M., Mountain, B. W., Toole R. O., Stott, M. B. (2008). Relating microbial community and physicochemical parameters of a hot spring: champagnepool, wai-o-tapu, New Zealand. *Geomicrobiology Journal*, 25: 441–453.
- [17] Song, Z. Q., Chen J. Q., Jiang, H. C. (2010). Diversity of Crenarchaeota in terrestrial hot springs in Tengchong, China. *Extremophiles*, 14: 287–296.
- [18] Sharma, B., Verma, R., Dev, K., Thakur, R. (2012). Molecular characterization of Manikaran hot spring microbial community by 16S rRNA and RAPD analysis. *Biotechnology An Indian Journal*, 6: 254–266.
- [19] Rainey, F. A., Fritze, D., Stackebrandt, E. (1994). The phylogenetic diversity of thermophilic members of the genus *Bacillus* as revealed by 16S rDNA analysis. *FEMS Microbiology Letters*, 115: 205–212.
- [20] Ronimus, R. S., Parker, L. E., Turner, N., Poudel, S., Ruckertand, A., Morgan, H. W. (2003). A RAPD-based comparison of thermophilic bacilli from milk powders. *International Journal of Food Microbiology*, 85: 45–61.
- [21] Obeidat, M., Khyami-Horani, H., Al-Zoubi, A., Otri, I. (2012). Isolation, characterization and hydrolytic activities of *Geobacillus* species from Jordanian hot springs. *African Journal of Biotechnology*, 11: 6763–6768.
- [22] Ahmet, A., Kadriye, I., Fikretin, S., Tulin, A., Medine, G., Ali O. B., Ozlem, B. (2011). Molecular diversity of thermophilic bacteria isolated from Pasinler hot spring (Erzurum, Turkey). *Turkish Journal of Biology*, 35: 267–274.
- [23] Greenberg, A. E., Clesceri, L. S., Eaton, A. D. (1992). Standard method for the examination of water and waste water, 18<sup>th</sup> edition published jointly by APHA, AWWA, and WPCF, Wasington DC.
- [24] Smibert, R. M., Krieg, N. R. (1994). Phenotypic characterization. In: Gerhardt P., Murray R.G., Wood W.A., Krieg N.R., (eds) *Methods for General and Molecular Bacteriology. American Society for Microbiology*, Washington DC, 5: 611–654.
- [25] Sambrook, J., Fritsch, E. F., Maniatis, T. (1989). *Molecular cloning: A laboratory Manual*. II edn. Cold Spring Harbour Laboratory, Cold Spring Harbour, N.Y.
- [26] Jiang, H., Dong, H., Zhang, G., Yu, B., Chapman, L. R., Fields, M. W. (2006). Microbial Diversity in Water and Sediment of Lake Chaka, an Athalassohaline Lake in Northwestern China. *Applied and Environmental Microbiology*, 72: 3832–3845.
- [27] Nazina, T. N., Tourova, T. P., Poltarau, A. B., Novikova, E. V., Grigoryan, A. A., et al., (2001). Taxonomic study of aerobic thermophilic bacilli: descriptions of *Geobacillus subterraneus* gen. nov., sp. and *Geobacillus uzenensis* sp. nov. from petroleum reservoirs and transfer of *Bacillus stearothersophilus*, *Bacillus thermocatenulatus*, *Bacillus thermoleo-vorans*, *Bacillus kaustophilus*, *Bacillus thermoglucosidasius* and *Bacillus thermodenitrificans* to

- Geobacillus* as the new combinations *G. stearothermophilus*, *G. thermocatenulatus*, *G. thermoleovorans*, *G. kaustophilus*, *G. thermoglucosidasius* and *G. thermodenitrificans*. *International Journal of Systematic and Evolutionary Microbiology*, 51: 433–446.
- [28] Sung, M. H., Kim, H., Bae, J. W., Rhee, S. K., Jeon, C. O., Kim, K., Kim, J. J., *et al.*, (2002). *Geobacillustoebii* sp. nov., a novel thermophilic bacterium isolated from hay compost. *International Journal of Systematic and Evolutionary Microbiology*, 52: 2251–2255.
- [29] Zarilla, K. A., Perry, J. J. (1987). *Bacillus thermoleovorans* sp. nov., a species of obligately thermophilic hydrocarbon utilizing endospore-forming bacteria. *Systematic and Applied Microbiology*, 9: 258–264.
- [30] Daniel, R. Z. (2014). The *Geobacillus* paradox: why is a thermophilic bacterial genus so prevalent on a mesophilic planet? *Microbiology*, 160: 1–11.
- [31] Huber, R., Huber, H., Stetter, K. O. (2000). Towards the ecology of hyperthermophiles: biotopes, new isolation strategies and novel metabolic properties. *FEMS Microbiology Reviews*, 24: 615–623.
- [32] Herbert, R. A. (1992). A perspective on the biotechnological potential of extremophiles. *Trends in Biotechnology*, 10: 395–402.
- [33] Madigan, M. T., Mairs, B. L. (1997). Extremophiles. *Scientific American*, 276: 82–87.
- [34] Adams, M. W. W., Perler, F. B., Kelly, R. M. (1995). Extremozymes: Expanding the limits of biocatalysis. *Nature Biotechnology*, 13: 662–668.
- [35] Demiorijan, D. C., Moris-Varas, F., Cassidy, C. S. (2001). Enzymes from extremophiles. *Current Opinion in Chemical Biology*, 5: 144–151.
- [36] Eichler, J. (2001). Biotechnological uses of archaeal extremozymes, *Biotechnology Advances*, 19: 261–278.
- [37] Fujiwara, S. (2002). Extremophiles: Developments of their special functions and potential resources. *Journal of Bioscience and Bioengineering*, 94: 518–525.
- [38] Baker, G., Gaffar, S., Cowan, D. A., Suharto, A. R. (2001). Bacterial community analysis of Indonesian hot springs. *FEMS Microbiology Letters*, 200: 103–109.
- [39] Sharma, P., Gupta, S., Sourirajan, A., Dev, K. (2015). Characterization of Extracellular thermophilic amylase from *Geobacillus* sp. Isolated from Tattapani Hot Spring of Himachal Pradesh, India, *Current Biotechnology*, 4 (2): 202–209.
- [40] Stackebrandt, E., Goebel, B. M. (1994). Taxonomic note: A place for DNA-DNA reassociation and 16S rRNA sequence analysis in the present species definition in bacteriology. *International Journal of Systematic Bacteriology*, 44: 846–849.
- [41] Maugeri, T. L., Gugliandolo, C., Caccamo, D., Panico, A., Lama, L., Gambacorta, A., Nicolaus, B., A. (2002). halophilic thermotolerant *Bacillus* isolated from a marine hot spring able to produce a new exopolysaccharide. *Biotechnology Letters*, 24: 515–519.
- [42] Nazina, T. N., Sokolova, D. S., Grigoryan, A. A., Shestakova, N. M., Mikhailova, E. M., *et al.*, (2005). *Geobacillusjurassicus* sp. nov., a new thermophilic bacterium isolated from a high-temperature petroleum reservoir and validation of the *Geobacillus* species. *Systematic and Applied Microbiology*, 28: 43–53.
- [43] Rhee, S. K., Jeon, C. O., Bae, J. W., *et al.*, (2002). Characterization of *Symbiobacteriumtoebii*, an obligate commensal thermophile isolated from compost. *Extremophiles*, 6: 57–64.
- [44] Obeidat, M., Khyami-Horani, H., Al-Zoubi, A., Otri, I. (2012) Isolation characterization and hydrolytic activities of *Geobacillus*

- species from Jordanian hot springs. *African Journal of Biotechnology*, 11: 6763–6768.
- [45] Mavromatis, K., Ivanova, N., Anderson, I., Lykidis, A., Hooper, S. D., *et al.*, (2009). Genome Analysis of the Anaerobic Thermohalophilic Bacterium *Halothermothrixorenia*. *PLoS ONE*, 4: e4192.
- [46] Poli, A., Romano, I., Caliendo, G., Nicolaus, G., Orlando, P., *et al.* (2006) *Geobacillus toebii* sub sp. *decanicus* sub sp. nov., a hydrocarbon-degrading, heavy metal resistant bacterium from hot compost. *The Journal of General and Applied Microbiology*, 52: 223–234.
- [47] Ozdemir, S., Kilinc, E., Poli A., Nicolaus, B. (2013). Biosorption of Heavy Metals ( $Cd^{2+}$ ,  $Cu^{2+}$ ,  $Co^{2+}$ , and  $Mn^{2+}$ ) by thermophilic bacteria, *Geobacillus sthermantarcticus* and *Anoxybacillus amylolyticus*: Equilibrium and Kinetic Studies. *Annals of Microbiology*, 17: 86–96.
- [48] Ozdemir, S., Kilinc, E., Poli, A., Nicolaus B., Guven, K. (2009). Biosorption of Cd, Cu, Ni, Mn and Zn from aqueous solutions by thermophilic bacteria, *Geobacillus toebii* sub sp., *decanicus* and *Geobacillus thermoleovorans* sub sp. *stromboliensis*: Equilibrium, kinetic and thermodynamic studies. *Chemical Engineering Journal*, 152: 195–206.
- [49] Sharma, S., Sharma, P., Sourirajan, A., Baumler, D.J., Dev, K. (2018). Identification of Thermophilic *Flavobacterium* and *Anoxybacillus* in Unexplored Tatapani Hot spring of Kishtwar District of Jammu and Kashmir: A North Western Himalayan State. *Current Trends in Biotechnology and Pharmacy*, 12: 245-256.
- [50] Selvarajanm R., Sibanda, T., Tekere, M. (2018) Thermophilic bacterial communities inhabiting the microbial mats of “indifferent” and chalybeate (iron rich) thermal springs: Diversity and biotechnological analysis. *Microbiology open*, 7: e00560.
- [51] Aliyu, H., Lebre, P., Blom, J., Cowan, D., De Maayer, P. (2016) Phylogenomic re-assessment of the thermophilic genus *Geobacillus*. *Syst Appl Microbiol* 39:527–533. doi:10.1016/j.syapm. 2016.09.004
- [52] Sharma, P., Gupta, S., Sourirajan, A. Baumler, D.J., Dev, K. (2019). Draft Genome sequence of hyper thermophilic, halotolerant *Parageobacillus toebii* PW12 isolated from Tattapani hot spring of North West Himalayas. *Microbiology Resource Announcement*, 8 (4), e01163-18. DOI: 10.1128/MRA.01163-18.



## Differential Loss of ROS homeostasis and activation of anti oxidative defense response in tea cultivar due to aluminum toxicity in acidic soil

Sanjenbam Sanjibia Devi<sup>1</sup>, Bedabrata Saha<sup>1</sup>, Sanjib Kumar Panda<sup>1,\*</sup>

<sup>1</sup>Department of Life Science and Bioinformatics, Assam University, Silchar-788011, India

\*Corresponding Author : drskpanda@gmail.com

### Abstract

Tea plant is best known as an economically important crop, environment hardy and an Al hyper accumulator. North East India forms one of the largest tea producing regions of the world but 90% of its soil is acidic. Acidic soil has got major influence on overall crop production, hence it is of utmost necessity to understand the mechanisms of tea plant to adapt to such inhospitable conditions. Through this present investigation we try to understand the changes after exposure to various Al concentrations in TS462 clone of *Camellia sinensis* [L.] in hydroponic solution. The repercussions were measured in terms of generation of reactive oxygen species (ROS) and anti-oxidative enzyme activity in both root and shoot tissues of tea plant. When rooted tea cuttings were raised in hydroponic culture containing 50µm, 250µm and 500µm of Al for 60 days, a constant increase in uptake of Al by roots with the increase dose was observed. The increase in Al uptake with dose, corroborated with the production of super oxide anion ( $O_2^-$ ) hydrogen peroxide ( $H_2O_2$ ) and malondialdehyde (MDA). These all repercussions led to an increment in activity of antioxidant machinery during the study showing that better antioxidative response is behind the relatively better tolerance capability of tea plants.

**Keywords:** *Camellia sinensis* (L.), Aluminum, acid soil, Reactive oxygen species, antioxidant

### Introduction

Landscape of India is dotted with both acidic

and alkaline soils. pH is one of the important chemical property of soil that regulates the normal growth of plants. Soil in North Eastern states of India is characterized by low pH which when culminates with high concentration of Al, restricts plant growth and development due to the formation of complexes with intracellular substances and hence suppressing the plant metabolism (1). Reactive oxygen species (ROS) is induced by Al toxicity at low pH in plants and it is accompanied with the increase of lipid peroxidation. Plant root tips are typically the primary site of oxidative damage. Oxidative stress is the production of elevated amount of reactive oxygen species (ROS) including the hydrogen peroxide ( $H_2O_2$ ), super oxide anion ( $O_2^-$ ) hydroxyl radical ( $\cdot OH$ ) (2). Scavenging or detoxification of excess ROS is accompanied by an efficient antioxidative system consisting of non- enzymatic and enzymatic antioxidants. Ascorbate (AsA) glutathione (GSH), carotenoids, tocopherols and phenolic compounds serves as a potent non-enzymatic anti-oxidants within the cells. The enzymatic antioxidants includes catalase (CAT), superoxide dismutase (SOD), guaiacol peroxidase (GPX), enzymes of ascorbate-guthathione cycle (AsA-GSH) cycle such as ascorbate peroxidase (APX), glutathione reductase (GR), dehydro-ascorbate reductase (DHAR) and monodehydro-ascorbate reductase (MDHAR) (3). Due to multi-functional activity of ROS, it is necessary to control the levels of ROS for the cells tightly to avoid any oxidative damage and not to eliminate them completely (4).

Various studies has reported the increase of various antioxidant enzyme activities in plants is to combat oxidative stress induced by diverse environmental stressors. Increase in tolerance capacity of plants under stressed condition is correlated to the maintenance of a high antioxidant capacity to scavenge the toxic ROS (7; 8).

### Materials and methods

#### **Sample collection and hydroponic condition**

The cutting of TS462 variety of *Camellia sinensis* L.(O) of uniform age of one and half years were procured from Rosekandy Tea Estate, Cachar District silchar. The cuttings were grown in field soil in polythene bags were procured from the nursery tea garden. The seedlings were allowed to grow after removing the polythene sleeves and adding soil in the pots. The plants were kept to acclimatize for 30-35 days. After that of tea plantlets were allowed to grow on pots (10cm diameter) in modified nutrient solution (9). They were pre-cultured for a week before giving aluminum treatment, aluminum is added in the form of  $AlCl_3$  at three different concentrations  $50\mu m$ ,  $250\mu m$  and  $500\mu m$ . The pH was adjusted at 4.2 and replacing of nutrient solution for every week.

**$H_2O_2$  production** : The analysis of  $H_2O_2$  content was conducted following the protocol of Sagisaka (10) and color development by the addition of 0.4ml of ferrous ammonium sulfate (10mM). Absorbency measured at 480nm.

**Super oxide anion ( $O_2^-$ ) content** : The super oxide anion production content was quantified according to Elstner and Heupal (11), the absorbency was observed at 530nm.

**Glutathione and Ascorbate content in response to  $Al^{3+}$  stress** : Total glutathione and ascorbate contents were estimated as per the method Griffith (12) and Oser (13). Plant was homogenized with 5 ml sulpho-salicylic acid and centrifuged at 17000g for 15 min at 4°C. The supernatant was collected and used for assay preparation. The reaction mixture for ascorbate content contained 2% sodium molybdate, 0.1N  $H_2SO_4$ , 1.5(N)  $Na_2HPO_4$  and plant extract and incubated at 60°C again centrifuged at 3000g. Absorbency was taken

at 660nm. While, the glutathione assay mixture consist of plant extract, 0.1M phosphate buffer (pH6.8), DTNB and the absorbency was recorded at 412nm.

#### **Antioxidant enzymes extraction and assay :**

For the extraction and determination of enzymes, in chilled pestle and mortar the samples were homogenized in 0.1M  $PO_4$  buffer, pH 6.8. The resultant homogenate was centrifuged at 17000g for 15 min at 4°C and the supernatant was taken for the assay of enzyme SOD, POX and CAT enzyme.

#### **Superoxide dismutase (SOD, EC 1.15.1.1) :**

The assay of SOD was performed according to the method of Gianopolitis and Reis (14). The assay mixture for SOD (1.15.1.1) consist of 79.2mM Tris-HCl buffer (pH 6.8), containing 0.12 mM EDTA and 10.8 mM tetraethylene diamine, bovine serum albumin (0.0033%), 6 mM nitroblue tetrazolium (NBT), 600  $\mu M$  riboflavin in 5mM KOH and 0.2 ml enzyme extract. Reaction was induced by placing the glass test tubes in between two fluorescent tubes (Philips 20 W). By switching the light on and off, the reaction was started and terminated, respectively. The increase in absorbance due to formazan formation was quantitated at 560 nm. The activity was expressed as  $\mu molg^{-1} FW$ .

#### **Catalase (CAT, 1.11.1.6) :**

For CAT, the activity was estimated as per the method of Chance and Maehly (15). The reaction mixture for CAT (1.11.1.6) contained 2ml (0.1M) phosphate buffer, 0.5ml 30mM  $H_2O_2$ , and 0.5ml enzyme extract, incubated for 1 min. The absorbency was recorded at 240nm.

#### **Peroxidase (POX, EC 1.11.1.7) :**

POX was assayed using pyrogallol as a substrate according to Kar and Mishra (16) with some modification, where 5.0 ml of assay mixture contained 300 IM  $H_2O_2$  and 1.0 ml of enzyme extract. After the incubations at 25°C for 5 min, the reaction was stopped by the addition of 1.0 ml of 10%  $H_2SO_4$ . The purpurogallin formation was read at 430 nm.

**Ascorbate glutathione cycle** : For the extraction and estimation of enzymes, plant tissue was

homogenized in 0.1M PO<sub>4</sub> buffer, pH 6.8 in a chilled pestle and mortar. The homogenate was centrifuged at 17000g for 15 min at 4°C and the supernatant was used for the assay of enzyme GR, DHAR and MDHAR. But the extraction for the determination of APX activity, the buffer contained 1mM ascorbic acid additionally to restore the activeness of the enzyme.

**Ascorbate peroxidase (APX, EC 1.11.1.11) :** For APX (1.11.1.11) extraction, according to Nakano and Asada (17), the tissue sample was homogenized with 0.1M phosphate buffer (pH 6.8) containing 1mM ascorbate, centrifuged at 17000rpm for 15 mins at 4°C. The supernatant was used as enzyme extract for assay mixture. The assay mixture was prepared with 10mM H<sub>2</sub>O<sub>2</sub>, 0.5mM ascorbate, 0.1M phosphate buffer (pH 6.8), enzyme extract. The absorbency was taken at 290nm. With extinction co-efficient 2.8 mM<sup>-1</sup>cm<sup>-1</sup> the APX activity was expressed as μmolg<sup>-1</sup>FW.

**Glutathione reductase (GR, EC 1.6.4.2) :** Glutathione reductase (GR) was assayed by the method of Smith *et al.*, (18). The reaction mixture of GR (1.6.4.2) contained 1.0 ml of 0.2 M potassium phosphate buffer (pH 7.5) containing 1 mM EDTA, 0.5 ml of 3 mM DTNB (5, 5- dithiobis-2 nitrobenzoic acid) in 0.01 M potassium phosphate buffer (pH 7.5), 0.1 ml of 2 mM NADPH, 0.1 ml enzyme extract and distilled water to make up a final volume of 2.9 ml. Reaction was initiated by adding 0.1 ml of 2 mM GSSG (oxidised glutathione) and used as a substrate. The increase in absorbance at 412 nm was recorded at 25°C over a period of 5 min spectrophotometrically. Specific activity was calculated using 6.22 mM<sup>-1</sup>cm<sup>-1</sup> extinction coefficient and expressed μmolg<sup>-1</sup>FW.

**De-hydro ascorbate reductase (DHAR, EC 1.8.5.1) :** Measure the activity following the method of Wang and Cheng (19). The reaction mixture contained 0.2mM DHA which acts as substrate, 50mM Hepes buffer (pH 7.0) containing 0.1mM EDTA, 2.5mM GSH and the supernatant. The activity was determined by measuring the increased in the reaction rate at 265nm for 5 min.

Specific activity was calculated using 14 mM<sup>-1</sup>cm<sup>-1</sup> extinction coefficient and expressed unit.g<sup>-1</sup>FW.

**Mono de-hydro ascorbate reductase (MDHAR, EC 1.6.5.4) :** This enzyme activity was measured the following method adapted from Miyake and Asada (20). The reaction mixture contained ascorbate oxidase (8unit), used as a substrate, 50mM Hepes buffer with 2.5mM ASA and 0.25mM NADH, lastly the enzyme extract. . The activity was determined by measuring the decreased in the reaction rate at 340nm for 5 min. Specific activity was calculated using 6.22mM<sup>-1</sup>cm<sup>-1</sup> extinction coefficient and expressed unit g<sup>-1</sup>FW.

**Statistical analysis :** All the data recorded were subjected to one way analyses of variance (ANOVA) and, LSD test were used for comparing between the control and treated values. Values are mean ±SE (n = 3) of three different experiments and \* correspond significant differences with controls at P <0.05. The data analysis was carried out using statistical package, SPSS 21.0.

## Results

### Reactive Oxygen species (ROS)

With the increasing of the concentration of Al stressed in tea plant a gradual enhancement in ROS generation was observed. Superoxide anion (O<sub>2</sub><sup>-</sup>) production in the plant increased with increasing of Al concentration except at 50 μM of root. The content was highest by 500μM 284.94% of 250 μM 104.94% followed by reduction at 50μM 34.39% in roots, in case of leaf 6.4%, 11.4% and 32.08% with respective concentrations from control. With comparing from the control the TS462 variety has greater production of (O<sub>2</sub><sup>-</sup>) at the stress given plants in roots than of leaves with comparison from their respective controls.

The lipid peroxidation was measured by evaluating MDA content of both roots and leaves. Al significantly affected the production of MDA by indicating the lipid peroxidation the MDA content were observed increased the three concentrations of both roots and leaves with increasing concentrations of Al stressed. The increase was about 22.13%, and 36.34 % at 50 μm, 79.12 %, 66.38% at 250 μm, 500 μm 177.1% & 85.68 %

respectively in roots and leaves.  $H_2O_2$  production was also shown the same observations with that of MDA and ( $O_2^-$ ). In all the treated plants were increased their production with the increasing of Al concentrations. Same pattern with MDA and  $H_2O_2$  content that roots has shown the higher production of than leaves (Fig. 1.a, b and c).

**Ascorbate and Glutathione** : The non-enzymatic ascorbate and glutathione content shown an increased with the concentration increased. The highest content of glutathione shown in root at  $500\mu M$  at root by increasing of 140.33% in leaves only 30.50% but both the roots and leaves have shown their significant increased at highest concentration Al treated. In glutathione with increasing of concentration the higher the content of glutathione was observed 2.1%, 25.4%, 30.5% and 44.69% , 148.4% , 61.27% in roots and leaves respectively. Here in the glutathione

content at  $250\mu M$  in leaf have shown the highest activity, both the ascorbate and glutathione content the leaf is much higher content than that of roots (Fig. 1.d and 1.a).

**Antioxidant enzymes (CAT, SOD and POX)** : With the increasing of Al stress CAT activity was being increased in both root and leaves. There was an increase of CAT activity from control to the stress plant of leaves 4.5%, 9.0% and 26.59% was increased from untreated plant to  $50\mu M$  respectively. In root only 21.41%, 38.05% and 15.97%, was increased with respect from the control one.

SOD activity increased with concentration of stress in leaf was observed that there was highest activity at  $500\mu M$  of enzyme activity by giving an increment of 307.16%. Higher activity of this enzyme is shown by leaves. In the roots too

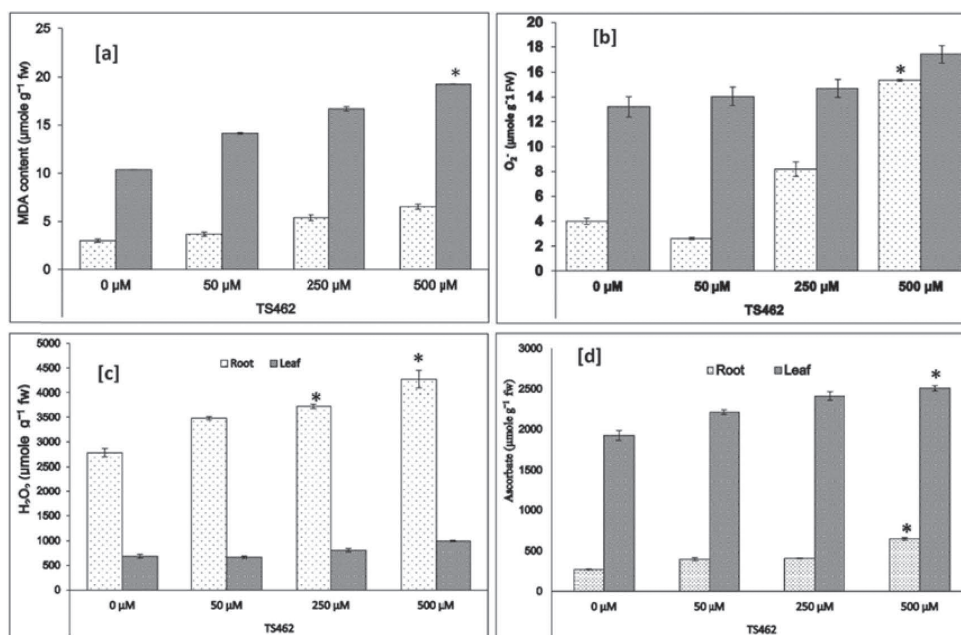


**Fig.1:** Biochemical assays of root and leaf samples of tea plant *var.*, TS462 after 2 months of aluminum treatment ( $50\mu M$ ,  $250\mu M$ ,  $500\mu M$ ) and control. a. Malondialdehyde (MDA) content b. Superoxide ( $O_2^-$ ) content; c. Hydrogen peroxide ( $H_2O_2$ ) content; d. Ascorbate content. Data represents mean values ( $n = 3$ )  $\pm$ SE, where  $n$  is the number of times experiment repeated and SE denotes Standard Error. Statistically significant values at  $P < 0.05$  using LSD analysis are indicated by star marks.



there was increased activity from control one (0 $\mu$ M). In comparison with roots and leaves their activity was higher with all the concentrations of Al treated.

There was a significant increase in the POX activity in the Al stressed tea plants in roots and leaves. Here also same observation was shown in between roots and leaves except 500  $\mu$ M of leaf, their activity was uniform same in both roots and leaf upto 250  $\mu$ M but by the highest concentration of there was significant increase of the activity was observed with an increment of 191.7% from the untreated one (Fig. 2. b, c and d).

**Ascorbate Glutathione cycle :** The ascorbate glutathione cycle enzymes has been shown a significant increased with the increasing of stressed given in roots and leaves. From the result it has been observed that there was a significant difference in the enzyme content in roots and

leaves, more enzymes were content at leaf in this study. The highest activity in ascorbate glutathione cycle is at 500  $\mu$ M except MDHAR 250  $\mu$ M in both roots and leaves. The lower activity among these four enzyme activity is GR and highest content shown by APX followed by MDHAR and DHAR. The DHAR enzyme activity have observed a significant increased at both roots and leaves at highest concentration Al treated (Fig.3).

### Discussion:

Al induces ROS production and lipid peroxidation (21) and oxidation of protein (22). In this present study Al treatment has induced oxidative stress, measured by MDA, H<sub>2</sub>O<sub>2</sub> and O<sub>2</sub><sup>-</sup> in both the roots and leaves of tea plant TS462 variety. Suggesting the loss of plasma membrane function and showed that the Al ions has the substantial affinity to bio-membranes (23, 24). Thus stimulated the rigidification of the

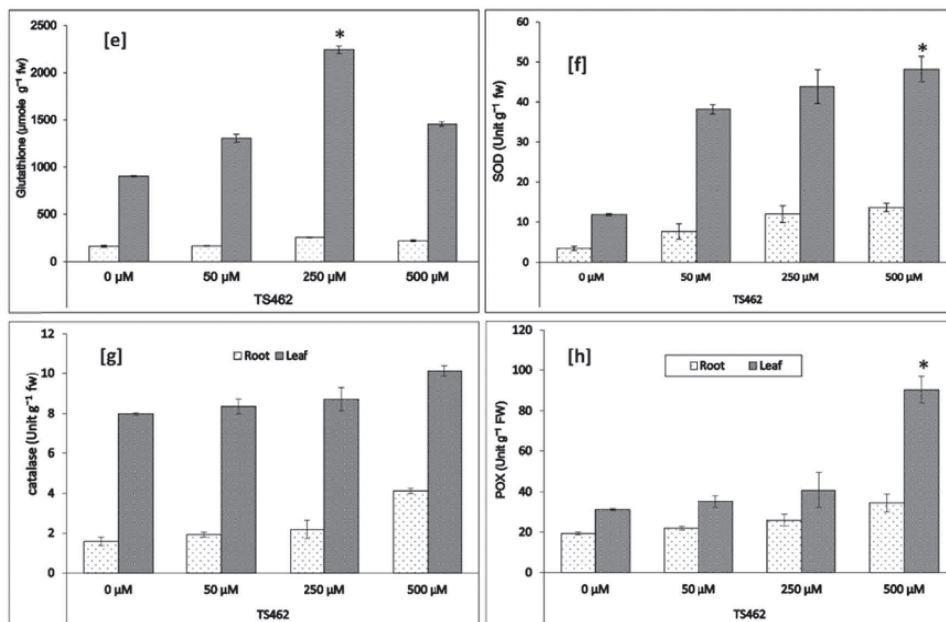


**Fig. 2:** Anti-oxidative enzyme assays for root and leaf samples of tea plant var., TS462 after 2 months of aluminum treatment (50 $\mu$ M, 250 $\mu$ M, 500 $\mu$ M) and control. a. Glutathione b. Superoxide dismutase (SOD) c. Catalase (CAT); d. Guaicol peroxidase (POX) Data represents mean values (n = 3)  $\pm$ SE, where n is the number of times experiment repeated and SE denotes Standard Error. Statistically significant values at P<0.05 using LSD analysis are indicated by star marks.

Loss of ROS homeostasis and anti oxidative responses in tea cultivar due to aluminium toxicity



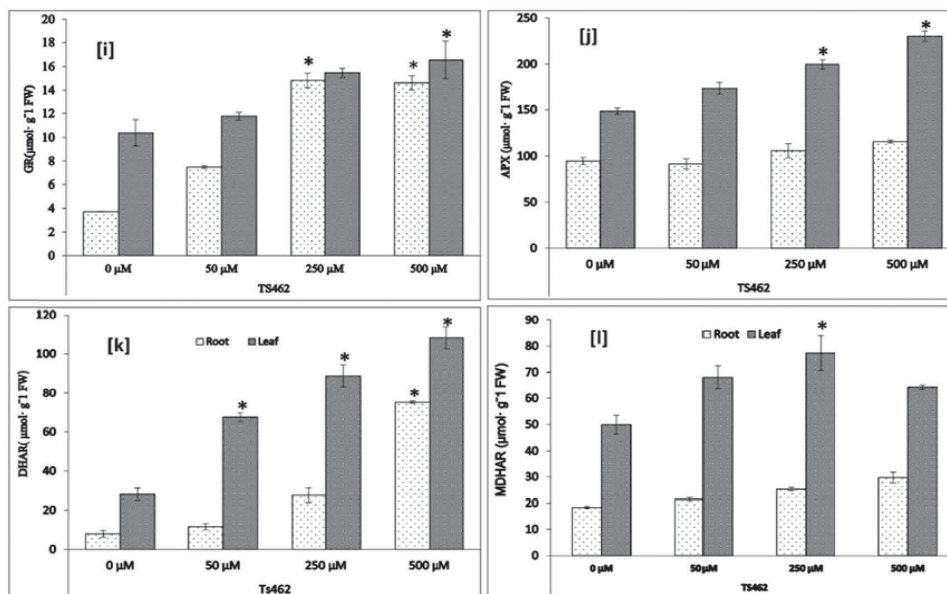


**Fig. 3:** Anti-oxidative enzyme assays AsA-GSH cycle for root and leaf samples of tea plant var., TS462 after 2 months of aluminum treatment (50μM, 250μM, 500μM) and control. a. Glutathione Reductase (GR) b. Ascorbate peroxidase (APX); c. Dehydroascorbate reductase (DHAR) d. Monodehydro ascorbate reductase (MDHAR); Data represents mean values (n = 3) ±SE, where n is the number of times experiment repeated and SE denotes Standard Error. Statistically significant values at P<0.05 using LSD analysis are indicated by star marks.

membranes (25), which looks to alleviate the radical chain reactions which is intermediated by iron (Fe) ions and finally heightened the lipid peroxidation of membrane. Lipid peroxidation is one of the eminent indication of oxidative damage. Induction of oxidative damage was observed from the result in both the roots and leaves of tea plant (TS462).

The increased in lipid peroxidation was due to the destructive effects of excessive levels of H<sub>2</sub>O<sub>2</sub> or its derivatives in the cellular components (26). Impairment of cell organelles like photosynthetic apparatus and ultimately leads to severe cellular damage and chlorosis of leaves. This results support that metal accumulator species has higher antioxidation capacity by regulating the antioxidant enzymes in leaves.

H<sub>2</sub>O<sub>2</sub> accumulation in the Al treated plants might be the consequences of circulating in the balance between its yields and scavenging. The

SOD enzyme is the first enzyme for the elimination of ROS and can be exchanged into O<sub>2</sub><sup>-</sup> radicals to H<sub>2</sub>O<sub>2</sub> at a very rapid rate. CAT can be expeditiously scavenged H<sub>2</sub>O<sub>2</sub> in the plants under many conditions of stress. In this study MDA, H<sub>2</sub>O<sub>2</sub> and O<sub>2</sub><sup>-</sup> contents increased up to 500μM of Al treated plants hence showing the induction of oxidative stress in tea plant. O<sub>2</sub><sup>-</sup> and H<sub>2</sub>O<sub>2</sub> can react by a metal catalyzed Haber-Weiss reaction that generates hydroxyl radicals (OH<sup>·</sup>), which speedily attack all types of biomolecules contributing to the catastrophic dysfunction and cell death (27). Their contents increases as the consequences of stress imposition and least stress was observed at 50μM followed by 250μM and 500 μM of treated plants of roots and leaves. This may suggest that tea plant treated with different concentrations upto 500 μM could attribute to its greater adaptation (Fig.1.b, c).

Al stress induced the increasing of non-

enzymatic antioxidant system in tea plant. Ascorbate is an abundant small molecules in plants which is a fundamental substance in the context of antioxidants that includes glutathione  $\alpha$ -tocopherol and a cascades of antioxidant enzymes. Ascorbate and glutathione are important antioxidants and redox buffers in plant cells but also a key role in growth and development as well as stress response (28, 29). Increase in the Ascorbate Glutathione content shows the protection against ROS and it acts as an electron donor for Ascorbate peroxidase (APX). Both ascorbate and glutathione are abundant antioxidants with appropriate redox potentials by interacting with numerous components and pathways and that are sustained in a general reduced state (30). Thus keeps the ROS (reactive oxygen species) under control. An important role plays by glutathione in protection of plants from the oxidative stress induced by some heavy metals (31). Increasing of glutathione in this study has observed in roots and leaves in this variety (fig 2.a). An increasing of glutathione content under the Al stress has been reported in pea plant roots(32).

In this study the higher production of glutathione revealed that tea plant under the Al stress is under the defense system to combat the stress given at different concentration.

Production of ROS is promoted under various environmental stresses. It causes oxidative damage to lipids, proteins and nucleic acids in the cell organelles. In preventing the cellular oxidative damaged caused by ROS is SOD enzyme. It is one of the most effective antioxidant enzyme which catalyzes the conversion of  $O_2^-$  to  $H_2O_2$ . The enzyme CAT has the ability to scavenge the  $H_2O_2$  and peroxidase (POX) used  $H_2O_2$  for the oxidation of various organic and inorganic substrates. Thus SOD, CAT and POX were regarded as the major antioxidant enzymes present in the plant cells (33). Plants have their own capability to defense the harmful effects of ROS with the help of both enzymatic and non-enzymatic antioxidant machinery to maintain their equilibrium level. ROS and oxidative stress caused by biotic and abiotic factor may contribute to cause lipid peroxidation (34).

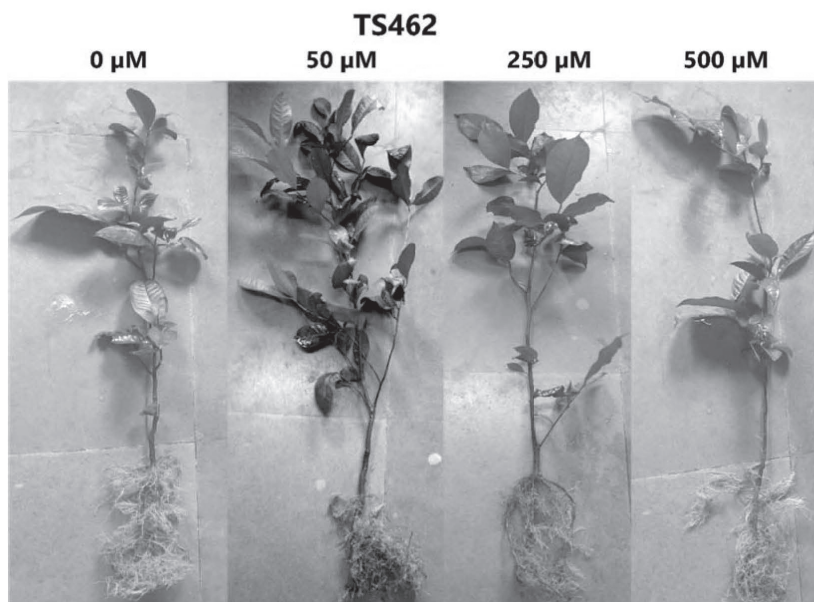


**Fig. 4:** Physiology of whole plant after two months aluminum treatment (0 $\mu$ M, 50 $\mu$ M, 250 $\mu$ M and 500 $\mu$ M)

Loss of ROS homeostasis and anti oxidative responses in tea cultivar due to aluminium toxicity

Different responses of anti-oxidative enzymes are reported under the Al stress of tea plant (9). In this study also gradually increasing of SOD enzyme with concentrations was observed in roots and leaves of both this variety it is an agreement with Ghanati *et al.*, (9, 35). SOD catalyzes the dismutation of  $O_2^-$  radicals to molecular  $O_2$  in the cytosol, mitochondria and chloroplast (36). SOD activity has been reported to increase in plants exposed to various environmental stresses which includes drought and metal toxicity (37,38). The over expression of SOD has been report to result in heighten of oxidative stress tolerance in plants (39). The increased activity of SOD is correlated with the increased tolerance of the plant against the environmental stresses. Increased of CAT activity under the Al stress has been reported (9,35, 40) and in our study also similar result has been observed with increasing of Al concentration in both roots and leaf and more production of CAT activity was shown on leaf than roots. An additional protection against the oxidative damage may render by CAT activity, induced by Al stress in tea plant. Tea is a  $C_3$  plant, higher CAT activity could scavenge the hydrogen peroxide formed in the photorespiratory pathway and hence cut down the photorespiration rate (41). The great different between the tea plant and other probably Al tolerant species (42, 43) and sensitive species (44) could be explained on the basis of their upregulation of SOD followed by by other ROS scavenging enzymes, mainly CAT and APX (9). SOD activity is mainly triggered by Al resulting in dismutation of  $O_2^-$  and more production of other toxic species and  $H_2O_2$  in Al sensitive plants. In Al treated tea plant the production of  $H_2O_2$  is afterwards detoxified by APX and CAT, the Peroxidase (POX) also eliminated  $H_2O_2$

Major sites of  $H_2O_2$  production are peroxisomes and CAT scavenges  $H_2O_2$  generated from this organelles during photorespiratory oxidation,  $\beta$ -oxidation of fatty acids and other enzyme systems like XOD which is coupled to SOD. Increased in the POX and PPO activity in all the Al stressed plants of tea may be an

acclimatization step against the given stress. In the presence of  $H_2O_2$ , theaflavin is formed in the oxidation of tea catechins by POX has also been reported (45), POX also eliminated  $H_2O_2$ .

The changes in the ratio of AsA to DHA and GSH to GSSG is a crucial for the cell to sense oxidative stress and respond accordingly. The AsA- GSH cycle is also denoted to as Halliwell Asada pathway, it is the recycling pathway of AsA- GSH cycle which requires in the successive oxidation and reduction of AsA, GSH and NADPH are catalyzed by enzymes APX, MDHAR, DHAR and GR. AsA- GSH cycle plays an important role in combating the oxidative stress induced by environmental stresses (37). APX is a central component of AsA- GSH cycle, an essential role is played in the controlling of intracellular ROS levels. APX activity was increased in stressed plants at both the roots and leaves (Fig.3.b). More activity was shown at leaves, there was a significant increase with respect from control. This result is agreement with the report of Ghanati *et al.*,(9) enhancement of APX activity was shown in tea plant under Al stress. APX is widely attributed antioxidant enzyme in plant cell and their isoforms has much greater affinity for  $H_2O_2$  than CAT. In several compartments of plants the MDHAR activity and their isoforms are widely found like chloroplast cytosol, mitochondria and peroxisomes (17). MDHAR could have two functions in chloroplast, the generation of AsA from MDHA and the resulting of the photoreduction of dioxygen to  $O_2^-$  when MDHAR substrate is absent (20). The MDHAR activity was shown in this study shown a significant increase in leaves from their untreated control (Fig.3.d). In this study enhancement of MDHAR activity under Al stress of tea was induced with the increasing concentrations of stress imposed and may show the tolerant like the salt and PEG stresses. In chloroplast, GR and GSH are involved in detoxification of  $H_2O_2$  generated by Mehler reaction (46). Same as the above enzymes GR have also reported an increased activity under several environmental stresses. Ghanati *et al.*,(9) reported with the increase of Al concentrations there was

an increase of GR activity in tea plant. In this study too there was a significant increase of GR activity in roots and leaves. Higher the activity shown in leaves of tea plant than the roots under Al stress. In maintain a high ratio of oxidized and reduced glutathione GR is involved, which is required for the regeneration of AsA, an important antioxidant plant cells (35). Catalysis of NADPH dependent reduction of oxidized glutathione was observed with the increase of GR activity.

### Conclusion

In conclusion, from this study suggested that Al toxicity is solely linked with the enhancement of oxidative stress in roots and leaves by showing the elevated amount of MDA, H<sub>2</sub>O<sub>2</sub> and O<sup>2-</sup>. And antioxidant CAT, SOD, POX and AsA- GSH cycle enzymes took the vital role in combating oxidative stress. As a hyper accumulator of Al the tea plant has the ability to adapt the acidic environment where the other plants could not survive for long. The tea plant enhances several defense mechanisms to combat the stress environment. The main defense mechanism to survive from ROS is antioxidant enzymes and non-enzymatic machineries.

### Acknowledgement

SSD sincerely thank UGC, New Delhi, India, for providing NON-NET fellowship throughout the research. In addition we would also like convey our thanks to the Manager and staffs of Rosekandy Tea Estate, Silchar, India to be generous enough to provide us the tea cultivars.

### References

1. Barthakur, I. K. (2018). Soil pH as a Phenotype Determinant in Humans: Proposing a Scientific Hypothesis. *Open Journal of Soil Science*, 8(01), 36.
2. Gechev, T. S., Van Breusegem, F., Stone, J. M., Denev, I., & Laloi, C. (2006). Reactive oxygen species as signals that modulate plant stress responses and programmed cell death. *Bioessays*, 28(11), 1091-1101.
3. Asada, K. (2006). Production and scavenging of reactive oxygen species in chloroplasts and their functions. *Plant physiology*, 141(2), 391-396.
4. Karuppanapandian, T., Moon, J. C., Kim, C., Manoharan, K., & Kim, W. (2011). Reactive oxygen species in plants: their generation, signal transduction, and scavenging mechanisms. *Australian Journal of Crop Science*, 5(6), 709.
5. Gill, S. S., & Tuteja, N. (2010). Reactive oxygen species and antioxidant machinery in abiotic stress tolerance in crop plants. *Plant physiology and biochemistry*, 48(12), 909-930.
6. Valero, E., Macià, H., Ildefonso, M., Hernández, J. A., González-Sánchez, M. I., & García-Carmona, F. (2015). Modeling the ascorbate-glutathione cycle in chloroplasts under light/dark conditions. *BMC systems biology*, 10(1), 11.
7. Mittler, R. (2002). Oxidative stress, antioxidants and stress tolerance. *Trends in plant science*, 7(9), 405-410.
8. Upadhyaya, H., Dutta, B. K., Sahoo, L., & Panda, S. K. (2012). Comparative effect of Ca, K, Mn and B on post-drought stress recovery in tea [*Camellia sinensis* (L.) O Kuntze]. *American Journal of Plant Sciences*, 3(04), 443-449.
9. Ghanati, F., Morita, A., & Yokota, H. (2005). Effects of aluminum on the growth of tea plant and activation of antioxidant system. *Plant and soil*, 276(1-2), 133-141.
10. Sagisaka, S. (1976). The occurrence of peroxide in a perennial plant, *Populus gelrica*. *Plant Physiology*, 57(2), 308-309.
11. Elstner, E. F., & Heupel, A. (1976). Inhibition of nitrite formation from hydroxylammoniumchloride: a simple assay for superoxide dismutase. *Analytical biochemistry*, 70(2), 616-620.
12. Griffith, O. W. (1980). Determination of glutathione and glutathione disulfide using glutathione reductase and 2-vinylpyridine. *Analytical biochemistry*, 106(1), 207-212.



13. Oser, B. L., 1979. Hawks physiological chemistry. *McGraw Hill*. N. Y. USA, 702–705.
14. Giannopolitis, C. N., & Ries, S. K. (1977). Superoxide dismutases I. Occurrence in higher plants. *Plant physiology*, 59(2), 309-314.
15. Chance, B., & Maehly, A. C. (1955). Assay of catalases and peroxidases. *Methods in enzymology*, 2, 764-775.
16. Kar, M., & Mishra, D. (1976). Catalase, peroxidase, and polyphenoloxidase activities during rice leaf senescence. *Plant physiology*, 57(2), 315-319.
17. Nakano, Y., & Asada, K. (1981). Hydrogen peroxide is scavenged by ascorbate-specific peroxidase in spinach chloroplasts. *Plant and cell physiology*, 22(5), 867-880.
18. Smith, I. K., Vierheller, T. L., & Thorne, C. A. (1988). Assay of glutathione reductase in crude tissue homogenates using 5, 5'-dithiobis (2-nitrobenzoic acid). *Analytical biochemistry*, 175(2), 408-413.
19. Wang Ma, F., & Cheng, L. (2004). Exposure of the Shaded Side of Apple Fruit to Full Sun Leads to Up-regulation of Both the Xanthophyll Cycle and the Ascorbate-glutathione Cycle. *HortScience*, 39(4), 887-887.
20. Miyake, C., Cao, W. H., & Asada, K. (1993). Purification and molecular properties of the thylakoid-bound ascorbate peroxidase in spinach chloroplasts. *Plant and cell physiology*, 34(6), 881-889.
21. Yamamoto, Y., Kobayashi, Y., & Matsumoto, H. (2001). Lipid peroxidation is an early symptom triggered by aluminum, but not the primary cause of elongation inhibition in pea roots. *Plant Physiology*, 125(1), 199-208.
22. Boscolo, P. R., Menossi, M., & Jorge, R. A. (2003). Aluminum-induced oxidative stress in maize. *Phytochemistry*, 62(2), 181-189.
23. Akeson, M. A. Munns DN and Burau RG 1989 Adsorption of Al<sup>3+</sup> to phosphatidylcholine vesicles. *Biochm. Biophys. Acta*, 986, 200-206.
24. Jones, David L., and Leon V. Kochian. "Aluminum interaction with plasma membrane lipids and enzyme metal binding sites and its potential role in Al cytotoxicity." *FEBS letters* 400.1 (1997): 51-57.
25. Deleers, M., Servais, J. P., & Wülfert, E. (1986). Neurotoxic cations induce membrane rigidification and membrane fusion at micromolar concentrations. *Biochimica et Biophysica Acta (BBA)-Biomembranes*, 855(2), 271-276.
26. Bowler, C., Montagu, M. V., & Inzé, D. (1992). Superoxide dismutase and stress tolerance. *Annual review of plant biology*, 43(1), 83-116.
27. Halliwell, B. (1999). Antioxidant defence mechanisms: from the beginning to the end (of the beginning). *Free radical research*, 31(4), 261-272.
28. Smirnoff, N. (2000). Ascorbic acid: metabolism and functions of a multi-facetted molecule. *Current opinion in plant biology*, 3(3), 229-235.
29. Pastori, G. M., Kiddle, G., Antoniw, J., Bernard, S., Veljovic-Jovanovic, S., Verrier, P. J., ... & Foyer, C. H. (2003). Leaf vitamin C contents modulate plant defense transcripts and regulate genes that control development through hormone signaling. *The Plant Cell*, 15(4), 939-951.
30. Foyer, C. H., & Noctor, G. (2011). Ascorbate and glutathione: the heart of the redox hub. *Plant physiology*, 155(1), 2-18.
31. Xiang, C., & Oliver, D. J. (1998). Glutathione metabolic genes coordinately respond to heavy metals and jasmonic acid in Arabidopsis. *The Plant Cell*, 10(9), 1539-1550.
32. Panda, S. K., & Matsumoto, H. (2010). Changes in antioxidant gene expression and induction of oxidative stress in pea (*Pisum*



- sativum L.) under Al stress. *Biometals*, 23(4), 753-762.
33. Eva, D., Helga, A., Eva, S. B., Jozsef, F., Ferenc, B., & Beata, B. (2004). Aluminum toxicity, Al tolerance and oxidative stress in an Al-sensitive wheat genotype and in Al-tolerant lines developed by in vitro microspore selection. *Plant Sci*, 66, 583-591.
  34. Awasthi, J. P., Saha, B., Chowardhara, B., Devi, S. S., Borgohain, P., & Panda, S. K. (2017). Qualitative Analysis of Lipid Peroxidation in Plants under Multiple Stress Through Schiff's Reagent: A Histochemical Approach. *PLOS ONE*.
  35. Li, C., Xu, H., Xu, J., Chun, X., & Ni, D. (2011). Effects of aluminum on ultrastructure and antioxidant activity in leaves of tea plant. *Acta physiologiae plantarum*, 33(3), 973-978.
  36. Salin, M. L. (1988). Toxic oxygen species and protective systems of the chloroplast. *Physiologia Plantarum*, 72(3), 681-689.
  37. Sharma, P., & Dubey, R. S. (2005). Lead toxicity in plants. *Brazilian journal of plant physiology*, 17(1), 35-52.
  38. Mishra, S., Jha, A. B., & Dubey, R. S. (2011). Arsenite treatment induces oxidative stress, upregulates antioxidant system, and causes phytochelatin synthesis in rice seedlings. *Protoplasma*, 248(3), 565-577.
  39. Gupta, A. S., Webb, R. P., Holaday, A. S., & Allen, R. D. (1993). Overexpression of superoxide dismutase protects plants from oxidative stress (induction of ascorbate peroxidase in superoxide dismutase-overexpressing plants). *Plant Physiology*, 103(4), 1067-1073.
  40. Mukhopadyay, M., Bantawa, P., Das, A., Sarkar, B., Bera, B., Ghosh, P., & Mondal, T. K. (2012). Changes of growth, photosynthesis and alteration of leaf antioxidative defence system of tea [*Camellia sinensis* (L.) O. Kuntze] seedlings under aluminum stress. *Biometals*, 25(6), 1141-1154
  41. Jeyaramraja, P. R., Kumar, R. R., Pius, P. K., & Thomas, J. (2003). Photoassimilatory and photorespiratory behaviour of certain drought tolerant and susceptible tea clones. *Photosynthetica*, 41(4), 579-582.
  42. Ogawa, M., Portier, R. J., Moody, M. W., Bell, J., Schexnayder, M. A., & Losso, J. N. (2004). Biochemical properties of bone and scale collagens isolated from the subtropical fish black drum (*Pogonia cromis*) and sheepshead seabream (*Archosargus probatocephalus*). *Food chemistry*, 88(4), 495-501.
  43. Ezaki, B., Katsuhara, M., Kawamura, M., & Matsumoto, H. (2001). Different mechanisms of four aluminum (Al)-resistant transgenes for Al toxicity in Arabidopsis. *Plant Physiology*, 127(3), 918-927.
  44. Cakmak, I., & Horst, W. J. (1991). Effect of aluminum on lipid peroxidation, superoxide dismutase, catalase, and peroxidase activities in root tips of soybean (*Glycine max*). *Physiologia Plantarum*, 83(3), 463-468.
  45. Sang, S., Yang, C. S., & Ho, C. T. (2004). Peroxidase-mediated oxidation of catechins. *Phytochemistry reviews*, 3(1-2), 229-241.
  46. Foyer, C. H., Descourvieres, P., & Kunert, K. J. (1994). Protection against oxygen radicals: an important defence mechanism studied in transgenic plants. *Plant, Cell & Environment*, 17(5), 507-523.

## Deciphering the Biological Activity of Recombinant Guinea Pig Proteins

Madhavan Omanakuttan<sup>1</sup>, Vijaya R. Dirisala<sup>1\*</sup>, Hanumohan R. Konatham<sup>1</sup>, M. Madhuri<sup>2</sup>,  
Malathi Jojula<sup>2</sup>, Shradha Mawatwal<sup>3</sup>, Rohan Dhiman<sup>3</sup>

<sup>1</sup>Department of Biotechnology, Vignana's University, Guntur-522213, AP, India

<sup>2</sup>Department of Microbiology, Sri Shivani College of Pharmacy, Warangal - 506001, Telangana, India.

<sup>3</sup>Laboratory of Mycobacterial Immunology, Department of Life Science, National Institute of Technology, Rourkela-769008, Odisha, India.

\*Corresponding Author : E-mail: drdirisala@gmail.com

### Abstract

The guinea pig is one of the most relevant small animal models for studying a large number of infectious and non-infectious diseases. The major roadblock for its effective utilization is the lack of readily available molecular and immunological reagents. In order to address this issue, some of the important recombinant proteins such as IL-4, IL-10, IL-1 $\beta$ , MCP-1, IFN- $\gamma$  and TNF- $\alpha$  which were generated previously were analyzed for their biological activity in terms of nitrite production in RAW cells. Interestingly, nitrite production was comparatively more in the presence of TNF- $\alpha$  in comparison with proinflammatory cytokine IFN- $\gamma$  and similar levels of nitrite production were observed in the presence of Th2 cytokines i.e IL-4 and IL-10. We have analyzed the biological activities of these recombinant proteins so that they could be used for a wide array of *in vitro* and *in vivo* biological assays.

**Keywords:** Th1; Th2; Guinea pig; Assay; Proteins

### Introduction

Guinea pig is an excellent animal model for studying infectious diseases such as tuberculosis and a number of other non-infectious diseases (1). The guinea pig model of pulmonary tuberculosis mimics human tuberculosis in the organization of granulomatous lesions, extra pulmonary dissemination and vaccine induced protection (2). One of the major roadblocks of effective utilization of this animal model is the lack

of readily available immunological reagents (3). Towards this initiative, coding sequences of genes pertaining to IL-4, IL-10, IL-1 $\beta$ , MCP-1, IFN- $\gamma$  and TNF- $\alpha$  were cloned and expressed for the generation of recombinant proteins (4, 5, 6, 7, 8, 9).

It has been well observed from different studies that Th1 cytokines alone cannot control tuberculosis. Hence a fine balance between Th1 and Th2 cytokines is crucial in combating tuberculosis (10). The objective of this study is to confirm the biological activities of the Th1 and Th2 proteins by a biological assay, so that they could be utilized for a wide array of *in vitro* and *in vivo* assays.

### Materials and methods

**Expression of recombinant proteins :** Thirty microlitres of the culture pertaining to positive clones of IL-1 beta, MCP-1, IL-4, IL-10, IFN- $\gamma$  and TNF- $\alpha$  were grown overnight in 5 ml of LB broth at 37 °C containing Kanamycin (15  $\mu$ g/ml). This culture was then added to 50 ml of identical culture medium and induced with 1.0 mM Isopropyl- $\beta$  d-thiogalactoside (IPTG) (Sigma, USA) at OD<sub>600</sub> of 0.8 for protein expression. After 5 hours of induction, protein expression was analyzed by polyacrylamide gel. The cells were harvested by centrifugation and the pellet was resuspended in 5 mL lysis buffer (50 mM NaH<sub>2</sub>PO<sub>4</sub>, 300 mM NaCl and 10 mM Imidazole, pH 8.0) followed by addition of lysozyme (Sigma) to 1mg/ml and incubation on ice for 30 minutes. The sample was subjected

to sonication (Misonix Inc., Farmingdale, NY) at 30 W for a total of 6 times (10 seconds each time with a pause of 10 seconds). The sonicated sample was centrifuged to obtain the cleared lysate and the pellet. A fraction of the cleared lysate or pellet was analyzed on 10-20% Tricine gel to determine the solubility of the target protein.

**Protein purification for soluble proteins and insoluble proteins :** The cleared lysates obtained after sonication were purified by immobilized metal affinity chromatography under native conditions as described in previous reports (7). The eluted fractions containing the protein of interest were pooled and concentrated using Amicon Ultra-5 centrifugal filter devices and the protein concentrations were determined using the Bradford assay.

For protein purification under denaturing conditions, the cell pellet after centrifugation was resuspended in 5 mL of lysis buffer (Qia Expressionist) containing 1mg/ml of lysozyme followed by incubation on ice for 30 minutes. The sample was then sonicated at 30 W for obtaining the cleared lysate and the pellet after centrifugation. The cleared lysate was further processed through denaturing conditions for lysing the pellet as described in previous reports and slightly modified protocol from Qiagen was adapted for renaturation of the denatured protein (8).

**In vitro biological activities of recombinant guinea pig proteins :** The biological activity of recombinant proteins were determined by measuring its ability to promote or inhibit nitric oxide (NO) production in RAW264.7 cell-lines (11). For estimation of NO,  $0.5 \times 10^6$  cells were plated per well and seeded overnight in a 24-well plate. The following day, cells were pre-treated with recombinant guinea pig proteins of IL-1  $\beta$ , MCP-1, IL-4, IL-10 and TNF- $\alpha$  (10 ng/ml) for 1 hour and some of them are stimulated with LPS (10  $\mu$ g/ml) for 48h. Supernatants were collected and the concentration of NO<sub>2</sub><sup>-</sup> was measured using Griess reagent through spectrophotometric method and the appropriate standard used was sodium nitrite

(12). In brief, 100  $\mu$ l of culture supernatant was mixed with 100  $\mu$ l of Griess reagent at room temperature for 10 minutes followed by measurement of absorbance at 550 nm using a microplate reader (Biobase, China).

## Results

**Analysis of recombinant proteins on SDS-PAGE :** Recombinant proteins such as IL-1 $\beta$ , MCP-1, TNF- $\alpha$  as expected were obtained in the soluble form and hence purified under native conditions. Other recombinant proteins such as IL4, IL-10, IFN- were obtained in the insoluble form and thus purified under denaturing conditions. The expressed proteins after purification were quantified and further run on SDS-PAGE which were of the expected size.

## Biological activities of recombinant proteins :

We checked the biological activity of recombinant proteins (IL-4, IL-10, IL-1 $\beta$ , MCP-1 and TNF- $\alpha$ ) in LPS-activated RAW264.7 cells by measuring NO production as published literature suggests that Th1 cytokines promote NO production in these cells upon LPS stimulation and Th2 cytokines inhibits NO production (10). As described in Materials and Methods, RAW264.7 cells were pre-treated with respective recombinant proteins for 1 hour before adding LPS either alone or in combination for 48 h. The nitrite assay in the culture supernatants clearly demonstrated the inhibitory effect of rgpIL-4 and rgpIL-10 on nitrite production. Notably NO production was enhanced in the presence of IFN- and TNF- $\alpha$ . (Figure 1). When anti-rgpIL-4 was added to the cells pretreated with IL-4, the production of NO was enhanced there by reversing the effect of IL-4 which is consistent with that of our previous report (Dirisala et al., 2019). It would be interesting to check the nitrite production in the presence of recombinant proteins generated from the variants generated by alternative splicing of genes. Interestingly, nitrite production was comparatively more in the presence of TNF- $\alpha$  in comparison with IFN- (Figure 1). Similar levels of nitrite production was observed in the presence of Th2 cytokines IL-4 and IL-10 (Figure 1).

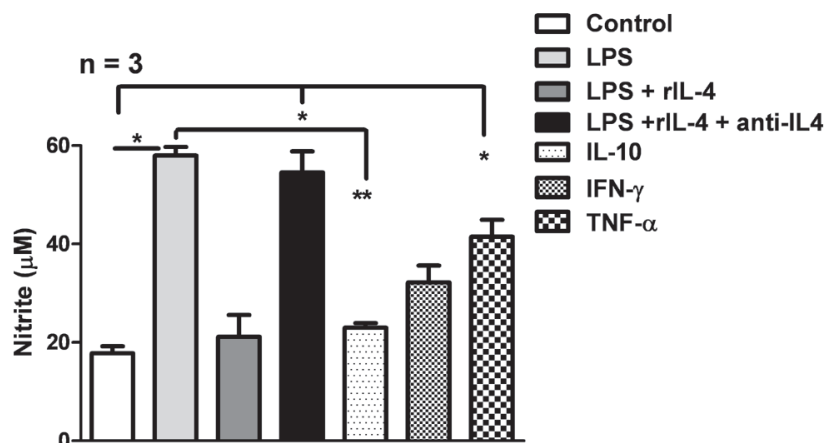


**Fig. 1.** RAW264.7 cells were plated and seeded overnight and were either stimulated with LPS (10 µg/ml) or left alone for 48 h. The nitrite assay was done on culture supernatants with the Griess reagent. Data shown are representative of the cumulative values of three independent experiments. Values are expressed as Mean ± SEM. \* signifies  $p < 0.05$ .

## Discussion

As per WHO estimates, 1.6 million deaths were reported for tuberculosis in 2017 alone (13). One of the major constraints associated with the widely used gold standard TB vaccine is that it is unable to offer 100% protection against tuberculosis and is efficient in the range of 0-80% in different individuals (14). Various vaccines are in different phases of clinical trials to replace BCG vaccine or enhance the efficacy of BCG (15). Although various animal models are used to evaluate the efficacy of novel vaccines, the guinea pig is considered as the most promising animal model for tuberculosis (Clark et al., 2015). Biological activities were not performed for IL-10 and only one biological assay was performed for recombinant proteins of IL-1 $\beta$  and MCP-1. Single assay or few assays were carried out for the recombinant proteins mentioned here but it would be worthy to perform additional assays to confirm their biological potential so that they could be used for a wide array of studies.

## Acknowledgments

The authors thank Vignan's University for providing facilities to execute this work. The

authors acknowledge the support of BEI resources wherein majority of the clones developed by the corresponding author and others were deposited in BEI through Dr. McMurray's lab. The authors also thank NIT, Rourkela for providing few of the facilities to execute the work. The authors acknowledge the support of SERB (ECR/2016/304) The authors acknowledge the support of FIST for providing infrastructure facilities to execute the work.

## References

1. Clark, S., Hall, Y., & Williams, A. (2015). Animal models of tuberculosis: Guinea pigs. *Cold Spring Harb. Perspec. Med.*, 5: 018572.
2. Ordway, D., Palanisamy, G., Henao-Tamayo, M., Smith E.E., Shanley, C., Orme, I.M., & Basaraba, R.J. (2007). The cellular immune response to Mycobacterium tuberculosis infection in the guinea pig. *J. Immunol.*, 179: 2532-2541.
3. Dirisala, V. R., Jeevan, A., Ly, L. H., & McMurray, D. N. (2015). Molecular and

- biochemical characterization of recombinant guinea pig tumor necrosis factor-alpha. *Mediat. Inflamm.*, 2015: 619480.
4. Lasco, T.M., Cassone, L., Kamohara, H., Yoshimura, T., & McMurray, D.N. (2005). Evaluating the role of tumor necrosis factor-alpha in experimental pulmonary tuberculosis in the guinea pig. *Tuberculosis*, 85:245-258.
  5. Jeevan, A., McFarland, C. T., Yoshimura, T., Skwor, T., Cho, H., Lasco, T., & McMurray, D. N. (2006). Production and characterization of guinea pig recombinant gamma interferon and its effect on macrophage activation. *Infect. Immun.*, 74: 213-224.
  6. Dirisala, V. R., Jeevan, A., Bix, G., Yoshimura, T., & McMurray, D. N. (2012). Molecular cloning and expression of the IL-10 gene from guinea pigs. *Gene*, 498: 120-127.
  7. Dirisala, V. R., Jeevan, A., Ly, L. H., & McMurray, D.N. (2013). Prokaryotic expression and in vitro functional analysis of IL-1 $\alpha$  and MCP-1 from guinea pig. *Mol. Biotechnol.*, 54: 312-319.
  8. Dirisala, V. R., Jeevan, A., Ly, L. H., & McMurray, D. N. (2013). Molecular cloning, expression and in silico structural analysis of guinea pig IL-17. *Mol. Biotechnol.*, 55: 277-287.
  9. Omankuttan M, Konatham HR, Dirisala VR, Jeevan A, Mawatwal S, Dhiman R, Ly LH, McMurray D (2019) Prokaryotic Expression, in vitro Biological Analysis and in silico Structural Evaluation of Guinea pig IL-4. *Mol. Biotechnol.*, (In Press)
  10. Zuniga, J., Torres-Garcia, D., Santos-Mendoza, T., Rodriguez-Reyna, T. S., Granados, J., & Yunis, E. J. (2012). Cellular and humoral mechanisms involved in the control of tuberculosis. *Clin. Dev. Immunol.*, 2012: 193923.
  11. Hiroi, M., Sakaeda, Y., Yamaguchi, H., & Ohmori, Y. (2013). Anti-inflammatory cytokine interleukin-4 inhibits inducible nitric oxide synthase gene expression in the mouse macrophage cell line RAW264.7 through the repression of octamer-dependent transcription. *Mediat. Inflamm.*, 2013: 369693.
  12. Rishi, L., Dhiman, R., Raje, M., & Majumdar, S. (2007). Nitric oxide induces apoptosis in cutaneous T-cell lymphomas (HuT-78) by downregulating constituting NF-KB. *Biochim. et Biophys. Acta.*, 1770: 1230-1239.
  13. Global tuberculosis report (2018) World health organization: Global tuberculosis control. Geneva, Switzerland.
  14. Roy, A., Eisenhut, M., Harris, R. J., Rodrigues, L. C., Sridhar, S., Habermann, S., Snell, L., Mangtani, P., Adetifa, I., Lalvani, A., & Abubakar, I. (2014). Effect of BCG vaccination against Mycobacterium tuberculosis infection in children: systematic review and meta-analysis. *The BMJ*, 2014: 349.
  15. Chang, K. C., & Leung, C. C. (2017). BCG Immunization: Efficacy, limitations, and future needs. In: Lu, Y., Wang, L., Duanmu, H., Chanyasulkit, C., Strong, A., Zhang, H. (Eds) *Handbook of Global Tuberculosis Control*. Springer, Boston, MA.
  16. Clark, S., Hall, Y., & Williams, A. (2015). Animal models of tuberculosis: Guinea pigs. *Cold Spring Harb. Perspec. Med.*, 5:018572.



## Pemphigus vegetans: a rare case report

**Inamdar SZ<sup>\*1</sup>, Pradeep R<sup>1</sup>, Akhila M<sup>1</sup>, Jangond A<sup>2</sup>, Pradeepthi K<sup>1</sup>, Kulkarni RV<sup>1</sup>**

<sup>1</sup>Department of Pharmacy Practice, BLDEA's SSM College of Pharmacy and Research Centre, Vijayapur – 586103

<sup>2</sup>Department of Dermatology, Shri B.M.Patil Medical College, Hospital & Research Centre, BLDE (Deemed to be university), Vijayapur-586103

\*For Correspondence Author : syedzia.inamdar@gmail.com

### Abstract

Pemphigus vegetans is a rare vesiculobullous autoimmune disease which is a rare variant of pemphigus vulgaris characterized by vegetating plaques in the flexures and lesions in the oral cavity. It is a less common disease and involves the mucosa and skin due to disintegration of cellular adherence (acantholysis) resulting in intradermal split. The lesions are usually painful and if untreated it may be fatal. A 68 years old male patient was admitted with complaints of fluid filled skin lesions over trunk since 3 months. The lesions later ruptured spontaneously and healed with crusting. The lesions gradually progressed to involve axilla, scalp and extremities with no itching. Successful implementation of dexamethasone –cyclophosphamide –pulse (DCP) therapy along with other adjuvant drugs has induced disease remission.

**Key words:** Pemphigus vegetans, Autoimmune disease, Acantholysis.

### Introduction

Pemphigus vegetans (Pveg) is a rare vesiculobullous autoimmune disease which is a less common variant of pemphigus vulgaris characterized by heaped up, cauliflower like vegetating plaques in the flexures and rarely in oral cavity. This disorder affects chiefly middle aged adults(1,2).It is caused by auto antibodies directed against desmogleins 1 and 3, which are transmembrane glycoprotein's and results in loss

of intercellular adhesion between intact keratinocytes which results in acantholysis. The incidence of the disease is 0.09 to 1.8%. In a study conducted in India majority of pemphigus patients have been diagnosed to have pemphigus vulgaris followed by pemphigus foliaceus, pemphigus erythematosus and pemphigus vegetans. This disease occurs mainly on intertriginous areas, scalp and face but may occur anywhere on the skin surface. The oropharynx, oesophagus, stomach, duodenum, anus, nasal vulvovaginal, laryngeal and conjunctival mucosa can also be affected (3). Oral involvement is reported in 60-80% of pemphigus cases and cerebiform tongue, characterized by a pattern of sulci and gyri of the dorsum of tongue has been reported in 50% cases of Neumann type vegetans (4). In Pemphigus vegetans blisters are fragile that usually rupture and leave an area of erosion and have a tendency to develop excessive granulation tissue and crusting in some patients. A positive Nikolsky sign (positive when gentle shearing pressure to pink or normal looking skin results in the formation of an erosion or extension of bulla) often can be elicited. Possible complications of pemphigus include infection of skin, sepsis, rarely death. Pemphigus isn't contagious and there is no way to predict who will get it.

### Case report

A 68 years old male patient was admitted in dermatology ward with complaints of fluid filled skin lesions over trunk since 3 months. The lesions later ruptured spontaneously to leave

behind raw areas, which got covered with crusts. The lesions gradually progressed to involve axilla, scalp and extremities. The lesions were painful and not associated with itching.

On Cutaneous examination, multiple crusted plaques well noted over anterior and posterior aspect of trunk and lower extremities, vegetating plaques, vesicles and bullae on bilateral axilla, umbilicus and hyper pigmented patches on scalp and upper extremities were observed (Fig. 1 and Fig. 2). Hyper pigmented ridges of the nails and buccal mucosa was observed with few hyper pigmented patches, some of the erosions were secondarily infected with pus formation.

On investigation complete haemoglobin and liver function tests were within normal limits except for mild hypoproteinemia. Culture from pus produced grants of gram positive cocci and gram negative bacilli.

**Diagnosis:** A provisional diagnosis of Pemphigus vegetans was made based on the clinical features. A Tzanck smear was prepared from a fresh vesicle and acantholytes cells were noted. Confirmation by skin biopsy is done after observing suprabasal split in histopathological examination and immunoglobulin G deposits within the epidermis in direct immunofluorescence.

**Medication:** After confirmation of diagnosis, patient was treated with DCP (140 mg of dexamethasone dissolved in 500 ml of 5% dextrose for 3 consecutive days, 500 mg of cyclophosphamide was also given on the second day) After 3 days patient was started on prednisolone 30 mg/day. Patient was also given appropriate antibiotics, calcium supplements, antacids and anti- histamines.

### Discussion

Pemphigus vegetans is a rare autoimmune disease and affects people irrespective of gender. This disease occurs mainly on interiginous areas, scalp and face, Similar to that in the present case patient developed fluid filled lesions initially over trunk which later ruptured and got covered with crusts. The lesions gradually progressed to axilla, scalp and extremities. The aetiology in the present case is unknown. As it is auto immune disease in most cases it is unknown what triggers the disease but the mechanism underlying the pathology is IgG auto antibodies directed against desmogleins , a keratinocytes protein which helps in intercellular adhesion and results in acantholysis histologically and bulla formation clinically. Sometimes, pemphigus develops as a side effect of medications, such as antihypertensive drugs and chelating agents, this



**Fig.1:** Pemphigus vegetans Lesions on neck



**Fig. 2:** Ruptured pemphigus vegetans lesions covered with crusts

type of disease disappears when medication is stopped. A preliminary diagnosis of Pemphigus vegetans was established in the present case on the basis of presenting clinical features and a Tzanck smear test, which reveals multiple acantholytic cells (Tzanck cells). The smear test is quite significant in the early diagnosis of Pemphigus vegetans and can be performed with ease and rapidity (5).

The goal of treatment is to induce complete remission while minimizing treatment related adverse effects. The first priority for patient management is to attain rapid disease control. This is typically achieved through the administration of systemic glucocorticoids. Although systemic glucocorticoids therapy is highly effective, the high doses and long treatment periods that are needed to maintain the clinical response may lead to serious or life-threatening side effects. Introduction of dexamethasone-cyclophosphamide pulse (DCP) therapy for pemphigus group of disorders by Pasricha and Gupta in 1984 has revolutionized the therapy of pemphigus. Administration of suprapharmacologic doses of drugs in an intermittent manner is known as "pulse therapy", which refers to intravenous (IV) infusion of high doses of steroids for one or more days for quicker, better efficacy and to decrease the side effects of long term steroids. The most common side effects of pulse therapy are mood and behavior alteration, hypokalemia, diarrhea, arrhythmias and shock. If administered properly, dexamethasone - cyclophosphamide pulse (DCP) therapy has the potential to affect lifelong recovery from pemphigus (6). In the present case, the patient was managed with dexamethasone - cyclophosphamide pulse (DCP) therapy to control and prevent the development of new lesions. The DCP regimen was followed by oral prednisolone therapy 30mg/day and the patient was managed symptomatically.

### Conclusion

The treatment of Pemphigus diseases is a challenge. However the mortality rate of pemphigus vegetans has reduced with the advent of new therapies and treatment modalities. Appropriate treatment and personal care helped patient to improve health condition. Untreated Pemphigus vegetans is often fatal because of many possible complications hence importance should be given for pemphigus vegetans treatment.

### Acknowledgement

The authors are thankful to the management of BLDE association for the required support.

### REFERENCES

1. Torres T, Ferreira M, Sanches M, Selores M (2009). Pemphigus vegetans in patients with colonic cancer. *Indian journal of Dermatology, Venerology and Leprosy* ; 75:603-605.
2. Dhamija A, D'souza P, Meherda A, Kothiwala RK (2012). Pemphigus vegetans: An unusual presentation. *Indian J Dermatol*; 3: 193-5.
3. Kanawar AJ, DE D (2011). Pemphigus in india. *Indian journal of Dermatology, Venerology and Leprosy* ; 77: 439-49.
4. Nanda S, Grover C, Garg VK, Reddy BS (2005). Pemphigus vegetans of hallopeau. *Indian J Dermatol*; 50:166 – 7.
5. Gupta LK, Singhi MK (2005). Tzanck smear: A useful diagnostic tool. *Indian J Dermatol Venerol Leprol* ; 71:295-9.
6. Abraham A, Roga G, Job AM (2016). Pulse therapy in pemphigus: Ready reckoner. *Indian J Dermatol*; 61:314-7.

## Comparative analysis of biofabricated silver nanoparticles as antibiofilm agents on *Pseudomonas aeruginosa*

Anju .S and Sarada J.

Bhavan's Vivekananda College of Science, Humanities and Commerce,  
Sainikpuri, Secunderabad.

\*For Correspondence author : anjunair227@gmail.com

### Abstract:

Microbial cells in the biofilm were characterized with significant features like antimicrobial resistance and bio fouling properties, which make them distinguishable from their planktonic forms. Although many antimicrobial drugs and antibiotics were reported for biofilm inhibition and dispersal, these compounds had limited applications because of drug resistance. Development of antibiofilm agents which could overcome the drug resistant bacteria had been a challenge over the years. In order to overcome development of drug resistance, silver nanoparticles were being used, to coat the medical devices. This strategy, though successful to some extent, suffer with toxic effects on eukaryotic cells in application .Hence there arises a need to explore natural compounds with antibiofilm activity. Natural products established as antibacterial agents were also found to have quorum quenching activity. *Garcinia* (*Garcinia cambogia*) and *Ginger* (*Zingiber officinale*) extracts were observed to possess quorum quenching activity in the lab, therefore used for biofabrication to enhance the antimicrobial activity of silver nanoparticles. *Pseudomonas aeruginosa* being a most potent biofilm forming bacteria in various environments, like infections, food spoilage and bio fouling in medical devices etc. The study aimed to figure out a novel antibiofilm agent, which could inhibit or eliminate biofilms by using a combination of biologically synthesized nanoparticles and natural quorum quenching agents. Comparative analysis of bio fabricated nanoparticles on the inhibition and dispersal of *Pseudomonas* biofilms

was performed with non fabricated nanoparticles using microtiter based assay, followed by SEM and Flow cell cytometry techniques. Fabricated GNP (fGNP) had showed 17.9% more inhibition which indicates ~ 2 fold enhancement in biofilm inhibition activity .Similarly 9.45% enhancement was found in dispersal activity by fGNP. These results were encouraging us to improve upon the combinatorial approach and to formulate an ideal antibiofilm agent with minimal scope for emergence of antimicrobial resistance.

**Key words:** Silvernanoparticles, biofabrication, *Garcinia cambogia*, *Zingiber officinale* *Pseudomonas aeruginosa*.

### Introduction

Formation of biofilms in different ecosystems has been a dynamic natural event (1). It is recognized as a matrix bound cell population that frequently includes most of the antibiotic resistant species. About 80% of the infectious diseases are biofilm induced. Biofilm formation is a sequential process that is influenced by various factors (4,5). Initially planktonic cells commence attachment to the surface, during which cells are found to uptake inorganic and organic nutrients. Once the cells and substratum interaction is conditioned, exopolysaccharide matrix secretion becomes prominent, that leads to firm attachment. A three dimensional complex is established as part of the maturation of biofilms (17). It develops as an assembly of cell population that function cordially and coherently to transform and represent resistance to many antimicrobial



agents, which they were otherwise susceptible (22). The cells in the biofilm community are recognized to alter physiological processes according to changes in the environment. Some of the cells may get detached from the biofilm, and get adhered to another surface or remain as unbound cells (25). The challenges to overcome the development of multidrug resistant bacteria in biofilms have been a matter of concern. Targeting these biofilms to overcome the resistance posed by the bacteria in the biofilm community has been part of most of the researches that aim to resolve spread of infectious diseases. Strategies that are suggested to fight pathogenic forms in the biofilms are to avoid attachment of cells to surface, disruption of biofilm matrix allowing penetration of antimicrobial substances and inhibition of maturation followed by dispersal (14, 32). Major fraction of biofilms consists of extracellular polymeric substances that comprises of biomolecules, extracellular DNA, exopolysaccharides and proteins. (27, 23).

To target the biofilm bacteria, antibiotics and other chemical drugs has been less effective due to their inability to either penetrate or development of drug resistance. Development of virulence and drug resistance in biofilms is Quorum Sensing(QS) regulated. Potential biofilm agents need to possess antivirulent property along with biofilm inhibition (30). Many compounds with Quorum Quenching activity (QQ) / Quorum Sensing inhibition (QSI) activity are demonstrated to disrupt the virulence factors in microorganisms. It is believed that the proven antimicrobial activity of metal nanoparticles combined with biofabrication through QQ agents can give a new dimension to target the bacterial biofilms (11)

Hence, silver nanoparticles (AgNPs) synthesized from a bacterial and plant source were used in the analysis and evaluated for their antibiofilm activity.

### Materials and Method

**Synthesis of Silver Nanoparticles (AgNPs) from *Garcinia* extract :** 100 g of dried *Garcinia cambogia* fruit rind was used to prepare the

extract in 100ml of milli Q water by boiling it for 15mins. The extract was filtered using Whatmann No.1 filter paper and stored at 4°C in screw cap vials. 1ml of the *Garcinia* extract was added to 100ml of filter sterilized AgNO<sub>3</sub>. It was incubated at room temperature for 5 hrs till there was a visual colour change. (21)

**Extracellular Synthesis of Silver Nanoparticles (AgNPs) from *Bacillus* sps :** *Bacillus subtilis*.SAJSB51 (2) culture reported for extracellular synthesis of AgNPs was used in the study. 1ml of the overnight grown culture supernatant was added to 100ml of filter sterilized AgNO<sub>3</sub> and incubated at room temperature for 20 minutes till there was a visual colour change.(12)

**Quorum quenching activity :** QSI activity of crude extracts of *Garcinia*, *Ginger* along with AgNP's was tested by violacein inhibition assay using *Chromobacterium violaceum* 12472 as bio indicator organism. Nutrient agar plates were pre-seeded with overnight grown culture of bioindicator. 50µl of the sample to be tested were loaded into agar wells made in the plate and incubated overnight at 30°C. The QSI activity was observed as colourless zone of inhibition of violacein pigment but not the growth (16; 28).

**Characterization of AgNP's :** Formation of nano silver was established by determining the optical density values for wavelength range of 300-600nm in a UV-Visible spectrophotometer (SYSTRONICS 117). The reduced silver nitrate solution was concentrated in the ROTOVAC for 2hrs and then subjected to FTIR analysis. Spectrum was recorded in the range of 4000-500cm<sup>-1</sup> using a SHIMADZU FTIR Spectrophotometer. The scanning data was obtained after 10 scans. The size and shape of the AgNP's was determined by Scanning Electron Microscopy using (SEM) S-3700 with accelerating voltage of 30000 Volts, emission current 82000nA and a magnification of 5000. (19)

**Fabrication of AgNPs with extract of *Zingiber officinale* :** Fresh *Ginger* was ground to make aqueous extract. This extract was filtered using a



disposable filter of 0.2 microns; fabrication of these nanoparticles was made by soaking the partially purified nanoparticles for 72hrs. The nanoparticles were centrifuged and dried for further analysis. (10, 3)

**Quantitative assay for biofilm inhibition :**

Biofilm inhibition assay was carried out in flat bottomed 96-wells microtitre plates. *Pseudomonas* culture (laboratory isolate) was inoculated in sterile 50ml of King's-B broth in an 100ml Erlenmeyer flask and incubated at 37°C for 24 hours under aerobic condition for the assay. 200 µl overnight grown culture was added into microtiter plates followed by 25µl and 50µl suspension of AgNPs, GNP's and fGNP's from stock solution of 10mg/ml were added to evaluate their antibiofilm inhibition activity. After setting with appropriate controls microtiter plate was incubated at 37°C for 48hrs. Microtiter plates were decanted after the incubation, and were stained with 50 µl of 0.1% crystal violet for 5 min. After rinsing twice with 200 µl of sterile water, the bound dye was removed from the stained cells using 200 µl of 70% acetic acid (26). Biofilm inhibition was quantified by measuring optical density of the suspension at 630 nm using a micro plate reader.

**Quantitative assay for biofilm dispersal :** For evaluating the biofilm dispersal activity, 25µl and 50µl suspension of three types of AgNPs along with control samples were added after 24hr incubation of the culture suspension in the microtiter plate. Biofilm dispersal was quantified by measuring the optical density after staining and destaining steps as mentioned above.

**SEM imaging to visualize the antibiofilm activity :** Culture samples treated with antibiofilm agents were subjected to SEM analysis to capture images showing inhibition in biofilm formation and dispersal activity with untreated controls. (34)

**Evaluation of bacterial cell viability after antibiofilm treatment by flow cytometry :** The biofilms of *Pseudomonas* treated with Ginger extract, AgNPs and fabricated AgNPs were analysed with a *BacLight Live/dead invitrogen Kit* to evaluate the percentage of live and dead bacteria

after the treatment. Samples were treated with green fluorescent dye CYTO9 and red fluorescent dye Propidium iodide (31,33).

**Results:**

*Garcinia cambogia* commonly known as Malabar tamarind is popularly used as a food preservative in many of the cuisines due to its antimicrobial activity. The fruit rind extract was observed to possess quorum quenching activity when tested in the laboratory. Hence it was used to synthesize AgNP's for bio fabrication and referred as GNP's. During initial screening of plant extracts for antibiofilm activity, it was also observed that *Ginger* (*Zingiber officinale*) extract had the potential of biofilm inhibition & dispersal activity. Interestingly it also has QSI activity when tested with the bio indicator organism (Figure 1). The intention in selecting these extracts for the study as they possess good antimicrobial activity along with QQ (Quorum Quenching) activity and normally used in diet as spices or as flavour enhancers.

**Characterization of AgNP's :** AgNP's synthesized from extract of *Garcinia* fruit rind and *Bacillus* culture supernatant were visually identified by the colour change from colourless to dark brown after 5hrs of incubation at room temperature (Figure.2).

UV-Visible spectroscopy analysis revealed the peaks between 300nm and 500nm. FTIR analysis generated peaks 1361.79, 1384.94, 1635.69, 2852.81, 3423.76, 3444.98 signifying the interaction of the groups C-N stretch, Aromatic groups, Primary and Secondary Amines, Aromatic stretch, Carboxylic acids respectively signifying the interactions with the amino acid domains. The SEM analysis revealed presence of spherical shaped AgNP's of different sizes. The sizes GNP's synthesized were 77.7nm, 74.7nm, 74.4nm, 110nm and 124nm (Figure 3). BNP's were of sizes 56.5nm, 68.1nm, 70.3nm, 77.1nm, 79.6nm, 89nm, 9nm, 119nm (Figure 4).

**Microtiter plate assays:** Assay was carried out in triplicates in a 96 well microtiter plate using overnight grown culture of *Pseudomonas*

Table 1 Antibiofilm activity of BNP & GNP				
Types of AgNp's	% of Biofilm Inhibition		% of Biofilm Dispersal	
	25µg/ml	50µg/ml	25µg/ml	50µg/ml
BNP	20.6	31.8	1.8	5.4
GNP	24.1	40.7	1.2	24.1

Table 1 Antibiofilm activity of BNP & GNP				
Types of AgNp's	% of Biofilm Inhibition		% of Biofilm Dispersal	
	25µg/ml	50µg/ml	25µg/ml	50µg/ml
BNP	20.6	31.8	1.8	5.4
GNP	24.1	40.7	1.2	24.1

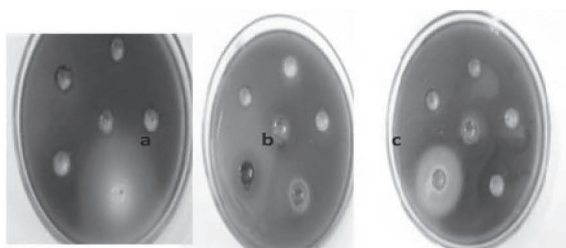


Figure 1: Quorum quenching (QQ) activity of (a) GNP (b) Ginger Extract (c) Garcinia Extract

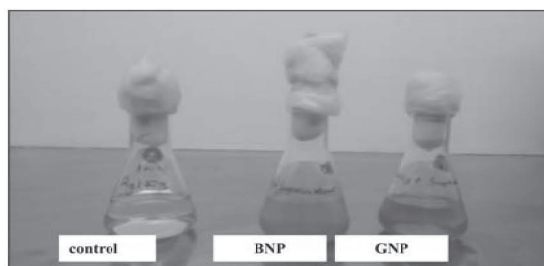


Figure 2: AgNP's Formation showing visual colour change

*aeruginosa*. Biofilm inhibition activity was evaluated using 200 µl of overnight grown *Pseudomonas* culture was mixed with 50µg/ml and 25µg/ml of BNP & GNP samples. After 48-hrs of incubation, the inhibition of treated samples were evaluated by measuring the optical density after staining and destaining steps as per the protocol (4, 26). Average values of triplicates were used to calculate the percentage of inhibition using untreated samples as control and results were represented in table 1. Among the two nanoparticles ( Table 1 & Figure 5 ), AgNp's from

*Garcinia* (GNP) showed enhanced biofilm inhibition (40.7%) than bacterial silver nanoparticles(BNP) (31.8%).

Dispersal assay was carried out by growing culture in King B medium in microtiter plates .After the 48 hrs of incubation, i.e after the biofilm formation the cultures were treated with the 50µg/ml and 25µg/ml AgNP's synthesized from *Garcinia* and *Bacillus Sps*. Dispersal activity of the samples was analysed by measuring the optical density (4, 26). Average values of triplicates were used to calculate percentage of dispersal using untreated samples as control and results were

represented in Table 1. From the data it is observed that GNP's had higher dispersal activity(40.7%) than BNP's (24.1%) at same concentration . (Figure 6) Present data reveals the fact that GNP's had potential for antibiofilm agent as they show biofilm inhibition& dispersal activity better than BNP's.(Table 1)

SEM images (Figure 7) were procured in order to visualize the treated biofilms matrix. From the SEM pictures,biofilm inhibition activity of GNP is more evident than the BNP's. Biofilm matrix was observed to be more inhibited with GNP's when compared with control *Pseudomonas* culture. BNP's show comparatively lesser amount of inhibition .This could be attributed to the phytocomponents present in *Garcinia* extract. Present data stands in support of the observation made in Microtiter plate assays.

**Biofabrication:** In order to enhance the potential of GNP's, bio fabrication with another natural antibiofilm agent was carried out. *Ginger* extract (*Zingiber officinale*) was identified with potential to inhibit *Pseudomonas* biofilms in preliminary screening of plant extracts in the laboratory. *Ginger* possess strong antioxidant, antibacterial, antifungal, anticancer and anti-inflammatory effect and used in food industry to prevent food spoilage. It was also identified as quorum sensing inhibitor. Hence this extract was used to further enhance the potential of GNP & BNP's as antibiofilm agents by bio fabrication. In present study, aqueous extract was used for biofabrication by soaking partially purified BNP's & GNP's for 72hrs. These nanoparticles were centrifuged and dried for further analysis.

AgNP's from *Garcinia* fabricated with *Ginger* extract was designated as fGNP while AgNP's synthesized by Bacteria was designated as fBNP's and used for evaluation of biofilm inhibition and dispersal activity testing. Microtiter plate based assays were performed to quantify the percentage of inhibition and dispersal activity as mentioned above. The data acquired in these experiments were represented in table 2 ,and Figure 5 . fGNP's depicted an increased biofilm inhibition activity i.e 70.5% after fabrication

whereas fBNP's showed only 29.4% inhibition. These results are in support of view that a combination of antimicrobial agent with QSI and antibiofilm activity would posses enhanced potential as antibiofilm agent. Dispersal activity of fGNP's was 31.25% when tested, whereas fBNP showed only 21.8% activity. Interestingly both type of fabricated depicted two –three fold enhanced activity at 50µg/ml when tested. (Table 2) (Figure 6).

**SEM analysis :** Biofilm images (Figure 8) were captured using scanning electron microscopy, for the fGNPs and fBNPs along with control culture. Biofilm network with cells trapped inside the matrix were seen in control. Samples treated biofabricated nanoparticle were found to have lost the integrity of the matrix and not many cells could be visualized in the SEM images after treatment.

#### **Evaluation of bacterial viability using Flow cytometry analysis**

After evaluating the biofilm inhibition and dispersal activity of fabricated GNP's & BNP's in microtiter plate assays and SEM analysis, attempts were made to understand the impact of these particles on *Pseudomonas* biofilms by studying the number of live and dead cells after the treatment. For this purpose, Invitrogen BacLight Viability Kit was used followed by flow cytometric analysis. Purpose of this analysis was to calculate the percentage of cell death caused by fabricated nanoparticles. Samples were treated with green fluorescent dye SYTO9 which was known to stain live cells alone and red fluorescent dye Propidium iodide specifically stain dead cells( 31). 2X working solution of Live/Dead BacLight staining reagent mixture was prepared and *Pseudomonas* culture was diluted with saline in order to obtain 400cells/µl. Standardization of remittance of fluorescence was carried out by mixing 400 µl (400cells/µl) with 3 µl of individual working solutions of staining dyes. Samples treated with GNP, fGNP and crude *Ginger* extract were prepared for flow cytometry by adding the staining mixtures for analysis .(Figure 9) has the analysis indicating percentage of live and dead cells. Flow cytometric analysis

gave clear picture regarding difference in the treatment of culture with fGNP & GNP. fGNPs showed 67.0% live cells and 20.3% of cells had early apoptosis while the GNP's treated samples showed 67.9% live cells. Early apoptotic cell death rate had been enhanced to 21.6%. Since Ginger extract was used to fabricate AgNP, its inhibition on growth was determined and found to be 12.5% induction of early apoptosis. The control (untreated cells) showed 7.18% early apoptosis which can be considered while evaluating the effect of antibiofilm agents. It was observed that there was 16.8% and 19% more death of cells when compared with the untreated control in case of

GE (ginger extract) and GNP respectively. However, the death rate increased to 20% when it was treated with fGNP. Induction of early apoptosis in treated samples than untreated was also noticed (Figure 11)

**Discussion:**

*P.aeruginosa* has the ability to survive in adverse conditions like scarcity of nutrients as well as stringent physical conditions. It is liable for both acute and chronic infections. Apart from having natural resistance to numerous drugs, its ability to form biofilm render this organism to

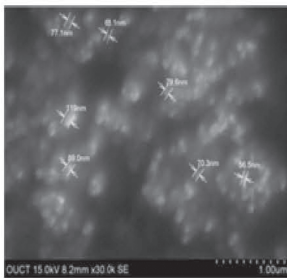


Figure 3: GNPs

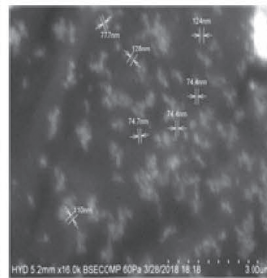


Figure 4: BNPs

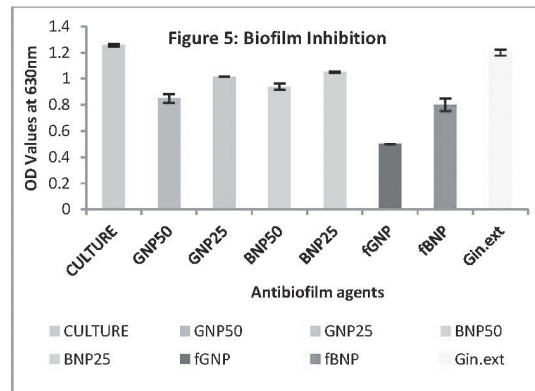


Figure : 5

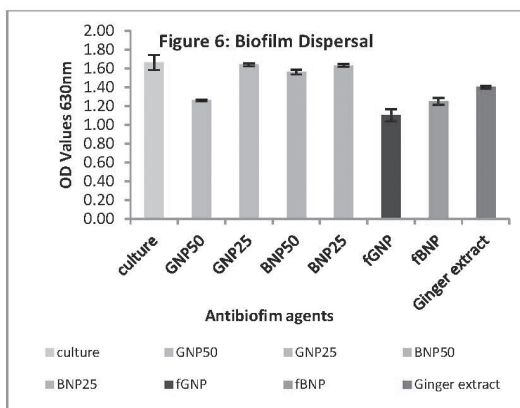


Figure : 6

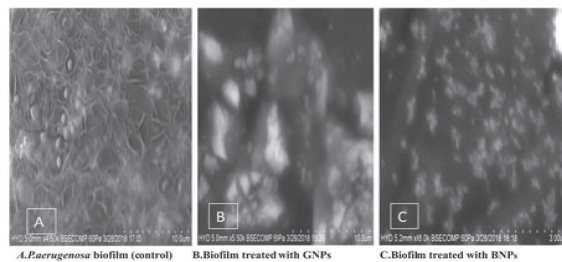
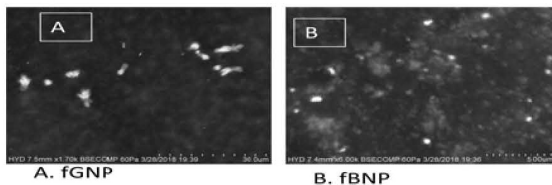
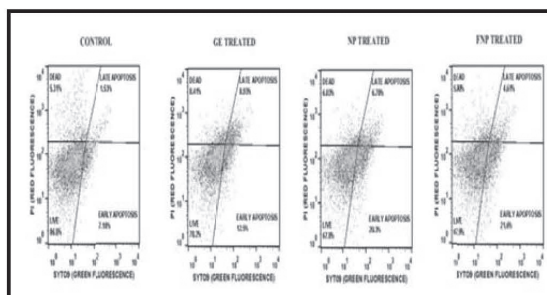


Fig. 7: SEM images of Pseudomonas biofilms treated with GNP & BNPs





**Figure 8.** SEM images treated with fabricated Nanoparticles



**Figure 9:** Flow Cytometric analysis of biofilms culture treated with GNP before and after fabrication.

unproductive antibiotic therapy (15, 1, 8). Strategies to control biofilm related infections can be either by inhibiting biofilm formation, dispersal, or by quenching quorum sensing mechanisms. Prevention of biofilm formation may not be always necessary to inhibit the growth alone but use strategies to disrupt the bacterial signalling. QS signalling is integral to biofilm formation as it is important for development of complex network of matrix. Current study aims to target this pathogen by a novel combination of biofilm inhibition with biocidal and QSI activity, that could make an effective anti biofilm agent (9).

With development of nanobiotechnology, use of biologically synthesized nanoparticles in various fields acts as a novel element to deal with antimicrobial resistance (5, 20). Biologically synthesized nano particles are elevated in properties, with the bioactive compounds that get associated with them during the production. In the present study, AgNP that has been made by green synthesis were further customized to enhance their antibiofilm activity. Earlier research, has established biocidal activity of several metal

nanoparticles, and among them silver nanoparticles is found to have a prominent action against many pathogenic bacteria (29, 36). Silver nanoparticles are being used, to coat the medical devices used for implantation, in order to inhibit the formation of biofilms. (19, 37)

Among the different AgNPs that has been biologically synthesized in the lab, initially comparative analysis of antibiofilm activity of BNP (extracellularly synthesized AgNP from *Bacillus* sps.) and GNP (AgNP from *Garcinia cambogia*) was carried out. This was to establish the difference in biocidal and quenching activity of AgNP formed from the plant extracts and bacterial supernatant. AgNPs as antibiofilm and quenching agents, these were used in a combination to make more effective in inhibiting or dispersing *Pseudomonas* biofilms.

During the screening of natural quorum quenching (QQ) agents, *Garcinia* extract was identified to have a prominent antibiofilm activity. *Garcinia cambodia* is known to have antibacterial activity on various infectious pathogens and food spoilage microorganisms (21). Hence, *Garcinia* commonly known as, *Malabar Tamarind* is traditionally used as a preservative in various cuisines.

The Ginger rhizome has phenolic compounds, volatile sesquiterpenes and monoterpenoids which were reported to inhibit *P. aeruginosa* biofilm formation. These compounds were involved to effect c-di-GMP production which in turn reduces biofilm matrix development. The major component zingerone (vanillyl acetone), showed to inhibit biofilm formation, and swimming as well as swarming in *Pseudomonas* (6).

In the present study after establishing the antibiofilm activity of aqueous Ginger extract, it was used to fabricate the GNP's. During fabrication GNP were soaked in the Ginger extract for 48 hrs in order to encapsulate the nanoparticles with the active compounds of Ginger that can enhance the QQ activity for GNP. This Fabricated GNP (fGNP) had showed 17.9% more inhibition which indicates ~ 2 fold enhancement in biofilm inhibition activity



.Similarly 9.45% enhancement was found in dispersal activity by fGNP. These results were encouraging us to improve upon the combinatorial approach and to formulate an ideal antibiofilm agent with minimal scope for emergence of antimicrobial resistance (13, 35).

Analysis by flow cytometry could reflect the biocidal action of the AgNPs by evaluating the live and dead cell ratios after treatment with fGNP and GNP. This was helpful to show the role of QQ agent against biofilm forming bacteria. There has been an enhanced antibiofilm activity (70.5% biofilm reduction) with fGNP when compared to GNP (40.7% biofilm reduction). But the Live/Dead cell ratios have not shown much difference with fabricated and non fabricated AgNP. From these results it is evident that additional factor like QSI activity other than biocidal action could be further explored to formulate an ideal anti biofilm agent.

Though individually both the AgNPs have been established with the quorum quenching activity (2), it would be beneficial to formulate an ideal AgNP after figuring the type of nanoparticles that have more potential antibiofilm activity. 8.9 % more biofilm inhibition activity for GNP was noticed than with BNP. In case of dispersal activity GNP showed 18.7% more activity than BNP. The results obtained indicated that GNP's were identified to have more potential than BNP's.

Since biofilm formation could be also targeted by quorum quenching activity, *Garcinia* and *Ginger* extracts alone were screened for antibiofilm activity in the lab. Quorum quenching activity of these extracts were proven by testing with standard strain of *Chromobacterium violaceum* 12472. In order to enhance the GNP activity, biofabrication with *Ginger* extract was done. Having established the individual abilities of *Garcinia* extract, and *Ginger* extract, AgNPs as antibiofilm and quenching agents, these were used in a combination to make more effective in inhibiting or dispersing *Psuedomonas* biofilms.

During the screening of natural quorum quenching (QQ) agents, *Garcinia* extract was

identified to have a prominent antibiofilm activity. *Garcinia cambodia* is known to have antibacterial activity on various infectious pathogens and food spoilage microorganisms (21). Hence, *Garcinia* commonly known as, *Malabar Tamarind* is traditionally used as a preservative in various cuisines.

The Ginger rhizome has phenolic compounds, volatile sesquiterpenes and monoterpenoids which were reported to inhibit *P. aeruginosa* biofilm formation. These compounds were involved to effect c-di-GMP production which in turn reduces biofilm matrix development. The major component zingerone (vanillyl acetone), showed to inhibit biofilm formation, and swimming as well as swarming in *Psuedomonas*. (6,7).

In the present study after establishing the antibiofilm activity of aqueous Ginger extract, it was used to fabricate the GNP's. During fabrication GNP were soaked in the Ginger extract for 48 hrs in order to encapsulate the nanoparticles with the active compounds of Ginger that can enhance the QQ activity for GNP. This Fabricated GNP (fGNP) had showed 17.9% more inhibition which indicates ~ 2 fold enhancement in biofilm inhibition activity. Similarly 9.45% enhancement was found in dispersal activity by fGNP. These results were encouraging us to improve upon the combinatorial approach and to formulate an ideal antibiofilm agent with minimal scope for emergence of antimicrobial resistance (13)

Analysis by flow cytometry could reflect the biocidal action of the AgNPs by evaluating the live and dead cell ratios after treatment with fGNP and GNP. This was helpful to show the role of QQ agent against biofilm forming bacteria. There has been an enhanced antibiofilm activity (70.5% biofilm reduction) with fGNP when compared to GNP (40.7% biofilm reduction). But the Live/Dead cell ratios have not shown much difference with fabricated and non fabricated AgNP. From these results it is evident that additional factor like QSI activity other than biocidal action could be further explored to formulate an ideal anti biofilm agent.

### Conclusion

Until now most of the studies that have been reported to target *Pseudomonas aeruginosa* biofilms by fabricated AgNP, are mostly in combination with antibiotics (24, 27, 18). This study introduces an innovative concept of fabricating biologically synthesized AgNP with QSI agents. This approach aims to overcome the development of antimicrobial resistance in biofilms bacteria and also minimize the toxicity of nanomaterial to eukaryotic cells by encapsulating them with natural QQ substances. Future studies would focus on raising the efficacy of fAgNP and establishing the components of *Garcinia* that targets the biofilm development.

### Acknowledgements

We thank Head, Department of Microbiology and Management of Bhavan's Vivekananda College for support and encouragement extended for research.

### References:

1. Allaker, R. P. (2010). The use of nanoparticles to control oral biofilm formation. *Journal of dental research*, 89(11), 1175-1186.
2. Anju, S., & Sarada, J. (2016). Quorum sensing inhibiting activity of silver nanoparticles synthesized by Bacillus isolates. *Int J Pharm Bio Sci*, 6, 47-53.
3. Auta, K. I., Galadima, A. A., Bassey, J. U., Olowoniyi, O. D., Moses, O. O., & Yako, A. B. (2011). Antimicrobial properties of the ethanolic extracts of Zingiber officinale (Ginger) on Escherichia coli and Pseudomonas aeruginosa. *Research Journal of Biological Sciences*, 6(1), 37-39.
4. Azeredo, J., Azevedo, N. F., Briandet, R., Cerca, N., Coenye, T., Costa, A. R., ... & Kačániová, M. (2017). Critical review on biofilm methods. *Critical reviews in microbiology*, 43(3), 313-351.
5. Baelo, A., Levato, R., Julián, E., Crespo, A., Astola, J., Gavaldà, J., ... & Torrents, E. (2015). Disassembling bacterial extracellular matrix with DNase-coated nanoparticles to enhance antibiotic delivery in biofilm infections. *Journal of Controlled Release*, 209, 150-158.
6. Bezalwar, P. M., & Shuddhalwar, P. P. (2015). A quest of anti-biofilm activity of zingiber officinale root and Coriandrum sativum seed extract against clinical isolates of Pseudomonas aeruginosa and Staphylococcus aureus. *Int. J. Sci. Res*, 4(2581), e2584.
7. Bhargava, S., Dhabhai, K., Batra, A., Sharma, A., & Malhotra, B. (2012). Zingiber officinale: Chemical and phytochemical screening and evaluation of its antimicrobial activities. *J. Chem. Pharm. Res*, 4(1), 360-364.
8. Billings, N., Millan, M. R., Caldara, M., Rusconi, R., Tarasova, Y., Stocker, R., & Ribbeck, K. (2013). The extracellular matrix component Psl provides fast-acting antibiotic defense in Pseudomonas aeruginosa biofilms. *PLoS pathogens*, 9(8), e1003526.
9. Brackman, G., & Coenye, T. (2015). Quorum sensing inhibitors as anti-biofilm agents. *Current pharmaceutical design*, 21(1), 5-11.
10. Chaturvedi, V., & Verma, P. (2015). Fabrication of silver nanoparticles from leaf extract of Butea monosperma (Flame of Forest) and their inhibitory effect on bloom-forming cyanobacteria. *Bioresources and Bioprocessing*, 2(1), 18.
11. Chen, M., Yu, Q., & Sun, H. (2013). Novel strategies for the prevention and treatment of biofilm related infections. *International journal of molecular sciences*, 14(9), 18488-18501.
12. Das, V. L., Thomas, R., Varghese, R. T., Soniya, E. V., Mathew, J., & Radhakrishnan, E. K. (2014). Extracellular synthesis of silver

- nanoparticles by the Bacillus strain CS 11 isolated from industrialized area. *3 Biotech*, 4(2), 121-126.
13. Deacon, J., Abdelghany, S. M., Quinn, D. J., Schmid, D., Megaw, J., Donnelly, R. F., ... & Taggart, C. C. (2015). Antimicrobial efficacy of tobramycin polymeric nanoparticles for Pseudomonas aeruginosa infections in cystic fibrosis: Formulation, characterisation and functionalisation with dornase alfa (DNase). *Journal of Controlled Release*, 198, 55-61.
  14. Desrousseaux, C., Sautou, V., Descamps, S., & Traoré, O. (2013). Modification of the surfaces of medical devices to prevent microbial adhesion and biofilm formation. *Journal of hospital Infection*, 85(2), 87-93.
  15. Duong, H. T., Jung, K., Kutty, S. K., Agustina, S., Adnan, N. N. M., Basuki, J. S., ... & Boyer, C. (2014). Nanoparticle (star polymer) delivery of nitric oxide effectively negates Pseudomonas aeruginosa biofilm formation. *Biomacromolecules*, 15(7), 2583-2589.
  16. Fatima, Q., Zahin, M., Khan, M. S. A., & Ahmad, I. (2010). Modulation of quorum sensing controlled behaviour of bacteria by growing seedling, seed and seedling extracts of leguminous plants. *Indian journal of microbiology*, 50(2), 238-242.
  17. Flemming, H. C., & Wingender, J. (2010). The biofilm matrix. *Nature Reviews Microbiology*, 8(9), 623.
  18. Forier, K., Raemdonck, K., De Smedt, S. C., Demeester, J., Coenye, T., & Braeckmans, K. (2014). Lipid and polymer nanoparticles for drug delivery to bacterial biofilms. *Journal of Controlled Release*, 190, 607-623.
  19. Franci, G., Falanga, A., Galdiero, S., Palomba, L., Rai, M., Morelli, G., & Galdiero, M. (2015). Silver nanoparticles as potential antibacterial agents. *Molecules*, 20(5), 8856-8874.
  20. Hasan, J., Crawford, R. J., & Ivanova, E. P. (2013). Antibacterial surfaces: the quest for a new generation of biomaterials. *Trends in biotechnology*, 31(5), 295-304.
  21. Jacob, K. M. P., Ali, M. A., Vishnu, H., Shylaja, G., Mythili, S., & Sathivelu, A. (2015). Evaluation of Antibacterial and Antioxidant Activity of Garcinia gummitutta. *Int. J. Drug Dev. Res*, 7, 57-59.
  22. Kim, H. S., & Park, H. D. (2013). Ginger extract inhibits biofilm formation by Pseudomonas aeruginosa PA14. *PLoS one*, 8(9), e76106.
  23. Kostakioti, M., Hadjifrangiskou, M., & Hultgren, S. J. (2013). Bacterial biofilms: development, dispersal, and therapeutic strategies in the dawn of the postantibiotic era. *Cold Spring Harbor perspectives in medicine*, 3(4), a010306.
  24. Loo, C. Y., Young, P. M., Cavaliere, R., Whitchurch, C. B., Lee, W. H., & Rohanizadeh, R. (2014). Silver nanoparticles enhance Pseudomonas aeruginosa PAO1 biofilm detachment. *Drug development and industrial pharmacy*, 40(6), 719-729.
  25. Oliveira, N. M., Martinez-Garcia, E., Xavier, J., Durham, W. M., Kolter, R., Kim, W., & Foster, K. R. (2015). Biofilm formation as a response to ecological competition. *PLoS biology*, 13(7), e1002191.
  26. O'toole, G. A., & Kolter, R. (1998). Initiation of biofilm formation in Pseudomonas fluorescens WCS365 proceeds via multiple, convergent signalling pathways: a genetic analysis. *Molecular microbiology*, 28(3), 449-461.
  27. Rasamiravaka, T., Labtani, Q., Duez, P., & El Jaziri, M. (2015). The formation of biofilms by Pseudomonas aeruginosa: a review of

- the natural and synthetic compounds interfering with control mechanisms. *BioMed research international*, 2015.
28. Rutherford, S. T., & Bassler, B. L. (2012). Bacterial quorum sensing: its role in virulence and possibilities for its control. *Cold Spring Harbor perspectives in medicine*, 2(11), a012427.
  29. Seil, J. T., & Webster, T. J. (2012). Antimicrobial applications of nanotechnology: methods and literature. *International journal of nanomedicine*, 7, 2767.
  30. Soto, S. M. (2014). Importance of biofilms in urinary tract infections: new therapeutic approaches. *Advances in biology*, 2014.
  31. Stiefel, P., Schmidt-Emrich, S., Maniura-Weber, K., & Ren, Q. (2015). Critical aspects of using bacterial cell viability assays with the fluorophores SYTO9 and propidium iodide. *BMC microbiology*, 15(1), 36.
  32. Vlamakis, H., Chai, Y., Beaugregard, P., Losick, R., & Kolter, R. (2013). Sticking together: building a biofilm the *Bacillus subtilis* way. *Nature Reviews Microbiology*, 11(3), 157.
  33. Webb, J. S., Thompson, L. S., James, S., Charlton, T., Tolker-Nielsen, T., Koch, B., & Kjelleberg, S. (2003). Cell death in *Pseudomonas aeruginosa* biofilm development. *Journal of bacteriology*, 185 (15), 4585-4592.
  34. Yang, J. L., Li, Y. F., Liang, X., Guo, X. P., Ding, D. W., Zhang, D., ... & Dobretsov, S. (2016). Silver nanoparticles impact biofilm communities and mussel settlement. *Scientific reports*, 6, 37406.
  35. Zhao, Y., Tian, Y., Cui, Y., Liu, W., Ma, W., & Jiang, X. (2010). Small molecule-capped gold nanoparticles as potent antibacterial agents that target gram-negative bacteria. *Journal of the American Chemical Society*, 132 (35), 12349-12356.
  36. Zhu, X., Radovic-Moreno, A. F., Wu, J., Langer, R., & Shi, J. (2014). Nanomedicine in the management of microbial infection—overview and perspectives. *Nano today*, 9(4), 478-498.
  37. Zodrow, K., Brunet, L., Mahendra, S., Li, D., Zhang, A., Li, Q., & Alvarez, P. J. (2009). Polysulfone ultrafiltration membranes impregnated with silver nanoparticles show improved biofouling resistance and virus removal. *Water research*, 43(3), 715-723.

## Statistical optimization of PolyHydroxy Butyrate (PHB) production by novel *Acinetobacter nosocomialis* RR20 strain using Response Surface Methodology

Ranganadha Reddy A<sup>1</sup>, Vidya Prabhakar K<sup>2</sup>, Venkateswarulu TC<sup>1</sup>, Krupanidhi S<sup>1</sup>,  
Md. Nazneen Bobby, Abraham Peele K, P. Sudhakar<sup>3</sup>, P. Vijetha<sup>4</sup>

<sup>1</sup>. Department of Biotechnology, VFSTR University, Guntur, Andhrapradesh, India 522 213

<sup>2</sup>. Department of Biotechnology, VS University, SPSR Nellore, Andhrapradesh, India 524 320

<sup>3</sup>. Department of Biotechnology, ANU University, Guntur, Andhrapradesh, India 522 510

<sup>4</sup>Department of Chemical Engineering, VFSTR University, Guntur, Andhrapradesh, India 522 213

Email: arr\_bt@vignan.ac.in, rangaaluri@gmail.com

### Abstract

Eco-friendly biopolymers, polyhydroxybutyrate, have been produced by many kinds of bacteria that possess most important applications in food packaging industries and also in medical field. In the present work, PHB production was economized through the statistical optimization of physical variables. The physical variables chosen for the enhanced production of PHB were incubation period, temperature, pH and inoculums size. The relative rate of production has been studied by understanding the complex interactions of variables using face-centred central composite design. The submerged fermentation with *Acinetobacter nosocomialis* RR20 produced PHB yield of 5.88 g/L at optimized conditions with a notable value change of sixfold increase in comparison with minimal salt medium and these findings have showed that the designed medium was significant in terms of higher of PHB production.

**Keywords** Polyhydroxybutyrate · *Acinetobacter nosocomialis* RR20 strain · Response surface methodology · Shake flask culture

### INTRODUCTION

Polyhydroxyalkanoates (PHA) are bioplastics which are nothing but a group of polyesters. They tend to accumulate as carbon reserves when exposed to low growth nutrient

availability in their surroundings such as phosphorus and nitrogen by many microorganisms intracellularly. PHB's are derivative of PHA's that have been profusely studied and thoroughly characterized. They are similar to traditional petroleum plastics such as polyethylene and polypropylene. This property has gained them much interest in past few decades. PHB is observed to be produced by many gram negative as well as gram positive bacterial species including *Alcaligenes caviae*, *Bacillus megaterium*, *Ralstonia eutropa*, *Bacillus subtilis* and *Pseudomonas putida* [1-2]. PHB homopolymers can be easily manipulated due to their short chain ring flexibility and low crystallinity. PHB polymers can also be produced by co-supplementing carbon sources leading to the construction of novel biopolymers including distinctive properties. Production of PHB has been a prime obstacle in replacing the traditional plastics with bioplastics masking all its advantages due to expensive production costs. Hence variety of approaches have been proposed to tackle this case regarding optimization approach and PHB utilizing waste materials. PHB production is highly affected by various physical, chemical and biological aspects [3-5]. Response surface methodology (RSM) is a suitable tool for investigating the effects of variables [6]. In the past, some studies have been reported the production of PHB by RSM from a variety of bacterial strains [7-8]. There was no evidence showing the previous work for medium optimization



of PHB production using RSM from *Acinetobacter nosocomialis* species. Considering the potency of the incubation period (A), temperature (B) pH (C) and inoculums size (D).

### MATERIALS AND METHODS

**Microorganism :** *Acinetobacter nosocomialis* RR20 used for the study was isolated from municipal sewage waste, Guntur, Andhrapradesh, India. Partial 16s RNA sequence of *Acinetobacter nosocomialis* RR20 was submitted to NCBI and provided with GenBank accession number KY913802. RR20 Strain was preserved as glycerol stock in our laboratory for future studies.

**Shake flask fermentation :** The liquid fermentation was conducted batch wise in 250 ml conical flask using 100 ml of mineral salt medium and is sterilized at 121°C for 15 min. Conical flasks were inoculated with 3% inoculums, incubated at 37 °C on rotary shaker driven at 150 rpm. The growth condition levels of incubation time, temperature, pH and inoculums size used in the optimization study, by an application of response surface methodology are given in Table 1.

**PHB assay Extraction and Quantification of PHB :** Extraction of PHB from fermented broth was done as per the method of Umesh et al., [9] using chloroform. *Acinetobacter nosocomialis* RR20 was grown in the culture medium. The cells were harvested by centrifugation at 10,000g for 10 min. The cell pellet was treated with 4% sodium hypochlorite solution and incubated at 37 °C for 45 min. Centrifugation of bacterial culture was carried out at 10,000g for 5 min to obtain the biopolymer followed by sequentially washing with phosphate buffer saline, distilled water and acetone-diethyl ether mixture (1:1 ratio). The resultant PHB granules were dissolved in boiling chloroform (80°C) and solvent was evaporated using rotary vacuum evaporator. Quantification of extracted PHB (grams per litre) was carried out by using crotonic acid assay with commercial PHA (Sigma-Aldrich) as reference standard [10].

**Optimization by Response Surface Methodology (RSM) :** RSM is a tool in Design

Expert software (Version 7.0.0, Stat-Ease Inc., Minneapolis, USA) and is used to optimize physical components of fermentation medium, namely where Y is dependent variable (PHB production) and X<sub>1</sub>, X<sub>2</sub>, X<sub>3</sub> and X<sub>4</sub> are independent variables (incubation time, temperature, pH and inoculums size respectively),  $\hat{a}_0$  is an intercept term,  $\beta_1, \beta_2, \beta_3$  and  $\beta_4$  are linear coefficients,  $\beta_{12}, \beta_{13}, \beta_{14}, \beta_{23}, \beta_{24}$  and  $\beta_{34}$  are the interaction coefficients, and  $\beta_{11}, \beta_{22}, \beta_{33}$  and  $\beta_{44}$  are the quadratic coefficients. Different levels, low (-1), medium (0) and high (+1), were used to study the independent variables. The experimental design used for this study is presented in Table 1. The effect of variables and regression analysis of experimental data was performed.

The following second-order polynomial equation explains relationship between dependent and independent variables:

$$Y = \beta_0 + \beta_1 X_1 + \beta_2 X_2 + \beta_3 X_3 + \beta_4 X_4 + \beta_{12} X_1 X_2 + \beta_{13} X_1 X_3 + \beta_{14} X_1 X_4 + \beta_{23} X_2 X_3 + \beta_{24} X_2 X_4 + \beta_{34} X_3 X_4 + \beta_{11} X_1^2 + \beta_{22} X_2^2 + \beta_{33} X_3^2 + \beta_{44} X_4^2$$

where Y is the predicted response (PHB yield);  $\beta_0$  is the intercept term; X<sub>1</sub>, X<sub>2</sub>, X<sub>3</sub> and X<sub>4</sub> are independent variables;  $\beta_1, \beta_2, \beta_3$  and  $\beta_4$  are linear coefficients;  $\beta_{12}, \beta_{13}, \beta_{14}, \beta_{23}, \beta_{24}$  and  $\beta_{34}$  are the interaction coefficients;  $\beta_{11}, \beta_{22}, \beta_{33}$  and  $\beta_{44}$  are the quadratic coefficients [11].

### RESULTS AND DISCUSSION

**Face centred central composite design for medium optimization :** The face-centred central composite design (FCCCD) is an effective method, and objective of this method is to run the selected variables powerfully with the route of increase towards optimum level and also recognizes the most excellent possible set of process variables for operating fermentation process effectively [12]. The FCCCD was used for optimization of medium components such as incubation period, temperature, pH and inoculums size. The input variables of present study are selected based on

finding of the one-factor-at-a-time (OFAT) analysis for production of PHB, and selected four variables showed the potential impact on PHB production [4]. The output variable of the process is PHB production. The FCCCD was generated a sum of 30 experiments with different combinations of physical variables, and among these experiments 08 are central points. The experiments were conducted at central points to establish the curve which indicates the importance of model (Table 2).

The response (Y) fitted with the second-order polynomial equation

$$\text{PHB Yield (R1)} = +5.52 + 0.23A - 0.099B - 0.49C - 0.016D + 0.079A^2 + 0.015A^2 - 2.500E-003 A^2 D + 0.083 B^2 C - 0.11 B^2 D + 0.099 C^2 D + 0.090 A^2 - 1.96 B^2 - 1.14 C^2 + 0.32 D^2$$

R<sub>1</sub> represents the response for PHB production, whereas Incubation period, Temperature, pH and Inoculums size represented by variables A, B, C and D respectively, and the R<sup>2</sup> coefficient value of 0.9723 suggested that predicted model was significant. The values of “Prob > F” less than 0.0500 indicate model terms are significant, and in this case and in this case C, B<sup>2</sup>, C<sup>2</sup> are significant model terms (Table 3). The model statistical parameter, low per cent CV (8.24), represents the reliability of experiment performed, and other parameters are shown in Table 4. The 3-D response surface curves were plotted to evaluate interactions of combinational medium variable effects on response and to find

out optimal concentrations of physical variables for PHB production (Fig. 1a–c). Maximum production of PHB was attained when fermentation medium was supplemented with 35.28°C of temperature and 54.34 h of incubation period (Fig. 1a). The oval shape 3D curve between pH and incubation time, inoculums size and incubation period, pH and temperature, inoculums size and temperature suggests that the interaction effects between four physical variables are significant (Fig. 1b, 1c, 1d, 1e). Similarly, the 3D plot related to inoculums size and pH showed the major effect on production and maximum production was achieved at 6.6 pH and 3.19 % of inoculums size (Fig. 1f).

For the production of PHB, the RSM model is validated by conducting an experiment at best predicted and precise solution. The PHB yield reached to 5.88 g/L from *A. nosocomialis* RR20, which is almost near to the RSM predicted value under very well optimized conditions (Table 5). The maximum PHB production reported previously was 3.32 g/L obtained in sub-merged fermentation with *Bacillus mycoides* DFC1. The process was run at optimum conditions of pH 7.3, temperature 37 °C, inoculums size 3% and incubation time 72 h in liquid medium containing 4% glucose, 3.5% peptone, 0.3% K<sub>2</sub>HPO<sub>4</sub>, 0.1% KH<sub>2</sub>PO<sub>4</sub>, 0.05% MgSO<sub>4</sub>·7H<sub>2</sub>O, and 0.03% l-cysteine [3]. Similarly, Umesh et al. [9] obtained highest yield of 5.09 g/L through submerged fermentation with *Bacillus subtilis* NCDC0671 with the optimized medium consisting of 2.23 (g/L) beef extract, 0.72 (g/L) sodium chloride and 48 h of incubation period. Nisha et al., [13] reported PHB yield of 2.2g/L by

**Table 1** Range of variables selected for optimization

S. No.	Physical variable	Code	Range of variables		
			-1(low)	0(middle)	+(high)
1	Incubation period	A	36	48	60
2	Temperature	B	30	35	40
3	pH	C	6	7	8
4	Inoculums size	D	3	4	5

culturing *Bacillus sphaericus* NCIM 5149 through submerged fermentation. Hidayah et al. [14] reported PHB yield of 1.40 g/L through submerged fermentation with *Comamonas* sp. EB172 with the optimized medium consisting of temperature 30 °C, pH 7.04, inoculum size 4.0 % (v/v), (NH<sub>4</sub>)<sub>2</sub>SO<sub>4</sub> 0.01 g/L and mixed organic acids 5.05 g/L. As reported by Sindhu et al. [15] the highest PHB yield of 0.194 g/L through submerged fermentation using *Comamonas* sp. with the optimized media consisting of 1% concentration of yeast extract, inoculum concentration of 5.5% and pH 6.0.: Sindhu et al. [16] reported the maximum production 1.697 g/L of PHB was obtained under the optimum concentrations of the medium through the fermentation from *Bacillus firmus* NII 0830 inoculum concentration of 6.5%, 90 h of incubation and

0.75% of xylose concentration. Poly- $\alpha$ -hydroxybutyrate obtained using molasses in this study was 6.36 g/L. Sowmya et al., [17] reported maximum PHB yield of 1.2 g/L at optimum conditions of pH 8.0, sodium chloride concentration 20 g l<sup>-1</sup>, inoculum size 0.5% (v/v), glycerol 20 g l<sup>-1</sup> and 72 h of incubation at 30°C. In comparison with these previous reports, the PHB production from RR20 strain (18-19) is said to be higher and raw materials of medium are also expected to reduce the estimated cost of the process.

#### PHB production comparison

The submerged fermentation with standard MSM is produced PHB, 0.89 g/L. After the optimization of low-cost

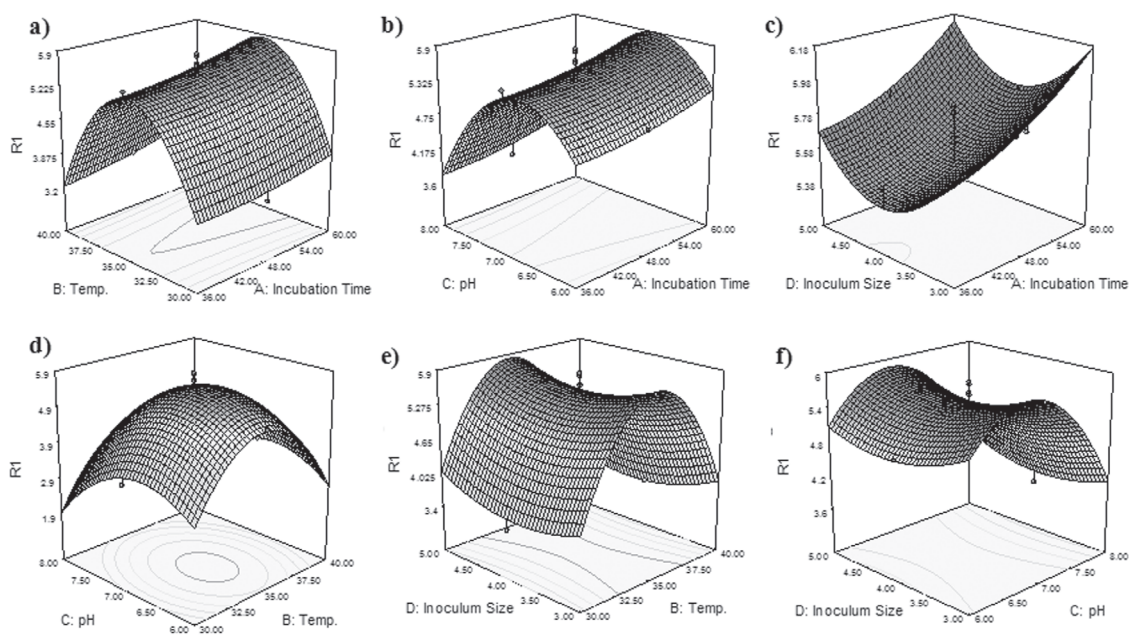


**Fig. 1** 3D graphs a) effect of temperature and incubation time b) effect of pH and incubation time c) effect of inoculums size and incubation time d) effect of pH and temperature e)effect of inoculums size and temperature f)effect of inoculums size and pH  
 Validation of RSM model

**Table 2** Actual data for design of experiments

S. No	Incubation period, h	Temp. (°C)	pH	Inoculums size (%)	PHB Yield (g/L)	
					Experimental	RSM predicted
1	48	35	7	4	5.65±0.013	5.52
2	48	35	7	3	5.82±0.005	5.86
3	36	30	8	3	1.78±0.002	1.99
4	48	35	7	4	5.42±0.012	5.52
5	60	40	8	3	2.61±0.014	2.66
6	36	40	8	5	2.00±0.016	1.97
7	60	40	6	5	3.54±0.009	3.21
8	60	40	6	3	3.75±0.013	3.66
9	60	30	6	5	3.21±0.023	3.63
10	60	30	8	5	3.24±0.003	2.7
11	48	35	8	4	3.67±0.006	3.89
12	60	40	8	5	2.35±0.005	2.61
13	36	40	6	3	3.56±0.011	3.37
14	48	35	7	4	5.62±0.010	5.52
15	36	30	8	5	2.21±0.009	2.38
16	48	35	7	5	5.68±0.009	5.82
17	60	30	8	3	2.32±0.003	2.33
18	36	35	7	4	5.5±0.014	5.39
19	36	40	6	3	2.65±0.012	3.07
20	36	40	8	3	2.36±0.008	2.01
21	48	48	7	4	5.84±0.010	5.52
22	48	48	7	4	5.8±0.004	5.52
23	36	36	6	5	2.56±0.008	2.63
24	36	36	6	5	3.54±0.007	3.36
25	60	60	6	3	3.74±0.006	3.65
26	48	30	7	4	3.46±0.013	3.66
27	48	35	7	4	5.45±0.005	5.52
28	60	35	7	4	5.52±0.009	5.84
29	48	35	6	4	4.89±0.011	4.88
30	48	40	7	4	3.45±0.007	3.46

**Table 3** ANOVA for response surface quadratic model

Source	Sum of squares	df	Mean square	F Value	p-value Prob>F	
Model	54.50	14	3.89	37.55	<0.0001	most Significant
A-Incubation time	0.94	1	0.94	9.10	0.0087	Significant
B-Temperature	0.18	1	0.18	1.72	0.2098	
C- pH	4.40	1	4.40	42.45	<0.0001	most Significant
D-Inoculums size	4.672E-003	1	4.672E-003	0.045	0.8347	
AB	0.099	1	0.099	0.96	0.3434	
AC	3.600E-003	1	3.600E-003	0.035	0.8547	
AD	1.000E-004	1	1.000E-004	9.646E-004	0.9756	
BC	0.11	1	0.11	1.05	0.3216	
BD	0.18	1	0.18	1.78	0.2016	
CD	0.16	1	0.16	1.51	0.2388	
A <sup>2</sup>	0.021	1	0.021	0.20	0.6586	
B <sup>2</sup>	10.00	1	10.00	96.48	<0.0001	most Significant
C <sup>2</sup>	3.37	1	3.37	32.47	<0.0001	most Significant
D <sup>2</sup>	0.26	1	0.26	2.48	0.1360	
Residual	1.56	15	0.10			
Lack of fit	1.41	10	0.14	4.68	0.0511	
Pure error	0.15	5	0.030			
Cor Total	56.06	29				

**Table 4** Model statistical parameters

R-Squared	0.9723
Adj R-Squared	0.9464
Pred R-Squared	0.8108
Adeq precision	17.073
SD	0.32
Mean	3.91
C.V. %	8.24

Physical variables, namely incubation period, temperature, pH and inoculums size, the production level is elevated to 5.88 g/L. In comparison with the standard MSM, the production of PHB improved to 6.60-fold (Fig. 2). The findings of the present study proved that designed medium could be used as potential alternative for commercial production of PHB.

**Table 5** Validation of RSM model for PHB production

S. No	Incubation (A), h	temperature (B), °C	pH (C)	Inoculums size (D), %	PHB production (R <sub>1</sub> ), g/L		
					RSM model predicted	Experimental value	Control
1	54.34	35.28	6.6	3.19	5.93	5.88	0.89



### Conclusion

The present study aimed in the PHB production using a novel *Acinetobacter nosocomialis* RR20 strain isolated from sewage waste. The operating conditions (physical variables) were optimized using Central Composite Design and the optimum incubation period, temperature, pH and inoculum size were 54.34 h, 35.28 °C, 6.6 and 3.19 % respectively. At these optimum conditions, PHB production of 5.88 g/L was reported which is sixfold enhanced. The findings of this study proved that the modified mineral salt medium could be used as potential alternative for commercial production of PHB.

### References

1. Otari, S.V., Ghosh, J.S. (2009). Production and characterization of the polymer polyhydroxy butyrate-co-polyhydroxy valerate by *Bacillus megaterium* NCIM 2475. *Current Research Journal of Biological Sciences*. 1:23–26
2. Yung, H.Y., Christopher, J.B., Charles, F.B., Paolo, B., Laura, B.W., Hassan, M.A., Yusof, Z.A.M., HoKyun, R., Anthony, J.S. (2010). Optimization of growth media components for polyhydroxyalkanoate (PHA) production from organic acids by *Ralstonia eutropha*. *Applied Microbiology Biotechnology*. 87: 2037–2045.
3. Aarthi, A., Venkataramana, N.K. (2012). Polyhydroxybutyrate production in *Bacillus mycoides* DFC1 using response surface optimization for physico-chemical process parameters. *3 Biotech*. 2:287–296.
4. Reddy, A.R., Venkateswarulu, T.C., Sudhakar, P., Krupanidhi, S., Prabhakar, K.V. (2018). Optimization of process parameters for polyhydroxybutyrate production from isolated *Acinetobacter nosocomialis* RR20 through submerged fermentation. *Current Trends in Biotechnology and Pharmacy*. 12:159–168.
5. Lee, W.H., Azizan, M.N.M., Sudesh, K. (2007). Magnesium affects poly (3-hydroxybutyrate-co-4-hydroxybutyrate) content and composition by affecting glucose uptake in *Delphacid acidovorans*. *Malaysian Journal of Microbiology*. 3: 31–34.
6. Venkateswarulu, T.C., Prabhakar, K.V., Kumar, R.B. (2017). Optimization of nutritional components of medium by response surface methodology for enhanced production of lactase. *3 Biotech*. 7:1–9
7. Sathiyarayanan, G., Kiran, G.S., Joseph, S., Saibaba, G. (2013). Optimization of polyhydroxybutyrate production by marine *Bacillus megaterium* MSBN04 under solid state culture. *International Journal of Biological Macromolecules*. 60: 253–261.
8. Kim, B.S. (2000). Production of poly (3-hydroxybutyrate) from inexpensive substrates. *Enzyme Microbial Technology*. 27:774–777.
9. Umesh, M., Manon Mani, V., Basheer, T., Preethi, K. (2017). Statistical Optimization of Process Parameters for Bioplastic (PHA) Production by *Bacillus subtilis* NCDC0671 Using Orange Peel-Based Medium *Iranian Journal of Science and Technology A Science*. doi.org/10.1007/s40995-017-0457-9.
10. John, H.L., Lepecky, R.A. (1961). Assay of poly- $\beta$ -hydroxy butyric acid. *Journal of Bacteriology*. 82:33–36.
11. Box, G.E.P., Behnken, D.W. (1960). Some new three level designs for the study of quantitative variables. *Technometrics*. 2:455–475.
12. Erva, R.R., Goswami, A.N., Suman, P., Vedanabhatla, R., Rajulapati, S.B. (2017). Optimization of L-asparaginase production from novel *Enterobacter* sp., by submerged fermentation using response surface methodology. *Preparative Biochemistry Biotechnology*. 47:219–228.

13. Nisha V. Ramadas Carlos R. Soccol Ashok Pandey. (2010). A Statistical Approach for Optimization of Polyhydroxybutyrate Production by *Bacillus sphaericus* NCIM 5149 under Submerged Fermentation Using Central Composite Design. *Applied Biochemistry Biotechnology*. 162:996–1007. DOI 10.1007/s12010-009-8807-5.
14. Noor Azman Mohd Johar, Mohd Ali Hassan, Mohd Rafein Zakaria, Phang Lai Yee, Yoshihito Shirai and Hidayah Ariffin. (2012). Evaluation of Factors Affecting Polyhydroxyalkanoates Production by *Comamonas* sp. EB172 Using Central Composite Design *Malaysian Journal of Microbiology*. 8(3) : 184-190.
15. Thunoli Payyanvalappil Prabisha, Raveendran Sindhu, Parameswaran Binod, Vandana Sankar, Kozhiparampil Gopalan Raghu, Ashok Pandey.(2015). Production and characterization of PHB from a novel isolate *Comamonas* sp. from a dairy effluent sample and its application in cell culture, *Biochemical Engineering Journal* <http://dx.doi.org/10.1016/j.bej.2015.05.012>
16. R. Sindhu, N. Silviya, P. Binod, A. Pandey. (2010). Pentose- rich hydrolysate from acid pretreated rice straw as a carbon source for the production of poly-3-hydroxybutyrate, *Biochemical Engineering Journal*. doi:10.1016/j.bej.2012.12.015.
17. Sowma, P., Mohandas, Linu Balan, Lekshmi, N., Sherine Sonia Cubelio, Rosamma Philip, Bright Singh I. S. (2016). Production and characterization of polyhydroxybutyrate from *Vibrio harveyi* MCCB 284 utilizing glycerol as carbon source. *JAM - Original Article*. doi:10.1111/jam.13359.
18. Reddy, A.R., Abraham, K.P., Krupanidhi, S., Prabhakar, K.V., Venkateswarulu, T.C. (2019). Production of Polyhydroxybutyrate from *Acinetobacter nosocomialis* RR20 strain using modified mineral salt medium: a statistical approach. *International Journal of Environmental Science and Technology*. 16: 6447-6452.
19. Reddy, A.R., Krupanidhi, S., Venkateswarulu, T.C., Bharath kumar, R., Sudhakar, P., Prabhakar, K.V. (2019). Molecular characterization of a biopolymer producing bacterium isolated from sewage sample. *Current Trends in Biotechnology and Pharmacy*. 13: 325-335.

## Extraction, Total phenol Content, Flavonoid content, Free Radical Scavenging Capacity and phytochemical screening of the Parts of Sri Lankan Pomegranate (*Punica granatum* L.) Fruit

Udeshika Y Bandara, Chamindri Witharana\* and Preethi Soysa

Faculty of Medicine, University of Colombo, No. 25, P.O. Box 271, Kynsey Road,  
Colombo 08, 0008, Sri Lanka

\*For Correspondence –Dr. Chamindri Witharana, [chamindri@bmb.cmb.ac.lk](mailto:chamindri@bmb.cmb.ac.lk)

### Abstract

Alteration of radical scavenging capacity (RSC), phenol (TPC) and flavonoid contents (FC) of pomegranate fruit parts were extracted using Boiling, Sonication, Microwave, Sonication followed by microwave and compared.

RSC was determined by DPPH activity and FRAP assay while TPC and FC were measured by Folin-Ciocalteu method and Aluminium chloride colourimetric assay, respectively. Sonicated peel extract exhibited maximum RSC ( $IC_{50}$  3.3 $\mu$ g/mL), PC (64.0W/W% Gallic Acid Equivalent) and FC (19.7w/w % Quercetin Equivalent). Fermented juice showed higher RSC (243 fold less  $IC_{50}$ ), TPC (4 folds) and FC (1.5 folds) than the fresh juice. Seeds had minimum phytochemical content; RSC ( $IC_{50}$  11698 $\mu$ g/mL), PC (2.0 W/W% Gallic Acid Equivalent) and FC (2.2W/W% Quercetin Equivalent). GC-MS enable to identify some functional groups (Furfural, Benzoic acid, and n-Hexadecanoic acid) in sonicated peel water extract. Thus, this study revealed Sri Lankan pomegranate peel presented with excellent TPC, FC and RSC than other parts of pomegranate fruit apart from extraction method.

### Total phenol Content

**Keywords:** Pomegranate, Polyphenols, Radical Scavenging Capacity, Sonication, DPPH

### Introduction

Natural phytochemicals play a major role in maintaining a healthy life in humans. These

phytochemicals can be consumed generally during diets. Phytochemicals, the bioactive plant compounds in fruits, vegetables, grains, and other plant foods, have been linked to reductions in the risk of major chronic diseases such as; cancer, diabetes, cardiovascular diseases, inflammation, and neurologic disorders. Fruits and vegetables contain a wide variety of phytochemicals with antioxidant properties such as polyphenols, flavonoids, isoflavones and carotenoids that may help to protect cellular systems from oxidative damage and lower the risk of chronic diseases (1).

*Pomegranate* (*Punica granatum* L.) is a medicinal herb belongs to *Lythraceae* family. Pomegranate in Sri Lankan home gardens has been revealed to have nutritional benefits (2). Even though in Indian ayurveda and siddha medicine have been used pomegranate as an anti-tumor remedy it was not based on scientific experiments (3). It is reported that pomegranate peel, pericarp (mesocarp), juice, seeds, leaves, bark have shown several health benefits such as antibacterial, antiviral, antioxidant, anti-inflammatory activities (4)(5)(6). Punicic acid, oleic acid, palmitic acid, stearic acid, linoleic acid, sterols, tocopherols were identified as the major constituents of the pomegranate seeds (7)(8). Pomegranate fruit is rich in tannins, phenolics (ellagic tannins, ellagic acid and gallic acid), which are potent antioxidants (9). Pomegranate peel which is inedible, constitutes about 50% of the total fruit weight and

it contains higher amounts of polyphenols than the juice, which is discarded as a waste (10). Department of Agriculture, Sri Lanka has been introduced three varieties of Sri Lankan pomegranate; *Nimali*, *Daya* and *Nayana* as Sri Lankan varieties. Health benefits of *Nimali* were investigated, as the most popular variety of pomegranate among three, due to its high yielding ability, soft seeded and sweet taste (11).

Efficiency of emerging extraction methods compared with its phytochemical analysis with selected five notable methods. SN considered as an emerging and efficient method which can intensely reduce extraction time while increasing extraction yields and antioxidant properties of extracts (12)(13). This highlighted the importance of extraction step for yield of total phenolic, flavonoid contents and antioxidant activities. Analysis of phenolic compounds and evaluation of anti-oxidant activity in different parts of Sri Lankan pomegranate fruit is not elucidated, hence the present investigation gains importance towards understanding its potential health benefits.

### Materials and Methods

**Materials** Gallic acid, Folin-Ciocalteu reagent, Trichloroacetic acid, Sodium carbonate ( $\text{Na}_2\text{CO}_3$ ), Aluminum chloride ( $\text{AlCl}_3$ ), Sodium nitrite ( $\text{NaNO}_2$ ), Sodium hydroxide ( $\text{NaOH}$ ) were purchased from Sigma Chemicals Co. (P.O.Box 14508, St. Louis, MO 63178 USA). 1, 1-Diphenyl-2-picrylhydrazyl (DPPH), polyvinyl-pyrrolidone (PVPP) and Quercetin (e+95%) were purchased from Fluka (Flukachemie GmbH, CH-9471 Buchs). Other chemicals were obtained from Sigma-Aldrich Co (St Louis, MO, USA) unless mentioned. All chemicals used were in analytical grade.

SHIMADZU UV 1601 UV/Visible spectrophotometer (Shimadzu Corporation, Kyoto, Japan) was used to measure absorbance. Deionized water was obtained from Labconco Water Pro-PS UV ultra-filtered water system (Labconco Corporation, Kansas City, Missouri). Labconco Free Zone Legacy 2.5 L Benchtop Vacuum Freeze Drier was used to obtain the lyophilized plant samples (Model No: 7670530, -

54° with SS interior, 220V). Sonication done with NEY ULTRASONIC cleaner controller 300 (The J M Ney Company Barkmeyer Division 13553 Calimesa Blvd, Yucaipa, CA, 50 kHz, 135 W). Memmert WNB 22 water bath (Memmert GmbH + Co. KG, Aeussere Rittersbacher Strasse, 38, D-91126, Schwabach) used for heating of samples.

**Plant materials** Sri Lankan *Punica granatum* L. (*Nimali*) obtained from Fruit Research Institute, Department of Agriculture, Kalpitiya, Sri Lanka (January 2017). Plant species was taxonomically identified and voucher specimen was deposited in Botany Department, Bandaranayake Memorial Ayurveda Research Institute, Nawinna, Colombo, Sri Lanka under number 2025). Pomegranates were handpicked, washed and stored in 4°C refrigerators (14). The fruit was separated to its parts (pericarp, peel, seeds, juice) manually.

**Sample Preparation** : Freeze-drying retains higher levels of phenolic content in herbal samples compared to air-drying (15). Pomegranate peel, pericarp, fresh juice, fermented juice and seed samples freeze dried at -40°C until a constant weight acquired.

**Preparation of Pomegranate peel and pericarp extracts** : Pomegranate peel and pericarp extracts were prepared by five different methods; boiling, sonication, heating in water bath, microwave and sonication followed by microwave. Lyophilized peel samples were grounded to obtain a powder and sieved to remove coarse particles. The fine powder was subjected to the following extraction methods. 1) Boiling water (45 minutes) 2) Sonication (50 kHz, 135 W, 30 minutes) 3) Sonication (50 kHz, 135 W, 30 minutes) followed by microwave (2450MHz, 1050W, 3 minutes) 4) Microwave (2450MHz, 1050W, 3 minutes) 5) Water bath (50°C, 20 minutes). Two grams of peel (n=6) / pericarp powder (n=6) was dissolved in 100mL deionized water for each extraction method. Extract was centrifuged (3000 rpm, 10 min) and filtered through Whatman No. 1 filter paper. Resulting filtrate of five extractions were freeze dried until obtained a constant weight and stored in -20°C freezer.

Lyophilized samples of peel and pericarp were prepared and the yield was calculated as a percentage of dry weight.

**Preparation of Juice extracts** Juice was separated into two portions. One portion was allowed to ferment with wine yeast (*Saccharomyces bayanus* – Lalvin EC-1118, from Lallemant, Montreal, Canada) (1g for 3.8L) for one week and filtered extract was freeze dried until a constant weight obtained. Other portion was allowed to remain as fresh juice and freeze dried until a constant weight obtained.

**Preparation of Seed Extract:** Seeds were cleaned with deionized water and freeze dried until a constant weight obtained. Dried seeds were grounded and refluxed for three hours. Resulting extract was centrifuged (3000rpm, 10 mins) and filtered through Whatman No. 1 filter paper. Resulting filtrate was freeze dried until obtained a constant weight and stored in -20°C freezer.

**Total Phenolic Content (TPC) :** TPC of Pomegrate peel, pericarp, juice and seed extracts was determined by Folin-Ciocalteu's method (16). Calibration curve was plotted with gallic acid as the standard. TPC was expressed as W/W% Gallic acid equivalents.

**Flavonoid content (FC)** FC was measured by aluminium chloride colorimetric assay (17). Calibration curve plotted with quercetin as the standard and FC was expressed as w/w% Quercetin equivalents.

#### **Determination of antioxidant activity**

Free radical scavenging capacity was assessed by the DPPH Radical Scavenging Method (18) with slight modifications and compared with IC<sub>50</sub> of ascorbic acid. The scavenging activity of each concentration (n = 6) were quantified by the decolorization of DPPH in solution at 517nm.

$$\% \text{ Inhibition capacity} = \frac{(Ab_{\text{control}} - Ab_{\text{sample}})}{Ab_{\text{control}}} \times 100$$

The Ferric Reducing Antioxidant Power (FRAP) was determined according to Sharma and Kumar, 2011 (19). The test samples (100 il) with different

concentrations were mixed with phosphate buffer (0.2 M, pH 6.6, 250il) and Potassium ferricyanide (1%, 250il). The mixture was incubated at 50°C for 20 min. Trichloroacetic acid (10%, 250il) was added and the samples were centrifuged at 6500rpm for 10 min. The supernatant was mixed with deionized water and Ferric chloride (0.1%) at a ratio of 1:1:2 respectively. The samples were vortexed and absorbance was measured at 700nm in UV-Visible spectrophotometer. The blank contained deionized water instead of test sample. L-ascorbic acid was used as the standard. Increased absorbance of the reaction mixture indicates stronger reducing power.

#### **Removal of Polyphenols from Pomegranate juice**

Polyphenols were removed using Polyvinylpyrrolidone (PVPP) column as described previously (20). A cotton wool plug was placed inside a 5cm<sup>3</sup> syringe after removing the plunger and the needle. Syringe was filled with PVPP (1.0g) and juice samples (3mL each) were layered over the PVPP column. The PVPP column was placed in a 15 mL falcon tube and centrifuged at 2,000g for 10 min. Centrifugation was repeated for 6 times with the same column adding 1mL of the extract and each fraction was collected to separate tubes. First fraction was discarded and remaining fractions were analyzed for the presence of polyphenols. The Absorbance of fermented juice before and after PVPP treatment were scanned for wave lengths using a UV/Visible spectrophotometer.

#### **Gas Chromatography/ Mass Spectrometry (GC/MS) Analysis:**

GC-MS analysis was performed for the freeze dried Sonicated peel water extract using a Agilent 6890 series instrument equipped with a Agilent 5973 N series mass selective detector. The sample was injected into the GC-MS on a 5% Phenyl methyl Siloxane glass capillary column with a film thickness of 0.25 µm (30 m × 0.25 mm) with helium as carrier gas at 0.9 mL/min constant flow mode. GC temperature programme was 60°C - 280°C at 15°C/min. The mass spectra were recorded in splitless mode. The scan repetition was 10 sec over a mass range of 15 - 550 atomic mass units.



**Statistical analysis** Results were presented as mean values of six replicates  $\pm$  standard deviation. The  $IC_{50}$  values were calculated from either linear or logarithmic dose response curves. A one way analysis of variance (ANOVA) was performed and the significant differences between mean values ( $p$  value) were determined.

**Results and Discussion** The effectiveness of the extraction method with reference to the antioxidant activity, total phenol content, and flavonoid content were determined by this study. Furthermore, the relationship between free radical scavenging activity with polyphenol and flavonoid contents were monitored. Several studies have been carried out to detect antioxidant activity, total phenol content and flavonoid content of edible parts of pomegranate fruit. However, this is the first study comparing the effect of extraction methods with the radical scavenging capacity, total phenol content, and flavonoid content for Sri Lankan variety of *Punica granatum* L. fruit.

Sonication or Ultrasound-Assisted Extraction (UAE) is a low cost and non-complex instrument, which is used for small and large scale extractions. With the acoustic waves generated by the shear force, can be disrupted the biological membranes which facilitate the release of endogenous substances (21). Faster kinetics, high extraction yield and safer method for thermolabile compounds are some benefits of UAE method (22) (23).

With microwaves a pressure generates inside cell and it causes the rupturing of the cell membrane, which will facilitate the release of active substances (23). Extraction yield depends on the microwave power, extraction time and type of solvent used. Microwaves can cause tremendous temperature elevation of the sample. Due to elevation of temperature in microwaves, thermolabile compounds may destroyed in the sample (24).

Boiling is the traditional extraction method used in ayurveda medicine for preparation of most of drugs. Therefore, in this study open boiling was

selected as an extraction method, which is only suitable for extracting heat-stable compounds, unbreakable plant materials (25). As UAE method is protective for thermolabile compounds, it may have given higher values for total phenol and flavonoid contents in this study(21) (22) .

**Extraction yield** Extraction yield for parts of the pomegranate fruit extracts are illustrated in Table 1 as a percentage of dry weight obtained after freeze drying. UAE extracts of peel and pericarp obtained the highest extraction yield of 38%, 24% respectively.

#### **Total phenolic and flavonoid contents**

UAE method has exhibited the highest mean value of total phenolic content in both peel ( $64.0 \pm 11.5$  W/W% GAE) and pericarp ( $43.5 \pm 6.5$  W/W% GAE) (Fig 1). A significant difference ( $p < 0.005$ ) was observed between extraction methods for both peel and pericarp. However, peel had the higher level of total phenolic content irrespective of the extraction method. Catechin, epicatechin, epigallocatechin-3-gallate, flavan-3-ol, kaempferol, luteolin, luteolin 7-O-glucoside, naringin, and quercetin available as flavonoids in peel (26). Total phenolic content of fermented juice ( $2.7 \pm 0.3$  W/W% GAE) is higher than fresh juice ( $0.7 \pm 0.05$  W/W% GAE) and seed ( $2.0 \pm 0.3$  W/W% GAE) extracts. But it was lower than peel. Gallic acid was considered as the standard phenolic compound and expressed as Gallic Acid Equivalent (W/W% GAE).

The flavonoid content was higher in peel than pericarp. UAE method demonstrated the highest value of flavonoid content for both peel ( $19.7 \pm 2.9$  W/W% QCE) and pericarp ( $15.2 \pm 1.5$  W/W% QCE) ( $p < 0.005$ ). Fermented juice ( $6.7 \pm 0.2$  W/W% QCE) had a higher value than fresh juice ( $4.6 \pm 0.7$  W/W% QCE) and seed ( $2.2 \pm 0.4$  W/W% QCE) extracts. Folin-Ciocalteu (F-C) assay is based on the reduction of Folin-Ciocalteu reagent from phenolic compounds, which is a mixture of tungsten and molybdenum oxides (16). Vinson *et al* reported that F-C method can be used for fruits (27). Total phenol content in pomegranate

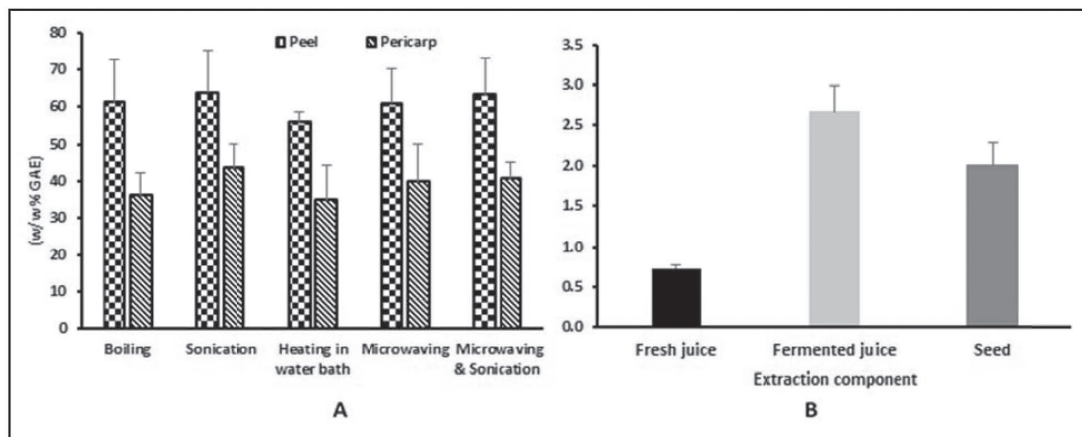


**Fig 1.** Total phenolic content (GAE W/W %) of peel, pericarp extracts with relative to extraction methods (A) and fresh juice, fermented Juice and seed extracts (B)

peel is ten folds higher than the pulp extract (10). A higher TPC was observed with 100% water extract of pomegranate peel, while 30% water: 70% ethanol extracts show the lowest. Though some reports suggest that there is a correlation between total phenol content and antioxidant activity, no correlation has been found in some studies (28). In this study, UAE method showed the highest TPC and antioxidant activity. Therefore, it revealed that there is a correlation between antioxidant activity and TPC.

#### Antioxidant activity

According to Gil, 2000 DPPH and FRAP methods were suggested as easy and precise methods for the detection of antioxidant activity of fruit and vegetable extracts (29). It is further reported that DPPH radical scavenging assay is easy, sensitive and rapid method to follow and 90% of antioxidant activity can be measured (30). It is revealed that the pomegranate juice consists with gallic acid, organic acids, simple sugars, ellagic acid, quinic acid, flavonols, amino acids, minerals, epigallocatechin-3-gallate (6) (31). In addition to that punicalagine, hydrolizable tannins, ellagitannins, anthocyanins, anthocyanidins can be found in pomegranate juice, as the main compounds which play a major role in antioxidant activity (29). Tezcan, 2009 has revealed that

glucose and fructose as the main sugar types present in juice (32). According to Rice-Evans *et al.* Glucose has been identified as the commonest sugar involved in the glycoside formation. As well as galactose, rhamnose, xylose and ructose are involved. Some compounds show a different antioxidant capacities with different solvents, depending on their structure and different binding affinities to the solvent. Further he says, if number of hydroxyl groups is higher, the free radical scavenging capacity is high due to the high conjugation ability (33).

DPPH free radical scavenging capacity was significantly higher ( $p < 0.005$ ) in UAE method both peel ( $IC_{50} 3.3 \pm 1.1 \mu\text{g/mL}$ ) and pericarp ( $IC_{50} 6.2 \pm 0.1 \mu\text{g/mL}$ ) extracts comparable to ascorbic acid standard than the other extraction methods. Pomegranate peel is composed with tannins, flavonoids, organic acids and alkaloids. With the presence of variety of tannins; punicalagin, punicalin, gallic acid and casuarinin, peel shows the antioxidant activity (29) (34). As tannins form strong complexes with proteins, they are less disposed to degradation even in the digestive tract, which is transported to other tissues. According to the suggestion from Marshall, 1990 tannins have the ability of replacing other antioxidants, therefore they prevent oxidative damage of proteins, carbohydrates and lipids during digestion

(35). Lowest DPPH free radical scavenging capacity was present with seed extract ( $IC_{50}$  11698 $\mu$ g/mL) and value for fermented juice extract was 243 fold higher than the fresh juice (Table 2).

PVPP is a polymer which is highly cross linked with a high affinity for polyphenols (36) and used to remove polyphenols from pomegranate fresh and fermented juice to investigate the effects of polyphenols on DPPH radical scavenging capacity. With the presence of PVPP, fresh juice and fermented juice have shown a very low % radical scavenging capacity at a concentration of 100  $\mu$ g/mL in DPPH assay. We performed the spectrum analysis especially for juice, as it showed a vast difference in % scavenging capacity

between two types of juice. According to photometric scanning spectrum, broadness of peaks and wave length were reduced after treatment with PVPP (Fig 3). The evidence of presence of polyphenols in fermented juice and fresh juice was represented with the peaks obtained between 190nm to 600nm. Phenol, nitrous compounds, carotenoids and other unidentified compounds can act as natural antioxidants other than polyphenols.

Percentage radical scavenging capacity of fresh juice and fermented juice were  $11.0 \pm 0.0$  % and  $42.5 \pm 0.0$  % before removal of polyphenols and  $0.03 \pm 0.0$  % and  $0.2 \pm 0.0$  % after removal of polyphenols consecutively at a concentration of

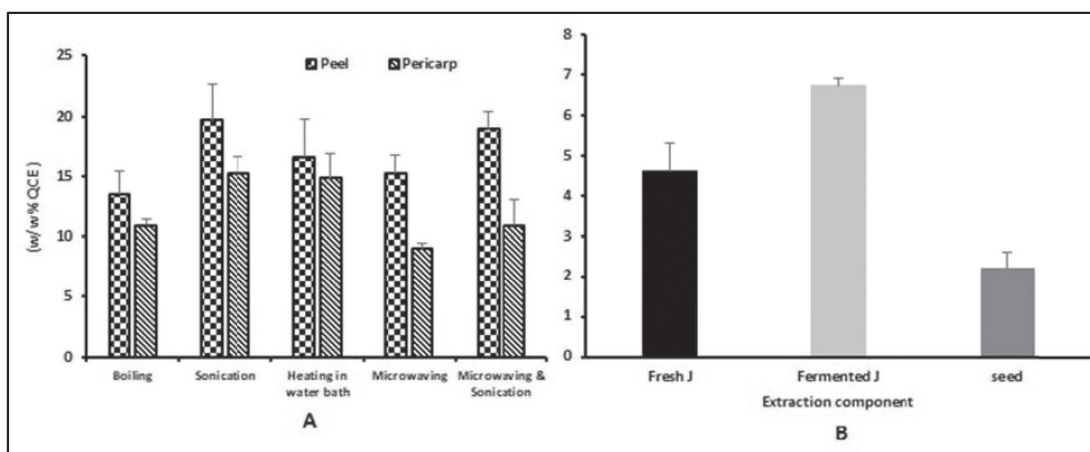


**Fig 2.** Flavonoid content (W/W % QCE) of peel, pericarp extracts with respect to extraction method (A) and fresh juice, fermented Juice, seed extracts (B).

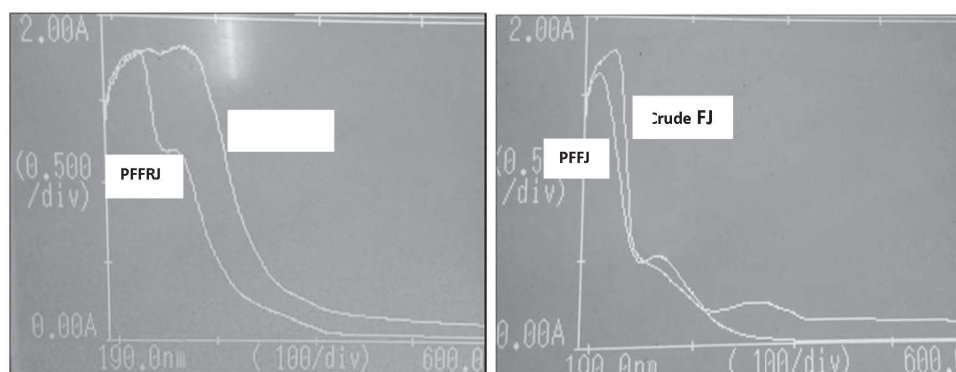


**Fig 3.** The photometric scanning spectrum for fermented juice (A) and fresh juice (B) before and after treatment with PVPP (PFFRJ – Polyphenol free fermented juice, PFFJ – Polyphenol free fresh juice)

100µg/mL which evidences polyphenols as the major component responsible for the antioxidant activity of Sri Lankan pomegranate.

Capacity of reduction of ferric ions ( $Fe^{3+}$ ) to ferrous ions ( $Fe^{2+}$ ) was greater in UAE method both peel and pericarp (Fig 4). Fermented juice has shown a significantly higher ( $p < 0.005$ ) value for  $Fe^{3+}$  reduction capacity comparable to fresh juice. Least reduction was obtained for seed extract comparing to ascorbic acid standard which is negligible.

**Gas Chromatography/ Mass Spectrometry (GC/MS) Analysis :** The GC/MS analysis of *Punica granatum* L. Sonicated peel powder extract exhibited five distinct peaks at retention times of 3.470, 6.716, 12.993, 13.943 and 14.260 minutes with 21.8%, 32.5%, 35.2%, 2.1% and 4.2% values respectively as area percent report (Fig 5).

It has been revealed that sonicated peel extract composed with furfural ring, benzoic acid, n-Hexadecanoic acid as functional groups.

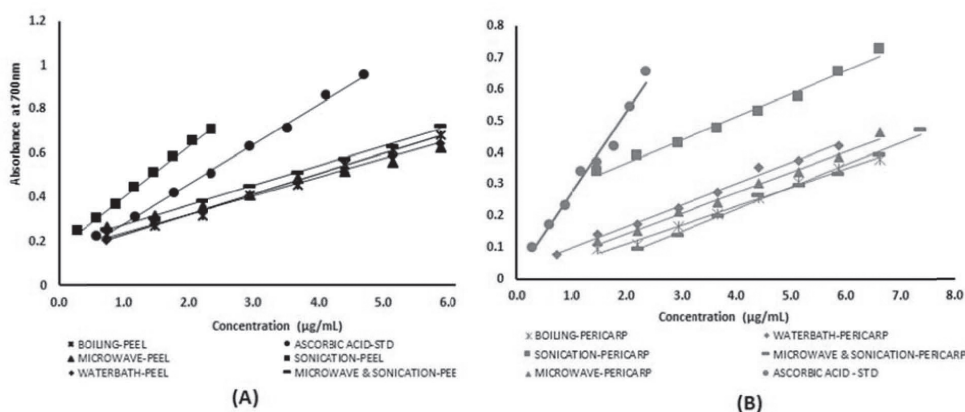


**Fig 4.** Ferric ion reducing power of peel (A), pericarp (B) with respect to extraction methods compared to ascorbic acid standard.

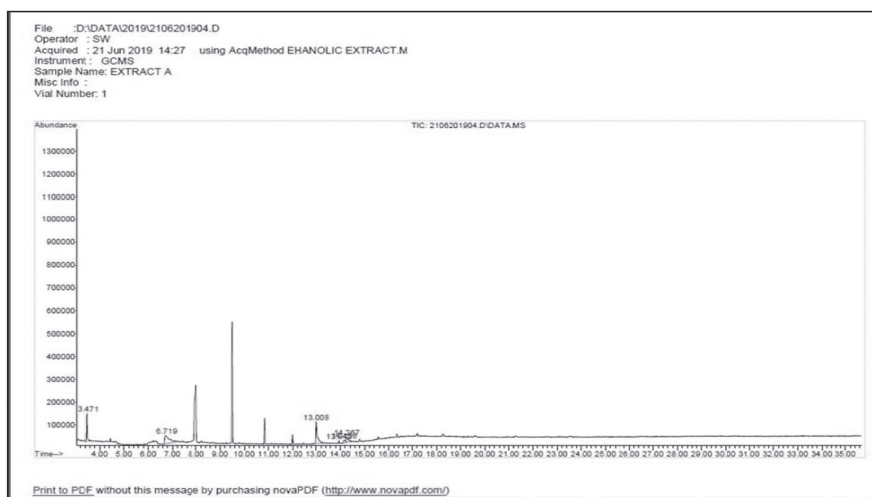


**Fig 5.** Total Ion Chromatogram of Volatile Compounds in the Sonicated Peel powder of *Punica granatum* L. fruit Analyzed by GC/MS

Extraction, Total phenol Content, Flavonoid content

**Table 1.** The extraction yield for pomegranate fruit extracts (W/W %)

Component	Extraction yield (W/W % of dry weight)
<b>Peel</b>	
a. Sonication	38.00
b. Microwave	15.00
c. Sonication & Microwave	20.00
d. Boiling	17.00
e. Waterbath	24.00
<b>Pericarp</b>	
a. Sonication	24.00
b. Microwave	9.00
c. Sonication & Microwave	15.00
d. Boiling	11.00
e. Waterbath	19.00
<b>Juice</b>	
a. Fresh juice	64.98
b. Fermented juice	48.76
Seed	39.12

Gunaseena 2017, revealed that 2, 5-dimethyl furan, Methyl beta-d-galactopyranoside have anticancer activity. Presence of Decanoic acid derivatives such as tridecane, 3-methylhexadecanoic acid, 9,12-octadecadienoic acid, 7-tetradecyne, 1-hexadecanol have antioxidant activity. Gallic acid which belongs to Hydroxybenzoic acids is a potent antioxidant component (37).

The polyphenols are the major compounds which are responsible for antioxidant activity according to the spectrum analysis of pomegranate fresh juice and fermented juice. Water extract of pomegranate peel showed the highest total phenolic and flavonoid contents among the other components of the fruit. Fermented juice has a higher antioxidant activity than fresh juice. UAE method shows the high total phenol and flavonoid contents in peel and pericarp extracts of pomegranate fruits.

**Conclusion** This study revealed that Sri Lankan *Punica granatum* L. peel extract indicated the highest total phenolic, flavonoid contents and antioxidant capacities compared to other extracts irrespective of the extraction method. As well as

**Table 2.** EC<sub>50</sub> values of pomegranate fruit extracts

Method of extraction <sup>1)</sup>	IC <sub>50</sub> value (µg/mL)		Method of extraction <sup>2)</sup>	IC <sub>50</sub> value <sup>1</sup>
	Peel	Pericarp		
Boiling	6.0±1.2 <sup>a</sup>	8.4±0.1 <sup>a</sup>	Fresh juice	754.5±83.2
Microwaving	4.3±0.9 <sup>a</sup>	9.5±1.0 <sup>a</sup>	Fermented juice	3.1±0.1
Heating in water bath	4.5±0.9 <sup>a</sup>	7.5±0.3 <sup>a</sup>	Seed	11698±159.3
Sonication	3.3±1.1 <sup>a</sup>	6.2±0.1 <sup>a</sup>		
Microwaving & Sonication	4.2±0.4 <sup>a</sup>	9.1±1.3 <sup>a</sup>		

<sup>1)</sup>IC<sub>50</sub> values of peel and pericarp extracts with respect to extraction methods and

<sup>2)</sup>fresh juice, fermented juice, seed extracts. <sup>a</sup>All values are mean±SD of 3 replicates;



UAE extraction method presented the highest value for all the evolutionary criteria mentioned above. The polyphenols in pomegranate fruit parts are mainly contributed to antioxidant activity.

#### Acknowledgements

The Staff, Department of Botany, Bandaranayake Memorial Ayurvedic Research Institute, Nawinna, Colombo, Sri Lanka for the identification of the plant. The technical assistance by technical staff, Department of Biochemistry & Molecular Biology, Faculty of Medicine, University of Colombo, Sri Lanka.

#### Conflict of Interest

The authors declare no conflict of interest.

#### Abbreviations:

IC<sub>50</sub> half maximal inhibitory concentration  
HEPES 2-[4-(2-hydroxyethyl)piperazin-1-yl]ethanesulfonic acid  
DPPH 2,2-diphenyl-1-picrylhydrazyl  
PVPP Polyvinylpyrrolidone

#### References

1. Yapa Bandara, U., Soysa, P., and Witharana, C. (2018). Medicinal herbs as a treatment for breast carcinoma, *Int J Herb Med*, 6(1): 05-09.
2. Amararatne Weerakkody, W., and Jayakody, J. D. (2012). Bioactive Properties of Fruit Juice of Pomegranate (*Punica granatum*) Grown in Dry Regions of Sri Lanka. *Trop Agric Res.*, 23(4):370–5.
3. central council for research in ayurveda & siddha. No Title Pharmacological investigations of certain medicinal plants & compound formulations used in ayurveda & siddha. department of Indian systems of medicine & homeopathy, Ministry of health & family welfare, Government of India, New Delhi; 1978. 88–89.
4. Fischer, U.A., Carle, R., Kammerer, D.R. (2011). Identification and quantification of phenolic compounds from pomegranate (*Punica granatum* L.) peel, mesocarp, aril and differently produced juices by HPLC-DAD–ESI/MSn. *Food Chem.*, 127(2):807–21.
5. Plumb, G.W., de Pascual-Teresa, S., Santos-Buelga, C., Rivas-Gonzalo, J.C., Williamson, G. (2002). Antioxidant properties of galocatechin and prodelphinidins from pomegranate peel. *Redox Rep.*, 7(1):41–6.
6. Lansky, E.P., Newman, R.A. (2007). *Punica granatum* (pomegranate) and its potential for prevention and treatment of inflammation and cancer. *J Ethnopharmacol.*, 109(2):177–206.
7. Schubert, S.Y., Lansky, E.P., Neeman, I. (1999). Antioxidant and eicosanoid enzyme inhibition properties of pomegranate seed oil and fermented juice flavonoids. *J Ethnopharmacol.*, 66(1):11–7.
8. Kim, N.D., Mehta, R., Yu, W., Neeman, I., Livney, T., Amichay, A., et al. (2002). Chemopreventive and adjuvant therapeutic potential of pomegranate (*Punica granatum*) for human breast cancer. *Breast Cancer Res Treat.*, 71(3):203–17.
9. Jaiswal, V., DerMarderosian, A., Porter, J.R. (2010). Anthocyanins and polyphenol oxidase from dried arils of pomegranate (*Punica granatum* L.). *Food Chem.*, 118(1):11–6.
10. Li, Y., Guo, C., Yang, J., Wei, J., Xu, J., Cheng, S. (2006). Evaluation of antioxidant properties of pomegranate peel extract in comparison with pomegranate pulp extract. *Food Chem.*, 96(2):254–60.
11. Department of Agriculture P. Annual performance report. (2010). 1–11.
12. Chemat, F., Zill-E-Huma., Khan, M.K. (2011). Applications of ultrasound in food technology: Processing, preservation and extraction. *Ultrason Sonochem*, 18(4):813–35.

13. Aybastier, Ö., Işık, E., Şahin, S., Demir, C. (2013). Optimization of ultrasonic-assisted extraction of antioxidant compounds from blackberry leaves using response surface methodology. *Ind Crops Prod.*, 44:558–65.
14. Pantuck, A.J., Leppert, J.T., Zomorodian, N., Aronson, W., Hong, J., Barnard, R.J., et al. (2006). Phase II study of pomegranate juice for men with rising prostate-specific antigen following surgery or radiation for prostate cancer. *Clin Cancer Res.*, 12(13):4018–26.
15. Abascal, K., Ganora, L., Yarnell, E. (2005). The effect of freeze-drying and its implications for botanical medicine: a review. *Phytother Res.*, 19(8):655–60.
16. Singleton, V.L., Rossi, J.A. (1965). Colorimetry of total phenolics with phosphomolybdic-phosphotungstic acid reagents. *Am J Enol Vitic.*, 16(3):144–58.
17. Zhishen, J., Mengcheng, T., Jianming, W. (1999). The determination of flavonoid contents in mulberry and their scavenging effects on superoxide radicals. *Food Chemistry.*, 64:555–9.
18. Blois, M.S. (1958). Antioxidant Determinations by the Use of a Stable Free Radical. *Nature.*, 181(4617):1199–200.
19. Sharma, U.S., Kumar, A. (2011). In vitro antioxidant activity of *Rubus ellipticus* fruits. *J Adv Pharm Technol Res.*, 2(1):47–50.
20. Ranatunge, I., Adikary, S., Dasanayake, P., Fernando, C.D., Soysa, P. (2017). Development of a Rapid and Simple Method to Remove Polyphenols from Plant Extracts., 2017.
21. Vinatoru, M. (2001). An overview of the ultrasonically assisted extraction of bioactive principles from herbs. *Ultrason Sonochem.*, 8(3):303–13.
22. Herrera, M.C., de Castro, M.D. (2005). Ultrasound-assisted extraction of phenolic compounds from strawberries prior to liquid chromatographic separation and photodiode array ultraviolet detection. *J Chromatogr A.*, 1100(1):1–7.
23. Chen Sung, J., and Lin, S. Y. (2015). Effect of Extraction Methods on the Active Compounds and Antioxidant Properties of Ethanolic Extracts of *Echinacea purpurea* Flower. *Am J Plant Sci.*, 6:201–12.
24. Mandal, V., Mohan, Y., Hemalatha, S. (2007). Microwave assisted extraction—an innovative and promising extraction tool for medicinal plant research. *Pharmacogn Rev.*, 1(1):7–18.
25. Handa, S.S., Khanuja, S.P.S., Longo, G., Rakesh, D.D. (2008). Extraction Technologies for Medicinal and Aromatic Plants., International Centre for science and high technology, Triste.
26. Vidal, A., Fallarero, A., Peña, B.R., Medina, M.E., Gra, B., Rivera, F., et al. (2003). Studies on the toxicity of *Punica granatum* L.(Punicaceae) whole fruit extracts. *J Ethnopharmacol.*, 89(2):295–300.
27. Vinson, J.A., Su, X., Zubik, L., Bose, P. (2001). Phenol antioxidant quantity and quality in foods: fruits. *J Agric Food Chem.*, 49(11):5315–21.
28. Ravipati, A.S., Zhang, L., Koyyalamudi, S.R., Jeong, S.C., Reddy, N., Bartlett, J., et al. (2012). Antioxidant and anti-inflammatory activities of selected Chinese medicinal plants and their relation with antioxidant content. *BMC Complement Altern Med.*, 12(1):173.
29. Gil, M.I., Tomás-Barberán, F.A., Hess-Pierce, B., Holcroft, D.M., Kader, A.A. (2000). Antioxidant activity of pomegranate juice and its relationship with phenolic composition and processing. *J Agric Food Chem.*, 48(10):4581–9.
30. Moon, J. K., Shibamoto, T. (2009). Antioxidant Assays for Plant and Food Components. *J Agric Food Chem.*

- 57(5):1655–66.
31. Amakura, Y., Okada, M., Tsuji, S., Tonogai, Y. (2000). Determination of phenolic acids in fruit juices by isocratic column liquid chromatography. *J Chromatogr A.*, 891(1):183–8.
32. Tezcan, F., Gültekin-Özgüven, M., Diken, T., Özçelik, B., Erim, F.B. (2009). Antioxidant activity and total phenolic, organic acid and sugar content in commercial pomegranate juices. *Food Chem.*, 115(3):873–7.
33. Rice-Evans, C., Miller, N., Paganga, G. (1997). Antioxidant properties of phenolic compounds. *Trends Plant Sci.*, 2(4):152–9.
34. Tanaka, T., Nonaka, G., Nishioka, I. (1990). Tannins and Related Compounds. C.: Reaction of Dehydrohexahydroxydiphenic Acid Esters with Bases, and Its Application to the Structure Determination of Pomegranate Tannins, Granatins A and B. *Chem Pharm Bull (Tokyo).*, 38(9):2424–8.
35. Marshall, T.A., Roberts, R.J. (1990). In vitro and in vivo assessment of lipid peroxidation of infant nutrient preparations: effect of nutrition on oxygen toxicity. *J Am Coll Nutr.*, 9(3):190–9.
36. Mitchell, A.E., Hong, Y.J., May, J.C., Wright, C.A., Bamforth, C.W. (2005). A comparison of polyvinylpyrrolidone (PVPP), silica Xerogel and a polyvinylpyrrolidone (PVP)-silica Co-product for their ability to remove polyphenols from beer. *J Inst Brew.*, 111(1):20–5.
37. Gunasena, K., Senarathana, W.T.P.S. (2017). Comparison of phytochemicals present in locally available Sri Lankan and imported (Indian) fruits of *Punica granatum* (Lythracea)., 3(1).

## Design and Development of Multifunctional Hybrids of Ferulic Acid and 1,3,4-Oxadiazoles for the Treatment of Alzheimer's Disease

Avanish Tripathi<sup>#</sup>, Priyanka Kumari Choubey<sup>#</sup>, Ankit Seth, Piyooash Sharma, Manish Kumar Tripathi and Sushant Kumar Shrivastava<sup>\*</sup>

Department of Pharmaceutical Engineering & Technology, Indian Institute of Technology (Banaras Hindu University), Varanasi 221005, India

<sup>\*</sup>For Correspondence - skshrivastava.phe@itbhu.ac.in

<sup>#</sup>Both the authors contributed equally.

### Abstract

Ferulic acid-based multifunctional molecular hybrids of 1,3,4-oxadiazoles were designed, synthesized, and biologically evaluated for the treatment of Alzheimer's disease. Among the synthesized compounds, the derivatives with 4-hydroxy-3,5-dimethoxy substituent (FA5 and CFA5) showed balanced inhibitory potential against hAChE, hBChE, and hBACE-1. Also, CFA5 displayed remarkable PAS-AChE binding with significant displacement of propidium iodide, and appreciable blood-brain barrier permeability predictions in PAMPA-BBB assay. The thioflavin T assay in self- and AChE-induced experiments established the considerable anti-A $\beta$  aggregatory activity of CFA5. Compound CFA5 also showed neuroprotective activity in A $\beta$ -induced oxidative stress against SH-SY5Y neuroblastoma cell lines. Moreover, *in vivo* behavioral studies showed amelioration of cognitive dysfunction in rats tested by Y-maze. *In silico* molecular docking study showed consensual binding interactions of CFA5 with active binding site residues of AChE and BACE-1.

**Keywords:** Alzheimer's disease; acetylcholinesterase (AChE);  $\beta$ -secretase-1 (BACE-1); A $\beta$  aggregation; molecular hybridization, multifunctional agents.

### Introduction

Alzheimer's (AD), a catastrophic brain disorder, has preyed life of millions (1). The silent creep of AD not only leads to the loss of memory but in many cases, "the loss of life" (2). The disease progresses gradually and relentlessly that causes degeneration of brain cells, diminished memory, obstruction in thinking and perception along with the disruption of the patient's capacity to function self-reliantly (3,4). Typically the AD originates in the hippocampal region of the brain and then advances to the other centers of the brain that control the rhetorical, physical, and judgmental activities of the patient (5). The dreadful disease is characterized by multifarious etiology in conjunction with its overlapping pathological mechanisms and clinical manifestations. Despite rigorous research efforts put up by scientists worldwide, there are still several unsolved mysteries surrounding this disorder (6). To date, about 46 million people are diagnosed with dementia worldwide. Regrettably, the figure was projected to reach 131.5 million by 2050. Substantial evidence has exposed the origin of AD from a combined array of neurochemical mechanisms causing cell death and tissue loss in the Alzheimer's brain (7).

The pathophysiological hallmarks of the disease include depleted levels of acetylcholine

(ACh)(8), accumulation of amyloid-beta(9), dysfunction of *N*-methyl-D-aspartate receptor(10), abnormally hyperphosphorylated tau proteins forming neurofibrillary tangles(11), neuro-inflammation (12), increased reactive oxygen species production (13), and so on(14). Irrespective of the extensive expansion in the high-throughput screening procedures and the colossal efforts for the discovery of novel molecules for AD, their numbers have not increased significantly over the last few decades(15). Only a handful of drugs are available that typically enhance cognitive function and improve the symptoms of AD, but none of them prohibit or halt the progression of the disease or offer a cure(16). Also, the clinical trials of several potential drug candidates failed to elicit positive outcomes(17). The researchers are now firmly convinced that the targeting of a single node of the Alzheimer's classical pathway by conventional therapeutics only exerts a little effect on the multifactorial AD network. These findings suggest an immense requirement of novel drugs with a strong potential of treatment that modulates multiple targets that decelerate the AD progression rather than a diminution of symptoms(18-20).

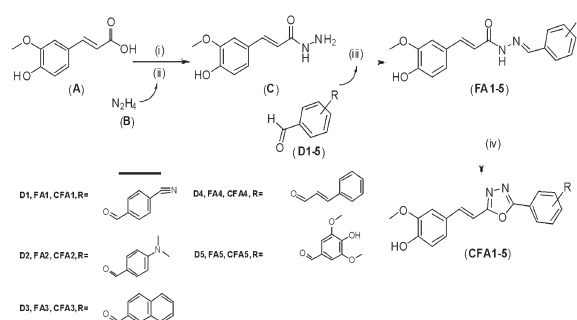
Cholinesterases, particularly AChE and BChE, were clinically proven as the crucial therapeutic target in the management of AD as they are responsible for the hydrolytic transformation of ACh(21). A depleted level of ACh is considered to be one of the critical pathogenic hallmarks of AD. It was revealed by numerous studies that the accumulation of extracellular senile plaques comprising of amyloid-Beta (A $\beta$ ) peptide is a prominent reason for neurotoxicity in AD(22). Studies have also demonstrated the involvement of cholinesterases along with another reported enzyme BACE-1 in the deposition and aggregation of A $\beta$  in AD(23). The generation of free radicals in mitochondria was reported owing to A $\beta$  buildup that leads to oxidative stress(24). Therefore the strategy of designing & synthesizing novel molecules for multiple targets was adopted in this research.

A series of ferulic acid tethered 1,3,4-oxadiazole hybrids were designed, synthesized,

and evaluated for all the pathogenic mechanisms reported above. Ferulic acid, a polyphenolic scaffold is profusely found in several plants like *Ferula foetida*, and it was reported previously in synthesizing several hybrids with potential antioxidant, anti-cholinesterase along with anti-A $\beta$  aggregation activities(25-27). However, owing to its poor water solubility, oral bioavailability, and BBB permeation, the clinical efficacy of this scaffold is compromised(28,29). Therefore, the concept of molecular hybridization was successfully utilized in the present work to synthesize novel hybrids of ferulic acid with 1,3,4-oxadiazole as multitarget-directed ligands (MTDLs) for AD.

## Results and Discussion

**Chemistry:** The target compounds FA1–5 and CFA1–5 were synthesized as per the reaction sequence of Scheme 1. Initially, ferulic acid (A) was reacted with *N*-hydroxybenzotriazole (HOBT) and 1-ethyl-3-(3-dimethylaminopropyl) carbodiimide (EDC) in acetonitrile to form its ester, which *in situ* reacted with hydrazine hydrate (B, 80 %v/v) under cold condition (0–5 °C) to yield 3-(4-hydroxy-3-methoxyphenyl)acryloylhydrazide (C). The FT-IR spectrum of compound C showed the stretching bands at 3654 and 3472 cm<sup>-1</sup> for —OH and —NH functional groups, respectively. Additionally, two stretching vibrations were observed at 3122 and 3117 cm<sup>-1</sup> for NH<sub>2</sub>, which confirmed the formation of hydrazide. The <sup>1</sup>H NMR spectrum showed D<sub>2</sub>O exchangeable peaks at  $\delta_{\text{H}}$  10.60 (1H) and  $\delta_{\text{H}}$  5.41 ppm (2H) for —NH and —NH<sub>2</sub>, respectively.



**Scheme 1.** Synthesis of target compounds.



**Reagents and conditions:** (i) HOBT, EDC.HCl, CH<sub>3</sub>CN, stirring, room temperature, 2 h; (ii) N<sub>2</sub>H<sub>4</sub> (2), CH<sub>3</sub>CN (0–5 °C) stirring, 3h; (iii) substituted benzaldehydes (D1–5), absolute C<sub>2</sub>H<sub>5</sub>OH, GAA, reflux, 6–8 h; (iv) chloramine T, absolute C<sub>2</sub>H<sub>5</sub>OH, stirring, room temperature, 30 min.

Subsequently intermediate (C) was refluxed in ethanol with a various substituted aldehyde in the presence of the catalytic amount of glacial acetic acid to yield respective imines (FA 1–5), which were further cyclized by chloramine T in absolute ethanol to afford molecular hybrids of ferulic acid-based 1,3,4-oxadiazole (CFA 1–5). The FT-IR spectra of imines showed characteristic HC=N stretching between 1625–1602 cm<sup>-1</sup>. Also, the disappearance of a dual stretching band of —NH<sub>2</sub> confirmed the formation of imines (FA 1–5). The disappearance of C=O peak in FT-IR spectra of CFA1–5 confirmed the formation of the oxadiazole ring. The <sup>1</sup>H NMR spectra of imines compounds (FA1-5) were characterized by the disappearance of D<sub>2</sub>O exchangeable peak of —NH<sub>2</sub> and appearance of HC=N (1H) peak. The characteristic HC=N (1H) and —NH (1H) signals were absent in <sup>1</sup>H NMR spectra of cyclized oxadiazoles (CFA1–5).

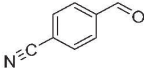
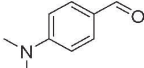
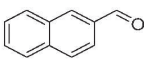
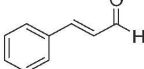
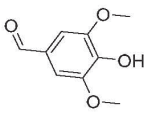
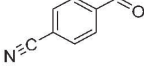
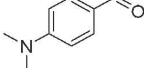
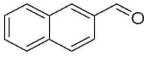
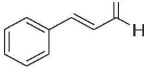
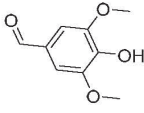
## 2.2 *In Vitro* Biological Evaluation

**Cholinesterase (AChE and BChE) and BACE-1 inhibition assays:** The cholinesterase inhibitory potential of synthesized compounds (FA1–5 and CFA1–5) was evaluated by Ellman colorimetric assay(30). The compounds displayed considerable inhibitory potential against both the cholinesterases (AChE and BChE). The Schiff bases (FA1–5) showed moderately lower inhibitory potential compared to their cyclic oxadiazole counterparts (CFA1–5), respectively. The compounds FA3 and CFA3 with naphthyl ring at the terminal group showed poor inhibition of AChE (> 5 μM) and BChE (> 10 μM). The replacement of naphthyl moiety with a substituted phenyl group significantly improved the inhibitory potential against AChE and BChE. The compounds with 4-dimethylamino, p-CN, and cinnamic substitution showed moderately lower inhibition of AChE and

BChE (> 1 μM). The substitution with a 4-hydroxy-3,5-dimethoxy group at the phenyl terminus showed maximum AChE (IC<sub>50</sub>, FA5: 0.98 μM and CFA5: 0.52 μM) and BChE (IC<sub>50</sub>, FA5: 2.13 μM and CFA5: 2.09 μM) inhibitory potential with IC<sub>50</sub> ranging in submicromolar to micromolar levels. In our quest to explore multifunctional therapeutic candidates, the FRET-based fluorometric BACE-1 inhibition assay was performed. Conversely to the cholinesterase inhibition, the results elicited that all the Schiff bases (FA1–5) were better BACE-1 inhibitors compared to their cyclized counterparts (CFA1–5). All the tested compounds showed micromolar inhibitory potential against BACE-1, with the maximum inhibition was observed in 4-hydroxy-3,5-dimethoxy substituted compounds (FA5 and CFA5). The results of *in vitro* enzyme assays signified the balanced inhibitory potential of FA5 and CFA5. The results of enzyme assays are summarized in Table 1.

**Enzyme kinetics study:** The enzyme kinetics study of most potential lead candidate CFA5 was evaluated against AChE using six different concentrations of substrate, i.e., acetylthiocholine iodide (ATCI). Three different concentrations of compound CFA5 were tested separately against each substrate concentration. The Lineweaver-Burk double reciprocal plot was drawn between the velocity of reaction (y-axis) and substrate concentrations (x-axis) to determine the type of enzyme inhibition. The plots revealed decreased V<sub>max</sub>, while K<sub>m</sub> increased with increasing the concentration of test compound CFA5, which suggested the mixed type of AChE inhibition (Figure 1A). In Lineweaver-Burk plot, the lines intersection point was at less than zero at x-axis and greater than zero at the y-axis, which indicated that ligand preferentially binds to free enzyme rather than enzyme-substrate complex(31). Further, Dixon plot was constructed between the slopes of Lineweaver-Burk plots and the concentration of test compound CFA5 (Figure 1B). The intersection point at the x-axis of the plot can be considered as dissociation constant K<sub>i</sub>, which was found to be 0.305 μM(32).

**Table 1.** Results of hAChE, hBChE and hBACE-1 inhibition assays by target compounds.

comp	Ar-group	IC <sub>50</sub> ± SEM (µM) <sup>a</sup>			selectivity for hAChE <sup>b</sup>
		hAChE	hBChE	hBACE-1	
<b>FA1</b>		1.18 ± 0.016	3.48 ± 0.062	4.62 ± 0.063	2.94
<b>FA2</b>		2.73 ± 0.062	7.63 ± 0.096	5.34 ± 0.057	2.79
<b>FA3</b>		>5	>10	nd	--
<b>FA4</b>		1.53 ± 0.050	3.96 ± 0.037	4.21 ± 0.098	2.58
<b>FA5</b>		0.98 ± 0.051	2.13 ± 0.074	3.25 ± 0.071	2.17
<b>CFA1</b>		1.02 ± 0.072	3.29 ± 0.074	6.25 ± 0.062	3.5
<b>CFA2</b>		1.26 ± 0.068	4.80 ± 0.089	5.98 ± 0.084	3.80
<b>CFA3</b>		>5	>10	nd	--
<b>CFA4</b>		1.21 ± 0.041	2.69 ± 0.045	7.95 ± 0.740	3.68
<b>CFA5</b>		0.52 ± 0.046	2.09 ± 0.081	3.38 ± 0.085	4.01
	donepezil <sup>c</sup>	0.046 ± 0.003	1.94 ± 0.093	0.220 ± 0.006	42.2
	rivastigmine <sup>c</sup>	2.58 ± 0.032	1.07 ± 0.054	nd	0.41

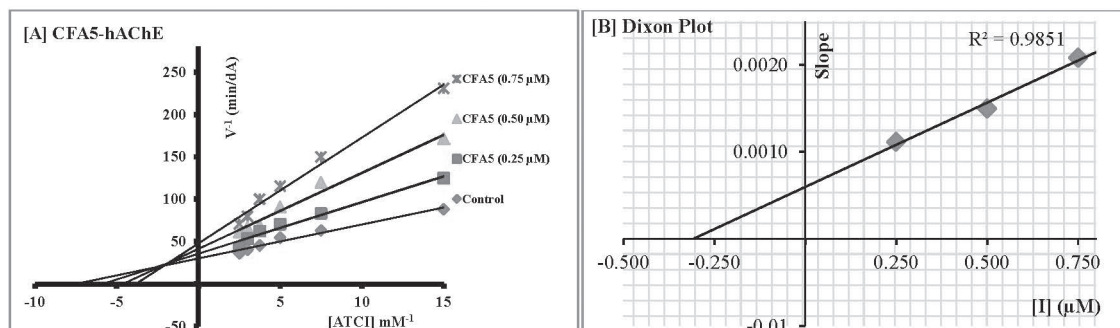


**Fig. 1.** Results of enzyme kinetics of **CFA5** on AChE; [A] Lineweaver-Burk plot; [B] Dixon plot.

**Propidium iodide displacement assay:**

Regardless of the non-cholinergic function of AChE, it also interacts with the structural motif of the peripheral anionic site (PAS) of AChE and potentiates A $\alpha$  aggregation(33). This hypothesis is supported by propidium iodide, a known ligand bind specifically to PAS-AChE, and responsible for increasing the fluorescence intensity up to 8-10 folds. The experimental affinity of selected compounds FA5 and CFA5 towards AChE-PAS were evaluated through propidium iodide displacement assay. Compounds FA5 and CFA5 were evaluated at two different concentrations (10 and 50  $\mu M$ ). Results of assay revealed that compound FA5 has lower propidium iodide displacement ability, while CFA5 demonstrated significantly higher displacement, compared standard donepezil at both the tested concentrations. The results pointed out that CFA5 could bind significantly to PAS-AChE (Table 2).

**2.2.4 Blood-brain barrier (BBB) permeability assay:**

Blood-brain barrier (BBB) permeability is the most important criterion while designing a drug for CNS activity(34). Parallel artificial membrane permeation assay (PAMPA) was performed to determine the permeation potential of new hybrids(35). The assay was validated by comparing the experimental ( $P_{e(exp)}$ ) and reference ( $P_{e(ref)}$ ) permeability values of nine commercial drugs and define a permeability range for excellent, uncertain, and poor permeability values as per our previously prescribed protocols. Compound CFA5 exhibited appreciable BBB permeability, while FA5 showed uncertain BBB permeability predictions (Table 2). These results suggested that compound CFA5 exhibited balanced inhibition of both cholinesterases (hAChE and hBChE) and hBACE-1. This compound also has commendable propidium iodide displacement capability along with appreciable BBB permeability predictions suggested by PAMPA assay. Therefore,

**Table 2.** Results of propidium iodide displacement and PAMPA assays.

compd PI displacement from PAS-hAChE (%) <sup>a</sup>		PAMPA-BBB permeability	
[I] = 10 $\mu M$	[I] = 50 $\mu M$	$P_{e(exp)}$ ( $10^{-6} cm s^{-1}$ )	Prediction
<b>FA5</b> 15.15 $\pm$ 1.35	21.98 $\pm$ 1.52	3.6 $\pm$ 0.32	CNS <sup>+c</sup>
<b>CFA5</b> 24.26 $\pm$ 1.15	33.24 $\pm$ 1.20	6.3 $\pm$ 0.29	CNS <sup>+b</sup>
donepezil 22.14 $\pm$ 1.50	31.52 $\pm$ 1.29	6.4 $\pm$ 0.20	CNS <sup>+b</sup>

compounds **CFA5** was selected as lead candidates for further pharmacological investigations.

<sup>a</sup>The PI assay was performed at 10  $\mu\text{M}$  and 50  $\mu\text{M}$  concentrations of respective inhibitors. <sup>b</sup>'CNS+' suggested excellent ( $P_e > 4.4 \times 10^{-6} \text{ cm s}^{-1}$ ) and <sup>c</sup>'CNS±' suggested uncertain ( $4.4$  to  $1.8 \times 10^{-6} \text{ cm s}^{-1}$ ) brain permeability values. Data are expressed as the mean  $\pm$  SEM of three separate experiments ( $n = 3$ ).

**2.2.5 Self- and AChE-induced A $\beta$  aggregation inhibition by thioflavin T assay:** The A $\beta$  deposition in the neuronal cell is one of the major causes of AD. The thioflavin T assay was performed to determine the A $\beta$  aggregation inhibition potency. Compound **CFA5** has shown significant displacement of propidium iodide from PAS-AChE, which indicated that it could inhibit AChE accelerated A $\beta$  aggregation. Therefore, a thioflavin T based fluorometric assay was performed for **CFA5** to ascertain its efficacy against self- and AChE-induced A $\beta$  aggregation. The experiment was performed at three different concentration ratios of A $\beta$  and inhibitor (10:5  $\mu\text{M}$ , 10:10  $\mu\text{M}$ , and 10:20  $\mu\text{M}$ , respectively). The results were reported as normalized fluorescence intensity (NFI) (Figure 2). The results revealed that

the inhibitory potential of the compound is directly proportional to the concentration of the inhibitor. The inhibitory potential of compound **CFA5** (self-induced: 0.75-0.46; and hAChE-induced: 0.52-0.17) was significantly higher with reduced NFI compared to donepezil (self-induced: 0.76-0.64; hAChE-induced: 0.73-0.26).

**2.2.6 Neuroprotection studies on SH-SY5Y cell lines:** To determine the neuroprotective effect of compound **CFA5** on neuroblastoma SH-SY5Y cell lines by 3-(4,5-dimethylthiazol-2-yl)-2,5-diphenyl tetrazolium bromide (MTT) assay(36). The cells were exposed to different concentrations of compound **CFA5**(10, 20, 40, and 80  $\mu\text{M}$ ) for 48 hours to determine their potential in preventing cell death against A $\beta$ -induced oxidative stress. In this assay, 20  $\mu\text{M}$  of A $\beta$  was incubated with SH-SY5Y cells, which attenuated the cell viability to 61% compared to control. The incubation of A $\beta$  and SH-SY5Y cells in the presence of test compounds **CFA5** (68-88%) lead to significantly augmented % cell viabilities. Overall results suggested the neuroprotective activity of compound **CFA5** towards SH-SY5Y neuroblastoma cell lines against A $\beta$ -induced oxidative stress (Figure 3).

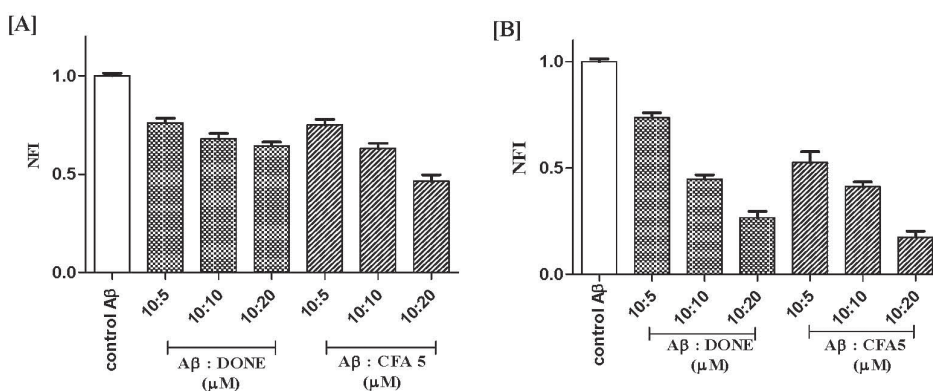


**Fig. 2.** Results of thioflavin T assay for compounds **CFA5** in [A] self-induced; [B] AChE-induced experiments. Each bar displays the values of normalized fluorescence intensity (NFI) as the mean  $\pm$  SEM of three separate experiments ( $n = 3$ ).

### 2.3 *In Vivo* Behavioral Studies

**2.3.1 Acute oral toxicity study:** The acute oral toxicity study was performed as per OECD guidelines 423 on healthy female Wistar rats (37-39). The results showed no adverse effects up to the dose of 500 mg/kg of **CFA5**. The results signified a significant margin of safety of compound **CFA5** and thereby processed for further *in vivo* investigations.

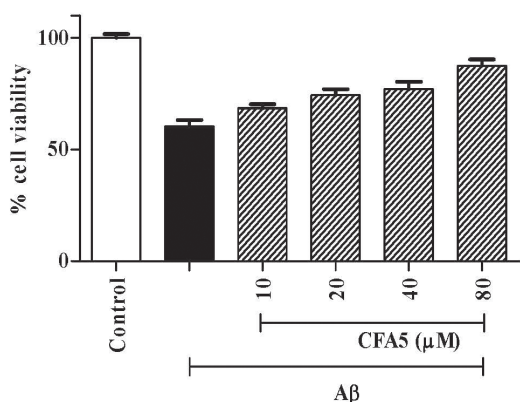


**Fig. 3.** The effect of compounds **CFA5** on neuroprotective ability on SH-SY5Y neuroblastoma cell lines. The results are expressed as the mean  $\pm$  SEM of three separate experiments (n = 3).

### 2.3.2 Scopolamine-induced amnesia model:

**Y maze test:** The Y-maze test was performed to evaluate the hippocampal-dependent spatial working memory in the rats. The test compound **CFA5** was administered daily for seven consecutive days to healthy male Wistar rats at the dose of 2.5, 5, and 10 mg/kg, p.o. On the seventh day, scopolamine was administered after thirty minutes of the treatment, and the Y-maze test was performed. This significantly decreased % alternation score in the scopolamine-group of animals (###p < 0.001, Figure 4A) compared to healthy control revealed induction of memory and learning impairment. Compound **CFA5** at the dose of 5 and 10 mg/kg exhibited statistically nonsignificant differences with donepezil (ns, Figure 4A). The total number of arm entries by all groups showed a nonsignificant difference indicated that scopolamine does not affect locomotive behavior in animals (Figure 4B). Overall results advocated that compound **CFA5** can revert scopolamine induce amnesia.

### 2.5 Molecular docking studies

The *in silico* molecular docking studies were performed to determine the binding affinity and of **CFA5** on both the target enzymes, i.e., AChE (PDBID: 4EY7) and BACE-1 (PDBID: 2ZJM). Initially, docking protocols and prepared grids were

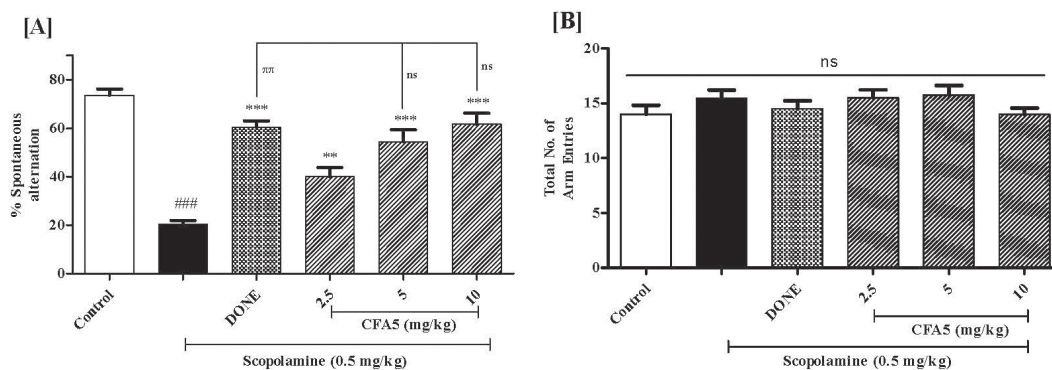


**Fig. 4.** The effect of compounds **CFA5** on scopolamine-induced amnesia model by Y maze test in rats. [A] Percentage spontaneous alterations and; [B] total arm entries. Data are expressed as the mean  $\pm$  SEM (n = 6). ###p < 0.001 versus control; \*\*\*p < 0.001, \*\*p < 0.01 versus scopolamine; °°p < 0.01, ns = nonsignificant versus donepezil (DONE).



validated by using the Superposition tool of Schrödinger. For this, the co-crystallized ligand was extracted and re-docked in the generated grids. Further, RMSD value was calculated by aligning the co-crystallized and redocked ligands using the superposition tool, which was found to be within the limit, i.e., below 2 Å for both the prepared grids of AChE and BACE-1(40). The result of docking studies showed that ferulic acid moiety of **CFA5** was aligned towards PAS of AChE, while phenyl terminal part was lined up towards catalytic anionic site (CAS). The ferulic acid moiety showed  $\delta$ - $\delta$  stacking and hydrophobic interaction with Trp286, while 1,3,4-oxadiazole active interactions with Tyr72, Tyr124 and Trp286 residues of PAS. The phenyl terminal moiety showed polar interactions with Ser203 and His447, with additional  $\delta$ - $\delta$  stacking interaction with His447 residue of CAS. Also, this terminal phenyl part showed  $\delta$ - $\delta$  stacking and hydrophobic interactions with Phe338 and Trp86 residues at the anionic subsite (Figures 5A and 5B). To accomplish our rationale of multifunctional activities, compound **CFA5** was also docked within the active site of BACE-1. The results showed that ferulic acid-based hybrid formed charged interactions with the aspartate dyad (Asp32 and Asp228) of BACE-1 (Figures 6A and 6B).

## CONCLUSION

AD is multifaceted, which involved the simultaneous involvement of several pathophysiological pathways in its progression. This multifactorial nature of AD has prompted the researchers to search multifunctional drug candidates that can affect multiple targets at one time. Herein, we have designed and synthesized a series of ferulic acid-based 1,3,4-oxadiazole hybrids. These hybrids were screened for their inhibitory potential against several targets such as AChE, hBChE, and hBACE-1. Among the tested derivatives, compounds **FA5** and **CFA5** with 4-hydroxy-3,5-dimethoxy substituent showed balanced inhibition of target enzymes. The enzyme kinetics study of compound **CFA5** suggested mixed-type of AChE inhibition. The results of propidium iodide displacement assay showed significant PAS-AChE binding by **CFA5**, with PAMPA assay predicted the appreciable BBB permeability. Also, **CFA5** elicited a remarkable disassembling of A $\beta$  aggregation in self- and AChE-induced experiments confirmed by thioflavin T assay. Further, MTT assay proved the neuroprotective activity of **CFA5** against A $\beta$ -induced oxidative stress in neuroblastoma SH-SY5Y cell lines. Furthermore, **CFA5** showed amelioration of cognitive dysfunction in the

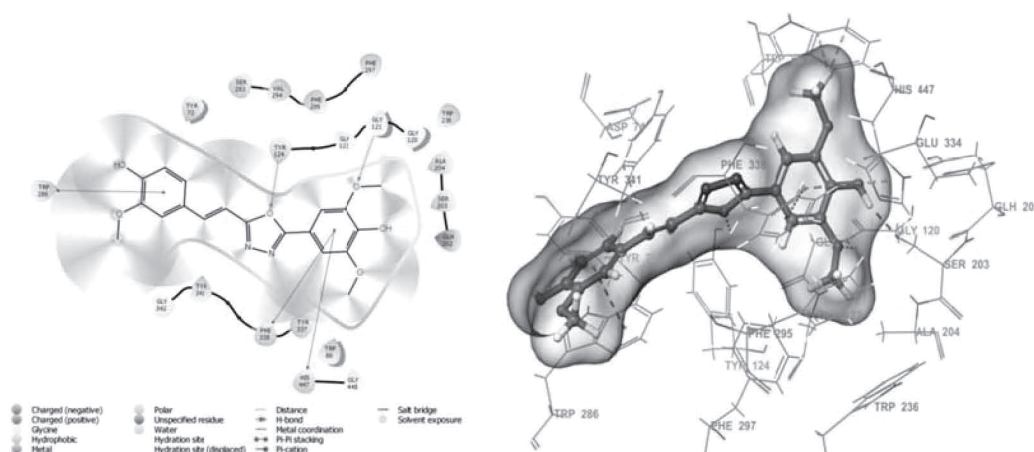


**Fig. 5.** The docked pose of **CFA5** within the active binding site of AChE. (A) 2D and; (B) 3D poses.

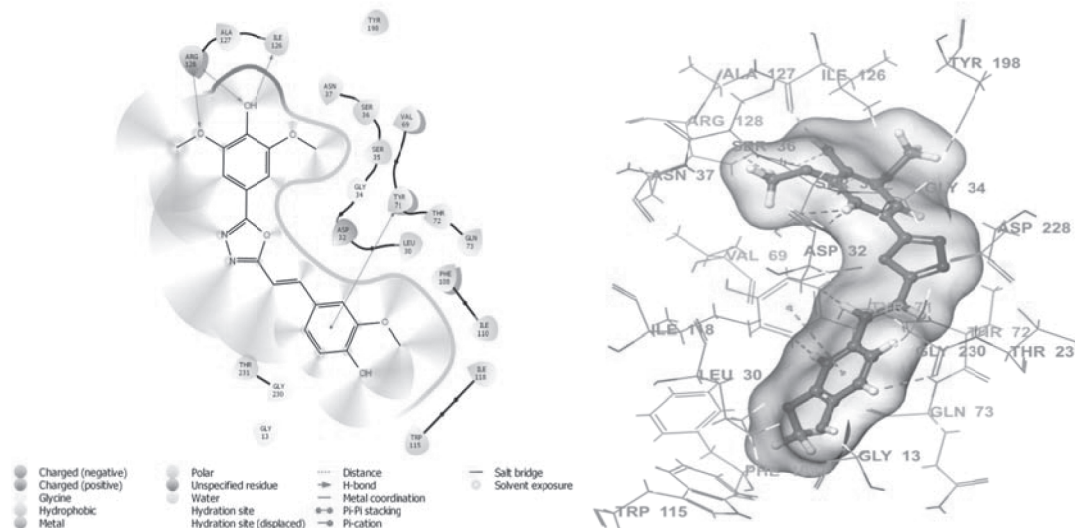


**Fig. 6.** The docked pose of **CFA5** within the active binding site of BACE-1. (A) 2D and; (B) 3D poses.

scopolamine-induced amnesia model performed by the Y-maze test. These results of behavioral studies were also observed to be nonsignificant with the standard drug donepezil at the tested dosage. Moreover, to confirm the consensual binding, molecular docking studies were envisaged, which proved significant interactions of **CFA5** with PAS and CAS of AChE and aspartate dyad of BACE-1. Overall results suggested compound **CFA5** to be the potential multifunctional lead candidate for the treatment of AD.

#### 4.1 Chemistry

**4.1.1 Chemicals and instrumentations:** All the reagents and chemicals were purchased from commercial suppliers and used without further purification. The reaction progress was monitored by thin-layer chromatography (TLC) using precoated silica gel G60 stationary phase and visualized by ultraviolet light (254 nm) or iodine vapors. Melting points were determined by using an automated melting point apparatus (Bamstead Electrothermal, UK) and reported as uncorrected. FT-IR spectra were recorded on Bruker ALPHA-T (Germany) ATR. The  $^1\text{H}$  and  $^{13}\text{C}$  NMR spectra were recorded on Bruker Avance 500 MHz spectrophotometer in  $\text{DMSO-}d_6$  with

tetramethylsilane (TMS) was used as an internal standard. The chemical shift was measured in the ppm ( $\delta$ ). The physicochemical and spectra data are given in Table 3.

**General procedure for the synthesis of compound C.** Briefly, ferulic acid (**A**, 0.52 mmol) was mixed with HOBT (0.78 mmol) in acetonitrile, and the reaction was stirred continuously with the addition of EDC (0.78 mmol) at room temperature for 2h. The formed intermediate ester, as confirmed by TLC was further added dropwise in a solution of hydrazine hydrate (**B**, 0.52 mmol) and acetonitrile(3ml) under cold condition ( $0-5^\circ\text{C}$ ). The completion of reaction was monitored by TLC, and organic layer was evaporated under reduced pressure. The reaction mixture was treated with DCM (2 x 10 ml) and extracted with water. The organic layer was passed through saturated solution of NaCl (30 ml) and dried over  $\text{Na}_2\text{SO}_4$ . The organic layer was evaporated under reduced pressure to obtain crude product, which was further purified with column chromatography. The white needle shape crystals of 3-(4-hydroxy-3-methoxyphenyl)acrylohydrazide (**C**) was obtained.

**3-(4-Hydroxy-3-methoxyphenyl)acrylohydrazide (C).** White needles, yield 73%;

**Table 3.** The results of physicochemical and spectra data for the synthesized target compounds (FA1-5 and CFA1-5).

Comp	% Yield	M.P (°C) <sup>a</sup>	R <sub>f</sub> value <sup>b</sup>	FT-IR (ν cm <sup>-1</sup> )	<sup>1</sup> H NMR δ <sub>H</sub> (ppm)	<sup>13</sup> C NMR δ <sub>C</sub> (ppm)
<b>FA1</b>	73	181-183	0.63	3664 (—OH), 3248 (—NH), 1690 (C=O), 1612 (C=N)	9.20 (s, 1H), 7.83 – 7.75 (m, 3H), 7.56 (d, J = 15.2 Hz, 1H), 7.45 (d, J = 7.5 Hz, 2H), 7.08 – 7.01 (m, 2H), 6.87 (d, J = 7.4 Hz, 1H), 6.56 (d, J = 15.2 Hz, 1H), 4.28 (s, 1H), 3.82 (s, 3H)	166.78, 149.54, 149.45, 148.12, 145.36, 138.52, 133.51, 129.12, 127.48, 123.68, 122.29, 119.12, 116.28, 115.81, 111.26, 56.80
<b>FA2</b>	76	186-188	0.68	3654 (—OH), 3242 (—NH), 1680 (C=O), 1602 (C=N)	9.38 (s, 1H), 7.81 (s, 1H), 7.40 (d, J = 11.2 Hz, 1H), 7.28 (d, J = 4.5 Hz, 2H), 7.14 (d, J = 7.5 Hz, 2H), 7.07 – 6.99 (m, 2H), 6.87 (d, J = 3.5 Hz, 1H), 6.57 (d, J = 11.0 Hz, 1H), 4.25 (s, 1H), 3.84 (s, 3H), 2.88 (s, 6H)	166.43, 153.38, 149.16, 149.01, 148.50, 145.41, 128.66, 127.65, 123.18, 122.29, 120.97, 115.81, 111.78, 111.65, 56.68, 42.01
<b>FA3</b>	79	176-178	0.67	3668 (—OH), 3254 (—NH), 1692 (C=O), 1616 (C=N)	9.41 (s, 1H), 8.15 (s, 1H), 8.00 (d, J = 7.5 Hz, 1H), 7.89 – 7.78 (m, 3H), 7.76 (d, J = 7.5 Hz, 1H), 7.50 (d, J = 15.8 Hz, 1H), 7.46 (dd, J = 9.3, 3.8 Hz, 2H), 7.08 – 6.98 (m, 2H), 6.85 (d, J = 7.5 Hz, 1H), 6.57 (d, J = 12.30 Hz, 1H), 4.21 (s, 1H), 3.86 (s, 3H)	166.56, 149.24, 148.41, 145.74, 134.99, 133.83, 133.19, 129.84, 128.47, 127.58, 126.93, 126.47, 123.92, 123.18, 122.29, 115.51, 111.47, 56.32
<b>FA4</b>	83	188-190	0.61	3674 (—OH), 3265 (—NH), 1698 (C=O), 1625 (C=N)	9.07 (s, 1H), 8.46 (d, J = 6.0 Hz, 1H), 7.27 (dd, J = 35.7, 11.8, Hz, 6H), 7.07 – 7.02 (m, 2H), 6.87 (dd, J = 14.3, 6.7 Hz, 2H), 6.79 (d, J = 15.5 Hz, 1H), 6.51 (d, J = 15.0 Hz, 1H), 4.29 (s, 1H), 3.88 (s, 3H)	166.36, 149.52, 148.54, 147.08, 145.52, 136.44, 130.52, 129.12, 128.46, 127.81, 125.30, 123.15, 122.51, 115.55, 111.45, 56.71
<b>FA5</b>	87	191-193	0.66	3678 (—OH), 3265 (—NH), 1698 (C=O), 1620 (C=N)	9.43 (s, 1H), 7.65 (s, 1H), 7.56 (d, J = 15.2 Hz, 1H), 7.09 – 6.99 (m, 2H), 6.87 (d, J = 7.5 Hz, 1H), 6.56 (d, J = 15.0 Hz, 1H), 6.37 (s, 2H), 4.28 (s, 1H), 4.16 (s, 1H), 3.81 (s, 9H)	166.73, 149.57, 148.68, 147.70, 145.84, 137.36, 128.15, 127.58, 123.18, 122.29, 115.81, 111.76, 107.50, 56.89
<b>CFA1</b>	77	121-123	0.76	3680 (—OH)	7.76 (s, 4H), 7.19 (d, J = 15.2 Hz, 1H), 6.82 (d, J = 15.2 Hz, 1H), 6.71 – 6.64 (m, 3H), 4.10 (s, 1H), 3.83 (s, 3H)	168.61, 163.89, 149.57, 148.42, 137.78, 130.78, 129.65, 127.51, 127.01, 123.18, 119.12, 115.81, 111.78, 110.46, 110.14, 56.84

Comp	% Yield	M.P (°C) <sup>a</sup>	R <sub>f</sub> value <sup>b</sup>	FT-IR (ν cm <sup>-1</sup> )	<sup>1</sup> H NMR δ <sub>H</sub> (ppm)	<sup>13</sup> C NMR δ <sub>C</sub> (ppm)
<b>CFA2</b>	79	129-131	0.71	3698 (—OH)	7.38 (d, <i>J</i> = 7.5 Hz, 2H), 7.08 (d, <i>J</i> = 15.0 Hz, 1H), 6.86 (d, <i>J</i> = 15.2 Hz, 1H), 6.81 – 6.74 (m, 4H), 6.68 (d, <i>J</i> = 7.2 Hz, 1H), 3.99 (s, 1H), 3.82 (s, 3H), 2.92 (s, 6H)	168.84, 162.56, 156.95, 149.45, 148.69, 137.12, 127.51, 123.31, 118.68, 115.98, 111.73, 111.14, 110.32, 56.32, 42.01
<b>CFA3</b>	78	118-120	0.78	3678 (—OH)	8.04 (d, <i>J</i> = 2.9 Hz, 1H), 7.96 (d, <i>J</i> = 8.9 Hz, 1H), 7.88 – 7.78 (m, 2H), 7.77 – 7.72 (m, 1H), 7.52 – 7.39 (m, 2H), 7.13 (d, <i>J</i> = 15.0 Hz, 1H), 6.89 (d, <i>J</i> = 15.2 Hz, 1H), 6.80 (dd, <i>J</i> = 9.8, 1.5 Hz, 2H), 6.69 (d, <i>J</i> = 7.3 Hz, 1H), 3.97 (s, 1H), 3.82 (s, 3H)	167.95, 166.22, 149.52, 148.53, 137.84, 134.51, 134.02, 130.64, 129.70, 129.33, 128.22, 127.61, 127.00, 126.50, 125.93, 123.36, 122.41, 115.62, 111.25, 110.36, 56.85
<b>CFA4</b>	81	117-119	0.81	3696 (—OH)	7.30 – 7.25 (m, 2H), 7.21 (t, <i>J</i> = 7.3 Hz, 2H), 7.18 – 7.13 (m, 1H), 7.09 (d, <i>J</i> = 3.5 Hz, 1H), 7.06 (d, <i>J</i> = 3.5 Hz, 1H), 6.97 (d, <i>J</i> = 15.2 Hz, 1H), 6.85 (d, <i>J</i> = 15.0 Hz, 1H), 6.81 – 6.77 (m, 2H), 6.68 (d, <i>J</i> = 7.3 Hz, 1H), 3.95 (s, 1H), 3.82 (s, 3H)	166.78, 149.57, 148.50, 138.51, 137.82, 135.88, 129.46, 129.12, 128.15, 127.58, 123.18, 115.81, 111.78, 110.14, 109.93, 56.79
<b>CFA5</b>	83	114-116	0.88	3668 (—OH)	7.09 (d, <i>J</i> = 15.2 Hz, 1H), 6.84 (d, <i>J</i> = 15.2 Hz, 1H), 6.81 – 6.77 (m, 2H), 6.73 (s, 2H), 6.69 (d, <i>J</i> = 7.3 Hz, 1H), 4.40 (s, 1H), 3.98 (s, 1H), 3.81 (s, 9H)	168.61, 163.03, 149.57, 148.50, 147.52, 142.66, 137.82, 127.58, 123.18, 118.05, 115.81, 111.78, 110.14, 107.25, 56.58

<sup>a</sup> Melting points are reported as uncorrected; <sup>b</sup> R<sub>f</sub> values were determined using DCM/Methanol 90:10 v/v as the mobile phase.

mp 158-160 °C; TLC (DCM/Methanol 90:10 v/v); R<sub>f</sub> = 0.32. FT-IR (*i* cm<sup>-1</sup>): 3654(—OH), 3472 (—NH), 3122, 3117 (—NH<sub>2</sub>), 1705(C=O). <sup>1</sup>H NMR (500 MHz) δ<sub>H</sub> 10.60 (s, 1H, —NH D<sub>2</sub>O exchangeable), 7.37 (d, *J* = 4.2 Hz, 1H), 7.16 (t, *J* = 7.5 Hz, 1H), 7.14(d, *J* = 1.2 Hz, 1H), 5.41(s, 2H, —NH<sub>2</sub>D<sub>2</sub>O exchangeable), 4.16 (s, 1H), 4.01(s, 3H).

**General procedure for the synthesis of FA 1–5.** The intermediate **C**(4.8 mmol, 1 eq) was reacted with respective aromatic aldehydes (**D1–5**, 1.2 eq) in absolute ethanol (10 mL) with the addition of few drops of glacial acetic acid. The reaction mixture was heated at reflux for 6–8 h till the completion of reaction as monitored by TLC using DCM:MeOH (90:10 v/v) as the mobile phase. The reaction mixture was kept overnight and obtained precipitate was filtered, washed, dried, recrystallized in absolute ethanol, and collected as the pure compounds.

**N'-(4-Cyanobenzylidene)-3-(4-hydroxy-3-methoxyphenyl)acrylohydrazide (FA1).** White solid, yield 73%; mp 181-183 °C; TLC (DCM/Methanol 90:10 v/v); R<sub>f</sub> = 0.63. FT-IR (*i* cm<sup>-1</sup>): 3664 (—OH), 3248 (—NH), 1690 (C=O), 1612 (C=N). <sup>1</sup>H NMR (500 MHz) δ<sub>H</sub> 9.20 (s, 1H), 7.83 – 7.75 (m, 3H), 7.56 (d, *J* = 15.2 Hz, 1H), 7.45 (d, *J* = 7.5 Hz, 2H), 7.08 – 7.01 (m, 2H), 6.87 (d, *J* = 7.4 Hz, 1H), 6.56 (d, *J* = 15.2 Hz, 1H), 4.28 (s, 1H), 3.82 (s, 3H). <sup>13</sup>C NMR (126 MHz) δ<sub>C</sub>: 166.78, 149.54, 149.45, 148.12, 145.36, 138.52, 133.51, 129.12, 127.48, 123.68, 122.29, 119.12, 116.28, 115.81, 111.26, 56.80.

**N'-(4-(Dimethylamino)benzylidene)-3-(4-hydroxy-3-methoxyphenyl)acrylohydrazide (FA2).** White solid, yield 76%; mp 186-188 °C; TLC (DCM/Methanol 90:10 v/v); R<sub>f</sub> = 0.68. FT-IR (*i* cm<sup>-1</sup>): 3654 (—OH), 3242 (—NH), 1680 (C=O), 1602 (C=N). <sup>1</sup>H NMR (500 MHz) δ<sub>H</sub> 9.38 (s, 1H), 7.81 (s, 1H), 7.40 (d, *J* = 11.2 Hz, 1H), 7.28 (d, *J* = 4.5 Hz, 2H), 7.14 (d, *J* = 7.5 Hz, 2H), 7.07 – 6.99 (m, 2H), 6.87 (d, *J* = 3.5 Hz, 1H), 6.57 (d, *J* = 11.0 Hz, 1H), 4.25 (s, 1H), 3.84 (s, 3H), 2.88 (s, 6H). <sup>13</sup>C NMR (126 MHz) δ<sub>C</sub> 166.43, 153.38, 149.16, 149.01, 148.50, 145.41, 128.66, 127.65, 123.18, 122.29, 120.97, 115.81, 111.78, 111.65, 56.68, 42.01.



**3-(4-Hydroxy-3-methoxyphenyl)-N'-(naphthalen-2-ylmethylene)acrylohydrazide (FA3).** White solid, yield 79%; mp 176-178°C; TLC (DCM/Methanol 90:10 v/v);  $R_f = 0.67$ . FT-IR ( $\nu$  cm<sup>-1</sup>): 3668 (—OH), 3254 (—NH), 1692 (C=O), 1616 (C=N). <sup>1</sup>H NMR (500 MHz)  $\delta_H$ : 9.41 (s, 1H), 8.15 (s, 1H), 8.00 (d,  $J = 7.5$  Hz, 1H), 7.89 – 7.78 (m, 3H), 7.76 (d,  $J = 7.5$  Hz, 1H), 7.50 (d,  $J = 15.8$  Hz, 1H), 7.46 (dd,  $J = 9.3, 3.8$  Hz, 2H), 7.08 – 6.98 (m, 2H), 6.85 (d,  $J = 7.5$  Hz, 1H), 6.57 (d,  $J = 12.30$  Hz, 1H), 4.21 (s, 1H), 3.86 (s, 3H). <sup>13</sup>C NMR (126 MHz)  $\delta_C$ : 166.56, 149.24, 148.41, 145.74, 134.99, 133.83, 133.19, 129.84, 128.47, 127.58, 126.93, 126.47, 123.92, 123.18, 122.29, 115.51, 111.47, 56.32.

**3-(4-Hydroxy-3-methoxyphenyl)-N'-(3-phenylallylidene)acrylohydrazide (FA4).** White solid, yield 83%; mp 188-190 °C; TLC (DCM/Methanol 90:10 v/v);  $R_f = 0.61$ . FT-IR ( $\nu$  cm<sup>-1</sup>): 3674 (—OH), 3265 (—NH), 1698 (C=O), 1625(C=N). <sup>1</sup>H NMR (500 MHz)  $\delta_H$ : 9.07 (s, 1H), 8.46 (d,  $J = 6.0$  Hz, 1H), 7.27 (dd,  $J = 35.7, 11.8$ , Hz, 6H), 7.07 – 7.02 (m, 2H), 6.87 (dd,  $J = 14.3, 6.7$  Hz, 2H), 6.79 (d,  $J = 15.5$  Hz, 1H), 6.51 (d,  $J = 15.0$  Hz, 1H), 4.29 (s, 1H), 3.88 (s, 3H). <sup>13</sup>C NMR (126 MHz)  $\delta_C$ : 166.36, 149.52, 148.54, 147.08, 145.52, 136.44, 130.52, 129.12, 128.46, 127.81, 125.30, 123.15, 122.51, 115.55, 111.45, 56.71.

**N'-(4-Hydroxy-3,5-dimethoxybenzylidene)-3-(4-hydroxy-3-methoxyphenyl) acrylohydrazide (FA5).** White solid, yield 87%; mp 191-193 °C; TLC (DCM/Methanol 90:10 v/v);  $R_f = 0.66$ . FT-IR ( $\nu$  cm<sup>-1</sup>): 3678 (—OH), 3265 (—NH), 1698 (C=O), 1620 (C=N). <sup>1</sup>H NMR (500 MHz)  $\delta_H$ : 9.43 (s, 1H), 7.65 (s, 1H), 7.56 (d,  $J = 15.2$  Hz, 1H), 7.09 – 6.99 (m, 2H), 6.87 (d,  $J = 7.5$  Hz, 1H), 6.56 (d,  $J = 15.0$  Hz, 1H), 6.37 (s, 2H), 4.28 (s, 1H), 4.16 (s, 1H), 3.81 (s, 9H). <sup>13</sup>C NMR (126 MHz)  $\delta_C$ : 166.73, 149.57, 148.68, 14 General procedure for the synthesis of CFA 1-5. The mixture of respective imines (FA1-5, 1 eq) and chloramine T (2.2 eq) in absolute ethanol was stirred at room temperature for 30 min to obtain a solid white precipitate, which was filtered, and purified by column chromatography using activated silica gel to afford pure oxadiazole hybrids (CFA1-5).

**4-(5-(4-Hydroxy-3-methoxystyryl)-1,3,4-oxadiazol-2-yl)benzotrile(CFA1).** White solid, yield 77%; mp 121-123°C; TLC (DCM/Methanol 90:10 v/v);  $R_f = 0.76$ . FT-IR ( $\nu$  cm<sup>-1</sup>): 3680(—OH). <sup>1</sup>H NMR (500 MHz)  $\delta_H$ : 7.76 (s, 4H), 7.19 (d,  $J = 15.2$  Hz, 1H), 6.82 (d,  $J = 15.2$  Hz, 1H), 6.71 – 6.64 (m, 3H), 4.10 (s, 1H), 3.83 (s, 3H). <sup>13</sup>C NMR (126 MHz)  $\delta_C$ : 168.61, 163.89, 149.57, 148.42, 137.78, 130.78, 129.65, 127.51, 127.01, 123.18, 119.12, 115.81, 111.78, 110.46, 110.14, 56.84.

**4-(2-(5-(4-(Dimethylamino)phenyl)-1,3,4-oxadiazol-2-yl)vinyl)-2-methoxyphenol (CFA2).** White solid, yield 79%; mp 129-131 °C; TLC (DCM/Methanol 90:10 v/v);  $R_f = 0.71$ . FT-IR ( $\nu$  cm<sup>-1</sup>): 3698(—OH). <sup>1</sup>H NMR (500 MHz)  $\delta_H$ : 7.38 (d,  $J = 7.5$  Hz, 2H), 7.08 (d,  $J = 15.0$  Hz, 1H), 6.86 (d,  $J = 15.2$  Hz, 1H), 6.81 – 6.74 (m, 4H), 6.68 (d,  $J = 7.2$  Hz, 1H), 3.99 (s, 1H), 3.82 (s, 3H), 2.92 (s, 6H). <sup>13</sup>C NMR (126 MHz)  $\delta_C$ : 168.84, 162.56, 156.95, 149.45, 148.69, 137.12, 127.51, 123.31, 118.68, 115.98, 111.73, 111.14, 110.32, 56.32, 42.01.

**2-Methoxy-4-(2-(5-(naphthalen-2-yl)-1,3,4-oxadiazol-2-yl)vinyl)phenol (CFA3).** White solid, yield 78%; mp 118-120 °C; TLC (DCM/Methanol 90:10 v/v);  $R_f = 0.78$ . FT-IR ( $\nu$  cm<sup>-1</sup>): 3678(—OH). <sup>1</sup>H NMR (500 MHz)  $\delta_H$ : 8.04 (d,  $J = 2.9$  Hz, 1H), 7.96 (d,  $J = 8.9$  Hz, 1H), 7.88 – 7.78 (m, 2H), 7.77 – 7.72 (m, 1H), 7.52 – 7.39 (m, 2H), 7.13 (d,  $J = 15.0$  Hz, 1H), 6.89 (d,  $J = 15.2$  Hz, 1H), 6.80 (dd,  $J = 9.8, 1.5$  Hz, 2H), 6.69 (d,  $J = 7.3$  Hz, 1H), 3.97 (s, 1H), 3.82 (s, 3H). <sup>13</sup>C NMR (126 MHz)  $\delta_C$ : 167.95, 166.22, 149.52, 148.53, 137.84, 134.51, 134.02, 130.64, 129.70, 129.33, 128.22, 127.61, 127.00, 126.50, 125.93, 123.36, 122.41, 115.62, 111.25, 110.36, 56.85.

**2-Methoxy-4-((E)-2-(5-((E)-styryl)-1,3,4-oxadiazol-2-yl)vinyl)phenol (CFA4).** White solid, yield 81%; mp 117-119 °C; TLC (DCM/Methanol 90:10 v/v);  $R_f = 0.81$ . FT-IR ( $\nu$  cm<sup>-1</sup>): 3696 (—OH). <sup>1</sup>H NMR (500 MHz)  $\delta_H$ : 7.30 – 7.25 (m, 2H), 7.21 (t,  $J = 7.3$  Hz, 2H), 7.18 – 7.13 (m, 1H), 7.09 (d,  $J = 3.5$  Hz, 1H), 7.06 (d,  $J = 3.5$  Hz, 1H), 6.97 (d,  $J = 15.2$  Hz, 1H), 6.85 (d,  $J = 15.0$  Hz, 1H), 6.81 – 6.77 (m, 2H), 6.68 (d,  $J = 7.3$  Hz, 1H), 3.95 (s, 1H), 3.82 (s, 3H). <sup>13</sup>C NMR (126 MHz)



$\delta_c$  166.78, 149.57, 148.50, 138.51, 137.82, 135.88, 129.46, 129.12, 128.15, 127.58, 123.18, 115.81, 111.78, 110.14, 109.93, 56.79.

**4-(5-(4-Hydroxy-3-methoxystyryl)-1,3,4-oxadiazol-2-yl)-2,6-dimethoxyphenol (CFA5).**

White solid, yield 83%; mp 114-116 °C; TLC (DCM/Methanol 90:10 v/v);  $R_f$  = 0.88. FT-IR ( $\nu$  cm<sup>-1</sup>): 3668 (—OH). <sup>1</sup>H NMR (500 MHz)  $\delta_H$  7.09 (d,  $J$  = 15.2 Hz, 1H), 6.84 (d,  $J$  = 15.2 Hz, 1H), 6.81 – 6.77 (m, 2H), 6.73 (s, 2H), 6.69 (d,  $J$  = 7.3 Hz, 1H), 4.40 (s, 1H), 3.98 (s, 1H), 3.81 (s, 9H). <sup>13</sup>C NMR (126 MHz)  $\delta_c$  168.61, 163.03, 149.57, 148.50, 147.52, 142.66, 137.82, 127.58, 123.18, 118.05, 115.81, 111.78, 110.14, 107.25, 56.58.

**4.2 In Vitro Biological Evaluation**

**4.2.1 Cholinesterase (AChE and BChE) and BACE-1 inhibition assays:** Cholinesterase inhibitory activities of all target compounds (**FA1–5** and **CFA1–5**) were evaluated following an Ellman colorimetric assay (30). The enzymes, hAChE (acetylcholinesterase from human erythrocytes, EC No. 3.1.1.7), and hBChE (butyrylcholinesterase from human, EC No. 3.1.1.8) were purchased from Sigma, India. The BACE-1 inhibition assay was performed using a FRET-based fluorometric assay kit (CS0010, Sigma, India). For detailed procedure, refer to Supporting Information- Experimental section.

**4.2.2 Enzyme kinetics study:** The enzyme kinetics study of compound **CFA5** against AChE was performed to establish the type of inhibition. Lineweaver-Burk double reciprocal(31) and Dixon plots (32) were constructed to evaluate the mechanism. For detailed protocol of enzyme kinetics study experiment, refer to Supporting Information- Experimental section.

**4.2.3 Propidium iodide displacement assay:** The PAS-AChE binding ability of test compounds was evaluated by propidium iodide displacement assay, as reported by Peauger et al.(41). For detailed protocol of propidium iodide displacement assay, refer to Supporting Information- Experimental section.

**4.2.4 PAMPA assay:** The BBB permeability of test compounds was predicted by parallel artificial

membrane permeation assay (PAMPA) reported by Di et al.(35,42). For detailed protocol of PAMPA assay, refer to Supporting Information- Experimental section.

**4.2.5 Self- and AChE-induced A $\beta$  aggregation inhibition by thioflavin T assay:**

Thioflavin T assay was performed to determine the anti-A $\beta$  aggregatory potential of test compounds. The self- and AChE-induced A $\beta$  aggregation inhibition were tested at three different ratios of A $\beta$  and inhibitor (10:5, 10:10, and 10:20  $\mu$ M, respectively)(43). For detailed experimental protocol, refer to the Supporting Information- Experimental section.

**4.2.6 Neuroprotection studies on SH-SY5Y cell lines:**

The neuroprotective ability of compounds was tested against neuroblastoma SH-SY5Y cell lines by the MTT assay. The percentage cell viabilities due to A $\beta$  in presence or absence of test compounds were compared and reported (16). For detailed experimental protocol, refer to Supporting Information- Experimental section.

**4.3 In Vivo Behavioral Studies**

**4.3.1 Animals:** The Wistar rats of either sex, weighing in the range of 200  $\pm$  20 g were procured from Central Animal House of Banaras Hindu University (BHU), Varanasi. The rats were kept in a group of six per cage under a regular dark-light cycle in a day with standard environmental conditions. Animals were kept for one week first to get acclimatized and were given free access to food and water. All the protocols and animal handling were performed with the prior approval of the institutional animal ethics committee (No. Dean/2018/CAEC/814).

**4.3.2 Acute oral toxicity study:** The acute oral toxicity study was performed as per OECD guidelines 423 on healthy female Wistar rats. Test compounds were given in the graded doses of 100–500 mg/kg, p.o. All the animals were monitored for any signs of toxicity, abnormal reactions, and changes in feeding behavior or mortality upto 14 days.

**4.3.3 Scopolamine-induced amnesia model- Y maze test:** The anti-amnesic activity of test

compounds was evaluated by the Y maze test following scopolamine-induced memory impairment. The scopolamine hydrobromide (Sigma, CAS No. 6533-68-2) solution was prepared in sterilized saline and given intraperitoneally at a dose of 0.5 mg/kg. The test compounds were prepared by suspending in 0.3% w/v Na-CMC and were given orally at three doses, 2.5, 5, and 10 mg/kg. Donepezil was used as reference standard and given at a dose of 5 mg/kg, p.o. For detailed experimental protocol, refer to the Supporting Information- Experimental section.

**4.5 Molecular docking studies :** The molecular docking studies of compound **CFA5** on AChE (PDB ID: 4EY7) and BACE-1 (PDB ID: 2ZJM) proteins were conducted using Schrödinger Maestro 2018.4 platform with Glide XP module. Supporting Information- Experimental section can be referred for the detailed experimental protocol of molecular docking studies.

**Supporting Information :** The supporting information includes the detailed experimental protocols of biological and *in silico* studies.

#### Acknowledgments

This work was assisted financially through the Young Scientist Project sanctioned by the Department of Health Research, Ministry of Health and Family Welfare, Government of India, New Delhi (Grants V25011/215-HRD/2016-HR).

#### References

1. Sharma, P., Srivastava, P., Seth, A., Tripathi, P.N., Banerjee, A.G. and Shrivastava, S.K. (2019). Comprehensive review of mechanisms of pathogenesis involved in Alzheimer's disease and potential therapeutic strategies, *Prog. Neurobiol.* 174: 53-89.
2. Schneck, M.K., Reisberg, B. and Ferris, S.H. (1982). An overview of current concepts of Alzheimer's disease, *Am. J. Psychiatry* 139: 165-173.
3. Coyle, J.T., Price, D.L. and DeLong, M.R. (1983). Alzheimer's disease: a disorder of cortical cholinergic innervation, *Science* 219: 1184-1190.
4. Reisberg, B., Borenstein, J., Salob, S.P. and Ferris, S.H. (1987). Behavioral symptoms in Alzheimer's disease: phenomenology and treatment, *J. Clin. Psychiatr.* 48: 9-15.
5. Roberts, G.W., Nash, M., Ince, P.G., Royston, M.C. and Gentleman, S.M. (1993). On the origin of Alzheimer's disease: a hypothesis, *Neuroreport* 4: 7-9.
6. Ibrahim, M.M. and Gabr, M.T. (2019). Multitarget therapeutic strategies for Alzheimer's disease, *Neural regeneration research* 14: 437.
7. Thies, W. and Bleiler, L. (2012). 2012 Alzheimer's disease facts and figures, *Alzheimers Dement.* 8: 131-168.
8. Perry, E.K. (1986). The cholinergic hypothesis—ten years on, *Br. Med. Bull.* 42: 63-69.
9. Hardy, J. and Selkoe, D.J. (2002). The amyloid hypothesis of Alzheimer's disease: progress and problems on the road to therapeutics, *Science* 297: 353-356.
10. Malinow, R. (2012). New developments on the role of NMDA receptors in Alzheimer's disease, *Curr. Opin. Neurobiol.* 22: 559-563.
11. Maccioni, R.B., Fariás, G., Morales, I. and Navarrete, L. (2010). The revitalized tau hypothesis on Alzheimer's disease, *Arch. Med. Res.* 41: 226-231.
12. Heneka, M.T., Carson, M.J., El Khoury, J., Landreth, G.E., Brosseron, F., Feinstein, D.L., Jacobs, A.H., Wyss-Coray, T., Vitorica, J. and Ransohoff, R.M. (2015). Neuroinflammation in Alzheimer's disease, *The Lancet Neurology* 14: 388-405.
13. Markesbery, W.R. (1997). Oxidative stress hypothesis in Alzheimer's disease, *Free Radical Biol. Med.* 23: 134-147.
14. Kumar, A. and Singh, A. (2015). A review on Alzheimer's disease pathophysiology and its management: an update, *Pharmacol. Rep.* 67: 195-203.

15. Tripathi, P.N., Srivastava, P., Sharma, P., Tripathi, M.K., Seth, A., Tripathi, A., Rai, S.N., Singh, S.P. and Shrivastava, S.K. (2019). Biphenyl-3-oxo-1, 2, 4-triazine linked piperazine derivatives as potential cholinesterase inhibitors with anti-oxidant property to improve the learning and memory, *Bioorg. Chem.* 85: 82-96.
16. Mishra, P., Sharma, P., Tripathi, P.N., Gupta, S.K., Srivastava, P., Seth, A., Tripathi, A., Krishnamurthy, S. and Shrivastava, S.K. (2019). Design and Development of 1, 3, 4-Oxadiazole Derivatives as Potential Inhibitors of Acetylcholinesterase to Ameliorate Scopolamine-Induced Cognitive Dysfunctions, *Bioorg. Chem.* 103025.
17. Cummings, J., Lee, G., Mortsdorf, T., Ritter, A. and Zhong, K. (2017). Alzheimer's disease drug development pipeline: 2017, *Alzheimer's & Dementia: Translational Research & Clinical Interventions* 3: 367-384.
18. Sharma, P., Tripathi, A., Tripathi, P.N., Prajapati, S.K., Seth, A., Tripathi, M.K., Srivastava, P., Tiwari, V., Krishnamurthy, S. and Shrivastava, S.K. (2019). Design and development of multitarget-directed N-Benzylpiperidine analogs as potential candidates for the treatment of Alzheimer's disease, *Eur. J. Med. Chem.* 167: 510-524.
19. Sharma, P., Tripathi, A., Tripathi, P.N., Singh, S.S., Singh, S.P. and Shrivastava, S.K. (2019). Novel Molecular Hybrids of N-Benzylpiperidine and 1, 3, 4-Oxadiazole as Multitargeted Therapeutics to Treat Alzheimer's Disease, *ACS Chem. Neurosci.* 10: 4361-4384.
20. Tripathi, A., Choubey, P.K., Sharma, P., Seth, A., Tripathi, P.N., Tripathi, M.K., Prajapati, S.K., Krishnamurthy, S. and Shrivastava, S.K. (2019). Design and development of molecular hybrids of 2-pyridylpiperazine and 5-phenyl-1, 3, 4-oxadiazoles as potential multifunctional agents to treat Alzheimer's disease, *Eur. J. Med. Chem.* 183: 111707.
21. Talesa, V.N. (2001). Acetylcholinesterase in Alzheimer's disease, *Mech. Ageing Dev.* 122: 1961-1969.
22. Tripathi, P.N., Srivastava, P., Sharma, P., Seth, A. and Shrivastava, S.K. (2019). Design and development of novel N-(pyrimidin-2-yl)-1, 3, 4-oxadiazole hybrids to treat cognitive dysfunctions, *Bioorg. Med. Chem.* 27: 1327-1340.
23. Yan, R. and Vassar, R. (2014). Targeting the  $\beta$  secretase BACE1 for Alzheimer's disease therapy, *The Lancet Neurology* 13: 319-329.
24. Moreira, P., Siedlak, S., Aliev, G., Zhu, X., Cash, A., Smith, M. and Perry, G. (2005). Oxidative stress mechanisms and potential therapeutics in Alzheimer disease, *J. Neural Transm.* 112: 921-932.
25. Mallikarjuna, G., Dhanalakshmi, S., Raisuddin, S. and Rao, A.R. (2003). Chemomodulatory influence of *Ferula asafoetida* on mammary epithelial differentiation, hepatic drug metabolizing enzymes, antioxidant profiles and N-methyl-N-nitrosourea-induced mammary carcinogenesis in rats, *Breast Cancer Res. Treat.* 81: 1-10.
26. Fang, L., Kraus, B., Lehmann, J., Heilmann, J., Zhang, Y. and Decker, M. (2008). Design and synthesis of tacrine-ferulic acid hybrids as multi-potent anti-Alzheimer drug candidates, *Bioorg. Med. Chem. Lett.* 18: 2905-2909.
27. Chen, Y., Sun, J., Fang, L., Liu, M., Peng, S., Liao, H., Lehmann, J. and Zhang, Y. (2012). Tacrine-ferulic acid-nitric oxide (NO) donor trihybrids as potent, multifunctional acetyl- and butyrylcholinesterase inhibitors, *J. Med. Chem.* 55: 4309-4321.
28. Zhao, Z. and Moghadasian, M.H. (2008). Chemistry, natural sources, dietary intake and pharmacokinetic properties of ferulic acid: A review, *Food Chem.* 109: 691-702.
29. Balasubashini, M.S., Rukkumani, R. and Menon, V. (2003). Protective effects of ferulic acid on hyperlipidemic diabetic rats, *Acta*

- Diabetol. 40: 118-122.
30. Ellman, G.L., Courtney, K.D., Andres Jr, V. and Featherstone, R.M. (1961). A new and rapid colorimetric determination of acetylcholinesterase activity, *Biochemical pharmacology* 7: 88-95.
  31. Lineweaver, H. and Burk, D. (1934). The determination of enzyme dissociation constants, *J. Am. Chem. Soc.* 56: 658-666.
  32. Dixon, M. (1972). The graphical determination of Km and Ki, *Biochem. J* 129: 197-202.
  33. Inestrosa, N.C., Alvarez, A., Perez, C.A., Moreno, R.D., Vicente, M., Linker, C., Casanueva, O.I., Soto, C. and Garrido, J. (1996). Acetylcholinesterase accelerates assembly of amyloid- $\beta$ -peptides into Alzheimer's fibrils: possible role of the peripheral site of the enzyme, *Neuron* 16: 881-891.
  34. Kumar, M., Sharma, P., Maheshwari, R., Tekade, M., Shrivastava, S.K. and Tekade, R.K., Beyond the Blood-Brain Barrier: Facing New Challenges and Prospects of Nanotechnology-Mediated Targeted Delivery to the Brain, in: *Nanotechnology-Based Targeted Drug Delivery Systems for Brain Tumors*, Elsevier, 2018, pp. 397-437.
  35. Di, L., Kerns, E.H., Fan, K., McConnell, O.J. and Carter, G.T. (2003). High throughput artificial membrane permeability assay for blood-brain barrier, *Eur. J. Med. Chem.* 38: 223-232.
  36. Kang, S.S., Lee, J.Y., Choi, Y.K., Kim, G.S. and Han, B.H. (2004). Neuroprotective effects of flavones on hydrogen peroxide-induced apoptosis in SH-SY5Y neuroblastoma cells, *Bioorg. Med. Chem. Lett.* 14: 2261-2264.
  37. Srivastava, P., Tripathi, P.N., Sharma, P., Rai, S.N., Singh, S.P., Srivastava, R.K., Shankar, S. and Shrivastava, S.K. (2019). Design and development of some phenyl benzoxazole derivatives as a potent acetylcholinesterase inhibitor with antioxidant property to enhance learning and memory, *Eur. J. Med. Chem.* 163: 116-135.
  38. Shrivastava, S.K., Sinha, S.K., Srivastava, P., Tripathi, P.N., Sharma, P., Tripathi, M.K., Tripathi, A., Choubey, P.K., Waiker, D.K. and Aggarwal, L.M. (2019). Design and development of novel p-aminobenzoic acid derivatives as potential cholinesterase inhibitors for the treatment of Alzheimer's disease, *Bioorg. Chem.* 82: 211-223.
  39. Banerjee, A.G., Kothapalli, L.P., Sharma, P.A., Thomas, A.B., Nanda, R.K., Shrivastava, S.K. and Khatanglekar, V.V. (2016). A facile microwave assisted one pot synthesis of novel xanthene derivatives as potential anti-inflammatory and analgesic agents, *Arabian Journal of Chemistry* 9: S480-S489.
  40. Kontoyianni, M., McClellan, L.M. and Sokol, G.S. (2004). Evaluation of docking performance: comparative data on docking algorithms, *J. Med. Chem.* 47: 558-565.
  41. Peauger, L., Azzouz, R., Gembus, V., Tintas, M.-L., Sopkova-de Oliveira Santos, J., Bohn, P., Papamicael, C. and Levacher, V. (2017). Donepezil-based central acetylcholinesterase inhibitors by means of a "bio-oxidizable" prodrug strategy: design, synthesis, and in vitro biological evaluation, *J. Med. Chem.* 60: 5909-5926.
  42. Seth, A., Sharma, P.A., Tripathi, A., Choubey, P.K., Srivastava, P., Tripathi, P.N. and Shrivastava, S.K. (2018). Design, synthesis, evaluation and molecular modeling studies of some novel N-substituted piperidine-3-carboxylic acid derivatives as potential anticonvulsants, *Med. Chem. Res.* 27: 1206-1225.
  43. LeVine III, H., [18] Quantification of  $\beta$ -sheet amyloid fibril structures with thioflavin T, in: *Methods Enzymol.*, Elsevier, 1999, pp. 274-284.



## Role of Nanoparticles as Antibiofilm Agents: A Comprehensive Review

Suruchi Chaudhary<sup>†</sup>, Anurag Jyoti<sup>†</sup>, Vikas Shrivastava<sup>\*\*</sup> and Rajesh Singh Tomar<sup>\*</sup>

Amity Institute of Biotechnology, Amity University Madhya Pradesh, Gwalior

<sup>\*</sup>Corresponding Author: rstomar@amity.edu

<sup>\*\*</sup>Co-corresponding Author: vshrivastava@gwa.amity.edu

### ABSTRACT

Biofilm forms with the colonization of different microorganism resulting in a microbial community which is complex and diverse in nature. Biofilms are enclosed with different microbial colonies in a matrix known as extracellular polymeric substance. Microorganisms together in this complex structure communicate through cell signaling molecules. This process is known as quorum sensing which helps in maintaining the complexity and diversity. Biofilms are involved in causing various infections in human beings. Oral cavity and wounds are very common two sites where biofilm formation takes place. The complexity of a biofilm makes it tenacious and it's tough to eradicate completely. There are several conventional methods such as physical, chemical, antibiotics, antiseptics and anti-biofilm agents for the eradication of dental/periodontal biofilms and biofilms associated oral wounds. Thus, various novel approaches can be proposed, one of them is Nanotechnology. Its extensive application in dentistry can be very helpful in curing various periodontal and dental diseases. Nanoparticles are one of new emerging potent system which can be really helpful in the complete eradication of complex biofilms due to their high anti-microbial properties. In this review, we have attempted to discuss dental/ periodontal biofilms; oral wounds, their relation with oral biofilm microbes and their treatment as well as conventional methods of treatment available till now. With this comprehensive review, it is proposed that with the help of nanotechnology, various nanoparticles can

be designed and an improvement can be done to the available methods or some new method can also emerge.

**Keywords:** Biofilm, Oral biofilms, Periodontal diseases, Nanoparticles, dental plaque.

### INTRODUCTION

Biofilm formation is a unique property of microbes. This property of microbes helps them to survive in harsh conditions and allow them to proliferate as a microbial community. Generally, biofilms have been depicted in several systems since Antony Van Leeuwenhoek examined the "animalcules" in the dental plaque on his own teeth in the seventeenth century, but the general theory of biofilm predominance was not promulgated until 1978 [1]. In human body, apart from normal microflora, microbe gets adhere to a surface and results in the formation of biofilm. The best salient description of a biofilm is given by Donlan and Costerton in 2002, who stated that a biofilm is "a microorganisms derived sessile community which are characterized by those cells that are irreversibly attached to a biotic/ abiotic substratum or interface or to each other, are embedded in a matrix of extracellular polymeric substances that they have produced, and exhibit an altered phenotype with respect to growth rate and gene transcription" [2]. Such film like structures formed by the combination of different microbes is involved in etiopathogenesis of various diseases in animals and humans as well. According to IUPAC, "Aggregate of microorganisms in which cells that



are frequently embedded within a self-produced matrix of extracellular polymeric substances (EPSs) adhere to each other and/or to a surface” [3].

Microbial community adheres to biotic or abiotic surface and start to secrete some polymeric substances which result in a layer like structure. Later on, other microbes come and gets associated with this slime layer and a microbial community is formed. In a biofilm, microorganisms yield extracellular polymeric substances, such as exopolysaccharides (EPS), which procreate a high counteraction to host immune responses and limited penetration of antibiotic into biofilm [Figure 1] [4-6]. ‘Biofilm’ is a term given by Wilderer and Charaklis in 1989, depicted the comparatively ineffable microbial summation which is allied with a surface or some different substantial non-flicking material, conjecturally dispensed in a framed matrix or glycocalyx [7].

Biofilm implicated in etiology of different dental & periodontal diseases as the major cause of plaque formation in oral cavity. Some studies showed that biofilms are also responsible for causing severe periodontal inflammations, oral wound formation, acute to chronic. Presently, in a milestone study, James et al., used light and scanning electron microscopy to scrutinize the existence of microbial biofilms, manifestation of agglomerated colonies of microbes occupied by EPS, in wounds acute and chronic stages [8]. According to them, biofilm formation exhibit only in 60% of chronic wounds whereas in acute wounds only 6% of biofilm is incorporated.

Oral cavity is surrounded by various microbes present in the form of dental plaque and involved in the formation of biofilm. Though, it is not articulate whether chronic wounds with or without biofilms are impudence or sanative. Biofilms are mostly existing in chronic wounds than in acute ones [9-13].

#### **DENTAL AND PERIODONTAL MICROBIOLOGY**

Complete microflora located in the oral cavity is commonly referred as the oral microbiota,

or oral microbiome, which can be defined as “whole microorganisms that are found on or in the human oral cavity and its proximate expansion”. In early 1970’s, dental plaque was a challenging field among dental scientists. Scientists emphasized to find out the tenor rendering the multicity of oral microbial ecosystem such as pH, nutritional requisition etc. The importance of the plaque ecosystem was recognized by Loesche in 1976 and he proposed both nonspecific and specific plaque hypothesis individually for oral disease progression. Approximately, 1000 microbial species have been recognized in oral biofilms till now using different techniques [14].

Dental plaque is defined as, “a variable structural formation of highly organized intercellular matrix in which different microbes and their secreted products present forming a slime layer on the outer surface of the teeth enamel”. It is colourless layer at first but after tartar formation, it becomes yellow to brown in colour, covering teeth as well as the gum line. Progression of the dental plaque may lead to several oral problems like tooth decay, dental caries, gingivitis, etc.

#### **DENTAL AND PERIODONTAL MICROBIAL COMPLEXES**

In oral cavity the commonly found microbes, responsible for biofilm formation are *Streptococcus* spp., *Lactobacillus* spp., *Actinomycetes* spp., *Propionibacterium* spp., *Veillonella* and other anaerobes which may vary as per the location in the mouth. Examples of such anaerobes include *Fusobacterium* spp., etc. [Figure 3] [15]. *S. mutans* and other anaerobes play important role in the initial colonization on tooth surface for the establishment of the early biofilm community [16]. In oral cavity, various microbial communities form complexes with each other and results in the formation of a tough layer which shows a characteristic color of plaque shown in Figure 4 [17].

#### **CLASSIFICATION OF DENTAL BIOFILMS:**

Dental and periodontal surfaces are peerlessly hard and non-flicking, unlike other parts of body. So, the dank and torrid environment of

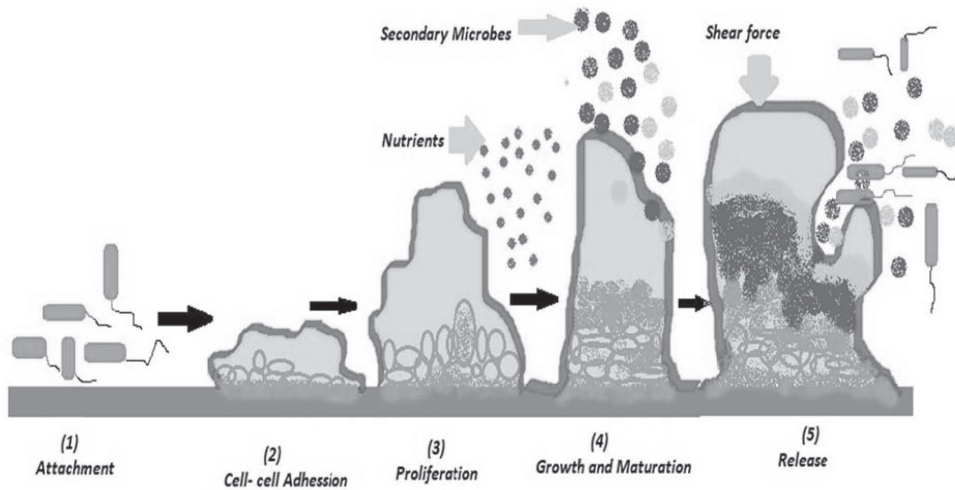


Figure 1: Diagrammatic representation of a common biofilm formation.

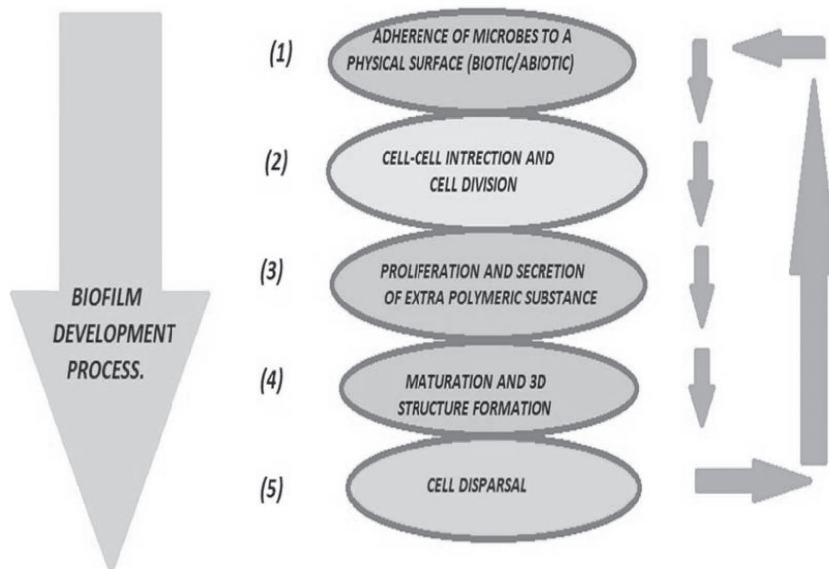


Figure 2: Flow-chart representation of various aspects of biofilm formation.

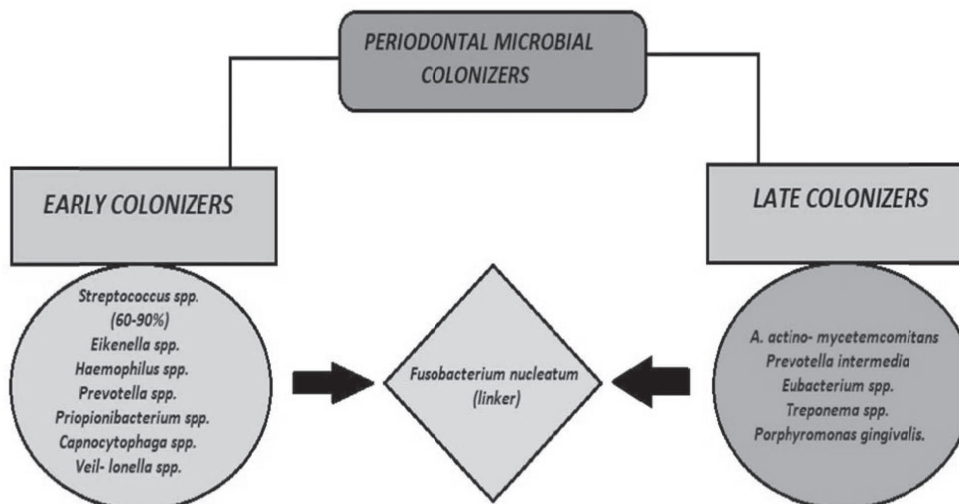


Figure 3: Pictorial representation of early and late colonizer microbial community.

the oral cavity and the presence of rigid surface (teeth) create best condition for growth and development of dental plaque.

**Biofilm present on the teeth and gum-line can be classified on two bases:**

1. **On the basis of the location:** -[18]
  - a) **Supra-gingival biofilm:** It is the type of biofilm which forms on gum-sit. It is the initial stage of plaque which commonly forms after the brushing and generally found in between the teeth, tooth-pits, tooth-grooves and in gums. The deposited layer of plaque consists of aerobic bacteria. Prolong persistence of initial plaque allows growth of anaerobic bacteria and convert into complex matrix of biofilm [19].
  - b) **Sub-gingival biofilm:** Sub-gingival biofilm proliferates upon the supra-gingival biofilm. This type of biofilm grows in downward direction up to the gum line (from top of the teeth to bottom). It constitutes anaerobic bacteria, which cause infections [20].
2. **On the basis of pathogenicity of**

**microbes:**

**a) Cariogenic biofilm:** Its formation takes place due to the deposition of acidogenic and gram- positive bacteria which particularly forms due to the regular long term uptake of cariogenic diet such as sugars.

**b) Preiopathogenic biofilm:**

Its formation takes place due to the basophilic and gram negative bacteria.

#### FORMATION OF DENTAL BIOFILMS

The complex process of oral biofilm formation begins with association and attachment of free microbes and sessile microbes present in the oral cavity on to the tooth surface. A film like layer started to form after the secretion of extra polymeric substances and some of host molecules.

The whole process of formation of dental biofilm is ensued by passive transport of bacteria mediated by weak long-range forces of attraction. Strong and short-range forces exerted by covalent and hydrogen bonds results in irreversible

attachment. [21]

The cell in the microbial community of oral cavity biofilms communicates with each other by process of Quorum sensing. It is a very important process of cell to cell signaling in dental biofilms as well as in other biofilms. This process is vastly carried out by different varieties of gram-positive and gram-negative bacterial species to commensurate with other species of microbes present in biofilm for various metabolic activities. This cell to cell signaling is the means of

communication between all microbes present in the microbial community to regulate a wide range of behavior patterns among them. The various interfering compounds generated by the bacteria have an effect which can be either positive or negative on the expression of bacterial phenotypes generally regulated by quorum sensing (a process of communication between microbes in biofilm community). [22]

By the process of auto-aggregation (same species attraction) and co-aggregation (different

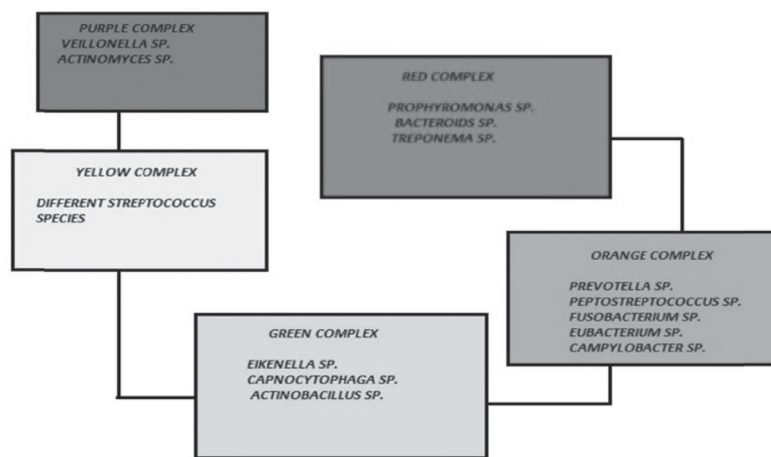


Figure 4: Showing periodontal microbial biofilm complexes.

<b>ASSOCIATION</b>	DENTAL PELLICLE FORMATION ON TOOTH WHICH PROVIDES MICROBES A SURFACE TO ADHERE.
<b>ADHESION</b>	WITHIN HOURS MICROBES LOOSELY BINDS TO THE PELLICLE.
<b>PROLIFERATION</b>	MICROBES STARTED TO SPREADS THROUGHOUT THE MOUTH AND BEGINS TO MULTIPLY.
<b>MICROCOLONIES</b>	FORMATION OF MICROCOLONIES AND MICROBES STARTED TO SECRETE EPSs (SLIME LAYER)
<b>BIOFILM FORMATION</b>	FORMATION OF COMPLEX GROUPS BY TAKING METABOLIC ADVANTAGES.
<b>GROWTH &amp; MATURATION</b>	THE BIOFILM DEVELOP A PRIMITIVE CIRCULATORY SYSTEM

Figure 5: Descriptive information of dental plaque formation.

**STAGES OF FORMATION OF AN ORAL BIOFILM**

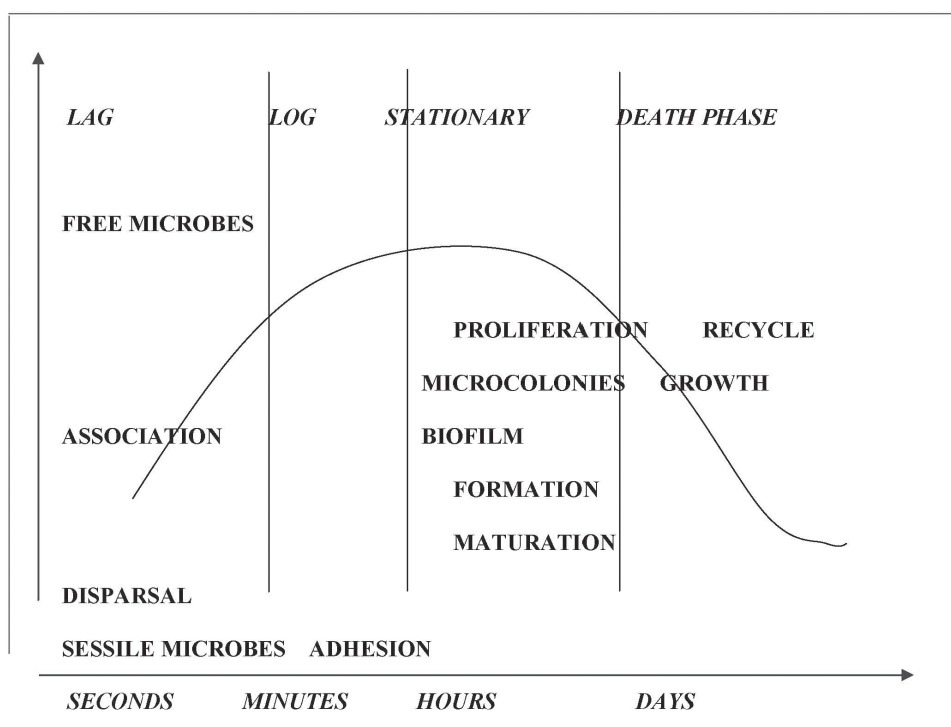


Figure 6: Showing stages of biofilm generation, growth, maturation and dispersal. [21]

species attraction) early colonizers form a biofilm. Functional organization of dental plaque microbes results in co-aggregation, and conformation of structures such as 'Corncobs' and 'Rosettes'. Now environment of oral cavity changes to facultative anaerobic from aerobic. Microbes which are already present started to multiply and secrete EPS, resulting in a paved mixed-population of microbes forming slime layer. [21] [23]

Fully organized mature complex slime layer formation takes place after one day, the term Biofilm is now suitable for it. Other new microbes get incorporated into the biofilm resulting in a complex summation. The plumpness of the dental

plaque rises slowly and steadily day by day; it grows up to 20 to 30  $\mu\text{m}$  in every three days. [21]

**PROBLEMS CAUSED BY PERIODONTAL MICROBES**

Oral problems/diseases have a significant economic impact on health care principles across the world, such as dental caries affects over 70-80% of the population in several countries, so there is an important impact of all dental problems on the quality of life, disease free life and implications for systemic health [24].

The dental biofilm is the basis of many oral problems; including endodontic infections, periodontal disease and dental caries. The most



common dental and periodontal problems among human community are tooth decay (*cavities, dental caries*) gingivitis, and periodontitis. Apart from this, evidences propounded that pathogenesis of systemic disease including rheumatoid arthritis, cardiovascular disease, respiratory disease, and other conditions are also caused by oral microbes [25-26].

The etiology of different dental and periodontal microbial diseases has been pervasively studied; however, the complexity of nature and diversity of composition in dental and periodontal biofilms makes it difficult to identify the main culprit involved to carry out the whole process. Early researches solely focus on identification of that pathogen which is responsible for oral problems such as dental caries, gingivitis, and chronic periodontitis. It is now generally accepted that these diseases result from the concerted actions of multispecies microbial communities [27].

There are several conventional culture methods available which have traditionally been used for the characterization of oral microbiota; however, most of the proportion remains unculturable, which leads to partial knowledge of wild type microbial communities involved in various oral problems. [28] Such microbial appurtenant and huddle of various pathogenic biofilms on surfaces of implant plays considerably important role in peri-implantitis pathogenesis [29-31].

#### **BIOFILMS ASSOCIATED WITH PERIODONTAL DISEASES AND WOUNDS**

For many years in periodontal infections, biofilms have been studied and accepted widely. Wounds can be extensively categorized according to the etiology condition as an acute or a chronic wound. Wounds in chronic condition generally have deferred healing pattern and repeatedly have some endogenous factors that conciliate the process of healing in which microbes associated with biofilms plays active role in wounds. In severe inflammation and wound/ ulcer formation inside the oral cavity, two anaerobic oral bacteria are

the subject of extensive study '*Porphyromonas gingivalis*' and '*Fusobacterium nucleatum*'. These two bacteria are commonly found in vicinity of periodontal region attached with the epithelium of the gingiva [32-33].

In recent years, most of the researchers are focusing on wound associated biofilms. It has been observed in few studies, that the wound healing gets delayed due to the persistence of pathogenic biofilms, which may lead to the several chronic diseases. [34-36].

**CONVENTIONAL METHODS AVAILABLE UP TO DATE:** Conventional methods available for the removal of dental biofilms which causes various oral problems are brushing, flossing, gargling, interdental brushing, tongue scraping and sub gingival irrigation. [37-41]

Conventional methods have been traditionally used to remove harmful oral microbiota; however, a large proportion remains as it is in mouth, leading to the formation of plaque and helpful in generating new oral problems. Microbial biofilms are generally characterized as highly resistant towards antibiotic treatment and host immune responses. There are several drugs which are used as a conventional method to control plaque and other inflammatory infections. One of the widely used drugs are;

**1. Chlorhexidine** which is an antibiotic used to control dental plaque and periodontal diseases caused by microbial community. It increases the staining of tartar present on teeth. Brushing helps in removal of tartar build up and staining. This medication is available as mouth rinse and gelatin- filled chips that are placed in deep gum pockets which released slowly over seven days.

**2. Doxycycline** is used to help treat periodontal diseases. It prevents growth of microbes. It is placed in gum pockets next to teeth and it dissolves naturally over seven days. This drug is having some side effects such as permanent discoloration of teeth, slow bone growth and therefore not recommended during breastfeeding, etc.

**3. Fluoride** used to prevent tooth decay. It is available in many types of toothpaste. It is absorbed by teeth and strengthens teeth to resist acid and blocks the cavity-forming action of microbes and helps in tooth sensitivity reduction.

**4. Tetracycline** used commonly in various therapies or alone, to reduce or eliminate microbes temporarily which are associated with periodontal diseases, to suppress the destruction of tooth attachment.

Dental antibiotics used conventionally are easily available in market in the form of gels, thread like fibers, microsphere, mouth rinses, and medicated toothpastes.

In general, the antibiotic drugs have certain chemical properties which lead to various side-effects. Moreover, regular use of antimicrobial drugs may raise anti-drug resistant property in microbes. Generally, microbes secrete certain products for stability maintenance of biofilm such as EPSs & eDNA which is an important component of both fungal and bacterial biofilms and both of these are related to antimicrobial resistance. [42]

In case of biofilms present in wounds treatments, modalities present up to date are;

**1. Debridement:** This process can be autolytic, enzymatic, surgical, or mechanical (hydrotherapy). Effective controlling of biofilms in oral wounds can be done by this method. In the case of chronic wounds, it is suggested for removal and suppression of biofilm [43, 44]. There are various debridement techniques present such as plasma-mediated bipolar radiofrequency ablation technique (PBRA).

**2. Antibiotics and antiseptics:** Biofilm generally consist of subpopulation of survivor cell of antibiotic resistance. In local oral wound infection, it is suggested that antibiotics are effective only 25-30% [45]. 0.2% solution of povidone-iodine, chlorhexidine gluconate, benzalkonium chloride or alkyl diamino ethyl glycine hydrochloride shown effective and fast bactericidal activity in the case of periodontal diseases [46, 47].

**3. Anti-biofilm agents:** A component which is present in human tears, mucus, and milk known as Lactoferrin. It is considered that this component clogs biofilm formation by commuting microbial motility and reduction in surface attachment. Lactoferrin synergistically with Xylitol impairs biofilm matrix development. Lactoferrin with xylitol in methylcellulose gel works as a good anti-biofilm agent. [45]. There are some polysaccharides designed by the researchers which shows the anti-biofilm property by inhibiting EPS formation. *P. aeruginosa* secretes Psl and Pel which show anti-biofilm property [48, 49].

### NANOPARTICLES AND NANOMATERIAL A NEW APPROACH IN THERAPEUTICS

The 'nano' is a Greek word, which means small in size which is used as the prefix for the billionth from the range 9 to 10. Nanoparticles are the particles which have two or more dimensions in the size range as 1 to 100 NM (ASTM International) [50]. It is well known with the ongoing researches nanoparticles have unprecedented physical and chemical properties in comparison to their solid bulk materials as their sublime surface area and unique electronic properties so it has been utilized in many aspects of science such as photochemical, electrochemistry, and biomedicine [51]. Nanoparticles have great application podium that can be exploit for various therapeutic aspects and different functions. Such particles can be easily synthesized from various inorganic and organic metals and compounds, but for simultaneous therapy and diagnosis, the inorganic materials are very important because they can be modifying easily, high loading capacity for drug and stability [52]. Such particles can also be utilizing in drug delivery systems and for the different drug determination in pharmaceuticals as well [53].

#### Types of Nanoparticles:

There are various types of nanoparticles differing in size, shape, compositions, and functions. Each type of NP's can potentially be concoct using various techniques, such as both nanoprecipitation and lithography for polymeric nanoparticles.

There are three basis of classification:

- 1) Origin, [54]
- 2) Dimension, [55-57] and
- 3) Structural organization [58-63].

**Synthesis of nanoparticles:**

To synthesize nanoparticles, there are two approaches: 1) Top down approach and 2) Bottom up approach. In the process of bottom up approach, the particles get arranged as smaller components into more complex assemblies. Chemical or physical forces are used for the operating at nanoscale for the assembling of basic units. Whereas, in the top down approach bulk material is converted into smaller sized nanostructure.

There are three methods of synthesis, physical, chemical and biological;

- 1) **Physical method:** It's been carried out via two different methods such as Mechanical method and Vaporization
- 2) **Chemical method:** It is the most promising method of nanoparticle synthesis. It's been carried out via colloids and colloids in solution and Sol gel method
- 3) **Biological method:** It is also known as green synthesis. It is done by three types, by the use of microorganisms such as fungi/ yeast, plant extracts or enzymes and

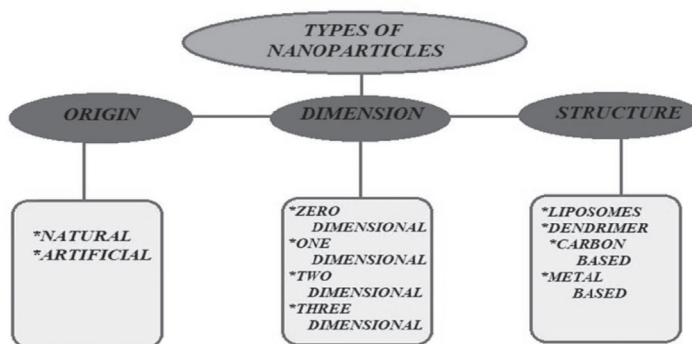


Figure 7: Types of nanoparticles

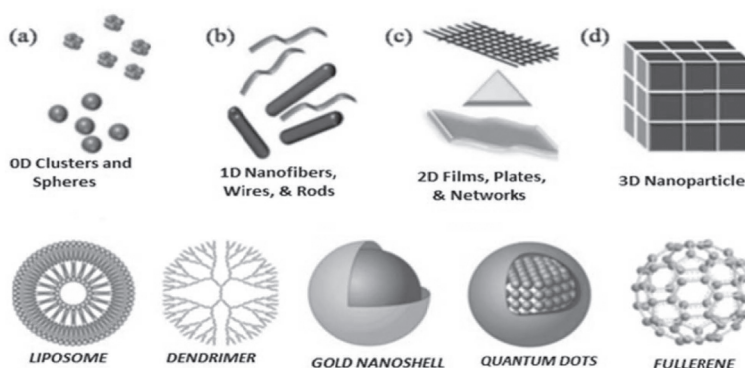


Figure 8: Diagrams showing different types of nanoparticles on the basis of dimension and structure [64] [65]

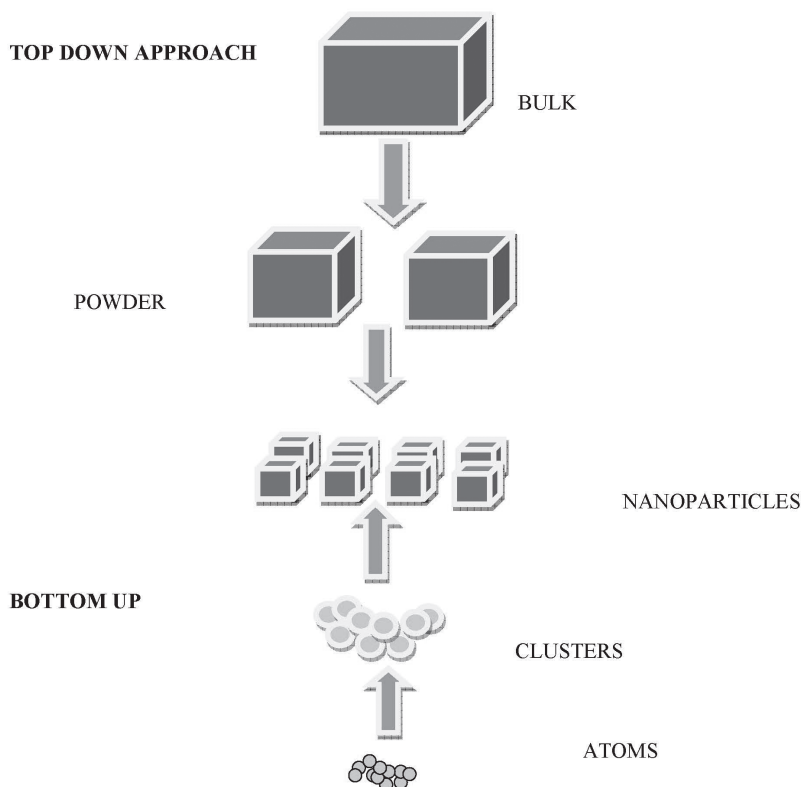


Figure 9: Figure showing two approaches to generate nanoparticles.

templates like DNA, membranes, viruses and diatoms.

#### ADVANCE CONTROL OF ORAL BIOFILMS

Dental and periodontal biofilms are intensely pliable microbial assemblies that are challenging to eradicate. Due to lacunae in existing methods of biofilm eradication and development of antimicrobial resistance in conventional drugs, there is necessity to explore the development of new anti-biofilm agents. Polysaccharides and eDNA, which are complex biofilm matrix, seem to be a good target for future therapeutic strategies [66].

Use of Nanoparticles is a suggestive approach in developing various methods to eradicate or control oral pathogenic microbes. Neoteric microbiological studies have umbilici on

developing novel antimicrobial agents with higher efficacy while being non-invasive and non-toxic and not causing drug resistance such as nanoparticles and new drug delivery systems which will be helpful in enhancement of medical therapeutics [67, 68]. Nanotechnology potentially benefited in the field of biomedical, it has become widely conceded for the treatment of various microbial diseases with a new generation of hopeful strategies [69]. Metals are widely used in the synthesis of nanoparticles due to the antibacterial properties commonly used metals as antimicrobials are silver, gold, zinc, copper, and titanium. For centuries, these metals have been known and been avail in modern medicine for infection control. Due to the broad-spectrum antibacterial activities Silver containing (Ag-containing) nanomaterials is of extensive interest [70-76]. Some of the metals showing antibacterial

**Table 1: Metal Nanoparticles with their special antimicrobial properties.**

Nanoparticles	Anti-microbial properties	References
<b>Zinc oxide</b>	Nanoparticles gets accumulated inside the cells, generation of H <sub>2</sub> O <sub>2</sub> , zinc ions release, cell membrane gets disrupted.	[63, 77]
<b>Titanium dioxide</b>	Reactive oxygen species formation takes place, cell wall and cell membrane gets disrupted.	[78]
<b>Copper oxide</b>	Lipid oxidation by reactive oxygen species and hydroxyl free radicals results in cell membrane disruption.	[79]
<b>Carbon nanotube</b>	Reactive oxygen species results in cell wall disruption, proteins and lipids gets oxidized within the cell membrane	[80]
<b>Chitosan</b>	Intracellular components gets leaked out due to increase in cell membrane permeability, microbial enzymes get deactivated.	[81]
<b>Gold</b>	Production of strong electrostatic effects, get reacted with microbial cell membrane.	[50, 82]
<b>Silver</b>	Silver ions release, disruption of bacterial cell membrane, electron impairment, DNA damage.	[83]
<b>Quaternary ammonia</b>	Penetration results in cell wall disruption.	[84]

properties which can be used as promising and effective agent to design nanoparticles which can increase the efficacy of conventional methods to combat with different infectious pathogens causing diseases in human body. A list has been compiled showing the metal nanoparticles having potential anti antimicrobial properties (Table 1).

**CONCLUSION**

Improper tooth care leads to the deposition of biofilm which is not easy to eradicate using conventional methods. Nanotechnology is a new approach in medical therapeutic field of dentistry as well as wound healing. It can be very helpful in providing sustainable methods to increase

accuracy, attributes and fast treatment procedure which will be economically cheap and easily available. The current review article enlightens the literal perspectives of nanotechnology in dentistry to cure problems caused by pathogenic oral microorganisms. In near future, this technology may become the core of therapeutics in dental and medical science.

**REFERENCES**

1. Costerton, J. W., Geesey, G. G., Cheng, K. J., *Sci.* 1978 Jan; 238(1) 86 – 95.
2. Donlan R. M., Costerton J. W., *Clin. Microbiol. Rev* 2002, 15(2), 167 – 93.



3. Vert, M., Doi, Y., Hellwich, K. H., Hess, M., Hodge, P., Kubisa, P., Rinaudo, M., Schué, F., *Pure and Applied Chemistry* 2012, 84 (2), 377–410.
4. Liu, Y., Busscher, H., Li, Y.Z., van der Mei, H. C., Y.R and L.S, *ACS Nano*.2016 (10), 4779–4789.
5. Jongsma, M. A., van der Mei, H. C., Atema-Smit J., Busscher, H. J. and R.Y., *Oral Science* 2015, (7), 42–48.
6. Zhou, J., Horev, B., Hwang, G., Klein, M. I., Koo, H. and Benoit, D. S., *Mater J., Chem. B.* 2016, (4), 3075–3085.
7. Socransky S.S, Haffajee A.D *Periodontol Dental biofilms* 2000. 2002, (28), 12-55.
8. James ,G.A., Swogger, E., Wolcott ,R., Pulcini ,E., Secor ,P., Sestrich ,J., *Wound Repair Regen.* 2008, 16(1), 37–44.
9. Kirketerp, M. K., Zulkowski, K., James, G., Bjarnsholt, T., Jensen, P.O., Moser, C., Hoiby, N., *Springer Science Business Media. LLC*, 2011.
10. Akiyama, H., Kanzaki, H., Tada, J., Arata, J., *Dermatol, J. Sci.* 1996, 11(3), 234–8.
11. Akiyama, H., Morizane, S., Yamasaki, O., Oono, T., Iwatsuki, K., *Dermatol Sci.* 2003, 32(3), 193–9.
12. Schaber, J.A., Triffo, W.J., Suh, S.J., Oliver, J.W., Hastert, M.C., Griswold, J.A., *Infect Immun.* 2007. 75(8), 3715–21.
13. Davis, S.C., Ricotti, C., Cazzaniga, A., Welsh, E., Eaglstein, W.H., Mertz, P.M., *Wound Repair Regen.*2008.16 (1), 23–9.
14. Loesche, W.J., *Oral Sci.Rev* 1976, 9, 65-107.
15. Darby, M. L., Walsh, M.M., *Dental Hygiene Theory and Practice.* 2010.
16. Kolenbrander, P., *Annu. Rev. Microbiol.* 2000, 54(1), 413–37.
17. Ten, C., Jacob, M., *Odontology*, 2006. 94 (1), 1–9.
18. Ximénez-Fyvie, L.A., Haffajee, A.D., Socransky, S.S., *J. Clin. Periodontol.* 2000. 27,648–57.
19. Chetrus, V., and Ion, I.R., *Int. J. Med. Dentistry.* 2013. 3, 139–43.
20. Wilkins, E., *Wolters Kluwer Health/ Lippincott Williams & Wilkins.* 2009.
21. Rita, C., Priyank, B., and Ruchi, B., *J. Indian Soc Periodontol.* 2011 Apr-Jun, 15(2), 111–114
22. Biradar, B., Devi, P., *J. Contemp Dent Pract.* 2011 Nov. 1, 12(6), 479-85.
23. Quirynen, M., Teughels, W., Haake, S.K., Newman, M.G., *Carranza’s Clinical Periodontology.* 10th ed. St Louis, Missouri: Elsevier (Saunders), 2006. pp. 134–69.
24. Petersen, P.E., Lennon, M.A., *Community Dent Oral Epidemiol.* 2004 Oct, 32(5), 319-21.
25. Sharma, V.K., Yngard, R.A., Liu, Y., *Adv Colloid Interface Sci* 2008, 145, 83-96.
26. Maddi, A., Scannapieco, F.A., *Am J Dent.* 2013. 26(5), 249–54.
27. Thuy, D., Deirdre, D., and Philip, D., *Clin Cosmet Investig Dent.* 2013. 5, 11–19.
28. Hiyari, S., Bennett, K.M.J., *Dent Hyg.* 2011. Fall, 85(4), 256-63.
29. Burgers, R., Gerlach, T., Hahnel, S., Schwarz, F., Handel, G., and Gosau, M., *Implants Res.* 2010. 21, 156–164.
30. Carcuac, O., Derks, J., Charalampakis, G., Abrahamsson, I., Wennstromand, J., Berglundh, T., *J. Dent. Res.* 2016. 95, 50–57.
31. Liu, Y., Busscher, H.J., Zhao, B., Li, Y., Zhang, Z., van der Mei, H. C., Ren, Y. and Shi, L., *ACS Nano.* 2016. 10, 4779–4789.

32. Kuboniwa, M., Tribble, G.D., Hendrickson, E.L., Amano, A., Lamont, R.J., *Expert Rev Proteomics*. 2012. 9, 311–323.
33. Han, Y.W., Shi, W., Huang, G.T., Kinder, H.S., Park, N.H., 2000.
34. James, G.A., Swogger, E., Wolcott, R., Pulcini, E., Secor, P., Sestrich, J., *Wound Repair Regen*. 2008. 16(1), 37–44.
35. Cooper, R., Okhiria, O., *Wounds U.K.* 2006. 2(3), 48–57.
36. Costerton, J.W., Stewart, P.S., Greenberg, E.P., *Science*. 1999. 284 (5418), 1318–22.
37. Cobb, C.M., Rodgers, R.L., Killoy, W.J., *Periodontol*. 1988 March. 59(3), 155–63.
38. Greenstein, G., *Compendium*. 1988. April. (4), 327–9, 332–4, 336–8.
39. Ciancio, S., *Biological Therapies in Dentistry*. 1988. 3, 33.
40. Fleming, T., AADR Abstract #1612, 1989. Irrigation Update
41. Darby, M., & Walsh, Margaret, M., *Theory and Practice*. 2010. St. Louis, M., Saunders/ Elsevier
42. Beatriz, H. D., & Cecilia Atem, G.D., *Curr Oral Health Rep* .2017, 4, 29–33.
43. Costerton, J.W., Lewandowski, Z., Caldwell, D.E., Korber, D.R., Lappin-Scott, H.M., *Annu Rev Microbiol*. 1995.49, 711–45.
44. Wolcott, R.D., Kennedy, J.P., Dowd, S.E., *J Wound Care*. 2009. 18(2), 54–6.
45. Black, C.E., Costerton, J.W., *Surg Clin North Am*. 2010. 90(6), 11, 47–60.
46. Kunisada, T., Yamada, K., Oda, S., Hara, O., *Dermatology*. 1997. 195(Suppl 2), 14–8.
47. Nakagawa, T., Hosaka, Y., Ishihara, K., Hiraishi, T., Sato, S., Ogawa, T., *Dermatology*. 2006. 212(Suppl 1):109–11.
48. Valle, J., DaRe, S., Henry, N., Fontaine, T., Balestrino, D., Latour-Lambert, P., *Proc Natl Acad Sci U S A*. 2006, 103(33), 12558–63.
49. Rendueles, O., Kaplan, J.B., Ghigo, J.M., *Environ Microbiol*. 2012.
50. Alanazi, F.K., Radwan, A.A., Alsarra, I.A., *J Saudi Pharm*. 2010, 18, 179-193.
51. Haruna, K., Saleh, T.A., AlThagfi, J., Al-Saadi, A.A., *Journal of Molecular Structure*. 2016. 1121, 7-15.
52. Saleh, T.A., *Recent Trends with Nanotechnology Detection*. 2014. 2, 27-32.
53. Huang, Z., Zheng, X., Yan, D., Yin, G., Liao, X., Kang, Y., *Langmuir*. 2008. 24, 4140-4144.
54. Tooba, M., *Journal of Pharmaceutical Sciences & Research* Vol. 9(2), 2017, 102-110.
55. Siegel, R.W., *Nanostructure Science and Technology*, Kluwer Academic Publishers.
56. Acharya, S., Hill, J.P., and Ariga, K., *Advanced Materials*. 2009. 21, 2959-2981.
57. Abhilash, M., *International Journal of Pharma and Bio Sciences*, 2010. 1.
58. Rawat, M., Singh, D., Saraf, S., *Biological and Pharmaceutical Bulletin*. 2006. 29, 1790-1798.
59. Wiener, E.C., Brechbiel, M.W., Brothers, H., Magin, R.L., Gansow, O.A., Tomalia, D.A., *Magn Reson Med*. 1994. 31, 1-8.
60. Kohler, J.M., *Nanostructuring Techniques*. Weinheim. 2004.
61. Tomalia, D.A., *Aldrichimia Acta*. 2004, 37.
62. Hughes, G.A., *Nanostructure mediated drug delivery*, 2005, 1.
63. Morris, D.S., *National Cancer Institute*, Maryland, 2015.
64. Alagarasi, A., <https://nccr.iitm.ac.in/2011.pdf>.
65. Klein, M.I., Hwang, G., Santos, P.H., Campanella, O.H., Koo, H., *Front Cell Infect Microbiol*. 2015. 5, 10.

66. Fux, C.A., Costerton, J.W., Stewart, P.S., Stoodley, P., Trends Microbiol 2005. 13, 34-40.
67. DelPozo, J.L., Patel, R., Clin Pharmacol Ther .2007. 82, 204-209.
68. Franci, G., Falanga, A., Galdiero, S., Palomba, L., Rai, M., Morelli, G., Galdiero, Silver M., Molecules. 2015. 20 (5), 8856"8874.
69. Agnihotri, S., Mukherji, S., Mukherji, S., RSC Adv. 2014, 4 (8), 3974"3983.
70. Song, J., Kim, H., Jang, Y., Jang, J., Mater. Interfaces 2013, 5 (22), 11563"11568.
71. Kong, H., Jang, J., Langmuir. 2008, 24 (5), 2051"2056.
72. Tian, Y., Qi, J., Zhang, W., Cai, Q., Jiang, X., ACS Appl. Mater. Interfaces 2014, 6 (15), 12038"12045.
73. Tan, P., Li, Y.H., Liu, X.Q., Jiang, Y., Sun, L.B., ACS Sustainable Chem. Eng. 2016, 4 (6), 3268"3275.
74. Sambhy, V., MacBride, M.M., Peterson, B.R., Sen, A., J. Am. Chem. Soc. 2006, 128 (30), 9798"9808.
75. Elif, E., Beatrice, G., Flavia, Z., Sergio, A., Benjamin, L.O., Selma, M., Applied materials and interfaces (2017), 9, 34762"34772.
76. Biradar, B., Devi, P., J Contemp Dent Pract. 2011 Nov 1, 12(6), 479-85.
77. Ren, G., Hu, D., Cheng, E.W., Vargas-Reus, M.A., Reip, P., Allaker, R.P., Int J Antimicrob Agents. 2009, 33, 587-590.
78. Dastjerdi, R., Montazer, M., B Biointerfaces. 2010. 79, 5-18.
79. Qi, L., Xu, Z., Jiang, X., Hu, C., Zou, X., Carbohydr Res. 2004, 339, 2693-2700.
80. Chamundeeswari, M., Sobhana, S.S., Jacob, J.P., Kumar, M.G., Devi, M.P., Sastry, T.P., biotechnol. Appl Biochem. 2010, 55, 29-35.
81. Maness, P.C., Smolinski, S., Blake, D.M., Huang, Z., Wolfrum, E.J., Jacoby, W.A., Appl Environ Microbiol. 1999, 65, 4094-4098.
82. Johnston, H.J., Hutchison, G., Christensen, F.M., Peters, S., Hankin, S., Stone, V., Crit Rev Toxicol. 2010, 40. 328-346.
83. Kang, S., Pinault, M., Pfefferle, L.D., Elimelech, M., Langmuir. 2007, 23, 8670-8673.

## Engineered nanoparticles: Hazards and Risk Assessment upon Exposure-A Review

Krishna Suresh Babu Naidu<sup>1\*</sup>,

1. Department of Biomedical & Clinical Technology, Durban University of Technology,  
Durban-4000, South Africa.

\*Corresponding author : Sureshk@dut.ac.za

### Abstract

The presence of engineered nanoparticles (ENPs) in the environment can have significant damaging effects for both environment and human health. Emergent nanoscience and nanotechnology are projected to revolutionise industrial production, economy and consumer crossing point, as we know them today. However, widespread use of nanotechnologies may invite and be a source of risks. People in many settings (academic, small and large industrial, and the public in industrialized nations) are either developing or using products containing engineered nanoparticles. However, our understanding of the occupational, health and safety aspects of ENMs is still in its formative stage. This review describes briefly, ENPs and their applications, safety and risk assessment upon exposure to engineered nanoparticles, the routes of human exposure, fate of engineered nanoparticles in the environment and make recommendations on future research in risk assessment of nanomaterials.

**Keywords:** Environmental risks, Human health, Nanomaterials, Risk characterizations,

### Introduction

Nanotechnology is a on the rise interdisciplinary technology that is often seen as part of a new industrial revolution. Added, nanotechnology is gradually attracting more global attention owing to its wide range of applications in end-uses and end users. Rapid advancements in nanotechnology in recent years have paved a

way for multibillion-dollar industry. For instance, it has been forecasted that the global nanotechnology industry will grow to reach US\$ 75.8 Billion by 2020 [1]. This scenario present huge opportunities for industry participants to tap the fast growing market.

Nanotechnology is defined as the design, characterization and application of structures, devices and systems by controlling shape and size at nanometer scale level (ranging from 1 to 100nm) [2]. The current and projected applications of nanomaterials include catalysts, lubricants and fuel additives; paints, pigments and coatings; cosmetics and personal care products; medical, dental, drug delivery and bionanotechnology; functional coatings; hydrogen storage and fuel cells; nanoelectronics and sensor devices; optics and optic devices; security and authentication applications: structural (composite) materials, conductive inks and printing; UV-absorbers and free-radical scavengers; construction materials; detergents; food processing and packaging; paper manufacturing; agrochemicals, plant protection products and veterinary medicines, plastics, and weapons and explosives [3-4].

A diversity of consumer products that include nanomaterials are already available in developed and developing countries worldwide. Case in point of these include self-cleaning glass, anti-microbial wound dressing, paints and coatings, fuel catalysts and cosmetics (The Woodrow Wilson Nanotechnology Consumer Products Inventory [www.nanotechproject.org](http://www.nanotechproject.org)). Current market

indicators suggest that many more applications of nanotechnologies will emerge in consumer products in the coming years and these are likely to impact on worker health and safety within a number of sectors [4]. The rapid use and integration of nanotechnologies in production of consumer products has therefore raised a number of technological, health and bio-safety, environmental, ethical, policy and regulatory issues worldwide [5]. This is partially because properties of manufactured nanomaterials may vary widely from the 'conventional' micro or macro-forms of the same materials [6]. This fear has arisen from a growing body of scientific evidence that specifies that free nanoparticles can penetrate cellular barriers, and that exposure to some forms of nanoparticle can lead to an increased production of oxyradicals and cause potential oxidative damage at the cell level (Fig 1) [5].

According to statistics published on the Stat Nano about 137500 articles on nanotechnology

have been indexed in the Web of Science (WoS) Database by the end of December 2016, which is 9.5% of all articles indexed in this database in 2016. China is in charge for 34% of these articles while USA has a share of 16%.

The overall objectives of this review paper are to 1) To reconnoiter the current state of knowledge of the safety and risks upon exposure to ENPs 2) Assess what safety mechanisms/practices are presently in place, and 3) and make recommendations on future research in risk assessment of nanomaterials.

#### Applications of engineered nanoparticles :

Advancements in the fields of nanoscience and nanotechnology have resulted in a myriad of possibilities for consumer product applications, many of which have already migrated from laboratory benches onto store shelves and e-commerce websites (Table 1) [6-7]. In 2009, it was estimated that nanotechnology would have impacted more than \$2.5 trillion worth of

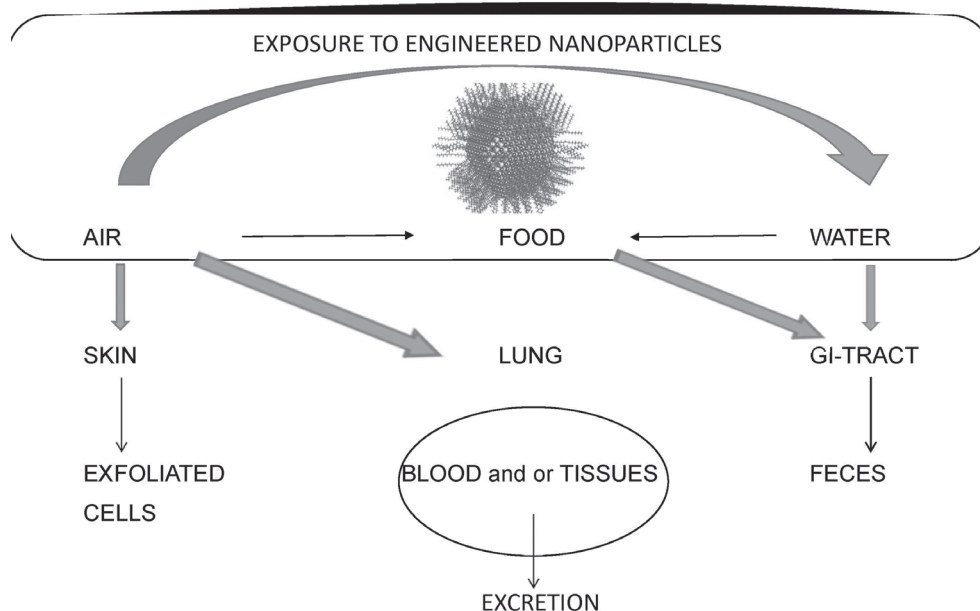
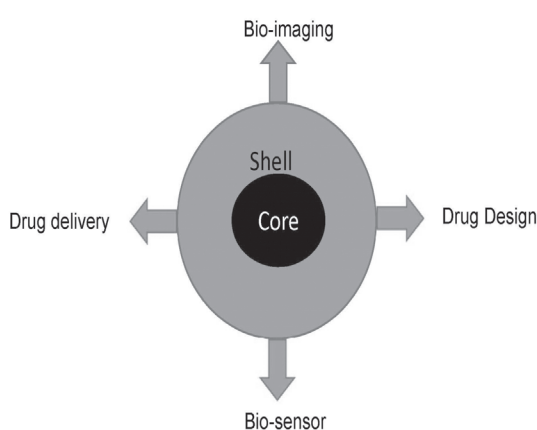


Fig.1. Environmental monitoring and biological exposure to engineered nanoparticles



manufactured goods by 2015 [8], although many of these goods may contain only minute amounts of intentionally engineered nanomaterials. According to Stat Nano report ([www.statnano.com](http://www.statnano.com)), studies carried out on 6432 products on the Nanotechnology Products Database (NPD) show that the United States and China are the largest producers of carbon nanotubes in the world. However, Japan has produced the largest number of products in which carbon nanotubes have been used. The International Risk Governance Council has observed that nanotechnology applications “will penetrate and permeate through nearly all sectors and spheres of life (e.g. communication, health, labour, mobility, housing, relaxation, energy and food) and will be accompanied by changes in the social, economic, ethical and ecological spheres” [9].

Nanomedicine, the application of nanotechnology to healthcare holds great promise for revolutionizing medical treatments and therapies in areas such as imaging, faster diagnosis, drug delivery and tissue regeneration, as well as the development of new medical products (Fig. 2). Indeed, materials and devices of nanometric dimensions are already approved for clinical use and numerous products are being



**Fig. 2.** Biomedical applications of core shell nanoparticles (11)

evaluated in clinical trials around the world [10]. The major advantages of nanoparticles over larger sized particles are their high surface-to-volume ratio and hence higher surface energy, unique optical, electronic, and excellent magnetic properties [11] and so on. The high surface area on nanoparticles are modified adequately to improve its pharmacokinetic properties, increase vascular circulation lifetime, along with improving bioavailability, especially for biomedical applications [12]. The improved properties are a boon in the field of drug delivery-: the increased vascular circulation lifetime increases the efficacy of the drug; the enhancement of the drug bioavailability means a lot lesser dosage could effectively work instead of bulk drugs [13]. As mentioned before, the most important property of nanoparticles, which has attracted the attention of researchers worldwide, is their ability to have better surface modifications, which not only helps in targeted drug delivery but can serve the dual purpose of drug monitoring and release. The use of nano materials provides unparalleled freedom to change fundamental properties such as solubility, diffusivity, blood circulation half-life, drug release characteristics, and immunogenicity [14]. Over last two decades, a number of nanoparticle-based therapeutic and diagnostic agents have been developed for the treatment of cancer, diabetes, pain, asthma, allergy and infections [15].

Despite these potential benefits, nanotechnology applications in the agricultural sector are still comparably marginal and have not yet made it to the market to any large extent in comparison with other industrial sectors[16]. The wave of research discoveries seems to be mainly claimed by the academic sector or small enterprises, while big industries reveal a large patent ownership.

#### **Safety & risk assessment upon exposure to engineered nanoparticles**

**Nanoparticle exposure pathways** : Critical information such as nanomaterial size and concentration are not generally known for most products listed on the Consumer Product Inventory (CPI) and therefore; the actual health risks of these

products remain largely unknown [17]. Nevertheless, the CPI may be useful for inferring potential exposure pathways from the expected normal use of listed products. Hansen et al. [18] developed a framework for exposure assessment in consumer products. In this framework, products that contain nanomaterials suspended in liquid and products that may emit airborne nanoparticles during use are expected to cause exposure (Fig .3).

Since metals and metal oxides are the most common nanomaterial composition in the CPI, they are also the most likely materials to which consumers will be exposed during the normal use of product via dermal, ingestion, and inhalation routes. Products containing nanomaterials of unknown composition are most likely to lead to exposure via the dermal route.

In another study piloted by Beaudrie et al. [20] presented a critique of the original CPI in 2010, which focused primarily on the lack of data pertinent to the dosages of nanomaterials to which consumers might be exposed through CPI-listed products. This is a valid criticism given that information used to populate the CPI is based

primarily on marketing claims made by manufacturers. However, the most recent modifications of the CPI offer a potential remedy for data gaps through the contributions of third-party research teams. These modifications are especially timely as there is a growing number of published studies assessing consumer exposure to nanomaterials released during the use of nanotechnology enhanced consumer products [1]. Added, major challenge is that there are no standardized methods for assessing consumer risks from using nanotechnology-enabled consumer products or a set of agreed upon metrics for characterizing nanomaterials to determine environmentally relevant concentrations [21]. The development of such standards is seen as a top policy for safe and sustainable nanotechnology development in the next decade.

**Risk assessment of engineered nanoparticles** : Concerns surrounding the health risk of engineered nanomaterials, effective regulation and the lack of specifically tailored insurance products for the nanotechnology sector are putting the industry's long-term economic viability at risk [22]. In U.S., federal mistake of potentially toxic

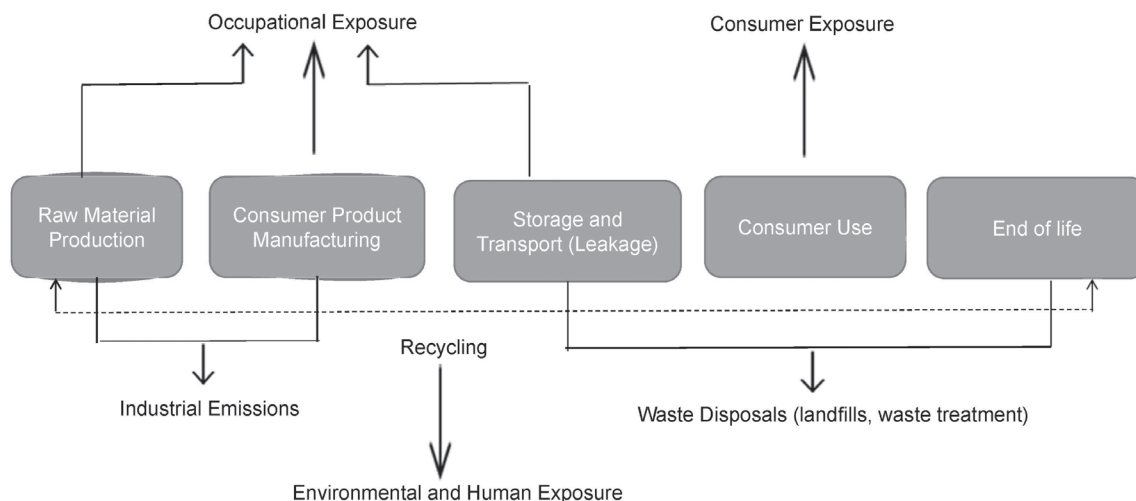


**Fig. 3.** Potential pathways of occupational, environmental and human exposure to ENPs (19)

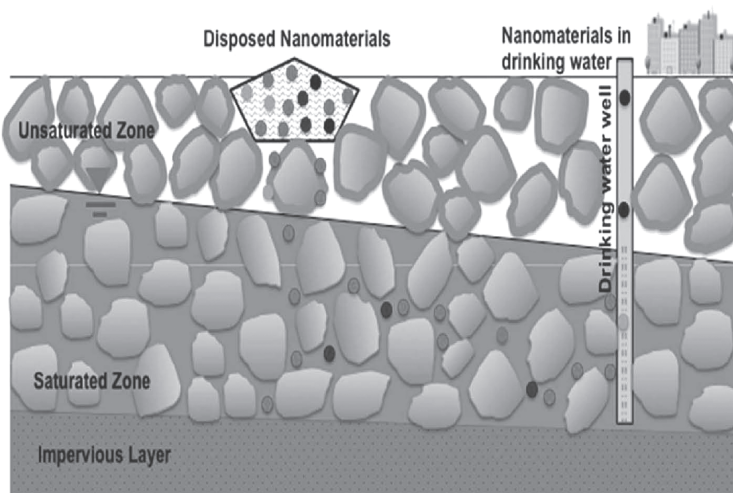


**Fig. 4.** Concerns for transport of nanomaterials from landfill sites to a drinking water well (35)

materials and products spans several federal agencies [20]. These include the Environmental Protection Agency (EPA), the Food and Drug Administration (FDA), the Occupational Safety and Health Administration (OSHA), and the Consumer Product Safety Commission (CPSC). Each agency is charged with enforcing regulations to control risks from specific types or uses of substances (i.e., chemicals, pharmaceuticals, and pesticides), or from potentially harmful releases in the workplace or into the environment.

The primary stage of Engineered Nano Materials (ENM) product life cycle comprises from the transformation of raw materials into nanomaterials (e.g., manufacturing bulk silver into nanoscale silver particles) to the incorporation of nanomaterials as a component of other products (e.g., nanosilver antimicrobial textile coatings). Three key statutes that come into effect at this stage depend on the intended application of the nanomaterial. In USA, chemical substances and pesticides are regulated under the Toxic Substances Control Act (TSCA) [23] and Federal Insecticide, Fungicide, and Rodenticide Act (FIFRA), respectively, and the EPA administers

both acts. Food additives and drugs are regulated under the Federal Food, Drug, and Cosmetic Act (FFDCA) [24] that is administered by the FDA. Together, TSCA, FIFRA, and FFDCA apply to chemical substances, pesticides, food additives, and drugs primarily through a “premarket” risk-assessment, registration, and management approach. With this approach, each substance is evaluated and risk-management decisions are typically made before a product is released for use on the market.

The United States Environmental Protection Agency (EPA), defines “risk” with “respect to the above definition of “hazard” as a measure of the probability that damage to life, health, property, and/or the environment will occur as a result of a given hazard. According to this definition, if the probability of an exposure to a hazardous material is high and the consequences for human health or the environment are significant, then the risk is considered high. It is important to consider both the frequency of the event and the degree of the hazard to estimate risk [25]. Usually two categories of risk are distinguished in literature: known “risks” and “potential risks”. When the

**Engineered nanoparticles: Hazards and Risk Assessment upon Exposure-A Review**

Table 1. Potential applications of engineered nanoparticles [modified 19]

Nanomaterial	Areas	Applications
Nano-CeO <sub>2</sub> ;	Automotive	Lightweight construction; Catalysts; Painting; Tires; Sensors; Windshield and body coatings
Nano-TiO <sub>2</sub>	Chemical	Fillers for paints; Composite materials; Impregnation of papers; Adhesives; Magnetic fluids
Nano-TiO <sub>2</sub> ; Nano-Ag	Construction	Materials; Insulation; Flame retardants; Surface coatings; Mortar
Nano-TiO <sub>2</sub> ; Nano-ZnO; Fullerene C <sub>60</sub>	Cosmetics	Sunscreen; Lipsticks; Skin creams; Toothpaste
Quantum dots	Electronics	Displays; Data memory; Laser diodes; Fiber optics; Optical switches; Filters; Conductive coatings; Antistatic coatings; Transistors
Carbon nanotubes (CNT)	Energy	Lighting; Fuel cells; Solar cells; Batteries; Capacitors
TiO <sub>2</sub> , SiO <sub>2</sub> , Ag, quantum dots	Engineering	Protective coatings for tools, machines; Lubricant-free bearings
Metals and metal oxides	Environmental	Environmental monitoring; Soil and groundwater remediation; Toxic exposure sensors; Fuel changing catalysts; Green chemistry
Ag, nanoclay, TiO <sub>2</sub>	Food and Drink	Packaging; Storage life sensors; Additives; Juice clarifiers
Copper species coated silica nanoparticles, TiO <sub>2</sub>	Household	Ceramic coatings for irons; Odor removers; Cleaners for glass, ceramics, metals
Fullerenes (carbon-60, carbon-70, carbon-80, derivatized), Multiwall Nanotubes,	Medicine	Drug delivery systems; Contrast medium; Rapid testing systems; Prostheses and implants; Antimicrobial agents; In-body diagnostic systems
Si or TiO <sub>2</sub> nanoparticles embedded in epoxy matrix, Iron nanoparticles in inert oil which hardens on stimulation with an electrical pulse (Magnetorheological Fluid)	Military	Neutralization materials for chemical weapons, bullet-proof protection
carbon nanotubes (CNTs), silica nanoparticles (SNPs), nanoclays, fullerenes	Sports	Ski wax; Tennis rackets; Golf clubs; Tennis balls; Antifouling coatings for boats; Antifogging coatings for glasses, goggles
TiO <sub>2</sub> , Al <sub>2</sub> O <sub>3</sub> , SiO <sub>2</sub> , CNT, ZnO, Polybutylacrylate.	Textiles	Surface coatings; Smart clothes (anti-wrinkle, stain resistant, temperature controlled)

relationship between a cause and an effect is established, we talk of known “risks”. The responsibility for such risks can generally be recognized. When the causal relationship is established, prevention is possible. When the relationship between a cause and damage is not well known, we talk of potential “risks”. In the case of potential risks, it is unclear whether there is a danger, how significant the damage can be or what is the probability of its occurrence [26]. This situation is considered by a state of suspicion (not awareness) and it is generally admitted that a precautionary approach can be applied in order to prevent potential damage [26]. The risks of ENPs for the environment and human health fall into the second category: potential risks. It is very important to assess the risks of hazardous agents like ENPs. The likelihood that a hazardous substance will cause harm (the risk) is the determinant of how cautious one should be and what preventative or precautionary measures should be taken.

Risk assessment of chemicals (CRA) has been reflected as the most relevant approach to understand and quantify the related risks [18]. CRA is a process, in which scientific and regulatory principles are applied in a systematic fashion in order to describe the hazards, associated with the environmental and/or human exposure to chemical substances. It is defined as “a process, intended to calculate or estimate the risk to a given target organism, system or (sub)population, including the identification of attendant uncertainties, following exposure to a particular agent, taking into account the inherent characteristics of the agent of concern, as well as the characteristics of the specific target system [27]. The CRA is a four-step process, consisting of: (1) hazard identification, (2) dose-response assessment, (3) exposure assessment and (4) risk characterization. Its main outcome is a statement of the probability that when humans or other environmental receptors (e.g., plants, animals) are exposed to a chemical agent, they will be harmed and to what degree. The CRA methodology is internationally recognized and

employed by major actors, such as the World Health Organization (WHO) and the Organization for Economic Co-operation and Development (OECD), as well as by several European and U.S. agencies [28].

In order to address the objective 2 of this chapter, the current methods adopted for the assessment of risks of ENPs for the environment and human health are summarized in relation to each of the four elements of the CRA framework important scientific advancements, research gaps and limitations are identified and discussed.

**Hazard identification** : “Hazard identification” (HI) is defined as the “identification of the adverse effects, which a substance has an inherent capacity to cause” [29]. Hansen et al. [18] identified 428 studies reporting on toxicity of ENPs. In these studies, adverse health effects of 965 tested ENPs of various chemical compositions were observed [30].

**Dose-response assessment** : “Dose-response assessment” (DRA) is defined as “an estimation of the relationship between dose, or level of exposure to a substance, and the incidence and severity of an effect”. It is the process of characterizing the relationship between the dose of an agent, administered to or received by an individual, and the consequent adverse health effects. In toxicological studies a “dose” is the quantity of anything that may be received by or administered to an organism. The “dose” is normally measured in mass units (i.e.,  $\mu\text{g}$ , mg, g), as higher doses of the same compounds are expected to cause more severe adverse effects. DRA studies with ENPs, however, suggest that the toxicity of some ENPs is not mass dependent, but influenced by other physico-chemical characteristics (e.g., surface area, chemical composition, and particle morphology) [31]. Several studies found that the toxicity of low-soluble ENPs was better described by their surface area than by their total mass [30], number of particles [32], functional groups [33]. Despite these findings, however, it is still largely unknown which properties influence the toxicity of most



ENPs and this gap in knowledge is partly attributable to the fact that the tested ENPs are seldom well characterized [19].

**Exposure assessment:** “Exposure assessment” (EA) is defined as an estimation of the concentrations/doses to which human populations (i.e., workers, consumers and citizens exposed indirectly via the environment) or environmental compartments (aquatic environment, terrestrial environment and air) are or may be exposed [19]. EA is a very important element in risk assessment of ENPs, since if no exposure to ENPs occur, it would be impossible that they cause any harm and there would be no risk at all. EA can be divided into three sub-areas: (1) occupational exposure assessment (OEA), (2) environmental exposure assessment (EEA) (including indirect human exposure from the environment) and (3) consumer exposure assessment (CEA).

**Fate of engineered nanoparticles in environment:** Engineered nanoparticles (ENPs) or Engineered nanomaterials (ENM) are exposed to environment during all stages of their life cycles: raw material production, transport and storage, industrial use (incl. processing and/or trade), consumer use, waste disposal (incl. waste treatment, landfill and recovery) [29]. Moreover, fate of ENPs, released in the environment is determined by their mobility in different media (i.e., soil, water, air), as well as by their potential to biodegrade or undergo chemical transformation [2]. A recent study by Keller and Lazareva [34] estimated that 63–91% of over 300 kilo tonnes of ENMs produced globally ended up in landfills by 2010; 8–28% entered the soils, 0.4–7% reached the surface water bodies, and 0.1–1.5% entered into the atmosphere. In the event of transport of nanomaterials present in landfills or soils, it may disperse into drinking water sources or major surface water bodies (Fig. 4). Given the large proportion of nanomaterials ending up in soils, an understanding of the impact of these nanomaterials on soil organisms or ecosystems is required for informed risk assessments and policy discussions. Interestingly, most of the potential hazards of these nanomaterials are

undocumented and there is lack of awareness among common people.

**Fate of engineered nanoparticles in air:** The fate of ENPs in the air is determined by three main factors: (1) the duration of time particles remain airborne, (2) their interaction with other particles or molecules in the atmosphere and (3) the distance they are able to travel in the air [36] deliberate the mechanisms of diffusion, agglomeration, and deposition for nanoparticle aerosols, and the possible resuspension of aerosol from deposited nanoparticles. In addition, the processes important to understand the dynamics of ENPs in the atmosphere are diffusion, agglomeration, wet and dry deposition and gravitational settling. With respect to the duration of time ENPs stay in the air, it is considered that they may follow the laws of gaseous diffusion.

It is generally considered that particles in the nanoscale ( $d < 100$  nm) have shorter residence time in the air, compared to medium-sized particles ( $100 \text{ nm} < d < 2,000$  nm), because they rapidly agglomerate into much larger particles and settle on the ground [37]. ENPs with anti-agglomerate coatings make an exception and their residence time cannot be predicted. It is well thought-out that deposited ENPs are usually not likely to be re-suspended or re-aerosolized in the atmosphere. However, many nano-sized particles are photoactive, but it is still unknown whether they are susceptible to photo degradation in the atmosphere.

**Fate of engineered nanoparticles in water:** The fate of ENPs in water is directed by several factors: (1) aqueous solubility, (2) reactivity of the ENPs with the chemical environment and (3) their interaction with certain biological processes [38]. Since ENPs have lower mass, ENPs generally settle more slowly to the bottom than larger particles of the same material. However, due to their high surface-area-to-mass ratios, ENPs readily sorb to soil and sediment particles and consequently are more liable to removal from the water column. However, some ENPs might be subjected to biotic and abiotic degradation [17],

which can remove them from the water column as well. In addition, abiotic degradation processes that may occur include hydrolysis and photocatalysis. Near to the surface ENPs are exposed to sunlight. It is likely that light-induced photoreactions can account for the removal of certain ENPs and for changing the chemical properties of others.

**Fate of engineered nanoparticles in soil :** The fate of ENPs in soil vary depending on physical and chemical properties of the material. Some ENPs can strongly sorb to the soil particles and become completely inert and immobile. Alternatively, if ENPs do not sorb to the soil matrix, they might show even greater mobility than larger particles, because their small size might allow them to travel easily through the pore spaces between the soil particles. The possibility to sorb to soil and the respective sorption strength of ENPs is influenced by their size, chemical composition and surface characteristics [36].

Study by Zhang [39], indicated considerable differences in mobility of some insoluble ENPs in porous media. The properties of soil, such as porosity and grain size, further influence the mobility of the particles. Just like the mineral colloids, the mobility of ENPs, agglomerated in colloid-like structures might be strongly affected by electrical charge differences in soils and sediments. Surface photoreactions might induce photochemical transformations on the soil surface.

### Conclusions & Recommendations

Though nanoparticles research is enduring since more than 30 years, the development of methods and standard protocols required for their safety and efficacy testing for human use is still in development [39]. ENPs are anticipated to affect living organisms in different ways than their bulk alternatives and considering their significant range, it is expected that ENPs would also differ a lot from each other in terms of toxicity.

As there are very limited number of studies are made in field of environmental fate of ENPs, their behavior in the environment is still largely

unmapped. When addressing the environmental fate of ENPs, most of the current literature available uses inaccurate general considerations and comparison with data, obtained for larger particles. It is very imperative to study the environmental fate of ENPs in order to understand their pathways of environmental and concern of human exposure.

Considering the availability of literature about nanoparticles for medical applications and taking into account of different participants in the field of nanomedicine including the community working in the field of nanotoxicology, we strongly recommend:

- A. Launching laboratories which allows a GMP like synthesis including functionalization of nanoparticles for medical application.
- B. Regulatory bodies should implement strict explicit checklist
- C. In vivo and In vitro models used for nanoparticle-cell interactions should be validated.
- D. To minimize damaging effects of ENPs it is essential to identify the exposure sources and pathways of ENPs in the working settings as well as to study the mechanisms behind their dispersion and measure their concentrations
- E. Comprehensive inventory of consumer exposure to ENPs and data generated needs to be elaborated and made easily accessible to scientists and risk managers.

Employing above recommendations leading to growth of nanomaterials for biomedical applications might be improved and hazard of exposure to ENPs would be reduced substantially. This would reassure community to reduce the risk of exposure to ENPs and protect the environment.

### References

1. Vance, M.E., Kuiken, T., Vejerano, E.P., McGinnis, S.P., Hochella, M.F., Jr., Rejeski, D., and Hull, M.S. (2015). Nanotechnology in the real world: Redeveloping the nanomaterial consumer products inventory. *Beilstein Journal of Nanotechnology* 6, 1769-1780.

2. Das, S.K., and Avasthe, R. (2015). Carbon farming and credit for mitigating greenhouse gases. *Current Science* 109, 1223.
3. Fiorino, D.J. (2010a). Voluntary Initiatives. Regulation and Nanotechnology Oversight: Charting a Path, Project on Emerging Nanotechnologies Publication 19.
4. Boxall, A.B., Chaudhry, Q., Sinclair, C. J., Alan, A., Robert, J., Bruce, W., and Chris. (2007). Current and future predicted environmental exposure to engineered nanoparticles. Central Science Laboratory, Department of the Environment and Rural Affairs, London, UK, 89.
5. Weissig, V., Pettinger, T.K., and Murdock, N. (2014b). Nanopharmaceuticals (part 1): products on the market. *International Journal of Nanomedicine* 9, 4357.
6. Dos Santos, C.A., Seckler, M.M., Ingle, A.P., Gupta, I., Galdiero, S., Galdiero, M., Gade, A., and Rai, M. (2014). Silver nanoparticles: therapeutical uses, toxicity, and safety issues. *Journal of Pharmaceutical Sciences* 103, 1931-1944.
7. Hristozov, D., and Malsch, I. (2009). Hazards and risks of engineered nanoparticles for the environment and human health. *Sustainability* 1, 1161-1194.
8. Research, L. (2009). Nanomaterials State of the Market Q1 2009 [www.luxresearch.com](http://www.luxresearch.com).
9. Fiorino, D.J. (2010b). Voluntary initiatives, regulation, and nanotechnology oversight: Charting a path. Project on Emerging Nanotechnologies, 19.
10. Zhang, L., Gu, F.X., Chan, J.M., Wang, A.Z., Langer, R.S., and Farokhzad, O.C. (2008). Nanoparticles in medicine: therapeutic applications and developments. *Clinical Pharmacology and Therapeutics* 83, 761-769.
11. Chatterjee, K., Sarkar, S., Jagajjanani Rao, K., and Paria, S. (2014). Core/shell nanoparticles in biomedical applications. *Advances in Colloid and Interface Science* 209, 8-39.
12. Chaudhry, Q., George, C., and Watkins, R. (2009). 11. Nanotechnology regulation: developments in the United Kingdom. *New Global Frontiers in Regulation: The Age of Nanotechnology*, p212.
13. Weissig, V., Pettinger, T.K., and Murdock, N. (2014a). Nanopharmaceuticals (part 1): products on the market. *International Journal of Nanomedicine* 9, 4357-4373.
14. Babu, A., Templeton, A.K., Munshi, A., and Ramesh, R. (2014). Nanodrug delivery systems: a promising technology for detection, diagnosis, and treatment of cancer. *Aaps Pharmscitech* 15, 709-721.
15. Ge, L., Li, Q., Wang, M., Ouyang, J., Li, X., and Xing, M.M. (2014). Nanosilver particles in medical applications: synthesis, performance, and toxicity. *International Journal of Nanomedicine* 9, 2399.
16. Parisi, C., Vigani, M and Rodríguez-Cerezo. (2015). Agricultural Nanotechnologies: What are the current possibilities? *Nano Today*, 10(2): 124-127.
17. Colvin, V.L. (2003). The potential environmental impact of engineered nanomaterials. *Nature Biotechnology* 21, 1166-1170.
18. Hansen, S.F. (2009). Regulation and risk assessment of nanomaterials: too little, too late. 2019 January; Accessed from the website: <http://www2.er.dtu.dk/publications/fulltext/2009/ENV2009-069.pdf>.
19. Hristozov, D., and Malsch, I. (2009). Hazards and risks of engineered nanoparticles for the environment and human health. *Sustainability* 1, 1161-1194.
20. Beaudrie, C.E.H., Kandlikar, M., and Satterfield, T. (2013). From Cradle-to-Grave at the Nanoscale: Gaps in U.S. Regulatory Oversight along the Nanomaterial Life Cycle.

- Environmental Science & Technology 47, 5524-5534.
21. Holden, P.A., Klaessig, F., Turco, R.F., Priester, J.H., Rico, C.M., Avila-Arias, H., Mortimer, M., Pacpaco, K., and Gardea-Torresdey, J.L. (2014). Evaluation of Exposure Concentrations Used in Assessing Manufactured Nanomaterial Environmental Hazards: Are They Relevant? *Environmental Science & Technology* 48, 10541-10551.
  22. McAlea, E.M., Mullins, M., Murphy, F., Tofail, S.A., and Carroll, A.G. (2016). Engineered nanomaterials: risk perception, regulation and insurance. *Journal of Risk Research* 19, 444-460.
  23. Bergeson, L. L., Campbell, L. M., and Rothenberg, L. (2000). TSCA and the Future of Chemical Regulation. *EPA Administrative Law Reporter*, 15(4), 23.
  24. Beckett, W.S., Chalupa, D.F., Pauly-Brown, A., Speers, D.M., Stewart, J.C., Frampton, M.W., Utell, M.J., Huang, L.-S., Cox, C., and Zareba, W. (2005). Comparing inhaled ultrafine versus fine zinc oxide particles in healthy adults: a human inhalation study. *American Journal of Respiratory and Critical Care Medicine* 171, 1129-1135.
  25. Helland, A. (2004). Nanoparticles: a closer look at the risks to human health and the environment perceptions and precautionary measures of industry and regulatory bodies in Europe. International Institute for Industrial Environmental Economics (IIIEE): Lund, Sweden, 2004. Available online: [http://www.iiiee.lu.se/Publication.nsf/\\$webAll/D9CA9F1E83E4FA12C1256F9D00539C39/\\$FILE/Asgeir%20Helland.pdf](http://www.iiiee.lu.se/Publication.nsf/$webAll/D9CA9F1E83E4FA12C1256F9D00539C39/$FILE/Asgeir%20Helland.pdf) (accessed November 2018).
  26. Perret, H., Audétat, M., Petriccione, B., Joseph, C., and Kaufmann, A. (2005). Approaches of risk: an introduction (RIBios et IUED: Geneva, Switzerland). Available online: <http://www.rezoscience.ch/rp/296/version/default/part/AttachmentData/data/ribiosbroch-approchesrisque-20061030.pdf>
  27. Boobis, A.R., Cohen, S.M., Dellarco, V.L., Doe, J.E., Fenner-Crisp, P.A., Moretto, A., Pastoor, T.P., Schoeny, R.S., Seed, J.G., and Wolf, D.C. (2016). Classification schemes for carcinogenicity based on hazard-identification have become outmoded and serve neither science nor society. *Regulatory Toxicology and Pharmacology* 82, 158-166.
  28. Reichwaldt, E.S., Stone, D., Barrington, D.J., Sinang, S.C., and Ghadouani, A. (2016). Development of toxicological risk assessment models for acute and chronic exposure to pollutants. *Toxins* 8, 251; doi:10.3390/toxins8090251
  29. Anwar, W., and Khitab, A. (2016). Risks and Preventive Measures of Nanotechnology. In *Advanced Research on Nanotechnology for Civil Engineering Applications* (IGI Global), pp. 253-276.
  30. Foss Hansen, S., Larsen, B.H., Olsen, S.I., and Baun, A. (2007). Categorization framework to aid hazard identification of nanomaterials. *Nanotoxicology* 1, 243-250.
  31. Strickland, J.D., Lefew, W.R., Crooks, J., Hall, D., Ortenzio, J.N., Dreher, K., and Shafer, T.J. (2016). In vitro screening of metal oxide nanoparticles for effects on neural function using cortical networks on microelectrode arrays. *Nanotoxicology* 10, 619-628.
  32. Schmid, O., and Stoeger, T. (2016). Surface area is the biologically most effective dose metric for acute nanoparticle toxicity in the lung. *Journal of Aerosol Science* 99, 133-143.
  33. Dobrovolskaia, M.A. (2016). Nanoparticle Toxicity: General Overview and Insights Into Immunological Compatibility. *Pharmaceutical Nanotechnology: Innovation and Production*, 2 Volumes. Edited by Jean Cornier, Andrew Owen, Arno Kwade, Marcel Van de Voorde

34. Keller, A.A., and Lazareva, A. (2013). Predicted releases of engineered nanomaterials: from global to regional to local. *Environmental Science & Technology Letters* 1, 65-70
35. Sharma, P. (2015). Nanomaterials from food packaging and commercial products into ecological and soil environment. *Current Science*, 109(7), 1223-1224
36. Aitken, R., Hankin, S., Ross, B., Tran, C., Stone, V., Fernandes, T., Donaldson, K., Duffin, R., Chaudhry, Q., and Wilkins, T. (2009). EMERGNANO: A review of completed and near completed environment, health and safety research on nanomaterials and nanotechnology (concise report) Defra Project CB0409. Institute of Occupational Medicine Report TM/09/01.
37. Dennekamp, M., Mehenni, O., Cherrie, J., and Seaton, A. (2002). Exposure to ultrafine particles and PM<sub>2.5</sub> in different micro-environments. *Annals of Occupational Hygiene* 46, 412-414.
38. Morris, J., & Willis, J. (2007). US Environmental Protection Agency nanotechnology white paper. US Environmental Protection Agency, Washington, DC.
39. Zhang, W. X. (2003). Nanoscale iron particles for environmental remediation: an overview. *Journal of nanoparticle Research*, 5(3-4), 323-332.





Registered with Registrar of News Papers for India  
Regn. No. APENG/2008/28877

# Association of Biotechnology and Pharmacy

(Regn. No. 28OF 2007)

## Executive Council

*Hon. President*

**Prof. B. Suresh**

*Hon. Secretary*

**Prof. K. Chinnaswamy**

*President Elect*

**Prof. T. V. Narayana**

Bangalore

*General Secretary*

**Prof. K.R.S. Sambasiva Rao**

Guntur

*Vice-Presidents*

**Prof. M. Vijayalakshmi**

Guntur

*Treasurer*

**Prof. P. Sudhakar**

**Prof. T. K. Ravi**

Coimbatore

## Advisory Board

**Prof. C. K. Kokate**, Belgaum

**Prof. B. K. Gupta**, Kolkata

**Prof. Y. Madhusudhana Rao**, Warangal

**Prof. M. D. Karwekar**, Bangalore

**Prof. K. P. R. Chowdary**, Vizag

**Dr. V. S.V. Rao Vadlamudi**, Hyderabad

## Executive Members

Prof. V. Ravichandran, Chennai

Prof. Gabhe, Mumbai

Prof. Unnikrishna Phanicker, Trivandrum

Prof. R. Nagaraju, Tirupathi

Prof. S. Jaipal Reddy, Hyderabad

Prof. C. S. V. Ramachandra Rao, Vijayawada

Dr. C. Gopala Krishna, Guntur

Dr. K. Ammani, Guntur

Dr. J. Ramesh Babu, Guntur

Prof. G. Vidyasagar, Kutch

Prof. T. Somasekhar, Bangalore

Prof. S. Vidyadhara, Guntur

Prof. K. S. R. G. Prasad, Tirupathi

Prof. G. Devala Rao, Vijayawada

Prof. B. Jayakar, Salem

Prof. S. C. Marihal, Goa

M. B. R. Prasad, Vijayawada

Dr. M. Subba Rao, Nuzividu

Prof. Y. Rajendra Prasad, Vizag

Prof. P. M. Gaikwad, Ahmednagar

Printed, Published and owned by Association of Bio-Technology and Pharmacy # 6-69-64 : 6/19, Brodipet, Guntur - 522 002, Andhra Pradesh, India. Printed at : Don Bosco Tech. School Press, Ring Road, Guntur - 522 007. A.P., India Published at : Association of Bio-Technology and Pharmacy # 6-69-64 : 6/19, Brodipet, Guntur - 522 002, Andhra Pradesh, India. Editors : Prof. K.R.S. Sambasiva Rao, Prof. Karnam S. Murthy